Effect of the gut microbiota metabolite urolithin A on the inflammatory responses induced by LPS or X-irradiation in BMDMs

Dissertation

der Mathematisch-Naturwissenschaftlichen Fakultät

der Eberhard Karls Universität Tübingen

zur Erlangung des Grades eines

Doktors der Naturwissenschaften

(Dr. rer. nat.)

vorgelegt von

Khalid Nady Mohammed Abdelazeem

aus Minia/Ägypten

Tübingen

2020

Gedruckt mit Genehmigung der Mathematisch-Naturwissenschaftlichen Fakultät der Eberhard Karls Universität Tübingen.

Tag der mündlichen Qualifikation:

Dekan: Prof. Dr. Wolfgang Rosenstiel

1. Berichterstatter: Prof. Dr. Friedrich Götz

2. Berichterstatter: Prof. Dr. Hans-Georg Rammensee

TABLE OF CONTENTS

LIST OF FIGURES

LIST OF TABLES

LIST OF ABBREVIATIONS

A

AKT	Protein kinase B
AMPK	AMP-activated protein kinase
APC	Allophycocyanin
APS	Ammonium per-sulphate
ATCC	American Type Culture Collection
ATM	Ataxia telangiectasia mutated
ATP	Adenosine triphosphate

B

BMDM	Bone marrow derived macrophage
53BP1	P53 Binding Protein 1
BSA	Bovine serum albumin

C

C/EBPβ	CCAAT-enhancer-binding proteins
Ca^{2+}	Calcium
CaM	Calmodulin
CaMKKβ	Calcium/ calmodulin dependent protein kinase kinase β
CCL	Chemokine (C-C motif) ligand
CD14	Cluster of differentiation 14
CLRs	C-type lectin-like receptors
CNS	Central nervous system

COX-2	Cyclooxygenase-2
CVD	Cardiovascular disease
CRAC	Ca^{2+} release-activated Ca^{2+} channels
CSF	Colony stimulating factors

D

DCs	Dendritic cells
DEPC	Diethyl pyrocarbonate
DNase I	Deoxyribonuclease I from bovine pancreas
DSB	Double strand breaks
DMSO	Dimethyl sulfoxide
DNA-PKcs	DNA-protein kinase catalytic subunit
DNA-PKcs	DNA-protein kinase catalytic subunit
DNA	Deoxyribonucleic acid
DDR	DNA damage response
DCFDA	2′,7′-Dichlorofluorescin diacetate
DMEM	Dulbecco's modified Eagle's medium
DAMPs	damage associated molecular patterns

E

EA	Ellagic acid
4E-BP1	Eukaryotic translation initiation factor 4E-binding protein 1
ECL	Enhanced Chemiluminescence

ECSIT	Evolutionarily conserved signalling intermediate in Toll pathways	**I**	
ELISA	Enzyme-linked immunosorbent assay	IBD	Inflammatory bowel diseases
ER	Endoplasmic reticulum	IFN	Type I interferon
ERK	Extracellular signal-regulated kinases	IGF-1	Insulin-like growth actor 1
Ex /Em	Excitation /Emission	IgG	Immunoglobulin G
		IKK	IκB kinase
F		IL	Interleukin
FBS	Fetal bovine serum	iNOS	Inducible nitric oxide synthase
FITC	Fluorescein isothiocyanate	IR	Ionizing radiation
FACS	Fluorescence Activated Cell Sorting	IRAK-1	Interleukin-1 receptor-associated kinase 1
Fc	Fragment crystallization		
		J	
G		JNK	c-Jun NH2-terminal kinase
GAPDH	Glyceraldehyde-3-phosphate dehydrogenase		
GF	Germ free		
GIT	Gastrointestinal tract	**L**	
Gy	Gray	LBP	LPS binding protein
		LOS	Lipooligosaccharides
H		LPS	Lipopolysaccharide
HR	Homologous recombination	LRRs	leucine-rich repeats
HRP	Horseradish peroxidase		
H2AX	Histone family member X	**M**	
h	Hour	M1	Classically activated macrophages
		M2	Alternatively activated macrophages
HCL	Hydrogen chloride	MAPKs	Mitogen-activated protein kinases
HBSS	Hank´s balanced salt solution	M-CSF	Macrophage colony stimulating factor
		MD2	Myeloid Differentiation factor 2
		MEK	MAPK/ERK Kinase
		Mg	Magnesium

ΔΨm	Mitochondrial membrane potential	**P**	
MHC	Major histocompatibility complex	PIP3	Phosphatidylinositol 3,4,5-triphosphate
miRNAs	MicroRNAs	PLC	Phospholipase C
MPS	Mononuclear phagocyte system	PM	Plasma membrane
mRNA	Messenger RNA	PPARδ	Peroxisome proliferator-activated receptor δ
mROS	Mitochondrial ROS	PRRs	pattern recognition receptors
mtDNA	Mitochondrial DNA	P/S	Penicillin-Streptomycin
mTOR	Mammalian target of rapamycin	PTKs	Protein tyrosine kinases
MyD88	Myeloid differentiation primary response 88	PVDF	Polyvinylidene difluoride
		PAMPs	Pathogen-associated molecular patterns
N		PBS	Phosphate buffer saline
NF-ATc	Nuclear factor of activated T cells	PCR	Polymerase chain reaction
NaN3	Sodium azide	PE	Phycoerythrin
NF-kB	Nuclear factor kappa-light-chain-enhancer of activated B cells	pH	Potential of hydrogen
NHEJ	Non-homologous end joining	PI3K	Phosphoinositide 3-kinase
NLS	Nuclear localization signals	PIKK	PI3K-related kinase family
NLR	NOD-like receptors	PIP2	Phosphatidylinositol 4,5-bisphosphate
NADPH	Nicotinamide adenine dinucleotide phosphate	PIP3	Phosphatidylinositol 3,4,5-triphosphate
NCTC	National Collection of Type Cultures		
NaCl	Sodium chloride	**R**	
nDNA	Nuclear DNA	^{222}Rn	Radium
		RA	Rheumatoid arthritis
NLRP3	NLR family pyrin domain containing 3	RAD	Radiation
NO	Nitric oxide	Raf	Rapidly Accelerated Fibrosarcoma
NOXs	NADPH oxidase	RLRs	RIG-I-like receptors
RNA	Ribonucleic acid		

RNS   Reactive nitrogen species

ROS   Reactive oxygen species

RT   Radiotherapy or room temperature

RT- PCR   Reverse transcriptase-PCR

RTK   Receptor tyrosine kinase

U

3′UTR   3′-untranslated region

UA   Urolithin A

UNC93B1   Unc-93 Homolog B1, TLR Signaling Regulator

V

VEGF   Vascular endothelial growth factor

S

5s rRNA   5S ribosomal RNA

S6K   S6 kinase

SAPK   Stress-activated protein kinases

SDS   Sodium dodecyl sulfate

SHP2   Src Homology Phosphatase 2

SOD   Superoxide dismutase

SSB   Single strand breaks

STAT1   Signal transducer and activator of transcription 1

STIM   Stromal interaction molecule 1

T

TNFs,   Tumor necrosis factor

TRIF   TIR-domain-containing adapter-inducing interferon-β

TLRs   Toll-like receptors

Th1   T helper type 1

TEMED   Tetramethylethylenediamine

TMRM   Tetramethylrhodamine

TIR   Toll/IL-1 receptor domain

TRAF6   Tumor necrosis factor receptor-associated factor 6

TGFs   Transforming growth factor

TSC 1/2   tuberous sclerosis complex

1 INTRODUCTION

1.1 Innate immunity and inflammation

The human body is populated with various microorganisms. Despite constant exposure to a large variety of microorganisms, the host immune system prevents the invasion of microbes. The human immune system is a critical subsystem of the body, performing many different roles and consists of the innate and adaptive immune systems (Chaplin 2010, Hirayama, Iida et al. 2017). The innate immune system is native and unique to humans and forms the first line of defense during infection and therefore plays a crucial role in the early recognition and subsequent triggering of a pro-inflammatory response to invading pathogens (Medzhitov, Preston-Hurlburt et al. 1997, Takeda and Akira 2005). On the other hand, the adaptive immune system is responsible for elimination of pathogens in the late phase of infection and in the generation of immunological memory (Iwasaki and Medzhitov 2004). Furthermore, in the adaptive immune system, antigen-specific T cells and B cells function to remove pathogens by cytotoxic reaction or producing antigen-specific antibodies, respectively. When the innate immune system is unable to destroy the pathogens completely, the adaptive immune system is activated (Hirayama, Iida et al. 2017). This shows the very close relationship of the two arms of the immune system, the innate and the adaptive arm, and it seems that nearly every aspect of the adaptive immune response is regulated and controlled by the innate immune system (Janeway 1989, Chaplin 2010).

Inflammation is a defense mechanism in which the immune system response to harmful stimuli, such as pathogens, damaged cells, toxic compounds, or irradiation (Takeuchi and Akira 2010, Mantovani, Biswas et al. 2013), and acts by eliminating injurious stimuli and initiating the healing process (Ferrero-Miliani, Nielsen et al. 2007, Nathan and Ding 2010). During the acute inflammatory responses, cellular and molecular events and interactions effectively decrease impending injury or infection. This mitigation process contributes to recovery of tissue homeostasis and resolution of the acute inflammation (Chertov, Yang et al. 2000, Ferrero-Miliani, Nielsen et al. 2007). However, uncontrolled acute inflammation may become chronic and lead to a variety of chronic inflammatory diseases such as cardiovascular (CVD) and bowel diseases (IBD), diabetes, arthritis, and cancer (Libby 2007, Zhou, Hong et al. 2016). Accordingly, macrophages play a key role in the initiation, maintenance, and resolution of inflammation. Macrophages perform three distinct functions during inflammation: antigen presentation, phagocytosis, and immunomodulation via production of various cytokines and growth factors (Fujiwara and Kobayashi 2005).

The inflammatory response is the coordination of signalling pathways that monitor inflammatory mediator levels in resident tissue cells and inflammatory cells recruited from the blood (Lawrence 2009). Inflammatory processes rely on the precise nature of the initial stimulus and its location in the body. However, they all share a common mechanism starting with recognition of damaging stimuli through cell surface pattern recognition receptors (PRR). Then, activation of

inflammatory pathways and followed by release of inflammatory markers. Finally, recruitment of inflammatory cells (Chen, Deng et al. 2017).

As mentioned before, the innate immune system is the first line of defense against invading pathogens, and inflammation is the defense mechanism of the immune system against harmful stimuli. In this context, the biological role of macrophages, as a prominent innate immune cell, in the regulation of inflammatory responses will be introduced. Firstly, the role of pattern recognition system, especially, pattern recognition receptors (PRRs) and toll like receptors (TLRs) in macrophages will be mentioned.

1.1.1 Pattern recognition receptors

Macrophages are an important component of the innate immune response, with a prominent role in host defense and clearance of foreign microorganisms (Mantovani, Sozzani et al. 2002). These cells express pattern recognition receptors (PRRs) for the initial detection of microbes. PRRs recognize microbe-specific molecular signatures known as pathogen-associated molecular patterns (PAMPs) as well as self-derived molecules derived from damaged cells regardless of the presence of a pathogenic infection, referred as damage associated molecular patterns (DAMPs) (Mogensen 2009, Hirayama, Iida et al. 2017).

PRRs activate downstream signalling pathways that lead to the induction of innate immune responses by producing inflammatory cytokines, type I interferon (IFN), and other mediators. These processes not only trigger immediate host defensive responses such as inflammation, but also prime and orchestrate antigen-specific adaptive immune responses (Charles A. Janeway and Medzhitov 2002). These responses are essential for the clearance of infectious microbes as well as crucial for the consequent instruction of antigen-specific adaptive immune responses (Kawasaki and Kawai 2014). Mammalian cells express five distinct families of PRRs, including Toll-like receptors (TLRs), RIG-I-like receptors (RLRs), NOD-like receptors (NLRs), C-type lectin-like receptors (CLRs) and cytosolic DNA sensors (Akira, Uematsu et al. 2006, Newton and Dixit 2012, Cai, Chiu et al. 2014). TLRs are the most well-studied of the known PRRs (Yamamoto and Takeda 2010). TLRs participate in the activation of the inflammatory response (Janeway and Medzhitov 2002). Thus, TLRs (especially, TLR2 and TLR4) are described in more detail.

1.1.1.1 Toll like receptors

Toll-like receptors (TLRs) were the first PRRs found in mammals. They play a crucial role in recognizing host cells and responding to microbial pathogens. The discovery of the Toll gene in the Drosophila fruit fly by Nusslein-Volhard and colleagues (Nüsslein-Volhard, Lohs-Schardin et al. 1980), opened a path towards the elucidation of recognition mechanisms by innate immunity cells against microbial components (Lemaitre, Nicolas et al. 1996, Hirayama, Iida et al. 2017). TLRs were discovered by Jules Hoffmann and Bruce Beutler, who, together with Ralph Steinman who discovered the Dendritic cell and get 2011 Nobel Prize in physiology and medicine (O'Neill, Golenbock et al. 2013).

The family of TLRs comprises 10 members of TLRs in human and 13 in mouse. TLRs are localized either to the cell surface (i.e. TLR1, TLR2, TLR4, TLR5, TLR6, and TLR10) or to intracellular compartments (i.e. TLR3, TLR7, TLR8, TLR9, TLR11, TLR12, and TLR13) such as the ER, endosome and lysosome (Kawai and Akira 2010, Celhar, Magalhães et al. 2012).

Each TLR is composed of an ectodomain with leucine-rich repeats (LRRs) that mediate PAMPs recognition, a transmembrane domain, and a cytoplasmic Toll/IL-1 receptor (TIR) domain that initiates downstream signalling (Figure 1). The ectodomain displays a horseshoe-like structure, and TLRs interact with their respective PAMPs or DAMPs as a homo- or heterodimer along with a co-receptor or accessory molecule (Botos, Segal et al. 2011).
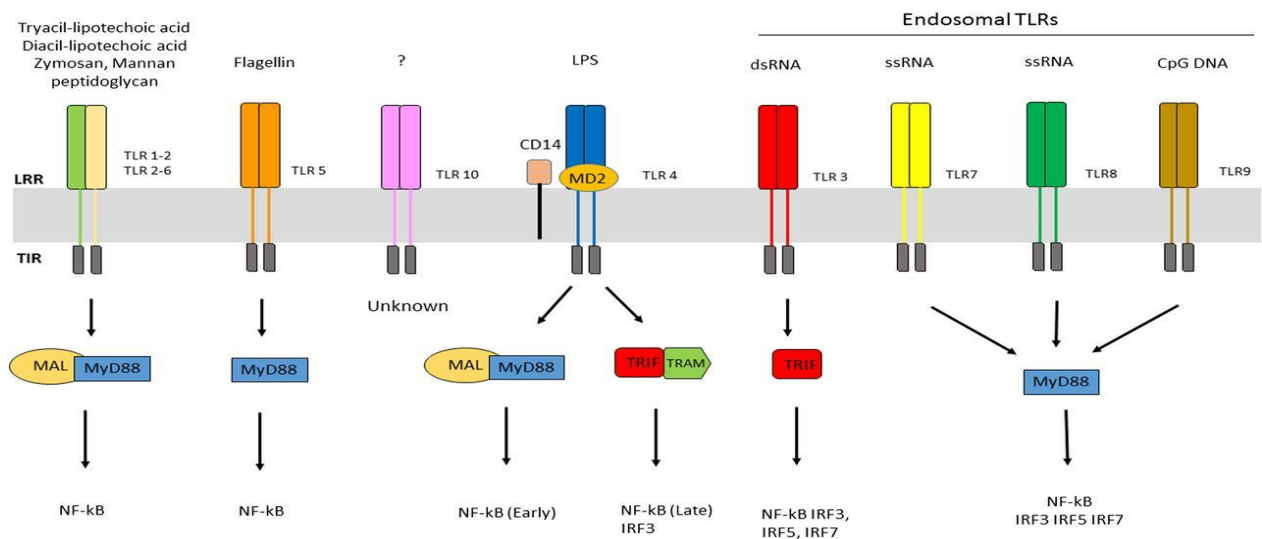
Figure 1 Toll-like receptors and their ligands

Distinct TLRs discriminate between different microbial patterns. The extracellular LRR domain of each TLR is involved in identification of its unique microbial ligand, where the intracellular TIR domain is used for the assembly of adaptor protein complexes. All TLRs, with the exception of TLR3, use MyD88 to activate downstream signaling pathways. In certain cases (as TLR2/6, TLR2/1, and TLR4), the MAL adaptor protein mediates the interaction between TLRs and MyD88. TLR3 and TLR4 use TRIF to transmit the downstream signal. In addition, TLR4 recruits TRAM as bridge. TLR4 is the only receptor that uses all four adaptors. The figure is used after permission from (Crifo and Taylor 2016).

TLRs recognize various kinds of components derived from bacteria or viruses (such as lipid, lipoprotein, protein, and nucleic acid) as ligands. Lipopolysaccharide (LPS), which is a component of the cell wall of Gram-negative bacteria, is recognized by the TLR4-MD2 complex, and bacterial lipopeptides and peptidoglycans are recognized by heterodimeric TLR2/TLR1 and TLR2/TLR6. In addition, nucleic acids such as bacterial genomic DNA or viral RNA can be recognized by TLR3, TLR7, TLR8, and TLR9, which develop in the phagosome (Kawai and Akira 2011, Hirayama, Iida et al. 2017).

All TLRs are synthesized in the ER then traffic to the Golgi and are recruited either to the cell surface or the intracellular compartments such as endosomes. The intracellular localization of

TLRs is thought to be important for ligand recognition as well as for preventing TLRs from coming into contact with self-nucleic acids that may induce autoimmunity (Tabeta, Hoebe et al. 2006, Lee, Moon et al. 2013). Noteworthy, the trafficking of intracellular TLRs from the ER to endosomes is regulated by the multi-pass transmembrane protein UNC93B1 (Lee, Moon et al. 2013).

Accumulative studies have revealed that Toll/TLRs carry out previously unanticipated functions in development, regulating cell fate, cell number, neural circuit connectivity and synaptogenesis. Furthermore, knowledge of their molecular mechanisms of action is expanding and has highlighted that Toll/TLRs function beyond the canonical NF-κB pathway to regulate cell-to-cell communication and signalling at the synapse (Anthoney, Foldi et al. 2018).

1.1.2 Inflammatory cytokines

Cytokines are small secreted proteins primarily released from immune cells, including monocytes and macrophages. Pro- and anti-inflammatory cytokines promote and inhibit inflammation, respectively (Turner, Nedjai et al. 2014). Cytokines modulate the immune response to infection or inflammation and regulate inflammation itself through a complex network of interactions. However, excessive inflammatory cytokine production can lead to tissue damage, hemodynamic changes, organ failure, and ultimately death (Czaja 2014, Liu, Wang et al. 2016). Inflammatory cytokines are classified as interleukins, colony stimulating factors (CSF), IFNs, TNFs, TGFs, and chemokines, and are produced by cells primarily to recruit leukocytes to the site of infection or injury (Turner, Nedjai et al. 2014). Importantly, a better understanding of how to regulate cytokine pathways would allow for more accurate identification of agent-mediated inflammation and the treatment of inflammatory diseases (Turner, Nedjai et al. 2014).

1.1.3 Macrophages

Monocytes/Macrophages are leukocytes which are characterised by their location, morphology, and as well as by their gene expression profile (Wynn, Chawla et al. 2013, Sica, Erreni et al. 2015). Macrophages were first described in sea stars by the Russian pathologist Elie Metchnikoff, the father of cellular immunology, who introduced the term "macrophage" that means "macro = big and phage = eater" (Metchnikoff 1893, Metchnikoff 1905, Divangahi, King et al. 2015). Blood monocytes and tissue macrophages possess various properties, but they adapt easily upon entering different tissue microenvironments, where they contribute to the general needs as well as specialized functions of individual organs (Epelman, Lavine et al. 2014, Gordon 2016). Macrophages induce an efficient and balanced inflammatory response through four orderly stages: 1) pathogens recognition by PRRs; 2) eradication of invading agents; 3) resolution of inflammation through the involvement of suppressing cells and the release of anti-inflammatory markers; 4) tissue repair and restoration of tissue homeostasis (Chen, Deng et al. 2017, Curtale, Rubino et al. 2019).

1.1.3.1 Macrophage origin

Macrophages are professional phagocytes belonging to the mononuclear phagocyte system (MPS) which includes monocyte and dendritic cells (DCs) (Ginhoux and Guilliams 2016, Orecchioni, Ghosheh et al. 2019). Their origin has been debated extensively in recent years. Van Furth et al. proposed that tissue-resident macrophages are continuously repopulated by blood-circulating monocytes, which arise from adult bone marrow progenitors (van Furth and Cohn 1968). Subsequently, several techniques have been developed to classify macrophage subsets, including flow cytometry, DNA microarray analysis, and lineage analysis using genetically modified mice. These scientific advances have revealed many facts: (1) almost all microglia in the central nervous system (CNS) are originated from the embryonic yolk sac and are preserved throughout life; (2) in the intestinal tract, macrophages derived from the embryonic yolk sac are replaced with macrophages from bone marrow monocytes immediately after birth; and (3) macrophages derived from the fetal liver are dominant in most tissues except the central nervous system and intestinal tract (Takahashi, Yamamura et al. 1989, Ginhoux and Guilliams 2016).

Gorden and Martinez-Pomaares indicated that macrophages are present in mammals from midgestation and contributing to physiologic homeostasis throughout life. Macrophages develop from yolk sac and fetal liver progenitors during embryonic development in the mouse and persist in different organs as heterogeneous, self-renewing tissue-resident populations. Bone marrow-derived monocytes are recruited after birth to replenish tissue-resident populations and to meet additional demands during inflammation, infection and metabolic perturbations. Macrophages of mixed origin and different locations vary in replication and turnover, but both are active in mRNA and protein synthesis, fulfilling organ-specific and systemic trophic functions, in addition to host defense (Gordon and Martinez-Pomares 2017).

1.1.3.2 Tissue distribution of macrophages

Macrophages are strategically positioned throughout the body tissues and constitute a dispersed organ system in the body (Figure 2)(Gordon and Martinez-Pomares 2017). Macrophages that reside in different tissues are known by different names, such as microglia in central nervous system (CNS), Kupffer cells (liver), Langerhans cells (skin), osteoclasts (bone), alveolar macrophages (lung) or histocytes (spleen) (Varol, Mildner et al. 2015, Ginhoux and Guilliams 2016).

Intestines are inhabited by various types of macrophages that have distinct phenotypes and functions, but work together to maintain tolerance to normal gut flora and orally administer antigens (Davies, Jenkins et al. 2013, Varol, Mildner et al. 2015). Secondary lymphoid organs also have distinct populations of macrophages, including marginal zone macrophages (spleen), which suppress innate and adaptive immunity to apoptotic cells, and sub-capsular sinus macrophages (lymph nodes), which clear viruses from the lymph and trigger anti-viral immune responses. Various macrophages reside in immune-privileged sites, such as the brain, eye, and testes, which have a vital role in tissue remodeling and homeostasis. These tissue-specific

macrophages orchestrate inflammatory processes and recruit additional macrophages on demand (Davies, Jenkins et al. 2013, Varol, Mildner et al. 2015). The distributions of macrophages in different tissues of the body as well as related homeostatic function are summarized in (Figure 2).
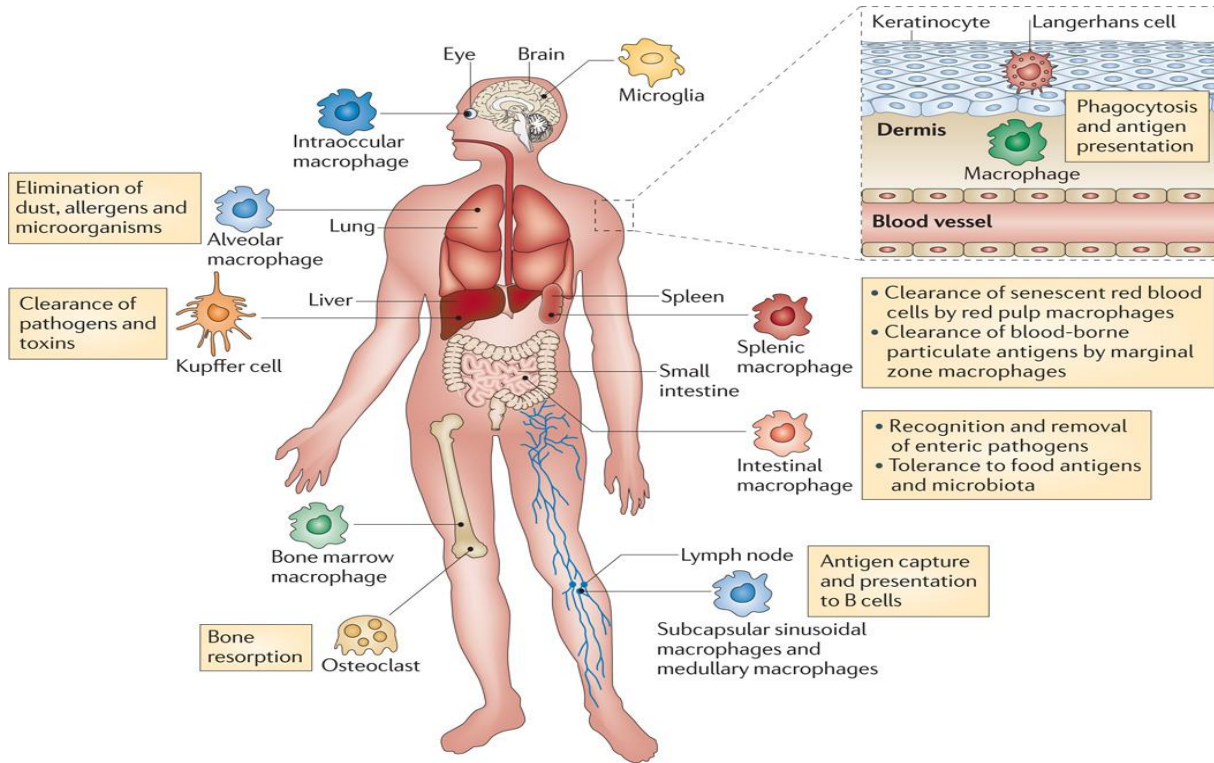
Figure 2 Tissue distribution of macrophages performs crucial homeostatic functions

Mononuclear phagocytes are generated from committed haematopoietic stem cells located in the bone marrow. Macrophage precursors are released into the circulation as monocytes and quickly migrate into nearly all tissues of the body, where they differentiate into mature macrophages. Different populations of mature tissue macrophages are strategically located throughout the body and perform important immune surveillance activities, including phagocytosis, antigen presentation and immune suppression. The figure is used after permission from (Murray and Wynn 2011).

1.1.3.3 Macrophage function (multi-role immune cell)

Macrophages are relatively long-lived cells with multiple important functions. One is to eliminate invading microorganisms by phagocytosis. Another crucial role of macrophages is to regulate adaptive immune responses to various pathogens through antigen processing and presentation by displaying processed antigens in association with major histocompatibility complex (MHC) molecules. They would either induce inflammation or repair damaged tissues by secreting different signalling proteins. In addition to these functions in the immune system, they can act as scavenger cells for clearing dead cells, cell debris, and other molecules such as cholesterol and fatty acids (Epelman, Lavine et al. 2014, Wang, Koenig et al. 2019).

Other different functions of macrophages are associated with the type of receptor interaction and the presence of cytokines (Epelman, Lavine et al. 2014). Heterophagy refers to uptake of extracellular cargo; autophagy is well known and developed in macrophages (Deretic 2016). In addition, they are able to detect and respond to the presence of microbial constituents, including RNA and DNA, within their cytoplasm, activating intracellular inflammasome (Guo, Callaway et al. 2015, Gordon 2016), caspase processing and release of IL-1β (Vieira, Botelho et al. 2002, Jaumouillé and Grinstein 2016). In addition, macrophages play important roles in the progression of inflammatory diseases, such as diabetes (Ehses, Böni-Schnetzler et al. 2008, Meshkani and Vakili 2016), cancer (Sica, Allavena et al. 2008, Ruffell and Coussens 2015), and atherosclerosis (Woollard and Geissmann 2010, Tabas and Bornfeldt 2016).

1.1.3.4 Macrophage plasticity and polarization

Macrophages possess a repertoire of cell surface receptors, intracellular mediators, and essential secretory molecules for recognition, engulfment, and destruction of invading pathogens as well as regulation of other types of immune cells and serve as a sentinel of the immune system, sensing the existence of pathogens through the membrane anchored and cytosolic detectors.

Macrophages participate in the inflammatory process by adapting their functional phenotype according to micro-environmental stimuli (Mantovani, Sica et al. 2004, Shapouri-Moghaddam, Mohammadian et al. 2018, Curtale, Rubino et al. 2019). Their plasticity, change from one phenotype to another, confers them the ability to organize host defense mechanisms to eliminate the pathogen and restore homeostasis in the host tissues (Aderem 2003, Mantovani, Sica et al. 2004, Mohammadi, Blesso et al. 2019).

Macrophages can be polarized into classically activated or pro-inflammatory (M1) and alternatively activated or anti-inflammatory (M2) macrophages. M2 macrophages are divided into M2a, M2b, M2c, and M2d subcategories. This phenomenon of the two different M1/M2 phenotypes is referred to term "macrophage polarization" (Cassetta, Cassol et al. 2011, Shapouri-Moghaddam, Mohammadian et al. 2018). Macrophage polarization is essential for tissue repairing and maintenance of homeostasis (Patel, Banerjee et al. 2019). Therefore, several classes of macrophages have been identified in human and mice based on the expression of their cell surface markers, production of specific factors and biological activities.

1.1.3.5 Classical activation (M1)

M1 macrophages are aggressive and highly phagocytic. They produce large amounts of reactive oxygen species (ROS) and reactive nitrogen species (RNS). They are typically induced by bacterial lipopolysaccharide (LPS) or Th1 cytokines (such as IFN-γ and TNF-α). M1 macrophages are characterized by TLR2, TLR4, CD80, CD86, iNOS, and MHC-II surface expression. These macrophages produce high levels of pro-inflammatory cytokines as TNF-α, IL-1α, IL-1β, IL-6, IL-12, IL-23 and cyclooxygenase-2 (COX-2) (Figure 3), and low levels of IL-10 (Beutler and Rietschel 2003, Shapouri-Moghaddam, Mohammadian et al. 2018, Mohammadi, Blesso et al. 2019).

Key transcription factors, such as NF-κB, STAT1, STAT5, IRF3, and IRF5 have been shown to regulate the expression of M1 specific genes. It seems that NF-κB and STAT1 signalling are the two major pathways involved in M1 macrophage polarization (Beutler and Rietschel 2003, Murray 2017).

Functionally, the M1 macrophages contribute to elimination of pathogens during infection through activation of the nicotinamide adenine dinucleotide phosphate (NADPH) oxidase system, and subsequent production of ROS. Therefore, M1 macrophages have vigorous - and anti-tumoral activity and mediate ROS-induced tissue damage, and impair tissue regeneration and wound healing. In order to provide a protection against such tissue damage, the chronic inflammatory response should be inhibited by regulatory mechanisms driven by the anti-inflammatory function of M2 macrophages (Mantovani, Sica et al. 2004, Sica, Erreni et al. 2015).

1.1.3.5.1 Alternative activation (M2)

M2 macrophages are anti-inflammatory and their polarization occurs in response to downstream signals of several cytokines such as IL-4, IL-13, IL-10, IL-33 and TGF-β (Wang, Liang et al. 2014, Hirayama, Iida et al. 2017). Notably, only IL-4 and IL-13 induce M2 macrophage activation, while other cytokines (such as IL-33 and IL-25) amplify M2 macrophage activation by producing Th2 cytokines (O'Shea and Paul 2010, Mohammadi, Blesso et al. 2019).

Key transcription factors, such as STAT6, IRF4, JMJD3, PPARδ, and PPARγ have been shown to regulate the expression of M2 specific genes. To date, the STAT6 pathway has been considered to be the main pathway to activate M2 macrophages (Martinez and Gordon 2014).

Functionally, M2 macrophages possess potent phagocytosis capacity, scavenge debris and apoptotic cells, promote tissue repair and wound healing, and have pro-angiogenic and pro-fibrotic properties (Kurowska-Stolarska, Stolarski et al. 2009, Sica and Mantovani 2012, Braga, Agudelo et al. 2015). Therefore, M2 macrophages take part in Th2 responses and parasite clearance (Chua, Brown et al. 2013), dampening of inflammation, orchestrate the promotion of tissue remodeling (Hinz, Phan et al. 2012, Mantovani, Biswas et al. 2013), angiogenesis, immunoregulation, tumor formation, and progression (Qian and Pollard 2010, Belgiovine, D'Incalci et al. 2016). (Figure 3) clarifies the main differences between M1 and M2 macrophages.

According to the activating stimulus, M2 macrophages are sub-grouped into M2a, M2b, M2c, and M2d (Martinez, Sica et al. 2008, Chistiakov, Bobryshev et al. 2015). **M2a** macrophages are activated by IL-4 or IL-13 and produce high levels of IL-10, TGF-β and CD206 expression. These macrophages enhance the endocytic activity, promote cell growth and tissue repairing (Martinez, Sica et al. 2008, Chistiakov, Bobryshev et al. 2015, Wang, Zhang et al. 2019).

M2b macrophages are activated by immune complexes, TLR ligands and IL-1β and release both pro-and anti-inflammatory cytokines, such as TNF-α, IL-1β, IL-6, and IL-10. Based on the expression profiles of cytokines and chemokines, M2b macrophages regulate the breadth and depth of immune responses and inflammatory reactions (Chistiakov, Bobryshev et al. 2015, Wang, Zhang et al. 2019).

M2c macrophages, also known as inactivated macrophages, are induced by glucocorticoids, IL-10 and TGF-β. These cells strongly exhibit anti-inflammatory activities against apoptotic cells by releasing high amounts of IL-10 and TGF-β, CCL16, and CCL18 (Martinez, Sica et al. 2008, Zizzo, Hilliard et al. 2012, Chistiakov, Bobryshev et al. 2015).

M2d macrophages**,** finally, are induced by TLR antagonists through adenosine receptor. Activation of adenosine receptor is followed by suppression of the production of pro-inflammatory cytokines and induction of secretion of anti-inflammatory cytokines (IL-10 high & IL-12 low), release of vascular endothelial growth factor (VEGF) and promote angiogenesis and tumor progression (Ferrante, Pinhal-Enfield et al. 2013, Chistiakov, Bobryshev et al. 2015). The characteristics of the M2 subtypes are summarized in (Figure 3).
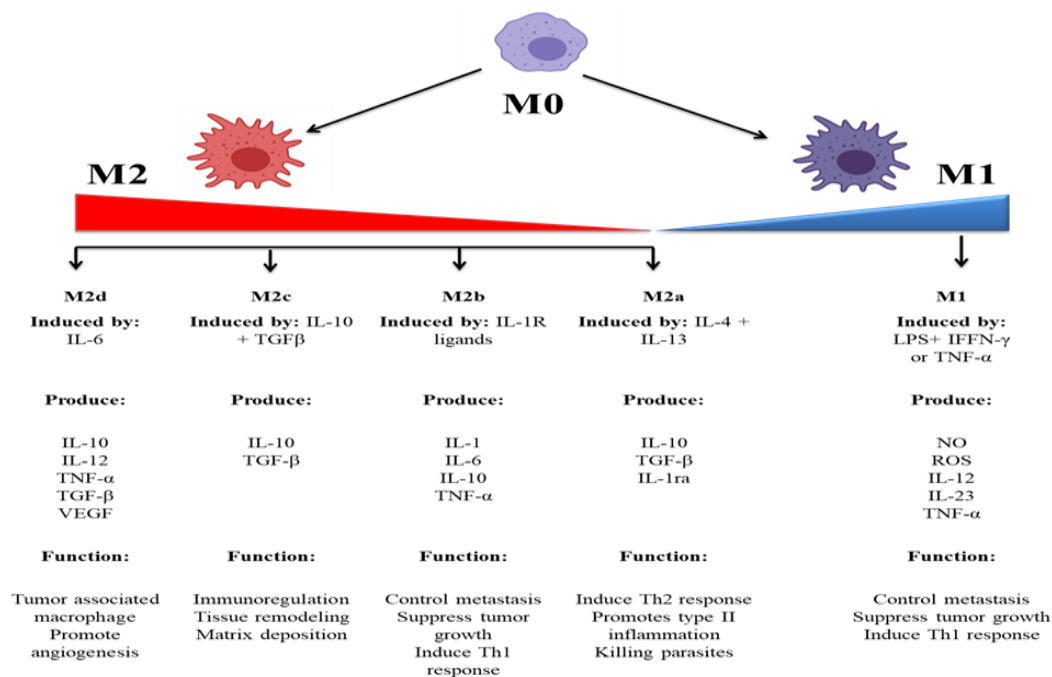
Figure 3 Macrophage polarization

Macrophage polarization to M1 (pro-inflammatory) and M2 (anti-inflammatory). M2 macrophages are subdivided into M2a, M2b, M2c, and M2d. See text for details. The figure adapted from (Weagel, Smith et al. 2015), changed.

1.1.4 MicroRNAs modulate immune responses in macrophages

MicroRNAs (miRNAs) are small single stranded non-encoding RNA molecules containing ~ 22 nucleotides. MicroRNAs induce gene silencing by modulating gene regulation at the post-transcriptional level through binding to the 3′-untranslated region (3′UTR) of target mRNA especially in immune cells as monocytes and macrophages (Liu and Abraham 2013, Wei and Schober 2016). Initial studies showed microRNA's ability to modulate the magnitude of the

innate immune response, participating as integral components of feedback loop regulatory mechanisms, which significantly shape the inflammatory response. Moreover, recent studies have also outlined their role in tuning macrophage differentiation, infiltration and polarization. In particular, a complex and highly controlled network of miRNAs are used to regulate inflammatory pathways by targeting multiple component of the TLR signalling pathway (Liu and Abraham 2013, Curtale, Renzi et al. 2018). Zhang et al. identified 109 miRNAs differentially expressed in human and murine M1- and M2-polarized macrophages, focusing particularly on miR-155, miR-181, and miR-451 in M1 macrophages, and miR-146a, miR-125a, and miR-145-5p in M2 macrophages (Zhang, Zhang et al. 2013).

1.1.4.1 The miRNAs involved in regulation of M1 polarization

Thulin et al. demonstrated that miR-9 stimulated M1 polarization by targeting peroxisome proliferator-activated receptor δ (PPARδ). The relative expression levels of miR-9 have been increased, while PPARδ levels have been decreased in primary human monocytes following exposure to LPS (Thulin, Wei et al. 2013). Interestingly, miR-155 was not only an M1 phenotypic marker, but also played a role in driving macrophage polarization as its inhibition resulted in impaired M1 polarization and its overexpression caused a re-polarization towards an M1 phenotype of M2- macrophages (Cai, Yin et al. 2012).

Taken together, miR-9 (Thulin, Wei et al. 2013), miR-127 (Ying, Kang et al. 2015), miR-155 (O'Connell, Taganov et al. 2007, Xu, Kang et al. 2013) and miR-125b (Chaudhuri, So et al. 2011) were shown to promote classical activation of macrophages (M1) and pro-inflammatory responses through inhibiting various factors. In addition, there were observations suggesting that Akt signalling is also involved in the miR-155-mediated promotion of M1 phenotype through targeting C/EBPβ and SOCS1 (Xu, Kang et al. 2013).

1.1.4.2 The miRNAs involved in regulation of M2 polarization

The miR-146a was the first miRNA associated with M2 polarization. Enforced expression of miR-146a in peritoneal macrophages resulted in reduced expression of M1-marker genes (e.g., iNOS, CD86, TNF, IL-12 and IL-6), and increased production of M2-phenotype markers (e.g., Arg1, CCL22 and CD206).

The subsequent studies confirmed that miR-124 (Veremeyko, Siddiqui et al. 2013), miR-223 (Chen, Wang et al. 2012, Haneklaus, Gerlic et al. 2013), miR-34a (Jiang, Liu et al. 2012), let-7c (Banerjee, Cui et al. 2013, Zhang, Liu et al. 2015), miR-132 (Liu, Li et al. 2015), miR-146a (Taganov, Boldin et al. 2006, Vergadi, Vaporidi et al. 2014) and miR-125a-5p (Banerjee, Cui et al. 2013) promote anti-inflammatory responses and M2 polarization in macrophages.

Finally, miRNAs play a critical role in many aspects of macrophage biology and can become an effective therapeutic strategy for macrophage-mediated immune diseases through modification of oligonucleotides (Rossato, Curtale et al. 2012, Curtale, Renzi et al. 2018). Unfortunately, the miRNAs specific networks are only poorly understood, making the drug development difficult.

Moreover, designing carriers to deliver miRNAs in a macrophage-specific manner could greatly increase potential applications of miRNA-based therapeutic strategies (Shapouri-Moghaddam, Mohammadian et al. 2018).

1.1.5 TLR signalling in innate immune response (activated macrophage)

Once macrophage recognize PAMPs and DAMPS, they can be activated to an inflammation promoting phenotype through members of the TLR family such as TLR4 (Kollmann, Levy et al. 2012, Nonnenmacher and Hiller 2018). TLRs recruit Toll/interleukin-1 receptor (TIR)-domain-containing adaptor proteins such as myeloid differentiation primary response 88 (MyD88) and TIR-domain-containing adapter-inducing interferon-β (TRIF), which initiate specific intracellular signalling pathways including MAPKs and NF-κB (Figure 4) (Vergadi, Ieronymaki et al. 2017, Wang, Pan et al. 2018).

Although TLR4 is the principal TLR species involved in LPS signalling, recent studies indicate that TLR2 is the primary signal transducing molecule for LPS from certain non enterobacterial Gram-negative organisms, including *Porphyromonas gingivalis* (Hirschfeld, Weis et al. 2001) and *Leptospira interrogans* (Werts, Tapping et al. 2001). TLR1 has also been implicated as a co-receptor for TLR2 as its co-expression in transfected cells augmented the TLR4-independent response to LPS of *Escherichia coli* and *Neisseria meningitidis* lipooligosaccharides (Wyllie, Kiss-Toth et al. 2000). However, TLR2 is best recognized as the predominant signal transducing molecule for diverse bacterial lipoproteins and the synthetic lipopeptides, Pam3Cys (Akira, Takeda et al. 2001).
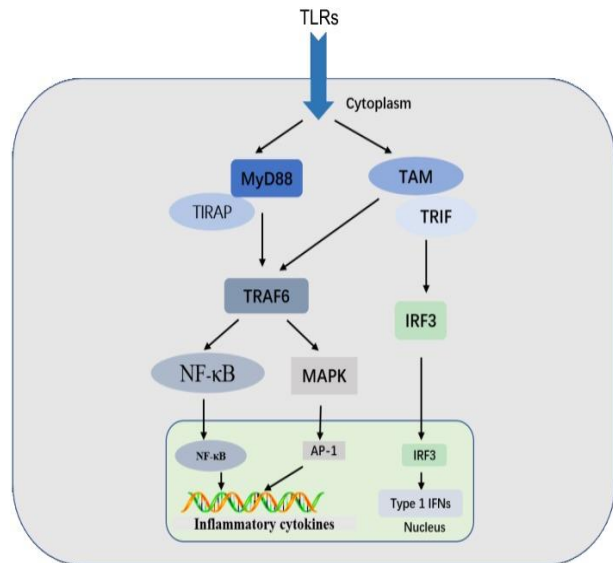
Figure 4 MyD88 and TRIF-dependent TLR signalling pathways

Signalling through TLRs activates intracellular signalling cascades that lead to nuclear translocation of AP-1 and NF-κB or IRF3, which regulate the inflammatory responses. The figure is used after permission from (Chen, Deng et al. 2017).

1.1.6 Mitochondria membrane potential regulates macrophage immune response

The crucial role of mitochondria in immune signaling and in innate immune response fits the function of this organelle in cell death and signaling. In fact, mitochondria might have a role as "signaling hubs", which can influence the phenotype of immune cells and possibly of other cell types (i.e., T and B lymphocytes and other circulating cells) to respond to infections (Angelini 2017, Ramond, Jamet et al. 2019). Interestingly, macrophages play a unique role in phagocytosis

and clearance of pathogens. This includes the secretion of anti-microbial effectors such as ROS, NO, proton generation, anti-microbial peptides, and the establishment of a deleterious nutritive environment (Weiss and Schaible 2015). In this context, bacteria have developed many tricks to subvert the intracellular environment and turn it beneficial for their own purpose, notably by altering mitochondrial integrity and function to influence energy generation, metabolism, and immune signaling (Ramond, Jamet et al. 2019).

The mitochondrial membrane potential ($\Delta\Psi$m), generated by proton pumps (Complexes I, III and IV), is an important component in energy storage process during oxidative phosphorylation. Together with the proton gradient (ΔpH), $\Delta\Psi$m forms the transmembrane potential of hydrogen ions which is utilized to make ATP. The levels of $\Delta\Psi$m and ATP in the cell are kept relatively stable although there are small fluctuations in each of these factors which may occur as a result of normal physiological activity. However, sustained changes in both factors can be deleterious. A long-lasting decrease or increase of $\Delta\Psi$m versus normal levels may induce undesired loss of cell viability. Among other factors, $\Delta\Psi$m plays a vital role in mitochondria homeostasis through selective elimination of dysfunctional mitochondria. It is also a driving force for transport of ions (other than H^+) and proteins which are required for healthy mitochondrial functioning (Zorova, Popkov et al. 2018).

1.1.7 Calcium signalling regulate macrophage immune response

Extracellular calcium influx across the plasma membrane is a major source of intracellular calcium production, which acts as a critical secondary messenger in regulating macrophage activation, such as phagosome maturation, activation of NLRP3 inflammasome, and transcriptional control of cytokines (Clapham 2007, Vogel, Schlickeiser et al. 2015). Microbial components as LPS are known to induce calcium influx in murine macrophages and thus increase the production of mediators like NO and IL-10 (Letari, Nicosia et al. 1991, Racioppi, Noeldner et al. 2012). Interestingly, intracellular calcium binds to calmodulin (CaM), activates CaM kinases, and further regulates transcriptional processes in inflammation and immunity. Calcium/ calmodulin dependent protein kinase kinase β (CaMKKβ) is a major CaM kinase activated by the increased intracellular calcium and plays a key role in calcium-mediated regulation of inflammation in innate immune cells (Racioppi, Noeldner et al. 2012).

1.1.8 Signalling pathways mediating macrophage activation

The phosphatidylinositol-3-kinase/Akt signalling pathway participates in macrophage polarization (Lim, Chung et al. 2017, Yu, Gao et al. 2019), while MAPKs, including extracellular signal-related kinase (ERK)-1/2, p38 and c-Jun NH2-terminal kinase (JNK), and NF-κB are signals related to classic inflammation and induce the expression of pro-inflammatory mediators (Sica and Mantovani 2012, Wang, Liu et al. 2017).

1.1.8.1 PI3K/AKT/mTOR signalling pathway

PI3K/Akt (Bellacosa, Staal et al. 1991) and the mammalian target of rapamycin (mTOR) (Sabers, Martin et al. 1995) are key signalling pathways that are not only regulating the survival, migration, and proliferation of macrophages, but also orchestrate the response to different metabolic and inflammatory signals (Song, Ouyang et al. 2005). They are interconnected and they could be regarded as a single, unique pathway (Porta, Paglino et al. 2014).

PI3Ks are unique members of a conserved family of intracellular lipid kinases. The PI3K/Akt pathway is activated by TLR4 and other PRR, cytokine, chemokine, and Fc receptors (Fukao and Koyasu 2003, Covarrubias, Aksoylar et al. 2015), modulating downstream signals that control cytokine production (Figure 5).

Activation of the PI3K/Akt pathway is critical in restricting pro-inflammatory and promoting anti-inflammatory responses in TLR-stimulated macrophages (López-Peláez, Soria-Castro et al. 2011), and has been considered as a negative regulator of TLR and NF-κB signalling in macrophages (Fukao and Koyasu 2003, Troutman, Bazan et al. 2012). The different functions of AKT in regulation of macrophage biology are summarized in (Figure 5).
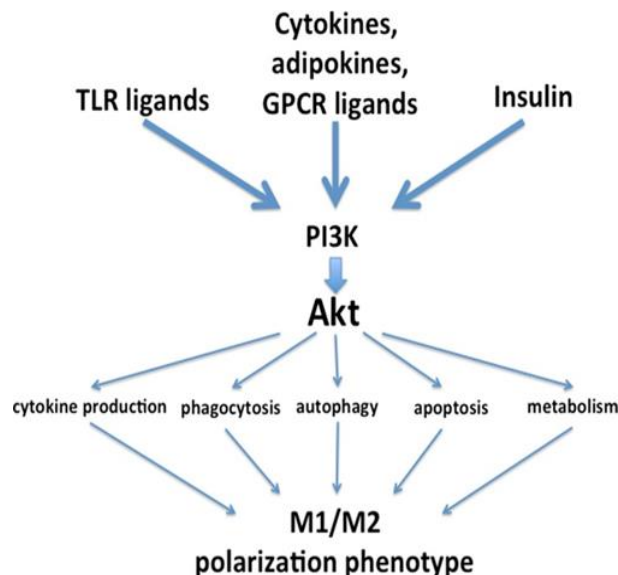
Figure 5 PI3K/AKT signalling regulate macrophage biology

Akt signalling converge extracellular signals to regulate macrophage biology and M1/M2 polarization. The figure used after permission from (Vergadi, Ieronymaki et al. 2017).

Importantly, mTOR is an evolutionarily conserved serine/threonine protein kinase that belongs to the PI3K-related kinase family (PIKK). In addition, mTOR is present in two distinct complexes inside the cells: mTOR complex 1 (mTORC1) and 2 (mTORC2). These complexes differ in their composition, mode of activation and rapamycin sensitivity, where mTORC1 is a rapamycin- and nutrient-sensitive multiprotein complex and mTORC2 is a growth factor sensitive but nutrient- and rapamycin-insensitive complex (Yang, Rudge et al. 2013, Liu, Gan et al. 2015).

Activated PI3K type I (Figure 6) phosphorylates phosphatidylinositol 4,5-bisphosphate (PIP2) to generate phosphatidylinositol 3,4,5-triphosphate (PIP3) (Vanhaesebroeck, Guillermet-Guibert et al. 2010, Thorpe, Yuzugullu et al. 2015) at the plasma membrane; PIP3, acts as a lipid secondary messenger, further recruits Akt and the mechanistic target of rapamycin complex (mTORC) 2, and facilitates Akt activation by mTORC2 (Song, Ouyang et al. 2005, Covarrubias, Aksoylar et al. 2015). Upon activation of the serine/threonine kinase Akt (Figure 6), also known as protein kinase B, subsequently phosphorylates and inactivates the tuberous sclerosis complex (TSC) 1/2. Inhibition of TSC1/2 by Akt leads to mTORC1 activation via Ras homolog (termed Rheb) suppression (Troutman, Bazan et al. 2012, Covarrubias, Aksoylar et al. 2015). Upon activation, mTORC1 regulates many cellular functions, such as cell growth, protein synthesis and autophagy via S6 kinase (S6K; RPS6K), eukaryotic translation initiation factor 4E-binding protein 1 (4E-BP1; EIF4EBP1) and ULK1, respectively (Laplante and Sabatini 2012).
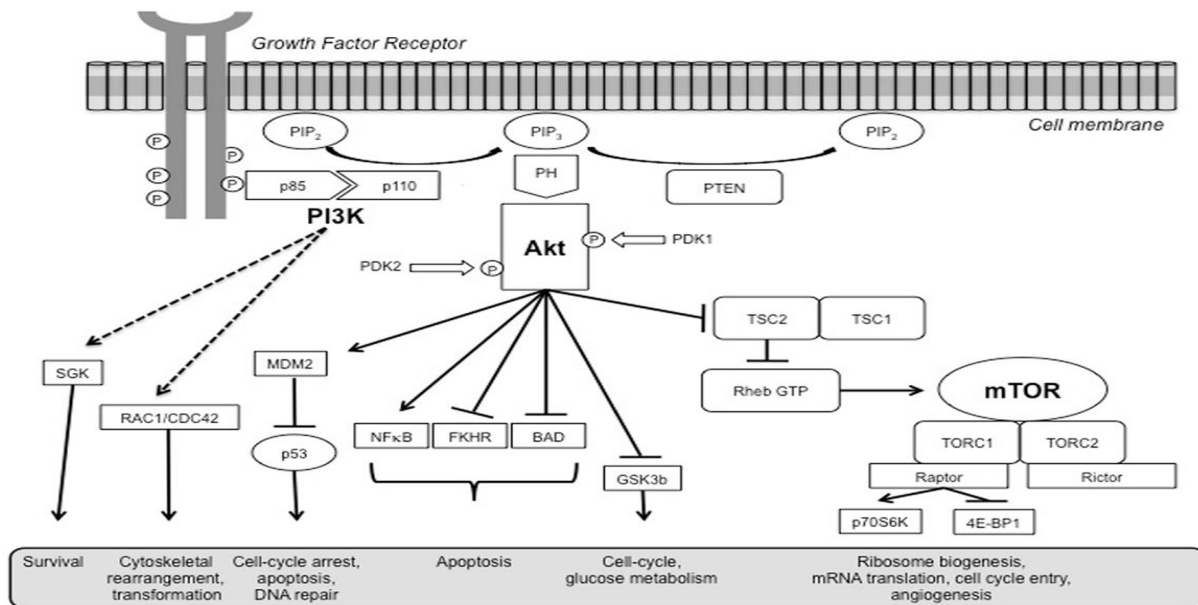
Figure 6 A schematic representation of the PI3K/Akt/mTOR pathway

PI3K/AKT/mTOR signalling consists of two parts: phosphatidylinositol 3-kinase (PI3K) and its downstream molecule serine/threonine protein kinase B (PKB; also known as AKT). The figure is used after permission from (Porta, Paglino et al. 2014).

1.1.8.2 MAPKs (Ras-Raf-MEK-ERK) signalling pathway

Mitogen-activated protein kinases (MAPKs) are protein kinases that phosphorylate their own serine/threonine residues (autophosphorylation), or those found on their substrates, either to activate or de-activate their target (Johnson and Lapadat 2002, Peti and Page 2013). MAPKs are involved in macrophage activities, including proliferation, differentiation, survival, apoptosis,

and immune responses (Kyriakis and Avruch 2001, Arthur and Ley 2013). There are three well-known MAPK pathways in mammalian cells (Figure 7): ERKs 1-4, the big MAPKs (ERK5), (JNK-1/2/3), and the isoforms of p38 MAPKs (α, β, δ, and γ) (Zhang and Liu 2002, McCain 2013). ERK, JNK, and p38 isoforms are grouped according to their activation motif, structure and function (Owens and Keyse 2007).
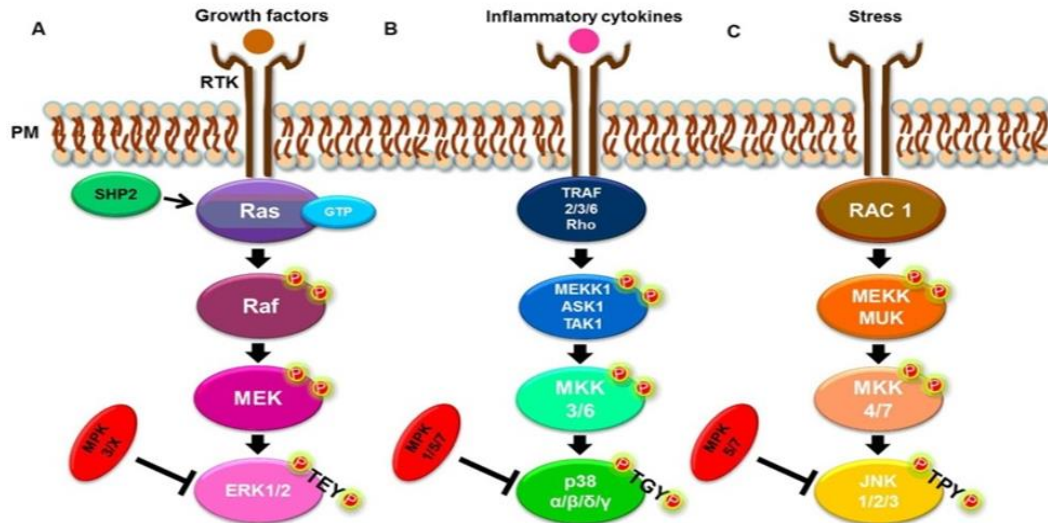
Figure 7 MAPK signalling pathway

The mammalian MAPK family includes (A) ERK1/2 pathway, (B) p38 α, β, δ, and γ pathways and (C) JNK 1, 2, and 3 pathways. This pathway mediates intracellular signaling initiated by extracellular stimuli, such as growth factors, cytokines and stress. In the Erk1/2 pathway, Erk1/2 is activated by MKK1/2, which is activated by Raf. In the p38 pathway, p38 is activated by MKK3/6, which is activated by MLK3, TAK, and DLK. In the JNK pathway, JNK is activated by MKK4/7, which is activated by MEKK1/4, ASK1, and MLK3. The figure is used after permission from (Soares-Silva, Diniz et al. 2016).

Activation of MAPK signalling pathway comprises at least three components: a MAPK, a MAPK kinase (MAPKK), and a MAPK kinase kinase (MAPKKK). The classical activation of MAPK is initiated by the binding of a ligand to a receptor tyrosine kinase (RTK) at the plasma membrane (PM), followed by activation of the small G-protein, Ras. In turn, Ras recruits and activates Raf, a MAP3K, which activates MEK, a MAP2K, that, in turn, phosphorylates the MAPK, ERK1/2, at both threonine and tyrosine residues within the TEY motif (Kolch 2000).

MKK1 and MKK2 activate ERK1/2, MKK4 and MKK7 activate JNK, and MKK3 and MKK6 activate p38. Activation of the MAPKs, including Erk1/2 and JNK leads to phosphorylation and activation of p38 transcription factors present in the cytoplasm or the nucleus, which initiates the inflammatory response (Raingeaud, Whitmarsh et al. 1996, Pearson, Robinson et al. 2001). In addition, the tyrosine phosphatase, SHP2, also acts on this signalling pathway by activating the G-protein, Ras (Zhang, Yang et al. 2004, Matozaki, Murata et al. 2009).

1.1.8.3 NF-κB signalling pathway

The transcription factor nuclear factor-κB (NF-κB) regulates multiple aspects of innate and adaptive immune functions and plays a vital role in orchestrating the inflammatory response to pathogens in macrophages and other innate immune cells (Figure 8). NF-κB induces the expression of different pro-inflammatory genes, including those encoding for cytokines and chemokines, and also participates in inflammasome regulation (Tak and Firestein 2001, Liu, Zhang et al. 2017, Dorrington and Fraser 2019).
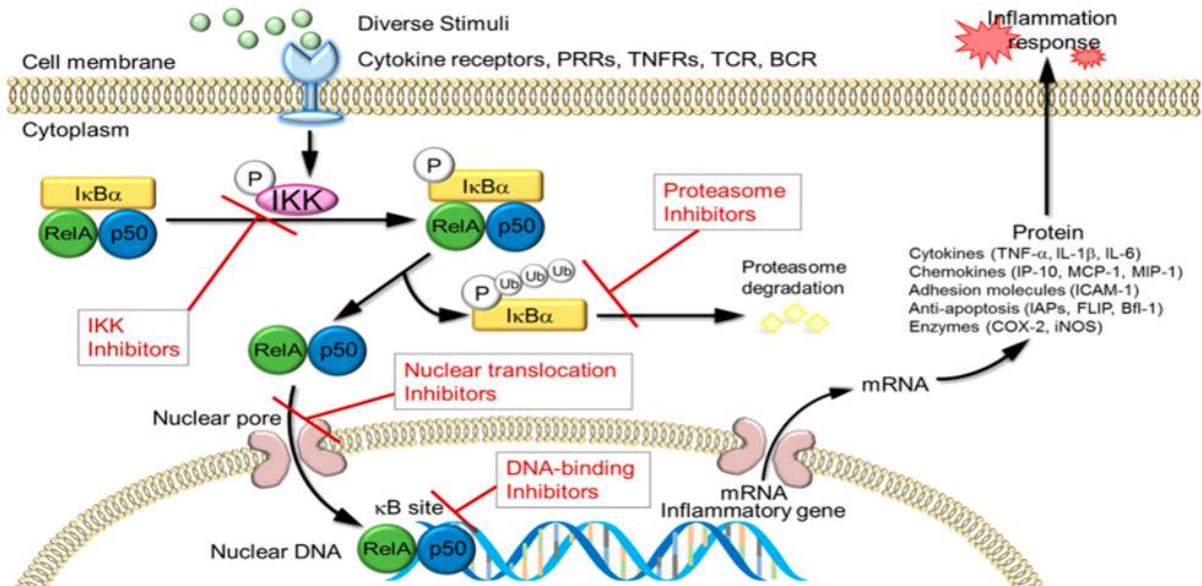
Figure 8 Role of NF-kB signalling pathway in inflammatory diseases

NF-κB signalling pathway plays a pathogenic role in various inflammatory diseases; therefore, there are many therapeutic strategies for inflammatory diseases aimed at blocking NF-κB activity. First, inhibition of IKK kinase activity preventing phosphorylation of IκBα. Second, inhibition of protease activity thereby preventing IκBα degradation. Third, inhibition of nuclear translocation through IκBα super-repressor which specifically prevents NF-κB subunits RelA, p50, c-Rel and other members from entering the nucleus. Finally, inhibition of DNA binding prevents NF-κB subunits from binding to target genes, and therefore inhibit the transcription. The figure is used after permission from (Liu, Zhang et al. 2017).

The NF-κB family includes five related transcription factors: p50, p52, RelA (p65), RelB, and c-Rel (Moynagh 2005, Sun, Chang et al. 2013). The activation of NF-κB involves two major signalling pathways, the classical (or canonical) and alternative (or non-canonical) pathways, both being important for regulating immune and inflammatory responses despite their differences in signalling mechanism (Karin 1999, Vallabhapurapu and Karin 2009, Sun 2011).

Briefly, under physiological conditions, IκB proteins, present in the cytoplasm, inhibit NF-κB (Kadhim, Tabarki et al. 2001). PRRs use similar signal transduction mechanisms to stimulate IκB kinase (IKK), which is composed of two kinase subunits (IKKα and IKKβ) and a regulatory subunit (IKKγ). IKK regulates NF-κB pathway activation by IκB phosphorylation (Lawrence

2009). Activation of IκB results in its degradation by the proteasome and the subsequent release of NF-κB for nuclear translocation and gene transcription activation (Hayden and Ghosh 2012). This pathway regulates pro-inflammatory cytokine production and inflammatory cell recruitment, which contribute to the inflammatory response. NF-κB signalling pathway provided with possible targets for blocking NF-κB activation are summarized in (Figure 8) (Liu, Zhang et al. 2017).

1.2 Lipopolysaccharides

One of the most studied bacterial surface molecules is lipopolysaccharide (LPS), which is the major component of the outer membrane of Gram-negative bacteria (Beutler and Rietschel 2003, Bertani and Ruiz 2018). Perhaps not surprisingly, LPS is an essential component of the cell envelope in most, though interestingly not all, Gram negative bacteria (Zhang, Meredith et al. 2013, Bertani and Ruiz 2018). One of the most abundant sources of LPS encountered by vertebrates is their resident gut microbiota and intestinal alkaline phosphatase detoxifies the LPS and prevents intestinal inflammation in response to the resident microbiota (Bates, Akerlund et al. 2007). Notably, the immune system greatly depends on the structure and composition of the bacterial cell surface.

1.2.1 Structure and function of LPS

In 1892, Richard Pfeiffer first defined endotoxin as a heat-stable, toxic substance that was released upon disruption of microbial envelopes (Beutler and Rietschel 2003) and based on their internal compounds it generally refers to lipopolysaccharide (LPS). This LPS is an amphiphilic molecule composed of two major components, hydrophobic lipid A which is covalently linked to a hydrophilic polysaccharide (made up of the O-specific chain, an outer core and an inner core) (Figure 9) (Bertani and Ruiz 2018). Both are important for endotoxin biological activity.

Toxicity is associated with the lipid component (Lipid A) which drives innate immune cell activation and immunogenicity is associated with the polysaccharide components (O-chain). LPS stimulates the immune responses (Yu and Kanost 2004) and enhances cellular immune reactions (Rietschel, Kirikae et al. 1994, Wassenaar and Zimmermann 2018). The overall structure of LPS is conserved, but there are many variations that can occur at the species and strain level (Heinrichs, Yethon et al. 1998, Iguchi 2016).

Similarly, the lipid A structure is conserved at the species level; however, it can undergo regulated modifications in response to environmental conditions (Raetz, Reynolds et al. 2007, Scott, Oyler et al. 2017). The core oligosaccharides vary among species and even between some strains of one species (Heinrichs, Yethon et al. 1998, Klein and Raina 2015). However, the most diverse component of LPS is the O antigen (Kalynych, Morona et al. 2014, Iguchi 2016). Some Gram-negative bacteria do not synthesize this component (O antigen) of LPS (Stevenson, Neal et al. 1994, Kalynych, Morona et al. 2014). In such cases, molecules composed of only lipid A and the core oligosaccharides are typically referred to as lipooligosaccharides, or LOS. Classically, LOS has been referred to as "rough" LPS, as opposed to "smooth" LPS, which includes the O

antigen (Raetz and Whitfield 2002, Bertani and Ruiz 2018). The smooth LPS is used in this study.
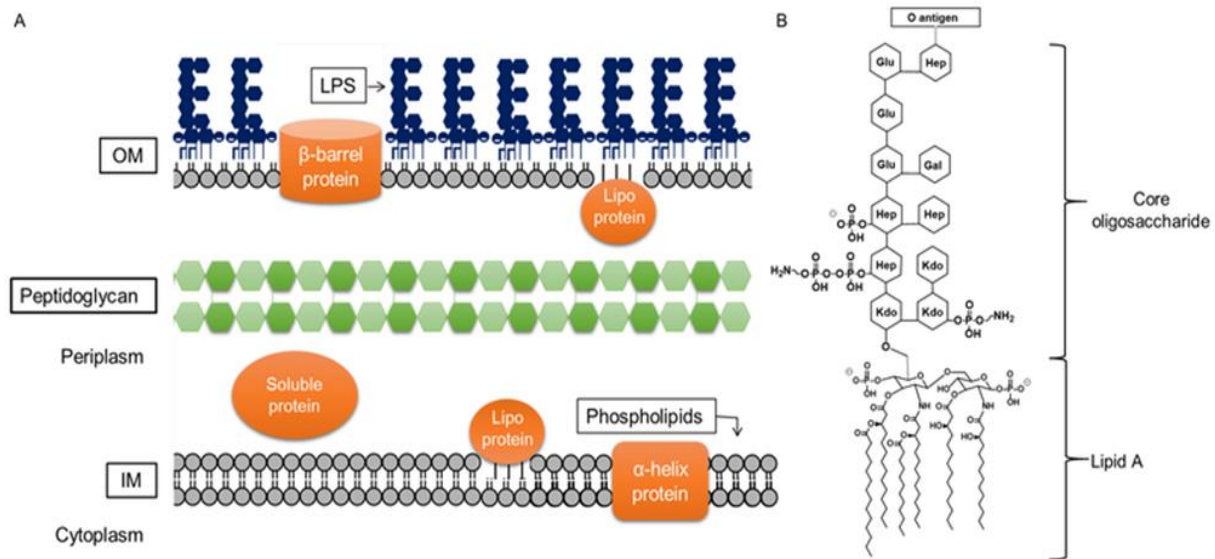
Figure 9 Architecture of the Gram-negative cell envelope

(A) Depiction of the Gram-negative cell envelope and its components. The inner membrane (IM) contains phospholipids, while the outer membrane (OM) contains phospholipids in the inner leaflet and lipopolysaccharide (LPS) in the outer leaflet. (B) Structure of prototypical LPS produced by E. coli (shown is the core structure associated with core type K-12). The figure used after permission from (Bertani and Ruiz 2018).

1.2.2 LPS signalling

As LPS decorates the surface of many bacterial pathogens, the host immune system has evolved to respond dramatically to its presence, making LPS a PAMP (Sassi, Paul et al. 2010, Needham and Trent 2013, Scott, Oyler et al. 2017). As mentioned before, the immune system has evolved to respond primarily to the most conserved feature of LPS, the lipid A structure, for which host TLR4 is the primary receptor (Sassi, Paul et al. 2010, Scott, Oyler et al. 2017). Bacterial LPS has been conventionally used to study inflammation, due to the abundance of inflammatory effects that it generates through TLR4 signalling (Takashiba, Van Dyke et al. 1999).

LPS is a potent activator of monocytes/macrophages and can induce an acute inflammatory response by triggering the release of vast number of inflammatory cytokines (such as TNF-α, IL-1β, IL-6, IL-8, IL-10, IL-12, IL-15, and TGF-β) in various cell types (Akira, Taga et al. 1993, Ngkelo, Meja et al. 2012, Tucureanu, Rebleanu et al. 2017). Cellular activation triggered by LPS requires extracellular proteins, including LPS binding protein (LBP) (Morrison and Ryan 1987) and CD14, a 55-kD glycosyl-phosphatidylinositol–linked membrane protein (Kielian and Blecha 1995), which play a role in transferring LPS to a signalling complex composed of MD2 and

MyD88 (Bryant, Spring et al. 2010, Borzęcka, Płóciennikowska et al. 2013). Hence, LBP and CD14 act as amplifiers of the LPS response. Like other TLR family members, TLR4 is a type I transmembrane protein with a leucine-rich repeat (LRR)-containing extracellular domain and a toll/interleukin-1 receptor (TIR) intracellular domain (Rossol, Heine et al. 2011).

There is evidence to suggest that G proteins (Daniel-Issakani, Spiegel et al. 1989), phospholipase C (Chen, Lei et al. 1992), protein kinase A, and protein kinase C (Shapira, Takashiba et al. 1994) are involved in LPS responsiveness. Some evidence indicates that protein tyrosine kinases (PTKs) play critical roles in LPS signalling. Considerable data support the idea that within minutes of LPS stimulation monocytes/macrophages activate MAPK (Weinstein, Sanghera et al. 1992, Tucureanu, Rebleanu et al. 2017).

1.3 Radiation

All living organisms are exposed continuously to radiation. In addition to diagnostic and therapeutic medical exposures, we are exposed daily to background radiation from cosmic rays, radioactive waste, radon decay, nuclear tests, and accidents. The contribution to dose from naturally occurring radionuclides is much larger. In recent years, it has become evident that inhalation of the short-lived decay products of ^{222}Rn is one of the important sources of natural exposure (Little 2006). Interestingly, ionizing radiation (IR) is classified as either electromagnetic radiation which include X and γ rays or particulate radiation which include energetic electrons, protons, neutrons, α particles and heavy charged particles (Hall and Giaccia 2006). The diagnostic applications of IR in medicine include the use of X-rays and radioisotopes in diagnostic imaging. Natural radiation and radioactivity in the environment, along with diagnostic medical exposure, make up the very largest part of the accumulated annual dose to human beings who are not occupationally exposed to ionizing radiation from other sources during their daily work activity. Despite the vast benefits derived from various medical applications, radiation can be harmful and is well established as a carcinogen to living organisms (Little 2006).

1.3.1 Direct and indirect effects of radiation

IR can be defined as electromagnetic waves that have enough energy to liberate electrons from atoms and this loss of electrons can disrupt covalent bonds and produce ROS (Einstein 1905). There are two mechanisms by which radiation ultimately affects cells including direct and indirect effects (Figure 10).

In direct action, IR can directly hit the DNA molecule and disrupt the molecular structure that may lead to cell damage or even cell death. On the other hand, the indirect action where the radiation hits the water molecules (radiolysis), the major constituent of the cell, and other organic molecules in the cell, whereby free radicals such as hydroxyl and alkoxy are produced that may damage nucleic acids, proteins and lipids (Desouky, Ding et al. 2015). Free radicals are characterized by an unpaired electron in the structure, which is very reactive, and therefore reacts with DNA molecules to cause a molecular structural damage. Together, the direct and indirect

effects of radiation initiate a series of biochemical and molecular signaling events that can repair the damage or culminate in permanent physiological changes or cell death (Spitz, Azzam et al. 2004).
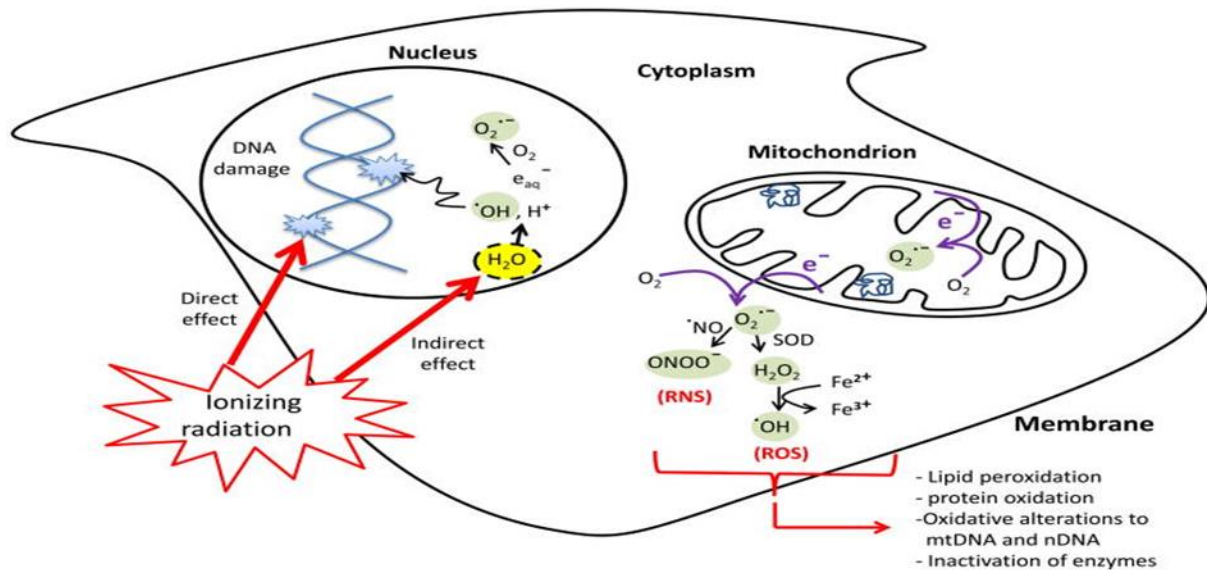
Figure 10 The direct and indirect cellular effects of ionizing radiation on macromolecule

Absorption of ionizing radiation by living cells directly disrupts atomic structures, producing chemical and biological changes and indirectly through radiolysis of cellular water and generation of reactive chemical species by stimulation of oxidases and nitric oxide synthases. Ionizing radiation may also disrupt mitochondrial functions significantly contributing to persistent alterations in lipids, proteins, nuclear DNA (nDNA) and mitochondrial DNA (mtDNA). The figure is used after permission from (Azzam, Jay-Gerin et al. 2012).

1.3.2 Immediate immunological effects of ionizing radiation

IR is able to induce an immune response that is displaced in time but also in space (i.e., abscopal effect). IR can induce inflammation in non-irradiated sites *in vivo* (Fajardo 1982, Mukherjee, Coates et al. 2014) as well as inflammatory bystander signals *in vitro* (Wright 2010, Blyth and Sykes 2011). Bystander factors are produced by irradiated cells and can activate non-irradiated cells (Mukherjee, Coates et al. 2014). It has been reported that the initial response to radiation therapy (RT) involves the recruitment of inflammatory cells at the site of injury as well as the production of DAMPs from irradiated cells (Rubin and Casarett 1968, Travis 1980, Vacchelli, Vitale et al. 2013), followed by a cascade of pro-inflammatory cytokine secretion leading to the initiation of inflammation (Vacchelli, Vitale et al. 2013). Inflammatory cytokines produced *in vivo* by irradiated cells could act as bystander factors to induce the abscopal effect (Travis 1980, Mukherjee, Coates et al. 2014, Meziani, Deutsch et al. 2018). Interestingly, upon activation, macrophages have been proposed as an important source of bystander signals *in vivo* and play a significant role in the development of radiation injury (Zhao and Robbins 2009, Meziani, Mondini et al. 2018).

1.3.3 Effects of ionizing radiation on macrophage immune response

After exposure to IR, macrophages are recruited at the irradiated site (Travis 1980, Meziani, Mondini et al. 2018) and they represent a novel pro-fibrogenic factor that plays an important role during radiation-induced normal tissue toxicity. Within the microenvironment, macrophages respond differently to radiotherapy in normal tissue depending on both time and IR/fractionation dose.

In vitro, human monocyte-derived macrophages remain viable with an active metabolism after cumulative doses of ionizing radiation (2 Gy/fraction/day), despite of DNA damages. Cumulative doses of 10 Gy increased proinflammatory, and decreased anti-inflammatory markers in macrophages (Teresa Pinto, Laranjeiro Pinto et al. 2016). *In vivo*, it is rather difficult to evaluate the direct effect of IR on macrophage activation. However, recent studies in the tumor stroma showed that high doses of IR (> 8 Gy) promote anti-inflammatory activation of macrophages (Meng, Beckett et al. 2010), and low doses (< 2 Gy) combined with immunotherapy induce pro-inflammatory activation of macrophages that favor tumor elimination (Klug, Prakash et al. 2013). These data indicate that there is a direct effect of IR on macrophage activation.

1.3.4 Radiation-induced oxidative stress, ROS production and DNA double strand breaks

As mentioned before, cells are continuously exposed to a barrage of DNA damage from both endogenous and external sources. Oxidative stress induced by extracellular and intracellular production of ROS is a fundamental mechanism that contributes to DNA damage. Overproduction of ROS that exceeds defense mechanisms can damage intracellular macromolecules, including nucleic acids, with the formation of DNA adducts and DNA strand breaks that may result in mutations (Figure 11A) (Imlay, Chin et al. 1988, Redon, Dickey et al. 2010). In irradiated cells, levels of ROS and RNS may be increased due to perturbations in oxidative metabolism and chronic inflammatory responses, thereby contributing to the long-term effects of exposure to ionizing radiation on genomic stability (Azzam, Jay-Gerin et al. 2012).

Interestingly, the early biochemical modifications, which occur during or shortly after radiation exposure, were thought to be responsible for most of the effects of IR in mammalian cells. However, oxidative changes may continue to arise for days and months after the initial exposure presumably due to continuous generation of ROS and RNS (Petkau 1987). Both ROS and RNS can attack DNA resulting in several alterations including DNA breaks, base damage, destruction of sugars, crosslinks, and telomere dysfunction (Valerie, Yacoub et al. 2007, Sahin, Colla et al. 2011). If unrepaired or mis-repaired, these damages may lead to mutations and promote neoplastic transformation or cell death (Kryston, Georgiev et al. 2011).
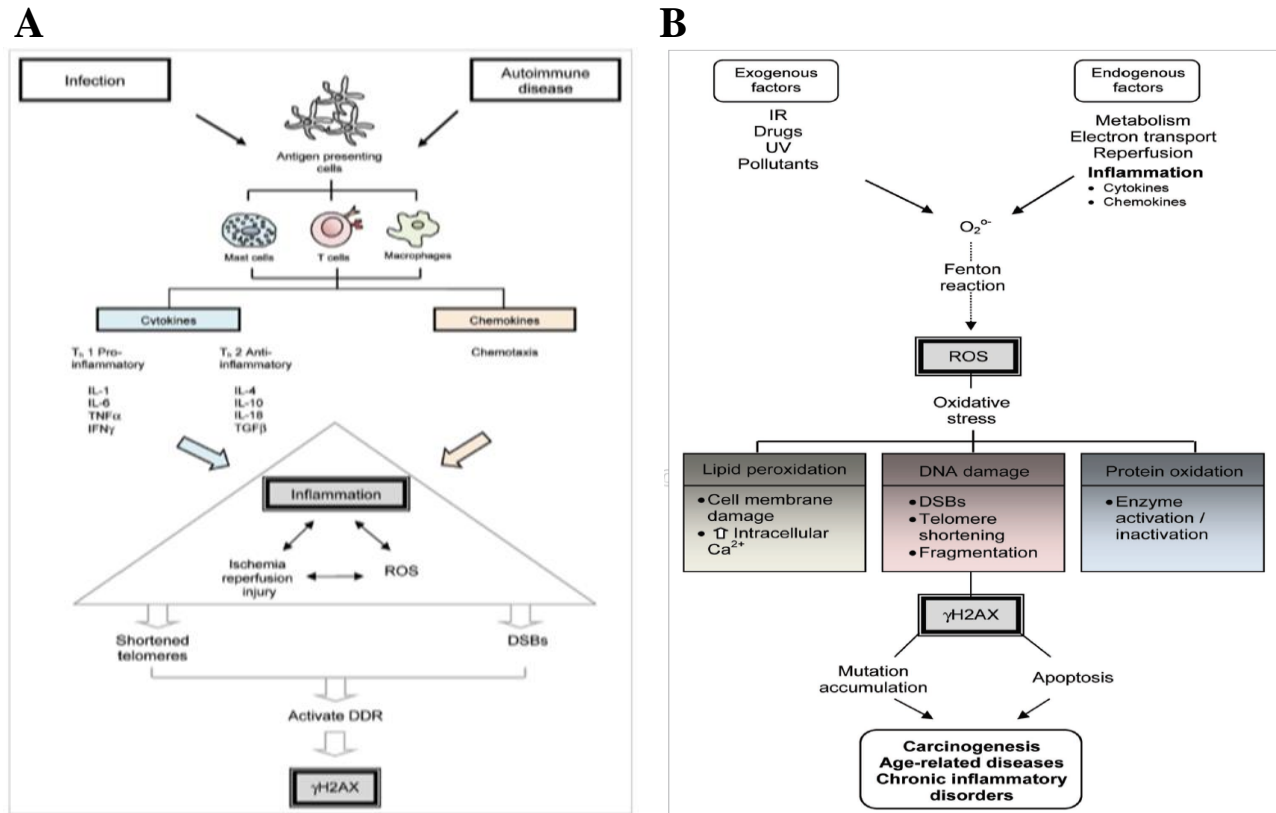
Figure 11 Production of DNA double strand breaks

(A) Cellular effects of reactive oxygen species leading to the production of DNA double strand breaks and γH2AX formation. (B) Potential pathway for inflammation-mediated induction of DNA double-strand breaks and γH2AX formation. The figure is used after permission from (Mah, El-Osta et al. 2010).

1.3.4.1 Mechanism of Double strand breaks (DSBs)

Among the different forms of DNA damage, double-strand breaks (DSBs) are the most dangerous to cells because failure to repair them can induce loss of genetic information and chromosome rearrangements. DSBs are formed when both strands of DNA are broken in close proximity (<20 bp) (Khanna and Jackson 2001, Lieber, Ma et al. 2003). Nevertheless, cells have developed multiple signaling pathways and biochemical mechanisms that counter-balance DNA damage and trigger DNA repair. As a result, cells undergo rapid and efficient error correction through a series of complex DNA pathways collectively known as the DNA damage response (DDR) (Stucki, Clapperton et al. 2005, Ciccia and Elledge 2010). Two major DSB repair pathways, homologous recombination (HR) and non-homologous end joining (NHEJ), both of which have been reviewed extensively, are employed by mammalian cells to overcome the deleterious effects of DSBs (Rothkamm, Krüger et al. 2003, Mahaney, Meek et al. 2009).

1.3.4.2 DNA breaks and formation of H2AX

Interestingly, several studies have used γH2AX as a marker for inflammation-induced DNA damage (Nichols, Schaack et al. 2009). H2AX is phosphorylated over a large region surrounding the DSB and forms easily visualized foci (Shroff, Arbel-Eden et al. 2004). Visualization of discrete γH2AX foci using immunofluorescence-based assays has provided a sensitive and successful method for detecting DSBs that may be involved in various pathologies including cancer, chronic inflammatory diseases and ischemia-reperfusion injury (Mah, El-Osta et al. 2010).The early cellular response to DNA breaks is the rapid phosphorylation of histone variant H2AX (Figure 11B) at Ser-139 to form γH2AX (Redon, Pilch et al. 2002). Phosphorylation occurs at the highly conserved SQ motif of H2AX, a common substrate for the PI3K family of proteins namely ataxia telangiectasia mutated (ATM), DNA-protein kinase catalytic subunit (DNA-PKcs) and ATM and RAD3-related (ATR) (Leatherbarrow, Harper et al. 2006).

ATM is activated by monomerization and autophosphorylation that in turn phosphorylates H2AX after IR-induced damage with some redundancy that can be compensated by DNA-PK while ATR is typically responsible for formation of γH2AX following damage associated with UV exposure, metabolic stress and ROS (Tanaka, Arakawa et al. 2000, Stiff, Walker et al. 2006).

Overall, H2AX phosphorylation represents an important step in the DDR, with a role in epigenetic signalling along with DSB repair initiation by increasing DNA accessibility and facilitating the recruitment and accumulation of specific DDR proteins at DNA ends. Furthermore, γH2AX modulates checkpoint responses, preventing cell cycle progression (Celeste, Petersen et al. 2002, Bouquet, Muller et al. 2006).

1.4 Gut microbiota

1.4.1 Background and definition

Gut microbiota is considered as hidden metabolic 'organ within an organ' because of its immense effect on health by influencing the host nutrient acquisition, metabolism, physiology, and immune functions (O'Hara and Shanahan 2006, Marchesi, Adams et al. 2016). The human gastrointestinal tract (GIT) is one of the largest interfaces (250–400 m^2) between the host, environmental factors and antigens in the human body. Approximately 60 tonnes of food pass through the human GIT, over an average life time, along with an abundance of microorganisms from the environment which impose a significant threat on gut integrity (Bengmark 1998).

The collection of bacteria, archaea and eukarya colonizing the GIT is referred to as the '**gut microbiota**' and has co-evolved with the host over thousands of years to establish a complex and mutually beneficial relationship (Bäckhed, Ley et al. 2005, Neish 2009). The GIT harbours complex microbial community as high as up to ~10^{14} microorganisms. As a result of the vast number of bacterial cells in the body, the host and the microorganisms inhabiting it are often referred to as a 'superorganism' (Luckey 1972, Gill, Pop et al. 2006).

Microbiota provides many benefits to the host, through a variety of physiological functions such as strengthening gut integrity or shaping the intestinal epithelium (Natividad and Verdu 2013), harvesting energy (den Besten, van Eunen et al. 2013), protecting against pathogens (Bäumler and Sperandio 2016) and regulating host immunity (Gensollen, Iyer et al. 2016). However, all these mechanisms can be disrupted as a result of dysbiosis (also called dysbacteriosis). With increasingly sophisticated methods to profile and characterise complex ecosystems being developed, a role for the microbiota in a large number of intestinal and extra-intestinal diseases has become steadily apparent (Schroeder and Bäckhed 2016).

1.4.2   Gut microbiota regulate immune responses

Participation of gut microbiota in host immunity development and immune response regulation at both local and systemic levels had been demonstrated, whereby reversal of the differentiation suppressed states of myeloid and lymphoid progenitor cells in germ free (GF) mice was observed after colonization with normal microbiota, indicating gut microbiota facilitates maturation of haematopoiesis (innate immunity) and lymphocytopoiesis (adaptive immunity) (Khosravi, Yáñez et al. 2014).

The balance between microbial controlled pro- and anti-inflammatory activities is critical to maintain gut homeostasis and regulate gut inflammation and colon carcinogenesis (Sobhani, Tap et al. 2011, Tomkovich and Jobin 2016). However, several external factors such as infection, diet and usage of antibiotics are known to disrupt the dynamics of microbial communities in the intestine and the host immune system (Ley, Hamady et al. 2008, Belkaid and Naik 2013).

1.4.3   Gut microbiota metabolites of polyphenols

One of the key functions of gut microbiota is to convert dietary components such as polyphenols to a spectrum of metabolites. Polyphenolic compounds are powerful anti-inflammatory dietary agents which can modify inflammation, drug and radiation resistance (Sánchez-González, Izquierdo-Pulido et al. 2016, Koch 2019). Polyphenols may also exert beneficial effects on microbiota by acting as prebiotics (Kawabata, Mukai et al. 2015). Importantly, the health benefits rendered by consumption of several natural plant products (e.g. pomegranates, walnuts and berries) have been associated with their high levels of polyphenolic compounds, specifically ellagitannins and ellagic acid (Heber 2008, Alasalvar and Bolling 2015).

Acid hydrolysis of ellagitannins releases free ellagic acid (EA) (Seeram, Henning et al. 2006) which are present in pomegranates, raspberries, strawberries, and walnuts (Cerdá, Tomás-Barberán et al. 2005). The absorption of ellagitannins and ellagic acid is very low and so, the unabsorbed compounds are further metabolised by gut microbiota to bioactive molecules including different urolithins compounds A, B, C, and D (Cerdá, Llorach et al. 2003, Seeram, Henning et al. 2006). Here, we will focus on urolithin A (UA).

1.4.3.1 Urolithins

Urolithins are microbial metabolites derived from EA or ellagitannins by commensal bacteria (Selma, Beltrán et al. 2014) and are dibenzopyran-6-one derivatives with different hydroxyl group substitutions. Urolithins represent a link between diet, gut microbiota and health, which has attracted increasing interest (Espín, Larrosa et al. 2013, Tomás-Barberán, González-Sarrías et al. 2017).

1.4.3.1.1 Chemical nature of urolithins

Chemically, urolithins can be considered a combination of coumarin and isocoumarin (benzo coumarins) (Cerdá, Periago et al. 2005). Urolithins are produced by the opening and decarboxylation of one of the lactone rings of ellagic acid and the successive removal of hydroxyls from different positions. After decarboxylation the first metabolite is urolithin M-5 (pentahydroxy-urolithin), and from this, several tetrahydroxy-urolithin isomers are produced by removal of one hydroxyl group from different positions (urolithin D, urolithin M-6). Trihydroxy-urolithins (urolithin C, urolithin M-7) were then produced and then dihydrox- urolithins (urolithin A and isourolithin A) (Figure 12). Monohydroxy-urolithin (urolithin B) was also detected, particularly in those cases in which isourolithin A was produced. Further degradation of urolithins to remove the second lactone ring has not been reported so far, although it should not be discarded (Espín, Larrosa et al. 2013). Recently, García-Villalba, et al. identified four unknown urolithins (M6R, M7R, CR, and AR) in human faces and urine after the intake of pomegranate extract (García-Villalba, Selma et al. 2019).

Among urolithins, urolithin A (UA; 3,8-dihydroxybenzo[c]chromen-6-one) is the most relevant urolithin and has been shown to influence the microbiota composition in rat models (Larrosa, González-Sarrías et al. 2010), but the significance of these changes remain to be established. UA is the most abundantly present metabolite in the mouse gut after consumption of pomegranate husks or extract, whereas in humans various sources of ellagitannins leads to different urolithins compounds including A, B, and C being formed (Tulipani, Urpi-Sarda et al. 2012).

1.4.3.1.2 Pharmacokinetics, production and tissue distribution of urolithin

The Iberian pig was used as a model to study urolithin production from ellagitannins as well as evaluation of ellagitannins metabolism and tissue distribution. This particular pig feeds on oak acorns which are very rich in ellagitannins (Espín, González-Barrio et al. 2007). This study revealed that different urolithins were produced in the gut starting with tetrahydroxy-urolithin through the removal of one of the lactone rings of ellagic acid, and by successive removal of hydroxyls to end with urolithins A and B. The analysis of plasma and urine samples indicated that urolithin A glucuronide and sulfate were the main metabolites, with urolithin C and B glucuronides and sulfates as minor metabolites. Ellagic acid dimethyl-ether-glucuronide was also a major metabolite. The analysis of the gall bladder and bile suggested that tetrahydroxy-urolithin

was absorbed in the first portion of the gut, and was detected in the liver, where it was conjugated and excreted with the bile to the small intestine (Espín, González-Barrio et al. 2007).

Concerning the tissue distribution, high concentration of urolithin metabolites only accumulated in the urine bladder and the gall bladder, but they did not accumulate in any of the analyzed tissues (muscle, adipose tissue, etc.) (Espín, González-Barrio et al. 2007). In parallel, Seeram et al. (Seeram, Aronson et al. 2007) described the pharmacokinetics and tissue distribution of urolithins in mice after oral or intraperitoneal administration of chemically synthesized urolithin A. Urolithin A peaked in plasma after 2 h and reached the highest concentrations in the prostate followed by the small intestine and colon, with a peak at 4 h (Seeram, Aronson et al. 2007). It has been suggested that potential health benefits rendered by these compounds *in vivo* are due to gut microbiota mediated conversion into metabolites called urolithins (Cerdá, Periago et al. 2005, Espín, Larrosa et al. 2013).

1.4.3.1.3 Bioavailability and tissue deconjugation of urolithin

Numerous studies of UA have been established in both humans and mouse models. These studies highlight that the concentration of UA reaches up to micromolar (μM) without displaying any toxic effects *in vivo* (Espín, Larrosa et al. 2013). For instance, upon consumption of pomegranate juice by humans, peak plasma levels of UA could reach from 14 to 40 μM but with large individual-variations (Cerdá, Espín et al. 2004, Seeram, Aronson et al. 2007).

Urolithin A and its conjugates, UA-glucuronide, are detected in some mouse tissues, including colon, prostate, liver, and kidney, at 1 to 6 h after oral administration of urolithin A (Surapaneni, Priya et al. 2014). The continuous circulation of urolithins may allow their accumulation in tissues, and thus facilitating their physiological functions. However, a recent study suggested that the process of tissue deconjugation in particular within the intestinal tract (in a systemic inflammation rat model) allows free availability of UA in inflammatory microenvironmental sites and could thus, have beneficial effects on inflammatory disease and colon cancer (Espín, Larrosa et al. 2013, Piwowarski, Stanisławska et al. 2017).

1.4.3.1.4 Biological function of urolithins

The gut microbiota metabolites of polyphenols have many biological health effects due to the anti-oxidant and anti-inflammatory activities. UA has an anti-inflammatory property in inflammatory bowel disease and improves the gut permeability (Tomás-Barberán, García-Villalba et al. 2014).

Urolithins have many biological functions including anti-malarial properties or topoisomerase inhibitors to quenchers of bacterial quorum sensing (Espín, Larrosa et al. 2013). Numerous studies demonstrated the vital role of UA in metabolic syndrome, improving cardiovascular function, downregulate the formation of triglycerides, inhibiting enzymes such as lipase or glucosidase, or relieving insulin resistance (Les, Arbonés-Mainar et al. 2018, Toney and Chung 2019). It has also been observed that UA may have an important role in the inhibition of certain

cancers, such as colorectal or prostate cancers (Liu, Cui et al. 2019, Mohammed Saleem, Albassam et al. 2019). In addition, many studies have described an anti-inflammatory activity (Larrosa, González-Sarrías et al. 2010), and preservation of the gut barrier integrity (Larrosa, González-Sarrías et al. 2010, Singh, Chandrashekharappa et al. 2019) in murine models after oral UA administration, which is consistent with the fact that the colon is the organ where the highest concentration of urolithins occurs (Nuñez-Sánchez, García-Villalba et al. 2014). Moreover, UA has an important role at the mitochondrial level, being able to activate mitophagy and prolonging lifespan in *Caenorhabditis elegans* worms, as well as beneficial mitochondrial effects in the skeletal muscle (Ryu, Mouchiroud et al. 2016, Singh, Andreux et al. 2017).
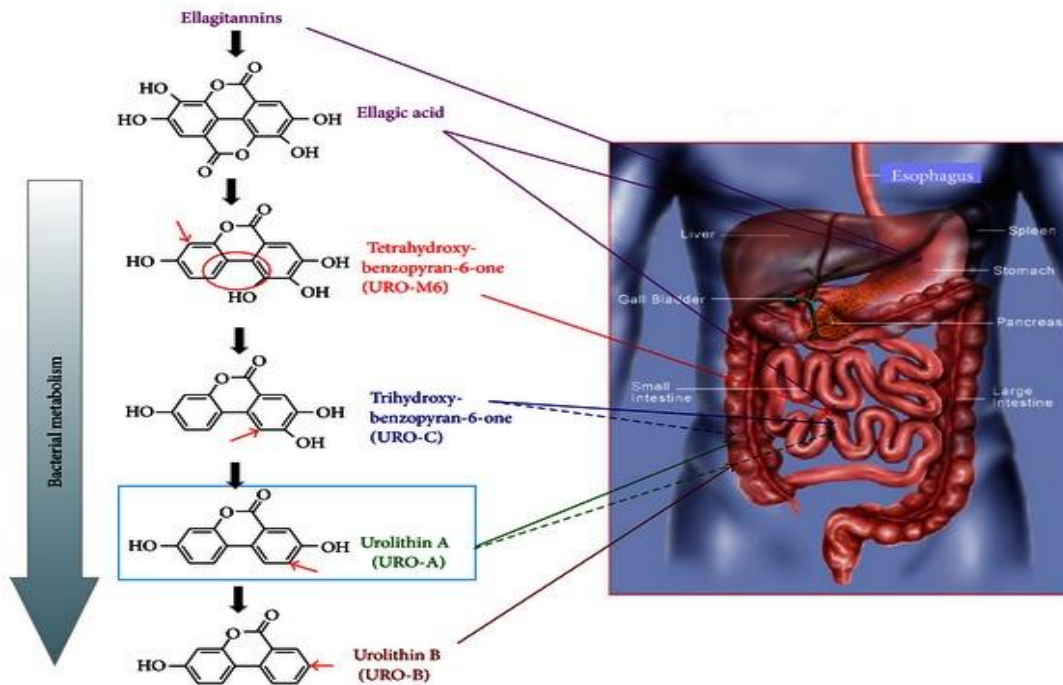
Figure 12 Gut microbiota metabolism of ellagitannins and ellagic acid

Catabolic pathway of ellagic acid includes loss of one of the two lactones (lactonase/decarboxylase activity) and by successive removals of hydroxyls (dehydroxylase activities) urolithin A and B are produced. The figure is used after permission from (Espín, Larrosa et al. 2013).

1.5 Aim of the thesis

Inflammation is a defense mechanism that is vital to health, in which the immune system's response to harmful stimuli, such as pathogens, toxic compounds, or irradiation. Inflammatory bowel disease (IBD) is a chronic intestinal inflammation that results from host-microbial interactions in a genetically susceptible individual. In addition, intestinal tissue is particularly radio-sensitive and remains the limiting factor in the application of radio-therapeutic schedules for the treatment of tumors located in the pelvis and abdominal area.

Macrophages are one of the first lines of defense in innate immunity and play a crucial role in host defense and inflammation. In response to an immune challenge, they have the pattern recognition receptor (PRR) system to sense and detect pathogen associated molecular pattern (PAMPs) through toll like receptors (TLRs). Although, macrophages produce a broad range of biologically active molecules participated in both beneficial and dangerous outcomes in inflammation, therapeutic strategies targeting macrophages and their products may open new pathways and opportunities for controlling inflammatory diseases. Accordingly, activation of TLRs enables the host to recognize a large number of PAMPs, ignite immune cells to distinguish between self and non-self, and then trigger the following innate and adaptive immune responses. Moreover, accumulated evidences have proven the crucial role of TLRs in autoimmune diseases, including inflammatory and tumor-associated diseases.

Urolithins are gut microbiota metabolites of the natural polyphenol ellagic acid. The molecular mechanisms underlying the beneficial effects of urolithins remain unclear. Urolithin A had been proposed as the bioactive metabolite responsible for the beneficial effects of pomegranates and other plants containing ellagitannins. The metabolism of polyphenols (including ellagic acid) from food seems to be insufficient to produce enough levels of urolithins in the body. In an attempt to participate in finding an effective treatment for inflammatory-response-associated diseases such as IBD and radiation sickness (as radioprotector agent) two inflammatory models will be used to investigate the effect of UA on:

1- Intracellular calcium, ROS production and mitochondrial membrane potential induced by LPS-stimulation or X-irradiation in BMDMs.

2- Mitochondrial superoxide production and accordingly the availability of double strand breaks (DSBs) induced by LPS-stimulation or X-irradiation in BMDMs.

3- Production of pro-inflammatory miRNA, mRNA, cytokines and mediators (NOS2) induced by LPS-stimulation or X-irradiation in BMDMs.

4- TLR2 and TLR4 expression and downstream signalling cascade as NF-κB (IκBα), MAPK (ERK, p38, JNK), and PI3K/AKT/mTOR in LPS-stimulated or X-irradiated murine BMDMs.

2 MATERIALS AND METHODS

2.1 Materials

2.1.1 Laboratory chemical and biochemical

Product	Reference number	Company & Origin
Accutase (cell dissociation solution)	#SCR005	Sigma-Aldrich, Germany
Acetic acid	#A9967	Merck, Germany
Acrylamide /Bis acrylamide, 30% solution	#A3699	Merck, Germany
Ambion RNase I	#AM2295	Invitrogen, Germany
Amersham Hybond P 0.45 PVDF blotting membrane 300mm × 4m	#10600023	VWR, France
Amersham Hyperfilm ECL (18 × 24cm)	#28906837	VWR, France
Ammonium persulfate	#A3678	Sigma-Aldrich, Germany
Bromphenol blue	#318744	Sigma-Aldrich, Germany
Bovine Serum Albumin (BSA)	#A2153	Sigma-Aldrich, Germany
β-Mercaptoethanol Sigma	#M7522	Sigma-Aldrich, Germany
Chemiluminescent HRP substrate A & B	#R-03031-D25 & #R-03025-D25	Advansta, USA
Deoxyribonuclease I from bovine pancreas (DNase I)	#90083	Thermo Fisher Scientific, USA
Dimethyl sulfoxide (DMSO)	#A994-2	Roth, Germany
Dulbecco's Phosphate Buffered Saline (PBS)	#D8537	Sigma-Aldrich, Germany
Ethanol	#20821-321	VWR, France
FACS Clean Solution	# 340345	BD Biosciences, Germany
FACS Flow Sheath Solution	#336911	BD Biosciences, Germany
FACS Shutdown Solution	#334224	BD Biosciences, Germany

Fast-SYBR Green Master Mix	#4385612	Thermo Fisher Scientific, USA
Formaldehyde	#158127	Sigma-Aldrich, Germany
Gel-blotting paper (Whatman)	#WHA10427812	Sigma-Aldrich, Germany
Glycine	#3908.3	Roth, Germany
Hank´s balanced salt solution (HBSS/Ca/Mg,)	#14025-092	Invitrogen, Germany
Hydrogen chloride (HCL)	#30721M	Sigma-Aldrich, Germany
Isopropanol	#190764	Sigma-Aldrich, Germany
Methanol (absolute)	#34860	Merck, Germany
Penicilin-Streptomycin	#P4333	Sigma-Aldrich, Germany
Ponceau S	#P7170	Sigma-Aldrich, Germany
ProLong GOLD Anti-fade Mountant with DAPI	#P36931	Thermo Fisher Scientific, USA
ReBlot Plus Strong Antibody Stripping Solution. 10x	#2504	Merck, Germany
Rotiphorese 10x-SDS-PAGE	#3060.2	Roth, Germany
Sodium azide (NaN3)	#71289	Sigma-Aldrich, Germany
Sodium chloride	#S9888	Sigma-Aldrich, Germany
Sodium dodecyl sulfate (SDS)	#0183.2	Roth, Germany
Tetramethylethylenediamine (TEMED)	#T9281	Sigma-Aldrich, Germany
Triton X-100	#T9284	Sigma-Aldrich, Germany
TRIZMA-Base	#T1503	Sigma-Aldrich, Germany
TRIzol Reagent	#15596018	Thermo Fisher Scientific, USA
Trypan blue solution 0.4%	#T8154	Sigma-Aldrich, Germany
Trypsin-EDTA solution (0.25%)	#25200056	Thermo Fisher Scientific, USA
Tween 20	#9005-64-5	Roth, Germany
Water (cell culture)	#W3500	Sigma-Aldrich, Germany
Nuclease free Water (DEPC)	#95284	Sigma-Aldrich, Germany
X-well tissue culture chamber	#94.6150.401	Sarstedt, Germany

2.1.2 Stock solutions for buffers

2M Tris (pH 8.8)	Volume / Weight	Components
	121 g	Trizma-Base
	Add to 500 ml	H_2O & adjust pH 8.8

0.5M Tris (pH 6.8)	Volume / Weight	Components
	30.25 g	Trizma-Base
	Add to 500ml	H_2O & adjust pH 6.8

2x Protein loading buffer (50ml)	Volume / Weight	Components
	10 ml	0.5M Tris-Base pH6.8
	5 ml	SDS (20 %)
	10 ml	Glycerol
	5 ml	β-Mercaptoethanol
	1 ml	0.1% Bromphenol blue
	Add 19 ml	$H2O_{dd}$

CoomassieR blue de-staining solution	Volume / Volume	Components
	40 %	Methanol
	10 %	Glacial acetic acid
	50 %	H2O

CoomassieR blue staining solution	Volume / Weight	Components
	50 %	Methanol
	10 %	Glacial acetic acid
	0.25 %	Coomassie R Blue
	40 %	H2O

TBST (1x - 2 liter)	Volume / Weight	Components
	20 ml	1M Tris-HCL pH 7.4
	60 ml	5M NaCl
	2 ml	% Tween 20

Separating gel buffer (1x -1liter)	Volume / Weight	Components
	3 g	Tris-Base
	14.4 g	Glycine
	5 ml	SDS (20 %)
	ad to 1 L	H_2O_{dd}

Running buffer (1x – 1liter)	Volume / Weight	Components
	14.4 g	Glycin
	3 g	Tris-Base
	0.75 g	SDS
	200 ml	Methanol
	Ad to 1 L	H_2O_{dd}

Stripping buffer (1x – 1liter)	Volume / Weight	Components
	15 g	Glycine
	1 g	SDS
	10 ml	Tween 20
	Add to I L	H_2O_{dd} (adjust pH 2.2)

Trypan blue solution	Volume / Weight	Components
	1x	PBS
	1:5 (v/v)	Trypan blue 0.4 %

2.1.3   Assay kits

2.1.3.1   Flow cytometry, western blot, miRNA and qRT-PCR Kits

Product	Reference number	Company & Origin
Annexin V apoptosis detection kit FITC	#88-8005- 72	eBioscience, Germany
ECL detection kit	# 345-57	Thermo Fisher Scientific, USA
miRNAeasy kit	#217004	Qiagen, Germany
miRNA universal cDNA synthesis kit II	#203301	Exiqon, Germany
Superscript III First-Strand synthesis system	#18080-51	Invitrogen, Germany

2.1.3.2   Mouse ELISA kits

Product	Reference number	Company & Origin
IL-1β	#88701322	Invitrogen, Germany
IL-4	#88704422	Invitrogen, Germany
IL-6	#88706422	Invitrogen, Germany
IL-10	#88710522	Invitrogen, Germany
IL-12	#88712188	Invitrogen, Germany
TGF-β	#88835022	Invitrogen, Germany
TNF-α	#88732422	Invitrogen, Germany
IFN-γ	#88831422	Invitrogen, Germany

2.1.4   Fluorescence dyes

Product	Reference number	Company & Origin
2′,7′-Dichlorofluorescin diacetate	#D6883	Sigma-Aldrich, Germany
Fluo-4	#F14200	Invitrogen, Germany
MitoSOX	#M36008D	Thermo Fisher Scientific, USA
Tetramethylrhodamine (TMRM)	#I34361	Invitrogen, Germany

2.1.5 Primers

2.1.5.1 Mouse primer for mRNA amplification

Primer name	Primer sequences	Company & Origin
IL-1β	F 5⁻ TACCTGTGGCCTTGGGCCTCAA - 3⁻ R 5⁻ GCTTGGGATCCACACTCTCCAGC - 3⁻	Sigma-Aldrich, Germany
IL-2	F 5⁻ AGGAACCTGAAACTCCCCAG - 3⁻ R 5⁻ CTTTCAATTCTGTGGCCTGCTT - 3⁻	Sigma-Aldrich, Germany
IL-4	F 5⁻ AGGAGAAGGGACGCCATGCAC - 3⁻ R 5⁻ GCGAAGCACCTTGGAAGCCCTAC - 3⁻	Sigma-Aldrich, Germany
IL-6	F 5⁻ TGGAGTCACAGAAGGAGTGGCTA - 3⁻ R 5⁻ TCTGACCACAGTGAGGAATGTCC - 3⁻	Sigma-Aldrich, Germany
IL-10	F 5⁻ GGCGCTGTCATCGATTTCTCCCC - 3⁻ R 5⁻ GGCCTTGTAGACACCTTGGTCTT - 3⁻	Sigma-Aldrich, Germany
IL-12	F 5⁻ AATCAGGGCTGCGAAGGTA - 3⁻ R 5⁻ AGGCCCTGGTTTCTTATCAA - 3⁻	Invitrogen, Germany
TGF-β	F 5⁻ GAGCCCGAAGCGGACTACTA - 3⁻ R 5⁻ TGGTTTTCTCATAGATGGCGTTG - 3⁻	Invitrogen, Germany
TNF-α	F 5⁻ ATAGCTCCCAGAAAAGCAAGC - 3⁻ R 5⁻ CACCCCGAAGTTCAGTAGACA - 3⁻	Sigma-Aldrich, Germany
IFN-γ	F 5⁻ GGCTGTTACTGCCACGGCACA - 3⁻ R 5⁻ CACCATCCTTTTGCCAGTTCCTC - 3⁻	Sigma-Aldrich, Germany
NOS2	F 5⁻ AGTCAACTGCAAGAGAACGGA - 3⁻ R 5⁻ TGAGAACAGCACAAGGGGTT - 3⁻	Sigma-Aldrich, Germany

2.1.5.2 MicroRNA LNA™ PCR primer set for amplification of different miRNAs

Primer	Reference number	Company & Origin
hsa-miR-9-5p	#204513	Exiqon, Germany
hsa-miR-10a-5p	#204778	Exiqon, Germany
has-miR-99b-5p	#205983	Exiqon, Germany
has-miR-146a-5p	#204688	Exiqon, Germany
has-miR-155-5p	#205930	Exiqon, Germany
Reference 5S rRNA	#203906	Exiqon, Germany

2.1.6 Antibodies

2.1.6.1 Immunofluorescence antibody

Primary antibody	Description and References	Company & Origin
$H_2A.X$	Polyclonal antibody #PA5-28778	Thermo Fisher Scientific, USA

Secondary antibody	Description and References	Company & Origin
Alexa Fluor 488 goat anti-rabbit IgG	1:500 in 1% BSA #A-11008	Thermo Fisher Scientific, USA

2.1.6.2 Antibodies for flow cytometry (macrophage phenotype staining)

Antibody	References	Company & Origin
CD11b - PE	#12-0112-82	Invitrogen, Germany
F4/80 - FITC	#11-4801-81	Invitrogen, Germany
MHCII – APC	#17-5321-82	Invitrogen, Germany

2.1.6.3 Antibody for western blot

Primary antibody	Description and References	Company & Origin
ERK1/2 (p44/42 MAPK)	Rabbit polyclonal antibodies #9102s	Cell signalling technology, Germany
pERK1/2 (phospho-p44/42 MAPK) (Thr202/Tyr204)	Rabbit polyclonal antibodies #9101s	Cell signalling technology, Germany
AKT	Rabbit polyclonal antibodies #9272s	Cell signalling technology, Germany
phospho-AKT (T308) (C31E5E)	Rabbit polyclonal antibodies #2965s	Cell signalling technology, Germany
mTOR	Rabbit monoclonal antibodies #2983s	Cell signalling technology, Germany
phospho-mTOR (Ser2448)	Rabbit polyclonal antibodies #2971s	Cell signalling technology, Germany
TLR2	Rabbit monoclonal antibodies #13744s	Cell signalling technology, Germany
TLR4	Rabbit monoclonal antibodies #14358s	Cell signalling technology, Germany
SAPK/JNK	Rabbit polyclonal antibodies #9252s	Cell signalling technology, Germany
phospho-SAPK/JNK (Thr183/Tyr185)	Rabbit monoclonal antibodies #4671s	Cell signalling technology, Germany
p38 MAPK	#8690S	Cell signalling technology, Germany
Phospho-p38 (Thr180/Tyr182)	Rabbit monoclonal antibodies #4511s	Cell signalling technology, Germany
IκBα	#4812S	Cell signalling technology, Germany
Phospho-IκBα (Ser32)	#2859S	Cell signalling technology, Germany
GAPDH	Rabbit monoclonal antibodies #2118s	Cell signalling technology, Germany

Secondary antibody	References and dilution	Company & Origin
HRP-conjugated anti-rabbit	1:1000 #7074s	Cell signalling technology, Germany

2.1.7 Cell line

Cell line	Organism	Tissue	Morphology	Description	Reference
L929	100-day-old male mouse	Subcutaneous connective tissue; areolar and adipose	Fibroblast	NCTC clone 929 (Connective tissue, mouse) Clone of strain L was derived in March 1948.	ATCC®, USA, #CCL-1™

2.1.8 Mice

Mice	Sex (gender)	Age
C57BL/6J	Male & Female	8-12 weeks age

2.1.9 Cell Culture media and supplements

Product	Reference number	Origin / Company
Dulbecco's modified Eagle's medium (DMEM)	#61965-026	Life Technologies, Germany
Fetal bovine serum (FBS)	#10270-106	Life Technologies, Germany
Lipopolysaccharide (LPS) from Escherichia coli O111:B4	#L4391	Sigma-Aldrich, Germany
MEM Non-essential Amino Acid Solution	#M7145	Sigma-Aldrich, Germany
β-Mercaptoethanol	#M7522	Sigma-Aldrich, Germany
Penicillin-Streptomycin (10000 U/ml, 10000 μg/ml) (Pen-Strep)	#P4333	Sigma-Aldrich, Germany
Urolithin A (UA)	#1143-70-0	Santa Cruz Biotechnology, USA

2.1.10 Laboratory equipment's

Instrument name	Origin /Company
Analytical Balance (AE163)	KERN plus, Germany
Cell culture incubator (Heraeus)	Thermo Fisher Scientific, USA
Centrifuge (ROTINA420R)	Hettich, Germany
Centrifuge (Eppendorf5417R)	Eppendorf, Germany
ELISA reader	BioTek, USA
Flow cytometry, BD FACS Calibur™	BD Bioscience, Germany
Fluorescence Mircroscope (AxioObserver Z1)	Carl Zeiss, Germany
Freezer -20°C	Thermo Fisher Scientific, USA
Freezer -80°C	Thermo Fisher Scientfic, USA
Fridge 4°C	Thermo Fisher Scientfic, USA
Heat block (Thermo mixer)	Eppendorf, Germany
Ice Machine	Hoshizaki, Germany
Linear accelerator	LINAC SL25 Philips, Germany
Liquid Nitrogen Tank (Cryosystem 6000)	MVE , Germany
Magnetic stirrer (heatable)	Heidolph Instruments, Germany
Microcentrifuge (Heraeus™ Fresco™ 17)	Thermo Fisher Scientfic, USA
Micro pipettes (2-10 µl)	Star lab, Germany
Microscopes	Zeiss, Jena, Germany
Milli-Q® Integral Water Purification System	Millipore, USA
Molecular imager VersaDoc system	Bio-Rad, Germany
Multichannel pipettes (200 µl ; 8, 12 channels)	Rainin, Germany
Neubauer haemocytometer	Brand, Germany
PCR Master cycle	Eppendorf, Germany
Pipettes (10 µl, 100 µl, 200 µl, 1000 µl)	Star lab, Germany
Quantitative Real-Time PCR	Bio-Rad Laboratories, Germany
Roller-Mixer (RM5)	Karl Hecht, Germany

Spectrophotometer (NanoDrop 2000c)	PEQLAB Biotechnology, Germany
Sterile Laminar Flow cabinet (Heraeus)	Thermo Fisher Scientific, USA
Vacuum Pump	NeoLab, Germany
Vortexer (Reax 2000)	Heidolph Instruments, Germany
Water Bath (SW21)	Julabo, Germany
XCell sureLock mini-cell electrophoresis system	Thermo Fisher Scientific, USA

2.1.11 Consumables

Product	Origin / Company
Cell-culture dishes, tissue-culture treated (100 x 20 mm and 150 x 20 mm)	Greiner Bio-One, Germany
Cell-culture flasks, tissue-culture treated with filter cap	Greiner Bio-One, Germany
Cell Scraper	Millipore, USA
Cryo vials with screw cap (2 ml)	Greiner Bio-One, Germany
Disposable needles – 20 G	B. Braun, Germany
Disposable needles – 27 G	B. Braun, Germany
Disposable scalpels	Feather, Germany
DNA LoBind Tubes (0.5 ml, 1.5 ml and 2 ml)	Eppendorf, Germany
Falcon conical centrifuge tubes (15 and 50 ml)	BD Falcon, Germany
Microscopical glass cover slips	VWR, France
Multiwell plates, tissue-culture treated (6-, 12-, 24-, 48- and 96-well)	TPP, Millipore, USA
Parafilm M®	Bemis NA, USA
Pasteur pipettes	Corning, Germany
PCR 96 multiwell plates	Thrermo Fisher Scientfic, USA
PCR tube (0.1 ml) and cap strips, domed	Eppendorf, Germany
Pipette filter tips (10 μl, 20 μl, 100 μl, 200 μl and 1000 μl)	Star lab, Germany
Pipette tips (10 μl, 200 μl and 1000 μl)	Gilson, Germany

Pipette tips (200 µl) for multi-channel pipettes	Rainin, Germany
Plastic serum pipettes (2 ml)	Greiner Bio-One, Germany
Polypropylene round bottom tubes (5 ml)	BD Falcon, Germany
Polystyrene round-bottom tube with cell-strainer cap	BD Falcon, Germany
Safe-lock tubes (0.5 ml, 1.5 ml, 2 ml and 5 ml)	Eppendorf, Germany
Sterile filter 0.22 µM and 0.45 µM	Eppendorf, Germany
Syringes with lock tip (1, 5, 10, 30 and 50 ml)	Millipore, Germany

2.1.12 Software

Software name	Company
AxioVision LE Rel. 4.8	Carl Zeiss
EndNote X9	Thomson Reuters
FACSDiva software v.6.1.3	BD Bioscience
Fiji imageJ	Free software
FlowJo software V.10	Tree Star, Inc.
Graphpad prism 6	GraphPad Software, Inc.
Image lab 4	Bio-Rad
Microsoft Office 2010	Microsoft Cooperation
Primer-Plast	NCBI
Primer3	Free software

2.2 Methods

2.2.1 Mice

C57BL/6J mice between 8-12 weeks of age (both male and female) were used for experiments. All experiments were performed according to the EU Animals Scientific Procedures Act and the German law for the welfare of animals. All procedures were approved by the authorities of the state of Baden-Württemberg.

2.2.2 Murine bone marrow-derived macrophages production

Bone marrow cells were gathered and cultured in the medium containing macrophage colony stimulating factor (M-CSF) (Stanley 1985) obtained from supernatant of murine fibroblast L929.

After 7 days in culture, non-adherent cells were eliminated, and adherent cells were harvested for assays. Adherent bone marrow–derived macrophages (BMDMs) are usually more than 90% pure, and, therefore, precisely defined numbers of macrophages can be plated for subsequent experiments. Virtually, all the cells in this population of macrophages could respond to exogenous stimuli, and, therefore, relatively uniform populations of macrophages can be generated and harvested for biochemical analysis.

2.2.2.1 Material and cultured media used:

1) Forceps and scissors (keep in sterile beaker containing 70% ethanol)
2) Ice-cold 1x phosphate-buffered saline (Sigma-Aldrich)
3) Macrophage complete medium (see recipe)
4) DMEM warmed to 37°C
5) 10-ml syringes with 25-G needles
6) Falcon tubes (15 ml & 50 ml), on ice
7) Centrifuge (Eppendorf)
8) Petri dishes 100×20 mm (Falcon, BD Labware)
9) 37°C, 5% CO2 incubator
10) Trypane blue
11) Hemocytometer
12) Additional reagents and equipment for mouse euthanasia.

2.2.2.2 Preparation of L929 cell supernatants

L-929 cells were used as a source of M-CSF (Austin, McCulloch et al. 1971, Stanley 1985). L-929 cells were cultured in DMEM (see recipe) at 37°C and 5% CO_2 to confluence. The

supernatants were collected and centrifuged at 600 x g for 5 minutes at RT. The pellets were discarded and the supernatants were stored in 15 ml falcon tubes in -20°C until used.

2.2.2.3 Preparation of mouse bone marrow suspension

1) The mice were euthanized by rapid cervical dislocation (in deep anaesthesia) with aseptic technique.

2) The skin was disinfected with 70% ethanol and peeled from the top of each hind leg and down over the foot.

3) The hind legs were cut off and the flesh and muscles adhering to the bones were removed.

4) The bones were placed in sterile petri dish containing ice cold 1x PBS.

5) Carefully, the leg bones proximal to each joint were cut using sharp scissors.

6) 10-ml syringe with 25-G needle was filled with complete media and the needle was inserted into the bone marrow cavity of femur and tibia.

7) The bone cavity was flushed out with 5 to 10 ml of complete media, until bone cavity appeared white.

8) The complete media containing bone marrow cells were collected in 50 ml falcon tube and further centrifuged at 450 x g for 10 minutes at 4°C.

9) The supernatants were discarded and the pellet was re-suspended in macrophage complete medium (containing 30% L929 cell supernatant) by pipetting up and down.

2.2.2.4 Bone marrow cells culture

1) The total numbers of bone marrow progenitor cells were counted using a hemocytometer and adjusted the cells to a concentration of ~ 3×10^6 cells per 100-mm culture dish in 10 ml complete media and incubated in 37°C, 5% CO2 incubator.

2) On the 2nd day, another 10 ml of fresh complete media was added to each culture dish.

3) On the 4th day, half of the media were changed with a new complete media. Cells were incubated for 3 additional days.

4) Under these conditions, the bone marrow monocyte/ macrophage progenitors proliferated and differentiated into a homogenous population of mature BMDMs.

2.2.2.5 Harvesting BMDMs

1) On day 7, the cultured supernatants were removed and BMDMs were washed two times with complete media.

2) BMDMs were detached by adding Accutase cell detachment solution to each dish and incubated 5 min at 37°C, 5% CO2 incubator.

3) BMDMs were collected in 50 ml falcon tubes and centrifuged at 450 x g for 10 minutes at RT.

4) The cell pellets were, gently, re-suspended in fresh complete media and counted in the presence of trypan blue.

5) The efficiency of differentiation was assessed by macrophage surface antigen expression (CD11b - PE, F4/80- FITC and MHCII - APC) using fluorescence-activated cell sorting (FACS) analysis. Once differentiated, the BMDMs were suitable for the experiment.

6) BMDMs were prepared as desired and left for overnight in complete media at 37°C and 5% CO2 (v/v).

2.2.3 Cell culture methods

Cells were cultured in cell culture flasks, dishes or plates under sterile conditions at 37°C and 5% CO_2 (v/v).

2.2.3.1 Determination of cell number and viability

A 10 μl aliquot of each sample was diluted 1:5 in trypan blue solution to determine viable cells in a cell suspension and transferred to a Neubauer haemocytometer. Trypan blue stains dead cells, so unstained (live) cells were counted using a hand tally counter on the four large squares of the counting chamber. The cell number per ml was calculated according to this formula:

$$\text{Nr of cells / ml} = \frac{\text{Nr of counted cells}}{\text{Nr of counted squares (4)}} \times \text{dilution factor (5)} \times \text{chamber factor } (10^4)$$

2.2.3.2 L-929 conditioned medium

L-929 cells were cultured in DMEM supplemented with 10% fetal bovine serum and 1% penicillin/streptomycin.

2.2.3.3 Macrophage complete medium

DMEM was supplemented with 30% (v/v) L929 conditioned medium (see recipe), 10% MEM Non-essential Amino Acid Solution and 0.1% 2-Mercaptoethanol.

2.2.4 Stimulation and treatment

BMDMs were stimulated with 1µg/ml lipopolysaccharides (LPS) and/or single dose of radiation (6 Gray) then treated with two concentrations (25 µM and 50 µM) of Urolithin A (UA, purity ≥ 94% HPLC) for 2h, 24h and 48h.

The radiated group received UA either 24h before or directly after irradiation. Both LPS and UA were dissolved in culture media and DMSO, respectively. BMDMs were classified into the following groups:

Control	LPS	Radiated (RAD)	DMSO + RAD
DMSO	LPS + 25 µM UA	RAD + DMSO	25 µM UA + RAD
25 µM UA	LPS + 50 µM UA	RAD + 25 µM UA	50 µM UA + RAD
50 µM UA		RAD + 50 µM UA	

Macrophage irradiation

BMDMs were irradiated (single dose of 6 Gy) with 6 MV photons by using a linear accelerator (LINAC SL25 Philips) at a dose rate of 2 Gy/min at room temperature. Open-field irradiation was applied. For a sufficient dose build up in the plane of the cells, a RW3 slab (1 cm thick) was placed above the cells. Energy deposition at the cell plane was calibrated by film dosimetry. Following IR, cells were treated and post-incubated in the respective cell culture media for 2h, 24h and 48h.

2.2.5 Fluorescence-Activated Cell Sorting (FACS)

2.2.5.1 Phenotypic Characterization of BMDMs by FACS

BMDMs were detached by Accutase and collected in a 96 well plate, then washed with 1x PBS and centrifuged at 600 x *g* for 5 minutes at 4°C. BMDMs were re-suspended in 50 µl of fresh 1x PBS and then to each well 0.5 µl fluorescently-labelled-antibodies CD11b-PE (Ho and Springer 1982), F4/80-FITC (McGarry and Stewart 1991) and MHCII–APC (Watts 1997) were added.

Cells were incubated in the dark for 30-45 minutes at 4°C. After incubation, 150 µl of 1x PBS was added to wash the stained cells (two times). Finally, 200 µl of 1x PBS was added and samples were acquired on the flow cytometry- BD FACS Calibur™ (BD Bioscience, Germany). The data were analysed by *FlowJo* software (FLOWJO, LLC, USA).

2.2.5.2 Apoptosis analysis (cell viability)

BMDMs were isolated, stimulated and treated as described above. The percentage of apoptotic cells was determined by flow cytometry using the Annexin V apoptosis detection kit FITC in accordance with the manufacturer's instructions. Briefly, BMDMs were collected and washed with 1x PBS and then 1× binding buffer. BMDMs were suspended in 1× binding buffer containing Annexin V-FITC solution (1:50 dilution). After that, cells were incubated at room temperature for 15 minutes, protected from light, and washed with 1× binding buffer again. After adding Propidium Iodide solution (1:100 dilution), cells were incubated at room temperature in the dark for 10 minutes prior to flow cytometry for cell apoptosis analysis. Data were analyzed by *FlowJo* software (FLOWJO, LLC, USA).

2.2.5.3 Measurements of intracellular calcium and mitochondrial membrane potential

BMDMs were treated as desired and then collected and washed once and re-suspended in 96 well plates with 200 µl of 1x PBS. In the following, 1 µM Fluo-4 or 100 nM Tetramethylrhodamine (TMRM) were added. Cells were incubated for 30 minutes at 37°C in the dark and then washed twice with 1x PBS buffer. Finally, cells were re-suspended in 200 µl of PBS prior to flow cytometry for measurement. Fluo-4 fluorescence intensity was measured in FL-1 with an excitation (Ex) wavelength of λ 494 nm and an emission (Em) λ wavelength of 506 nm. TMRM fluorescence intensity was measured in FL-2 with an Ex/Em wavelength of 488 nm / 570 ± 10 nm. Geometric mean of the FL-1 and FL-2 signal intensity was used to show the amount of Fluo-4 and TMRM fluorescence intensity, respectively. Data were analysed by *FlowJo* software (FLOWJO, LLC, USA).

2.2.5.4 Determination of intracellular reactive oxygen species (ROS)

BMDMs were treated as desired and then exposed to the ROS sensitive dye 2′,7′-Dichlorofluorescin diacetate (10 nM) for 30 min. BMDMs were washed two times with 1x PBS (at 600 x *g* for 5 minutes at RT). 200µl of 1x PBS was added and samples were acquired on the flow cytometry (FL1 channel) with a FACSCalibur™. Obtained values were corrected for autofluorescene of control cells without dye. DCFDA fluorescence intensity was measured in FL-1 with an excitation wavelength of λ 488 nm and an emission wavelength of 530 nm. Geometric mean of the FL-1 signal intensity was used to show the amount of ROS production. The data were analysed by *FlowJo* software (FLOWJO, LLC, USA).

2.2.6 Immunofluorescence microscopy

2.2.6.1 γH2AX for DNA double strand breaks

BMDMs (10.000 cells per well) were seeded on a X-well tissue culture chamber, treated as desired and further incubated for 2h and 48h. Thereafter, media was tipped off and cells were washed with 500 µl of PBS per well. The buffer was tipped off and BMDMs were fixed with 100 µl per well of 4% (v/v) formaldehyde for 10 min at RT. Then, BMDMs were washed three times

with 1x PBS. In all washing steps slides were rotated on an orbital mixer for 5 minutes. Next, BMDMs were permeabilized for 10 minutes at RT with 100 µl of 0.1% (v/v) Triton-X 100 per well then BMDMs were washed with 1x PBS for three times. Non-specific protein binding was blocked with 1% (v/v) Bovine serum albumin (BSA) for 20 minute at RT. Excess BSA was tipped off and BMDMs were incubated with 300 µl / well of primary mouse polyclonal anti-histone H2A.X antibody for 1h at RT in 1:500 dilution (in 1% BSA). BMDMs were washed with 1x PBS as mentioned and incubated with 300 µl of Alexa Fluor 488 goat anti-rabbit IgG diluted 1:500 in 1% BSA at RT for 45 minutes in the dark. Cells were washed with 1x PBS. The chambers were carefully removed from the slides, excess moisture was blotted, and slides were allowed to air dry. One drop of ProLong GOLD Anti-fade Mountant with DAPI was added per well. The slides were kept in the dark for 30 minutes at RT before sealing with nail polish. The slides were stored overnight at 4°C in dark before analysis. The fluorescence imaging was performed with an Axiophot Zeiss microscope using a digital camera with *AxioVision 4.8* software. The obtained images were analysed by *Fiji ImageJ* software.

2.2.6.2   MitoSOX Red mitochondrial superoxide indicator

Mitochondrial superoxide anion production can be measured using the MitoSOX Red mitochondrial superoxide indicator for live cell imaging. BMDMs (10.000 cells per well) were grown, stimulated and treated as desired in multiwell slides. BMDMs were washed twice with 1x PBS and subsequently incubated for 10 minutes at 37°C in 500 µl of 5 µM MitoSOX^{TM} red reagent protected from light (5 µM MitoSOX reagent working solution prepared by diluting the 5 mM MitoSOX reagent stock solution in Hank´s balanced salt solution (HBSS/Ca/Mg) to make a 5 µM MitoSOX reagent working solution). After the incubation, BMDMs were washed three times with warm buffer. To prepare the cells for viewing, one drop of ProLong GOLD Anti-fade Mountant with DAPI was added per well. The fluorescence imaging was performed with an Axiophot Zeiss microscope using a digital camera with *AxioVision 4.8* software. The obtained images were analysed by *Fiji ImageJ* software.

2.2.7   mRNA and miRNA qRT-PCR

To prevent RNase contamination, the workplace and all required equipment were wiped with RNaseZAP. In addition, only nuclease and RNase free eppendorf, tips and reagents were used. The TRIzol-phenol-chloroform protocol was used for total RNA (including miRNA) extraction. TRIzol reagent maintains the integrity of the RNA due to highly effective inhibition of RNase activity while disrupting cells and dissolving cell components during sample homogenization, allows for simultaneous processing of a large number of samples, and is an improvement to the single-step RNA isolation method developed by Chomcynski and Sacchi (Chomczynski and Sacchi 1987). TRIzol reagent allows performing sequential precipitation of RNA, DNA, and proteins from a single sample (Chomczynski 1993).

Sample preparation for both mRNA and miRNA

Following the manufacturer`s protocol, the growth media was removed and 300 µl of TRIzol reagent was added directly to the culture dish to lyse the cells. Then, the lysate was pipetted up and down several times to homogenize. After homogenizing, the samples were collected in a new tube and proceeded directly (or kept in -20°C) for RNA and miRNA isolation.

2.2.7.1 RNA isolation for qRT-PCR

To isolate RNA, 200 µl of chloroform was added to each sample (previously mixed with TRIzol reagent) and mixed by shaking. After 2-3 minutes of incubation, samples were centrifuged for 15 minutes at 12,000 × g at 4°C. A colourless upper aqueous phase (containing RNA) was transferred to a new tube containing 200 µl of ice-cold isopropanol (precipitation). Samples were then centrifuged for 15 minutes at 12,000 × g at 4°C. Total RNA was precipitated as a white gel-like pellet at the bottom of the tube.

The supernatant was discarded and the pellet was re-suspended in 400 µl of 75% ethanol (washing) then vortexed briefly and centrifuged for 15 minutes at 12,000 × g at 4°C. The supernatant was discarded and the RNA pellet was left for 5-10 minutes for air dry, then RNA pellet was re-suspended in 20 µl of RNase-free water. The concentration of RNA was determined (using biophotometer) by measuring the absorbance at 260 nm and 280 nm using the formula:

$A260$ × dilution × 40 = µg RNA/ml.

After measuring the concentration of RNA, the first strand cDNA synthesis step was started.

2.2.7.1.1 First-Strand cDNA Synthesis

Following the manufacturer`s protocol, the following components were added to each tube:

Component	Amount (1 Rxn)
Oligo(dT)20 (50 mM)	1 µl
10 mM dNTP Mix	1 µl

The samples were mixed gently and incubated at 65°C for 5 minutes then placed on ice for at least 2 minutes. The cDNA synthesis mix was prepared as shown:

Component	Amount (1 Rxn)
10X RT Buffer	2 µl
25mM MgCl$_2$	4 µl
0.1 M DTT	2 µl
RNaseOUT™ (40 U/µl)	1 µl
SuperScript™ III RT (200 U/µl)	1 µl
Total volume	**10 µl**

A 10 µl of cDNA synthesis mix was added to each mixture, mixed gently and collected by brief centrifuge. The samples were incubated in the thermal cycler at 50°C for 50 minutes. The reaction was inactivated at 85°C for 5 minutes. 1 µl of RNase H (2 U/µl) was added to the sample and incubated at 37°C for 20 minutes. For negative controls, 1 µl of sterile, distilled water instead of SuperScript™ III was used.

2.2.7.1.2 Detection of gene expression (amplification)

Gene expression was performed with KapaFast-SYBR Green and measurements were performed on a Bio-Rad iCycler iQ ™ Real-Time PCR detection system. Following the manufacturer`s protocol, the PCR reaction mix was prepared and plated out in a 96-well plate. The relative expression levels of mRNAs were normalized to GAPDH. The expression levels of the samples are provided as arbitrary units defined by the $\Delta\Delta C_T$ method. All measurements were performed in triplicates.

Melting curve analysis and agarose gel electrophoresis confirmed amplification specificity. The murine primers (see recipe) were used to detect IL-1β, IL-2, IL-4, IL-6, IL-10, IL-12, TGF-β, TNF-α, IFN-γ and NOS2 expression.

This table shows the mix for one well.

Component	Amount
Syber green	5 µl
Nuclease free water	3 µl
Primer (Forward & Reversible)	1 µl
Sample	1 µl
Total volume	**10 µl**

2.2.7.2   MicoRNA Isolation

Total RNA including miRNAs was extracted from BMDMs using miRNAeasy Kit. The miRNAs (100 ng) were separately reverse transcribed using miRNA universal cDNA synthesis kit for reverse transcript PCR (RT- PCR) and subsequent real-time quantitative PCR (qRT- PCR). Following the manufacturer`s protocol, briefly, 200 μl of chloroform was added to each sample (previously harvested and homogenized with TRIzol) and shaked vigorously for 15 seconds. Samples were incubated at room temperature for 2-3 minutes and centrifuged for 15 minutes at 12,000 x *g* at 4°C.The upper aqueous phase was transferred to a new collection tube, 1.5 volumes of 100% ethanol were added and mixed by pipetting up and down. Around 700 μl of each sample were transferred to RNeasy® Mini column in a 2 ml collection tube and centrifuged at 12,000 x *g* for 15 s at 4°C. The flow-through was discarded and 700 μl of buffer RWT was added to the RNeasy Mini column and centrifuged again for 15 s at 12,000 x *g*. The flow-through was discarded, 500 μl of buffer RPE was added to the RNeasy Mini column and centrifuged for 15 s at 12,000 x *g*. The flow-through was discarded again and 500 μl of buffer RPE was added to the RNeasy Mini column and centrifuged for 2 min at 12,000 x *g*. The RNeasy Mini column were placed into a new 2 ml collection tube and centrifuged at full speed for 1 min to further dry the membrane. To elute RNA, 30–50 μl of RNase-free water were added directly onto the RNeasy Mini column membrane after transferred the RNeasy Mini column to a new 1.5 ml collection tube and centrifuged for 1 min at 12,000 x *g*. The concentration of miRNA was determined using the biophotometer. Once calculated, the miRNA-cDNA synthesis step was started directly.

2.2.7.2.1   First-strand cDNA synthesis

Following the manufacturer`s protocol, the following components were added to each tube:

Component	Amount
5x Reaction buffer	2 μl
Enzyme Mix	1 μl
RNA (Total) =100ng	X μl
Nuclease free water	(7 μl - x)
Total volume	**10 μl**

The reaction was incubated for 60 minutes at 42°C then heated for 5 minutes at 95°C to inactivate the reverse transcriptase and immediately cooled to 4°C or stored at -20°C.

2.2.7.2.2 RT-PCR reaction

The cDNA templates were diluted (1:80) for the planned real-time PCR reactions in nuclease free water (e.g. add 395 µl of nuclease free water to each 5 µl of reaction). MicroRNA expression was performed with KapaFast-SYBR Green and measurements were performed on a Bio-Rad iCycler iQ^{TM} Real-Time PCR Detection System.

RT-PCR reaction:

Component	Amount
qPCR master mix –Syber green	5 µl
Diluted cDNA (1:80)	4 µl
PCR miRNA primer set	1 µl
Total volume	**10 µl**

The relative expression levels of miRNAs were normalized to 5S rRNA. The expression levels of the samples are provided as arbitrary units defined by the $\Delta\Delta C_T$ method. All measurements were performed in triplicates. Melting curve analysis and agarose gel electrophoresis confirmed amplification specificity. For amplification of different miRNAs (see recipe), hsa-miR-9-5p LNA™ PCR primer set, hsa-miR-10a-5p, has-miR-99b-5p, has-miR-146a-5p, has-miR-155-5p and reference 5S rRNA primer set were used and the reaction was set up as recommended by Exiqon.

2.2.7.2.3 PCR cycling conditions for miRCURY LNA miRNA PCR Assays

Assay	Time	Temperature
PCR initial heat activation	3 minutes	95°C
Denaturation	10 seconds	95°C
Combined annealing / extension	1 minutes	56°C
Number of cycles	40	
Melting curve analysis		60 - 95°C

2.2.8 Protein analysis methods

2.2.8.1 Lysis of cells

Whole cell protein extracts were obtained by direct lysis in 2x Laemmli Buffer diluted with H_2O to 1 x. Proteins were denatured at 95°C for 5-10 minutes and stored in -20°C.

2.2.8.2 SDS-polyacrylamide-gel electrophoresis (SDS-PAGE)

Equal amounts of proteins were separated on desired SDS polyacrylamide gels. The electrophoresis started with 80 V for 30 minutes and then changed to 120 V for 90 minutes. The components of gels are described in this table:

<u>**Separating (running) gel:**</u> For Bio-Rad mini gels, 10 ml are needed for each gel:

Components / Gel percentage	6%	8%	9%	10%	12%	15%	18%
Acry/Bis	2 ml	2.6 ml	2.9 ml	3.2 ml	3.8 ml	4.7 ml	5.6 ml
2M Tris pH 8.8	2 ml	2 ml	2 ml	2 ml	2 ml	2 ml	2 ml
H_2O	5.9 ml	5.3 ml	5 ml	4.7 ml	4.1 ml	3.2 ml	2.3 ml
20% SDS	50 µl	50 µl	50 µl	50 µl	50 µl	50 µ	50 µl
10% APS	50 µl	50 µl	50 µl	50 µl	50 µl	50 µl	50 µl
TEMD	5 µl	5 µl	5 µl	5 µl	5 µl	5 µl	5 µl

<u>**Stacking gel:**</u> 5 ml is needed for each gel.

Components /Gel	4%	5%
Acry/Bis	1.33 ml	1.25 ml
2M Tris pH8.8	2.5 ml	2.5 ml
H2O	6.1 ml	6.15 ml
20% SDS	50 µl	50 µl
10%APS	66.7 µl	66.7 µl
TEMD	12 µl	12 µl

2.2.8.3 Transfer of proteins on PVDF membrane

Proteins were transferred to PVDF membrane for 90 minutes at 25 V. Following blotting, proteins were stained with Ponceau S (0.1% in 5% acetic acid) in order to visualize and mark standard protein bands. The membrane was de-stained in water.

2.2.8.4 Protein detection

Nonspecific binding sites were blocked for 1 hour at RT with 3% BSA or 5% non-fat dry milk in Tris-buffered saline with 0.1% Tween.

Membranes were incubated overnight at 4°C with primary antibody (1:1000; see recipe): anti-ERK1/2, phospho-ERK1/2 (Thr202/Tyr204), AKT, phospho-AKT (T308) (C31E5E), mTOR, phospho-mTOR, TLR2, TLR4, SAPK/JNK, phospho-SAPK/JNK, p38, phospho-p38, Ikkβ, phospho-Ikkβ and anti-GAPDH (1:2000 dilution). Membranes were washed three times with TBS-T, followed by incubation with HRP-conjugated anti-rabbit secondary antibodies (1:1000). Protein complexes were visualized with enhanced chemiluminescent HRP substrate. For detection of signals, X-ray films or versa doc were used. To confirm loading control after detection of phosphorylated protein, membranes were stripped for 30 min at 50°C, blocked and re-probed with different antibodies against whole protein or GAPDH. Protein bands were quantified using *Image lab* & *ImageJ* software.

2.2.9 Enzyme linked immunosorbent assay (ELISA)

2.2.9.1 Cytokines determination in culture supernatants

Supernatants from co-culture assays were analyzed for IL-1β, IL-4, IL-6, IL-10, IL-12, TGF-β, TNF-α and IFN-γ production via sandwich ELISA kits recommended by eBioscience manufacturer's instructions. Cytokines were quantified by comparison to recombinant standard proteins.

2.2.10 Statistics

Given data are provided as means ± SEM. All data were tested for significance using unpaired Student's t-test or ANOVA (one way & two ways). Data were analysed by Excel 2010 or GraphPad Prism Software, USA. A value of $P \leq 0.05$ was statistically significant.

3 RESULTS

3.1 Phenotypic characterization of murine bone marrow derived macrophages (BMDMs) with directly conjugated cell surface antibodies

Bone marrow cells (BMCs) suspensions were prepared by flushing femurs and tibias of 8-12 week old mice as described in material and methods. BMCs were cultured for one week in DMEM complete media (see 2.2.3.3). The number of bone marrow cells obtained from each donor mice reached $70 \pm 10 \times 10^6$ cells. FACS-based analysis was used to verify the phenotypic characterization of BMDMs using fluorescently labeled monoclonal antibodies (mAbs) that specifically recognize proteins expressed by macrophages. Using flow cytometry, these sets of surface markers can be used to distinguish macrophages from other heterogeneous populations of hematopoietic cells. Three surface markers were used during the experiments, F4/80 and CD11b (Na, Jung et al. 2016), which are specific for macrophages as well as MHCII for non-macrophages. The inclusion of these markers in the analysis can provide information about the degree of non-macrophage cells in the cell suspension. After the cell suspension is incubated with the appropriate mAb cocktail, cells are processed for flow cytometry as described in detail in material and methods (see 2.2.5.1). The efficiency of differentiation was assessed directly after 7 days of culture in complete media. The data presented in Figure 13 revealed that the harvested BMCs were relatively favored to differentiate into macrophages with CD11b^{high} (almost 100%), F4/80^{high} (90% $\pm$ 7%) and MHCII^{low} (10% $\pm$ 4%).

A   **B**
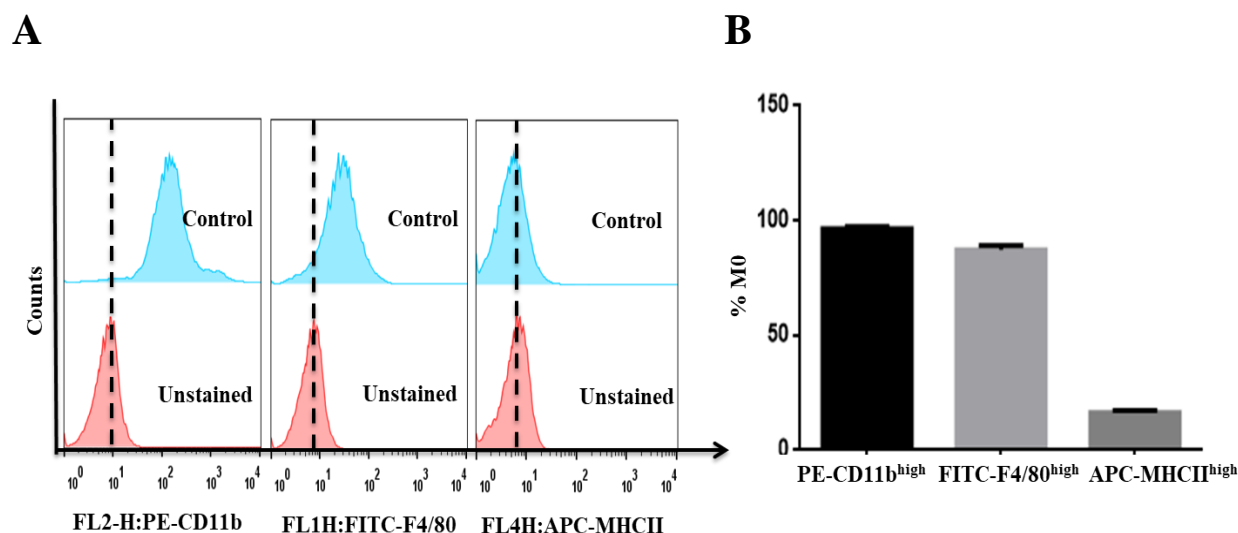
Figure 13 FACS phenotyping of BMDMs

Naive bone marrow cells were isolated and subsequently cultured for one week in DMEM complete media (M0) and then analyzed for macrophage markers. (A) FACS histogram displaying the harvested BMDMs (M0) which were defined as F4/80high, CD11bhigh and MHCIIlow. (B) Arithmetic means $\pm$ SEM (n = 5) of percentage of the positive gated populations of M0.

Data represented in Figure 14 revealed the second characterization after stimulation of BMDMs either with 1µg/ml of LPS or 6 Gy X-irradiation for 72h where all groups were still F4/80^{high}, CD11b^{high} and MHCII^{low}. Notably, F4/80 expression was higher in the LPS (with or without UA) group than irradiated (with or without UA) ones as compared to untreated control. But, CD11b expression was slightly higher in all groups compared to control as well as equal expression of MHCII$^+$ in all groups. In more detail, the F4/80 expression in BMDMs which received 50 µM UA, LPS, LPS+25 µM UA or LPS+50 µM UA (Figure 15) were significantly higher as compared to untreated control.
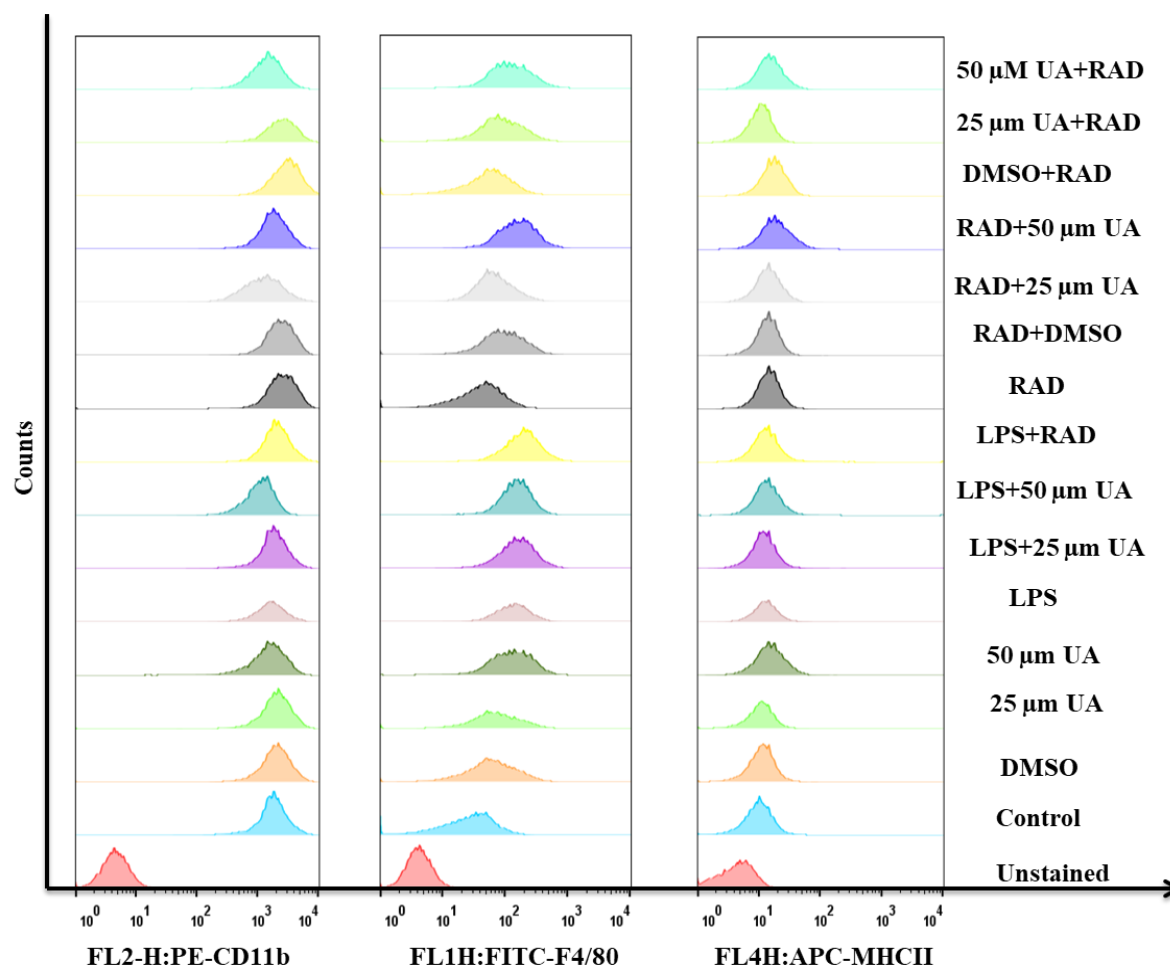
Figure 14 FACS phenotyping of BMDMs after 72h of stimulation (histogram)

Naive bone marrow cells were isolated and subsequently cultured for one week in DMEM complete media and then stimulated either with 1µg/ml LPS or 6 Gy X-irradiation in the presence or absence of UA. The radiated group was subdivided into two sub-groups, where one received UA (25 µM or 50 µM) 24h before irradiation and the other post-irradiation directly. FACS histogram displaying the expression of macrophage marker after 72h of desired treatment using CD11b, F4/80 and MHCII. Abbreviations: DMSO, dimethyl sulfoxide; UA, urolithin A; LPS, lipopolysaccharides; RAD, radiation.
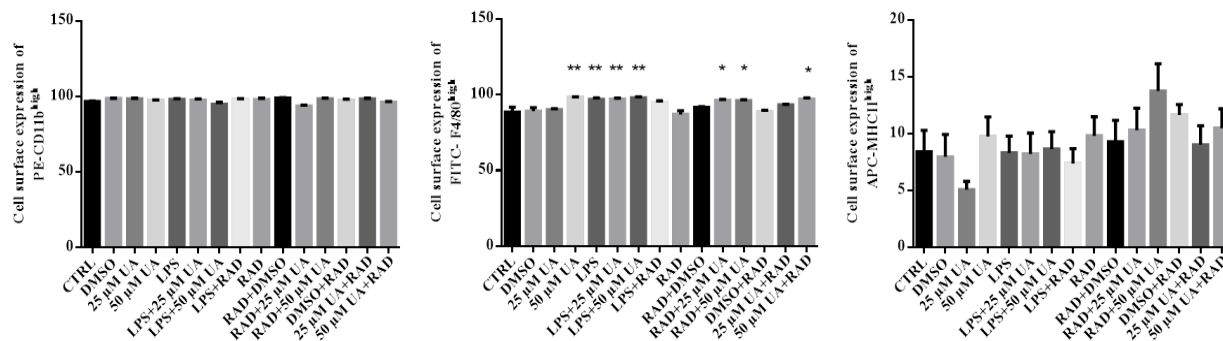
Figure 15 FACS phenotyping of BMDMs after 72h of stimulation (graph)

Naive bone marrow cells were isolated and subsequently cultured for one week in DMEM complete media and then stimulated either with 1µg/ml LPS or 6 Gy X-irradiation in the presence or absence of UA. The radiated group was subdivided into two sub-groups, where one received UA (25 µM or 50 µM) 24h before irradiation and the other post-irradiation directly. Arithmetic means ± SEM (n = 5) of percentage of the positive gated populations of stimulated macrophages. * (p<0.05) and ** (P<0.001) indicates statistically significant difference compared to control. Abbreviations: DMSO, dimethyl sulfoxide; UA, urolithin A; LPS, lipopolysaccharides; RAD, radiation.

3.2 Influence of urolithin A on the viability of murine BMDMs

Numerous studies suggested that UA influences various fundamental cell pathways such as apoptosis, cell proliferation of various cancer cell lines and primary cells including macrophages (Boakye, Groyer et al. 2018, Norden and Heiss 2018, Zhao, Shi et al. 2018, Gong, Huang et al. 2019, Zhang, Al-Maghout et al. 2019). Annexin-V (apoptosis) and Propidium Iodide (PI, necrosis) were used for measuring cell viability. BMDMs were treated with varying concentration of UA (for 72h) ranging from 10 µM - 300 µM to demonstrate the dose dependent effect on apoptosis (Figure 16). The observed data show that more than 95 % of the untreated control group were viable and non-apoptotic (Annexin V⁻ PI⁻).

Dot plots (Figure 16A) show the effects of two concentrations of UA on the stimulated BMDMs (LPS or irradiated) after 72h. Titration of BMDMs with different concentrations of UA revealed that the apoptotic effects start to appear after 50 µM and by increasing the concentration (above 50 µM), the percentage of apoptotic cells increased as illustrated in Figure 16B. According to these results, 25 µM UA and 50 µM UA were used for further experiments. As compared to untreated control, there was no significant change in all examined groups except a slightly decrease in the LPS group was observed (Figure 16C).
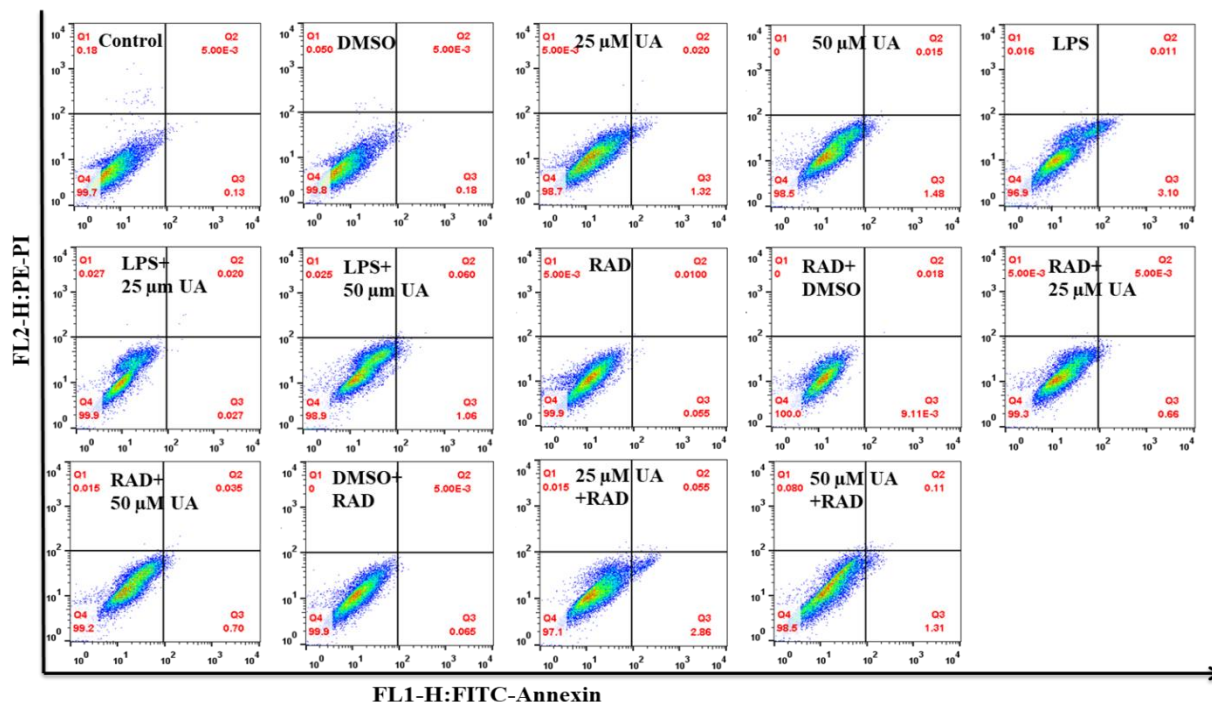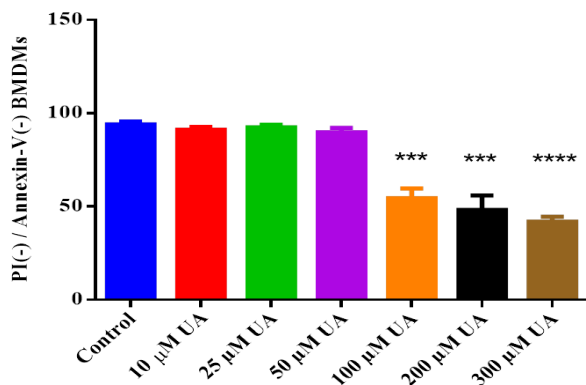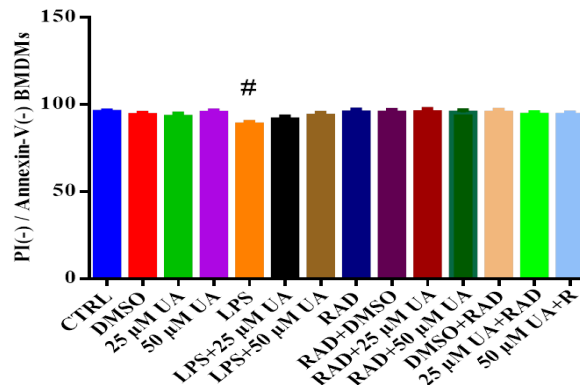
Figure 16 Influence of urolithin A on the viability of stimulated murine BMDMs after 72h

Naive bone marrow cells were isolated and subsequently cultured for one week in DMEM complete media and then stimulated either with 1µg/ml LPS or 6 Gy X-irradiation in the presence or absence of UA. The radiated group was subdivided into two sub-groups, where one received UA (25 µM or 50 µM) 24h before irradiation and the other post-irradiation directly. (A) Dot plots of mature BMDMs which were treated as indicated. After 72h the cell viability was measured by Annexin-V /PI compared to untreated control cells. (B) Arithmetic means ± SEM (n = 5) of BMDMs which were treated with different concentrations of UA for 72h. (C) Values show the percentage of live BMDMs Annexin-V⁻ /PI⁻ after indicated treatments. Arithmetic means ± SEM (n = 5). *** ($P<0.0001$) and # ($P<0.01$) indicate statistically significant differences compared to control. Abbreviations: DMSO, dimethyl sulfoxide; UA, urolithin A; LPS, lipopolysaccharides; RAD, radiation.

3.3 Urolithin A down-regulated intracellular calcium in LPS-stimulated or X-irradiated murine BMDMs

Intracellular calcium (Ca^{2+}) levels are essential indicators of any signaling mechanism involving Ca^{2+} as second messenger. Stimulation of cells including macrophages is involved with calcium influx across the cell membrane through ionophores and native calcium channels. This calcium influx or altered intracellular calcium concentration can be measured using a cell permeant dye, Fluo-4, which becomes fluorescent upon binding to calcium. The AM is a hydrophobic acetoxymethyl ester which allows passage across the cell membrane into viable cells and once inside the cell, intracellular non-specific esterases cleave the AM groups, leaving Fluo-4 free to bind intracellular calcium (Gee, Brown et al. 2000).
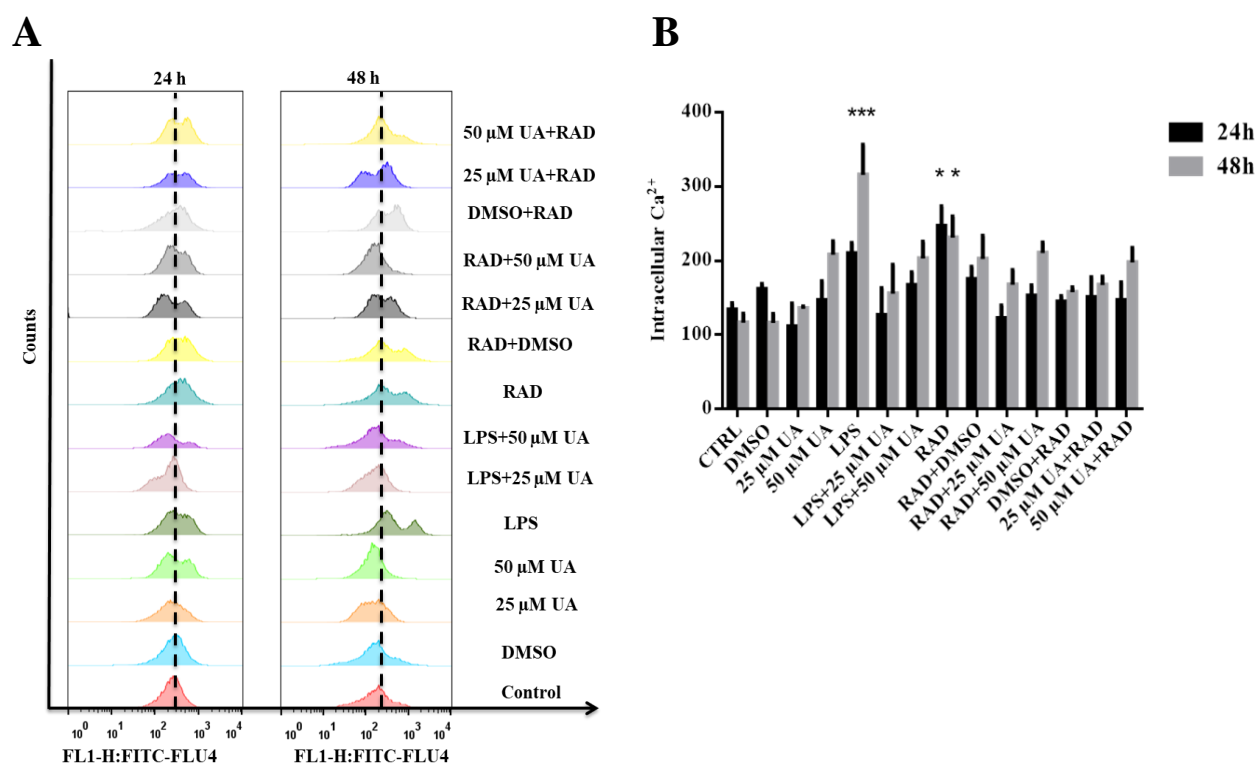
Figure 17 Influence of urolithin A on intracellular calcium in LPS-stimulated or X-irradiated murine BMDMs

BMDMs were stimulated either with 1μg/ml of LPS or 6 Gy of X-irradiation with or without UA (25 μM or 50 μM) for 24h or 48h. (A) Representative FACS histograms showing the effect of UA on stimulated BMDMs after 24h and 48h. The unstimulated BMDMs were used as untreated control. DMSO was used as negative control. The intracellular Ca^{2+} was measured with flow cytometry. The radiated group was subdivided into two sub-groups, where one received UA (25 μM or 50 μM) 24h before irradiation and the other post-irradiation directly. (B) Arithmetic means ± SEM (n = 5-7) show a significant difference in intracellular Ca^{2+} concentration between control and treated groups after 24h and 48h. Two way ANOVA was used * ($p < 0.05$) and *** ($p < 0.001$) indicate statistically significant differences compared to respective control. Abbreviations: DMSO, dimethyl sulfoxide; UA, urolithin A; LPS, lipopolysaccharides; RAD, radiation.

We were interested in studying the effect of UA (25 µM or 50 µM) on intracellular calcium levels after stimulating the BMDMs with 1µg/ml LPS or 6 Gy of X-irradiation for 24h and 48h. The obtained results showed that neither DMSO nor UA (25 µM or 50 µM) alone induced any significant change at all during the time intervals.

Results represented in Figure 17 show that stimulation of BMDMs with 1µg of LPS induced disturbance in intracellular calcium levels leading to a significant elevation after 24h and the upregulation keep going after 48h. The treatment of BMDMs with UA (25 µM or 50 µM) recorded a remarkable decrease of intracellular Ca^{2+} with values near to untreated control.

Concerning the X-irradiated BMDMs, a highly significant elevation of intracellular calcium was registered after 24h and 48h as compared to untreated control. Administration of UA pre- or post-irradiation was able to induce a significant decrease in intracellular calcium. The pre-administration of UA especially with 50 µM was able to preserve the values near to control during the time intervals.

In conclusion, UA was able to abolish the upregulation of intracellular calcium induced by LPS or X-irradiation in BMDMs after 24h and 48h. The source of variation between groups and time factor are summarized in supplementary Table 1.

3.4 Urolithin A diminished reactive oxygen species (ROS) production in LPS-stimulated or X-irradiated murine BMDMs

We were concerned in studying the effect of UA (25 µM or 50 µM) on ROS production in LPS-stimulated or X-irradiated BMDMs after 48h. The obtained results indicated that neither DMSO nor UA (25 µM or 50 µM) alone induced any significant changes in ROS production at all.

Results represented in Figure 18 depict a remarkable significant upregulation of ROS production levels in LPS-stimulated BMDMs after 48h. The treatment of BMDMs with UA (25 µM or 50 µM) recorded a remarkable decrease in ROS production with values near to untreated control.

Concerning the irradiated BMDMs, a highly significant elevation of ROS productions was registered after 48h as compared to untreated control. The administration of UA pre- or post-irradiation was able to induce significant improvement in the ROS production and preserved the values near to control ones.

In conclusion, the stimulation of BMDMs either with 1µg/ml of LPS or 6 Gy of X-irradiation induced equally remarkable elevation of ROS productions which were abolished by UA (25 µM or 50 µM) after 48h. The low concentration of UA (25 µM) achieved better results than the higher concentrations of UA (50 µM).

A

B
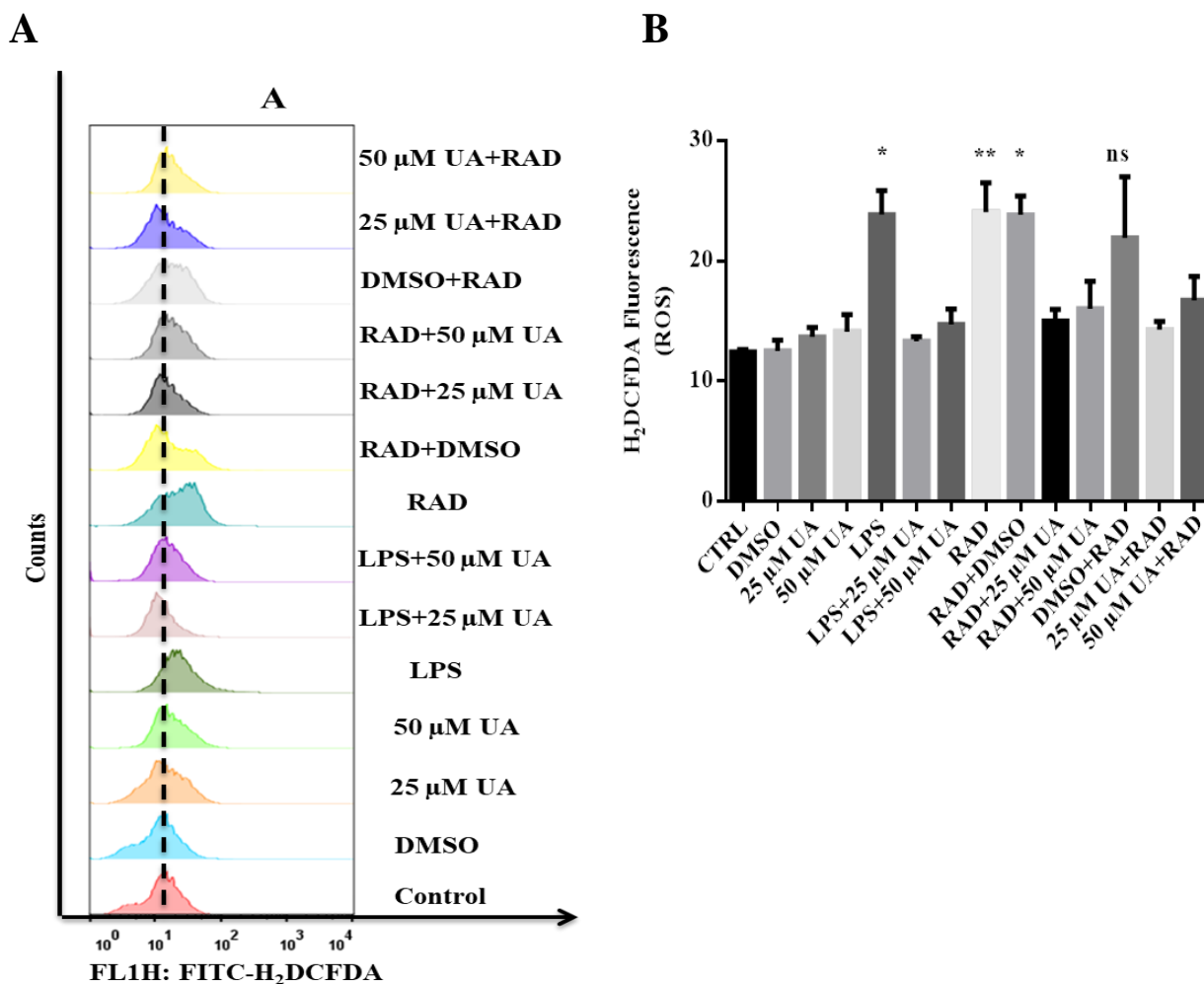
Figure 18 Influence of urolithin A on ROS production in LPS-stimulated or X-irradiated murine BMDMs

BMDMs were stimulated either with 1µg/ml of LPS or 6 Gy of X-irradiation in the presence or absence of UA (25 µM or 50 µM) for 48h. The irradiated group was subdivided into two sub-groups, where one received UA (25 µM or 50 µM) 24h before irradiation and the other post-irradiation directly. (A) Representative original FACS histograms showing the effect of UA on ROS production in LPS-stimulated or X-irradiated BMDMs after 48h. The unstimulated and untreated BMDMs were used as control. BMDMs treated with DMSO were used as negative control. The ROS production was measured with flow cytometry. (B) Arithmetic means ± SEM (n = 5-7). A significant difference in ROS production was observed between control and treated group after 48h. One way ANOVA was used and * (p < 0.05) and ** (P 0.01) indicate statistically significant differences compared to control. Abbreviations: DMSO, dimethyl sulfoxide; UA, urolithin A; LPS, lipopolysaccharides; RAD, radiation; ns, non-significant.

3.5 Urolithin A diminished the superoxide production in LPS-stimulated or X-irradiated murine BMDMs

BMDMs were stimulated either by 1 µg/ml LPS or 6 Gy X-irradiation in the presence or absence of UA (25 µM or 50 µM). BMDMs were then labeled with MitoSOX ™ Red reagent, which can be detected in red fluorescence when oxidized by superoxide, and nuclei were stained with blue – fluorescent DAPI. The obtained results showed that neither UA nor DMSO alone induce any significant changes on superoxide productions in murine BMDMs after 48h (Figure 19 and Figure 20).

Data represented in Figure 19 demonstrate that after 48h of LPS stimulation, BMDMs exhibited red immunofluorescence, indicating the highly significant changes in superoxide production as compared to untreated control cells. The post-administration of UA (25 µM or 50 µM) was able to inhibit the superoxide productions achieving values near to untreated control (Figure 20).

On the other hand, the immunofluorescence of live cell imaging and respective quantification of irradiated BMDMs demonstrated a significantly higher production of superoxide after 48h as compared to unradiated control. The administration of UA (25 µM or 50 µM) 24h pre- or post-irradiation inhibits the superoxide productions and preserved the values near to control (Figure 19 and Figure 20).

In conclusion, the mitochondria of stimulated BMDMs displayed a remarkable rising in red fluorescence after 48h, whereas the UA treated BMDMs showed a decrease in red fluorescence as compared to stimulated ones. The untreated or unstimulated BMDMs exhibited minimal fluorescence (Figure 19 and Figure 20). Notably, 25 µM UA exhibited a better effect than 50 µM UA.
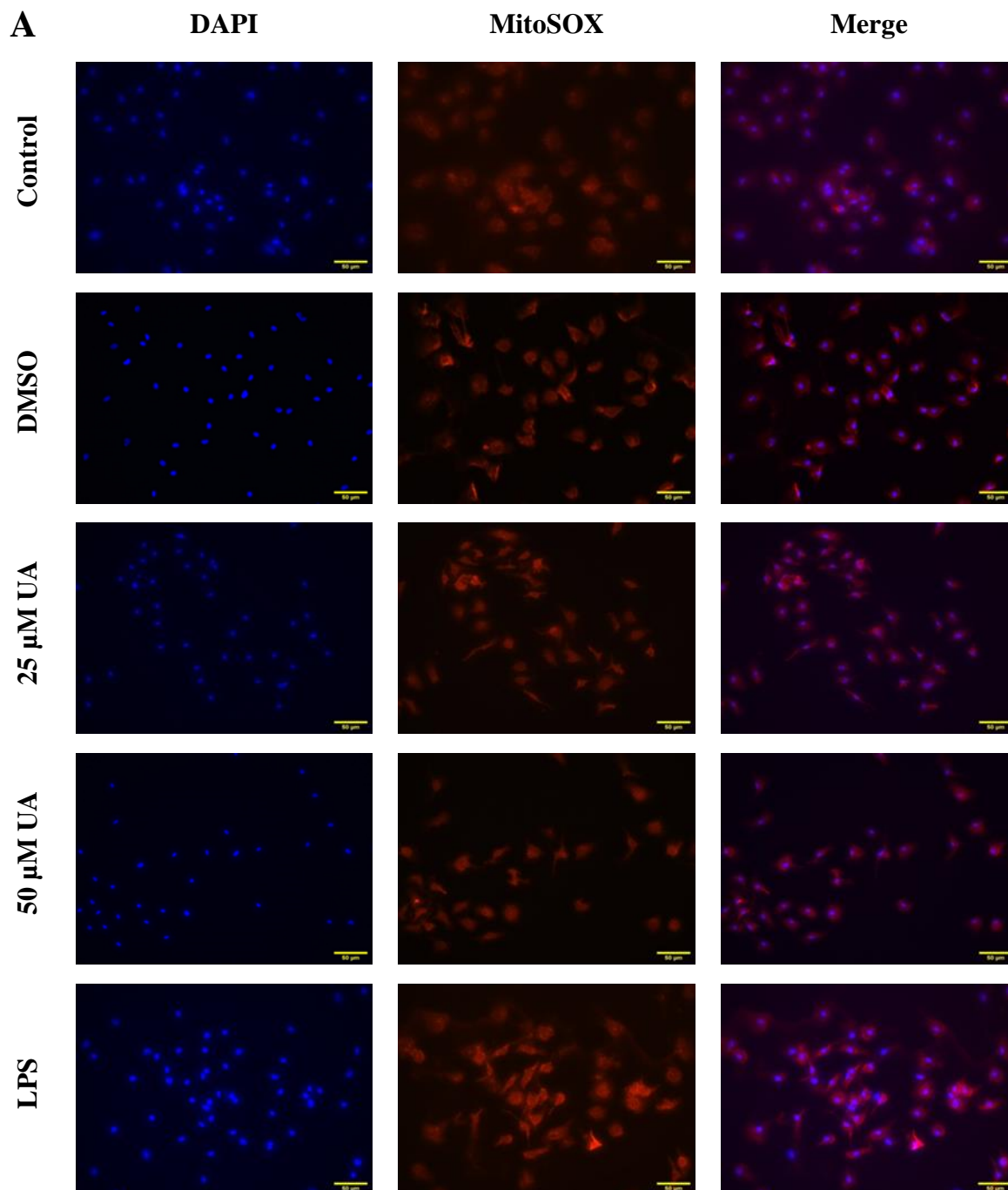
Figure 19 Effect of urolithin A on superoxide production in LPS-stimulated or X-irradiated murine BMDMs using MitoSOX ™ Red superoxide indicator

(A) BMDMs were stimulated either by UA (25 µM or 50 µM) or 1µg/ml of LPS for 48h. UA alone did not record any observable changes. Stimulation of BMDMs with LPS induced remarkable elevation of superoxide production demonstrated by red immunofluorescence while nuclei were counterstained with DAPI (blue). Scale bar represents 50 µm. The unstimulated and untreated murine BMDMs were used as control. Murine BMDMs treated with DMSO were used as negative control. Abbreviations: DMSO, dimethyl sulfoxide; UA, urolithin A; LPS, lipopolysaccharides.
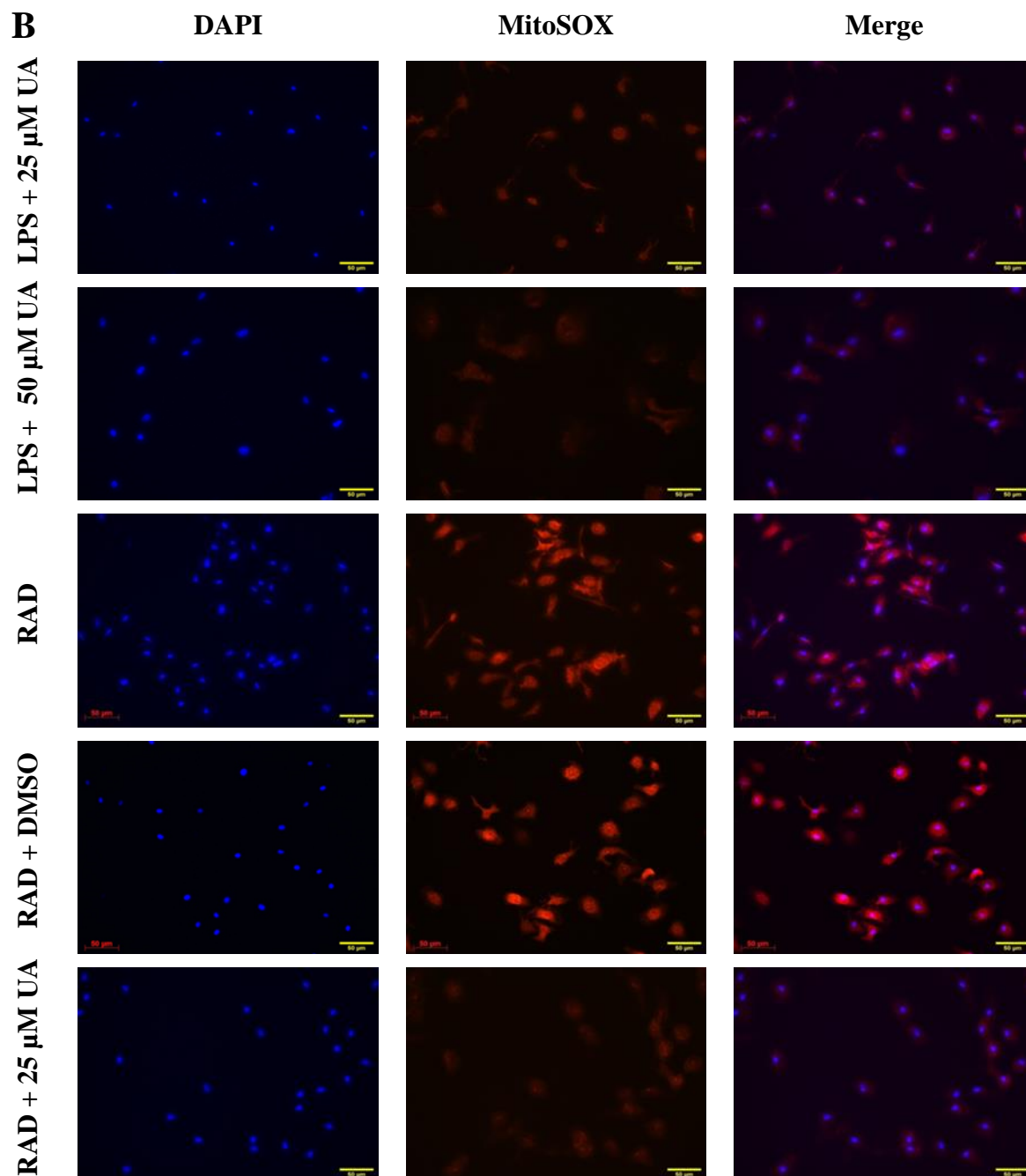
Figure 19 Continued: Effect of urolithin A on superoxide production in LPS-stimulated or X-irradiated murine BMDMs using MitoSOX ™ Red superoxide indicator

(B) BMDMs were stimulated either by 1µg/ml of LPS or 6 Gy of X-irradiation in the presence or absence of UA (25 µM or 50 µM) for 48h. The irradiated group was subdivided into two sub-groups, where one received UA (25 µM or 50 µM) 24h before irradiation and the other post-irradiation directly. Treatment of LPS-stimulated BMDMs with UA induced remarkable decrease of superoxide production demonstrated by obvious downregulation in red immunofluorescence while nuclei were counterstained with DAPI (blue). Post-administration of UA (25 µM) decreased the higher elevation of superoxide production induced by X-irradiation ± DMSO. Scale bar represents 50 µm. Abbreviations: DMSO, dimethyl sulfoxide; UA, urolithin A; LPS, lipopolysaccharides; RAD, radiation.

Figure 19 Continued: Effect of urolithin A on superoxide production in LPS-stimulated or X-irradiated murine BMDMs using MitoSOX ™ Red superoxide indicator

(C) BMDMs were stimulated with 6 Gy of X-irradiation in the presence or absence of UA (25 µM or 50 µM) for 48h. The irradiated group was subdivided into two sub-groups, where one received UA (25 µM or 50 µM) 24h before irradiation and the other post-irradiation directly. The pre- and post-administration of UA decreased the higher elevation of superoxide production induced by X-irradiation ± DMSO demonstrated an obvious decrease in red immunofluorescence. Nuclei were counterstained with DAPI (blue). BMDMs stained with DAPI without MitoSOX is also indicated. Scale bar represents 50 µm. Abbreviations: DMSO, dimethyl sulfoxide; UA, urolithin A; RAD, radiation; WO, without.
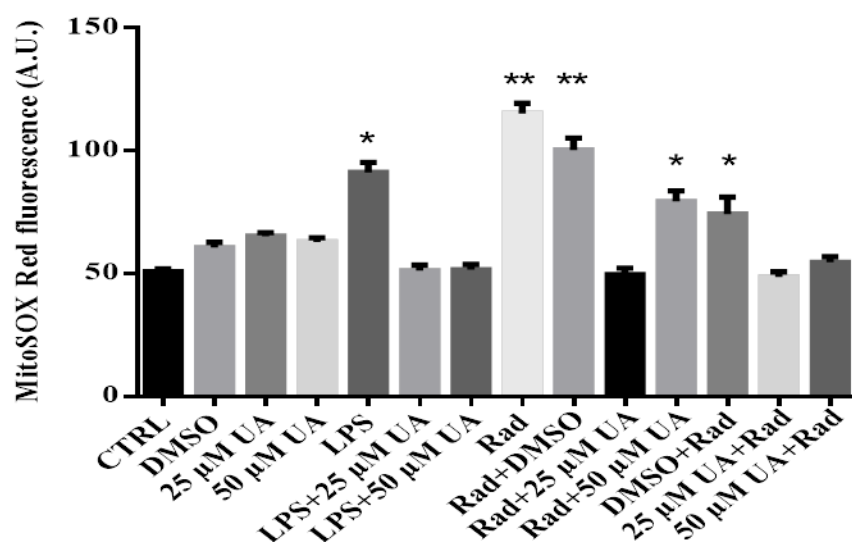
Figure 20 Quantification of superoxide production in LPS-stimulated or X-irradiated murine BMDMs using MitoSOX ™ Red superoxide indicator

BMDMs were stimulated either by 1μg/ml of LPS or 6 Gy of X-irradiation in the presence or absence of UA (25 μM or 50 μM) for 48h. Graph indicates the fluorescence intensity of superoxide production in BMDMs (n = 4 and 600 cells were counted). The unstimulated and untreated BMDMs were used as control. Murine BMDMs treated with DMSO were used as negative control. The radiated group was subdivided into two sub-groups, where one received UA (25 μM or 50 μM) 24h before irradiation and the other post-irradiation directly. Arithmetic means ± SEM. One way ANOVA was used and * (p < 0.05) and ** (P 0.01) indicate statistically significant differences compared to control. Abbreviations: DMSO, dimethyl sulfoxide; UA, urolithin A; LPS, lipopolysaccharides; RAD, radiation.

3.6 Effect of urolithin A on γ-H2AX phosphorylation in LPS-stimulated or X-irradiated murine BMDMs

Ionizing radiation (IR) generate a wide variety of DNA damage, among them double-strand breaks (DSBs), which considered the main actor responsible for cell death. These lesions can block genome replication and transcription, and if they are not repaired or improperly repaired, DSBs lead to mutations or chromosomal aberrations, which threaten the cell and induce human disorders including cancer (Jackson and Bartek 2009, Noda 2018). The early cellular response to DSBs in mammalian cells is the rapid phosphorylation of H2AX, the minor histone H2A variant, at Ser-139 to produce γ-H2AX (Redon, Pilch et al. 2002).

We were interested in studying the single shot dose scenario (6 Gy X-irradiation) and evaluating the effect of UA on DSBs induced by X-irradiation in BMDMs as well as investigating the impact of LPS-stimulation on DSBs in the presence or absence of UA in BMDMs. BMDMs were fixed and immunostained at different time intervals (2h and 48h) for phosphorylated H2AX (Ser139) after X-irradiation or LPS exposure.

As expected neither UA (25 μM or 50 μM) nor DMSO alone induced any significant effect on DSBs in BMDMs after 2h (Figure 21) and 48h (Figure 22). After 2h of LPS stimulation, immunofluorescence images did not show remarkable significant changes as compared to control cells (Figure 21). While, a highly significant increase of γH2AX foci was observed after 48h and the post-administration of UA (25 μM or 50 μM) was able to inhibit or repair the DSBs achieving values near to untreated control.

On the other hand, the immunofluorescence images and respective quantification of irradiated BMDMs demonstrated a significant higher number of γ-H2AX foci after 2h (Figure 21) which recorded a notably decrease after 48h of exposure but still significantly higher as compared to unradiated control (Figure 22). Administration of UA (25 μM or 50 μM) 24h pre- or post-irradiation induce decrease in DSBs and preserved the number of γ-H2AX foci near to control.

In conclusions, a higher significant number of γ-H2AX foci were observed in LPS (after 48h) and in irradiated (after 2h and 48h) BMDMs (Figure 23). Noteworthy, a prominent self-repair was recorded after 48h of irradiation compared to those observed at 2h. UA was able to induce a prominent decrease in DSBs. The source of variation between group factor and time factor are summarized in supplementary Table 2.
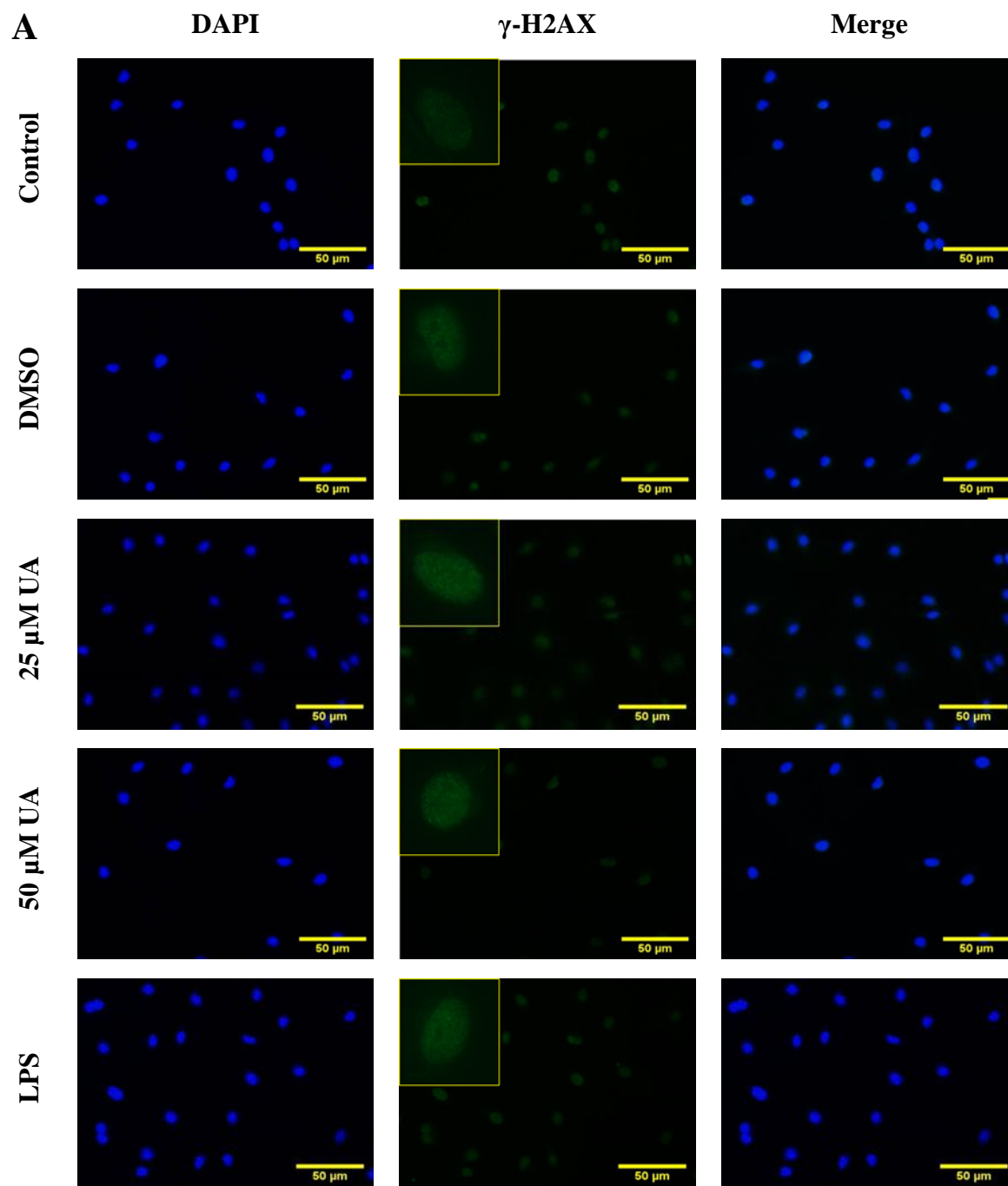
Figure 21 Influence of urolithin A on DSBs induced by LPS-stimulation or X-irradiation in murine BMDMs after 2h

(A) BMDMs were stimulated either by UA (25 μM or 50 μM) or 1μg/ml of LPS for 2h. Both UA and LPS did not register any significant effect on DSBs after 2h. Nuclei were counterstained with DAPI (blue). Scale bar represents 50 μm. The unstimulated and untreated BMDMs were used as control. BMDMs treated with DMSO were used as negative control. Abbreviations: DMSO, dimethyl sulfoxide; UA, urolithin A; LPS, lipopolysaccharides.
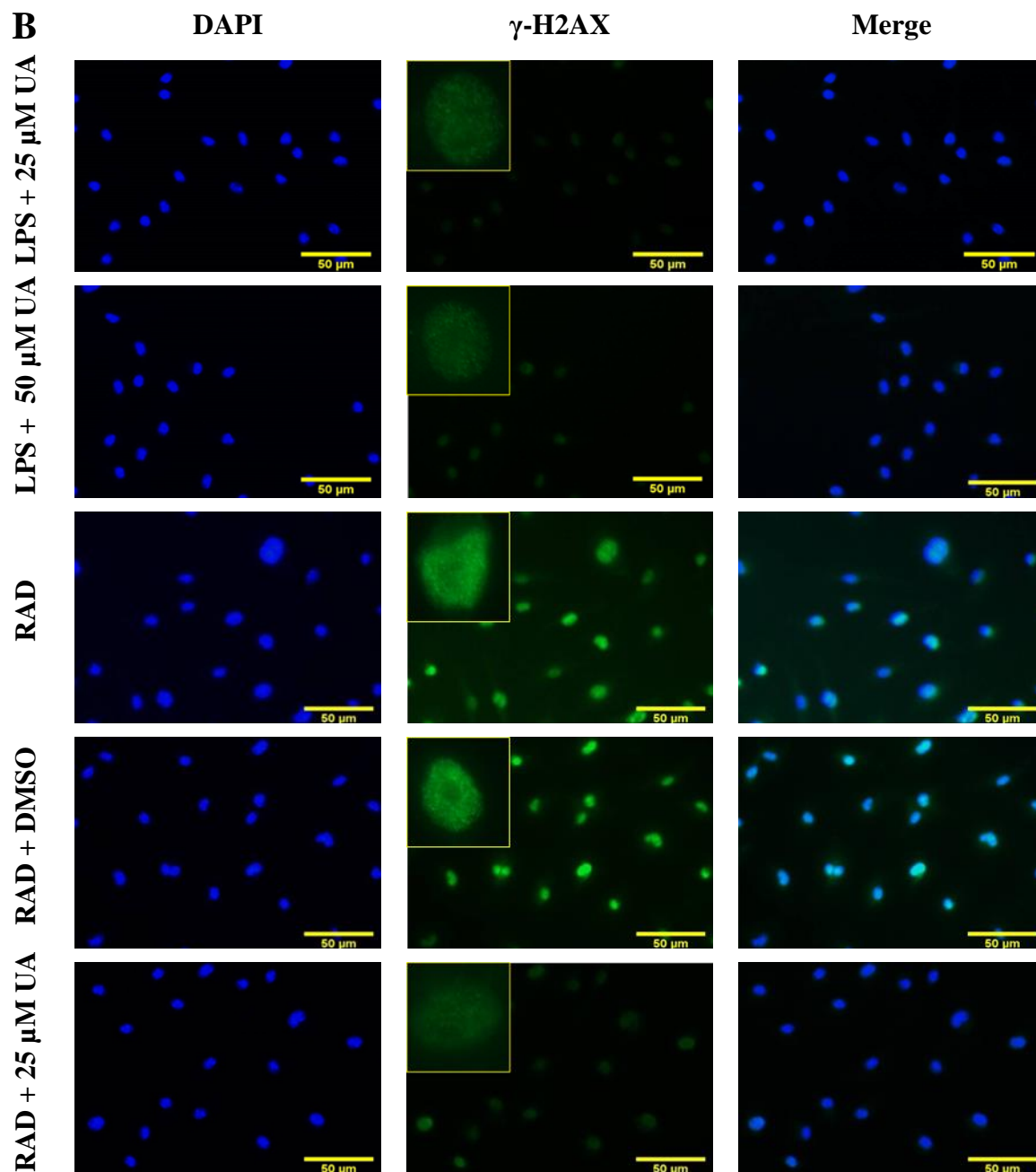
Figure 21 Continued: Influence of urolithin A on DSBs induced by LPS-stimulation or X-irradiation in murine BMDMs after 2h

(B) BMDMs were stimulated either by 1µg/ml of LPS or 6 Gy of X-irradiation in the presence or absence of UA (25 µM or 50 µM) for 2h. The irradiated group was subdivided into two, where one received UA before 24h of irradiation and the other one received it directly post-irradiation. Treatment of LPS-stimulated BMDMs with UA preserves the number of γH2AX foci as compared to control. X-irradiation ± DMSO induced DSBs which is demonstrated by a prominent green immunofluorescence for Ser139-phosphorylated H2AX (γ H2AX). Post-administration of UA (25 µM) repaired DSBs induced by X-irradiation. Nuclei were counterstained with DAPI (blue). Scale bar represents 50 µm. Abbreviations: DMSO, dimethyl sulfoxide; UA, urolithin A; LPS, lipopolysaccharides; RAD, radiation.

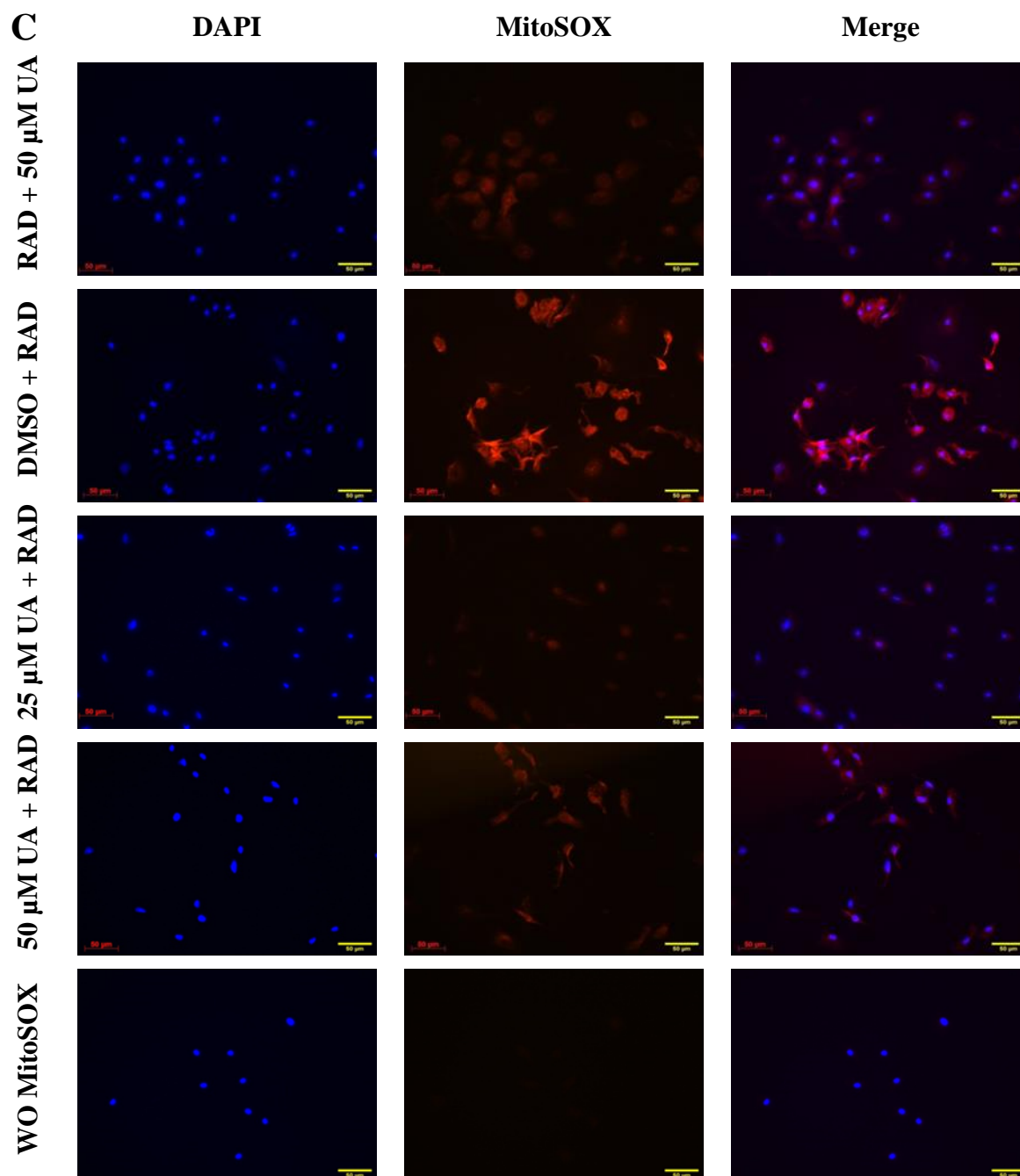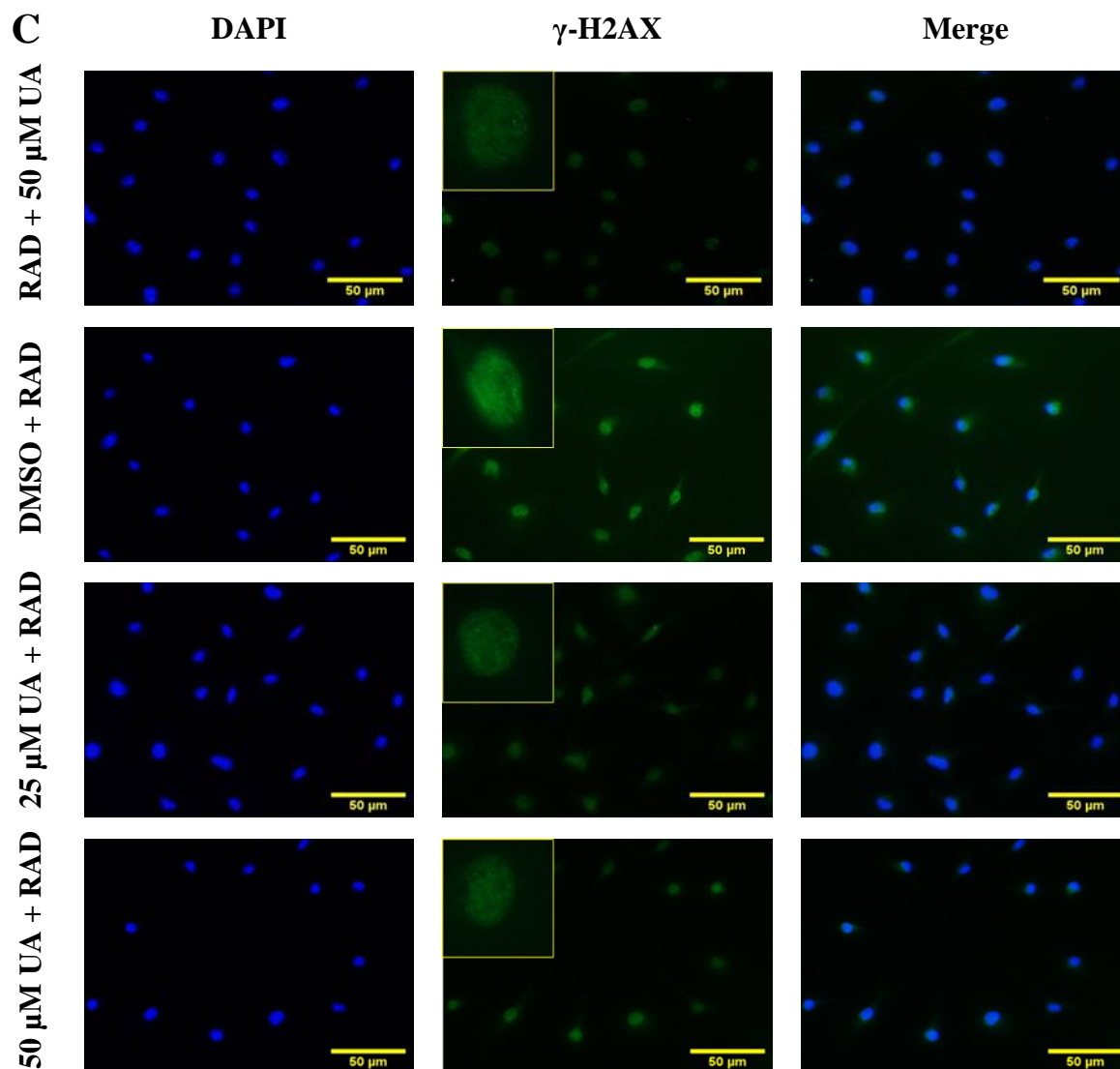**Figure 21 Continued: Influence of urolithin A on DSBs induced by LPS-stimulation or X-irradiation in murine BMDMs after 2h**

(C) BMDMs were stimulated with 6 Gy of X-irradiation in the presence or absence of UA (25 μM or 50 μM) for 2h. The irradiated group was subdivided into two, where one received UA (25 or 50 μM) 24h before irradiation and the other one received it directly post-irradiation. The pre- and post-administration of UA repaired the DSBs induced by X-irradiation ± DMSO demonstrated by obvious decrease in green immunofluorescence of Ser139-phosphorylated H2AX. Nuclei were counterstained with DAPI (blue). Scale bar represents 50 μm. Abbreviations: DMSO, dimethyl sulfoxide; UA, urolithin A; LPS, lipopolysaccharides; RAD, radiation.
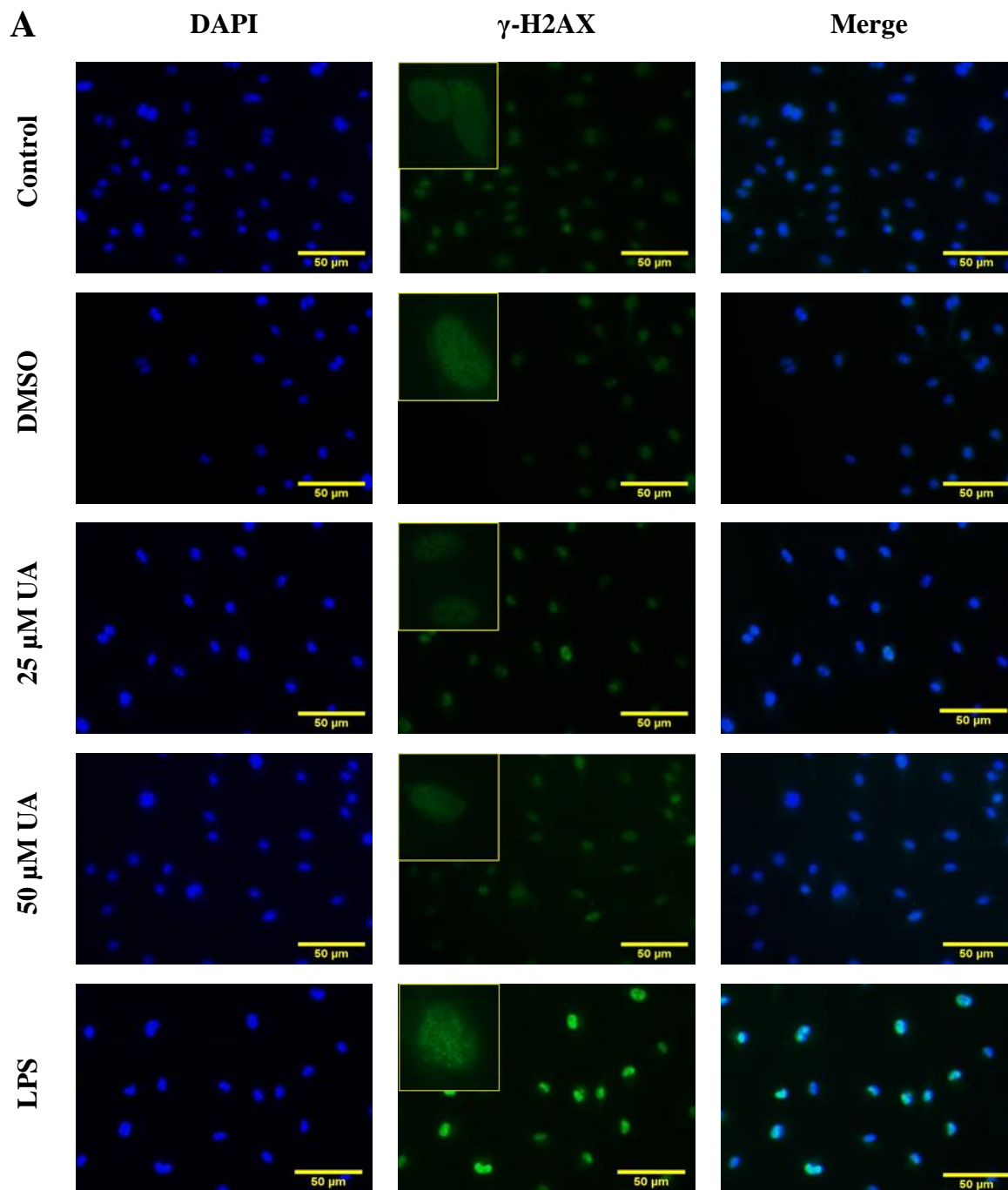
Figure 22 Influence of urolithin A on DSBs induced by LPS-stimulation or X-irradiation in murine BMDMs after 48h

(A) BMDMs were stimulated either by UA (25 µM or 50 µM) or 1µg/ml of LPS for 48h. LPS induced DSBs indicated by a prominent green immunofluorescence for Ser139-phosphorylated H2AX. Nuclei were counterstained with DAPI (blue). Scale bar represents 50 µm. The unstimulated and untreated BMDMs were used as control. BMDMs treated with DMSO were used as negative control. UA did not register any significant effect on DSBs after 48h. Abbreviations: DMSO, dimethyl sulfoxide; UA, urolithin A; LPS, lipopolysaccharides.
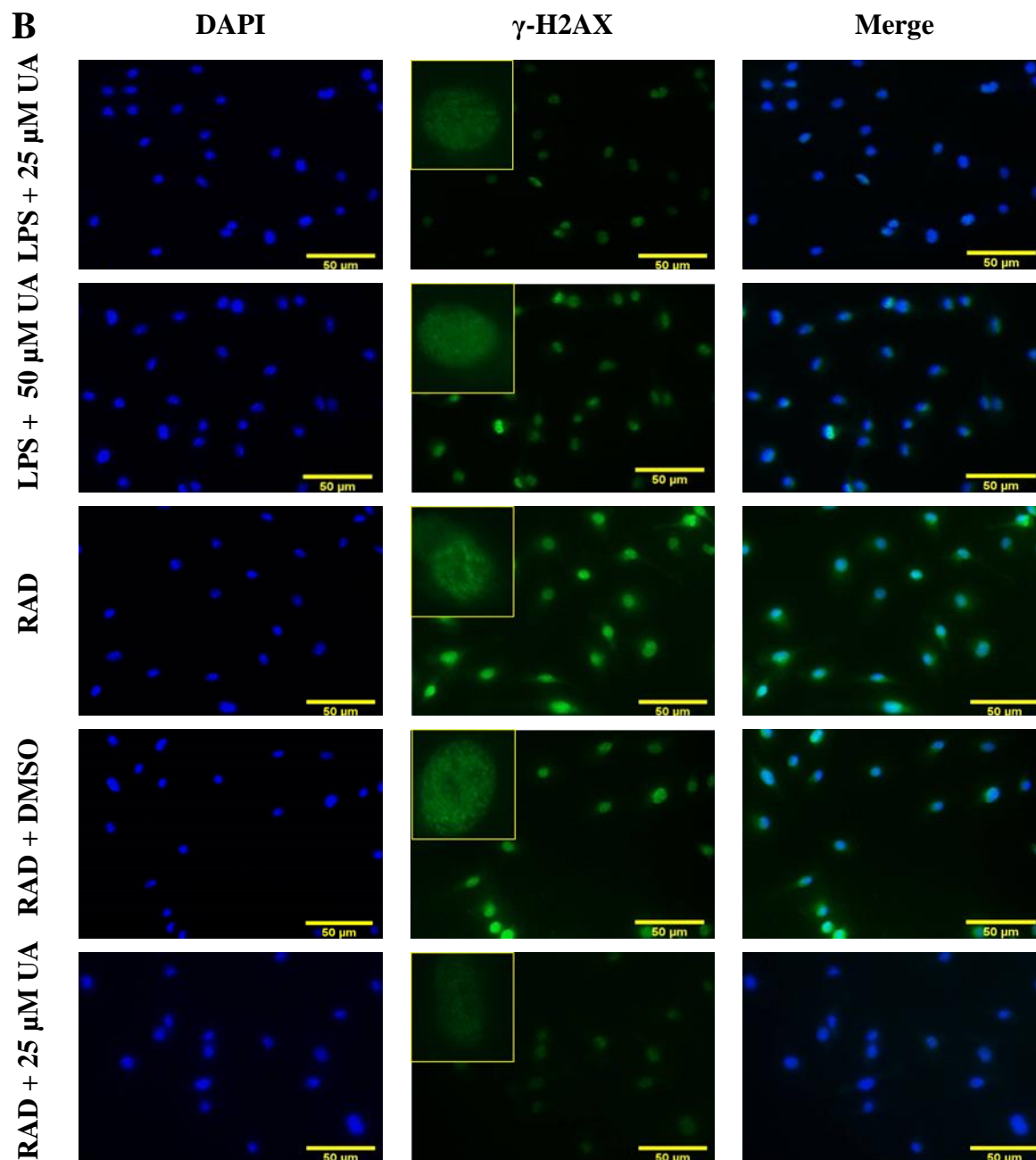
Figure 22 Continued: Influence of urolithin A on DSBs induced by LPS-stimulation or X-irradiation in murine BMDMs after 48h

(B) BMDMs were stimulated either by 1µg/ml of LPS or 6 Gy of X-irradiation in the presence or absence of UA (25 µM or 50 µM) for 48h. The irradiated group was subdivided into two, where one received UA 24h before irradiation and the other one received it directly post-irradiation. Treatment of LPS-stimulated BMDMs with UA induced prominent decrease in number of γH2AX foci. X-irradiation ± DMSO induced DSBs which are demonstrated by green immunofluorescence for Ser139-phosphorylated H2AX (γH2AX). Post-administration of UA 25 µM induced obvious decrease in DSBs induced by X-irradiation. Nuclei were counterstained with DAPI (blue). Scale bar represents 50 µm. Abbreviations: DMSO, dimethyl sulfoxide; UA, urolithin A; LPS, lipopolysaccharides; RAD, radiation.
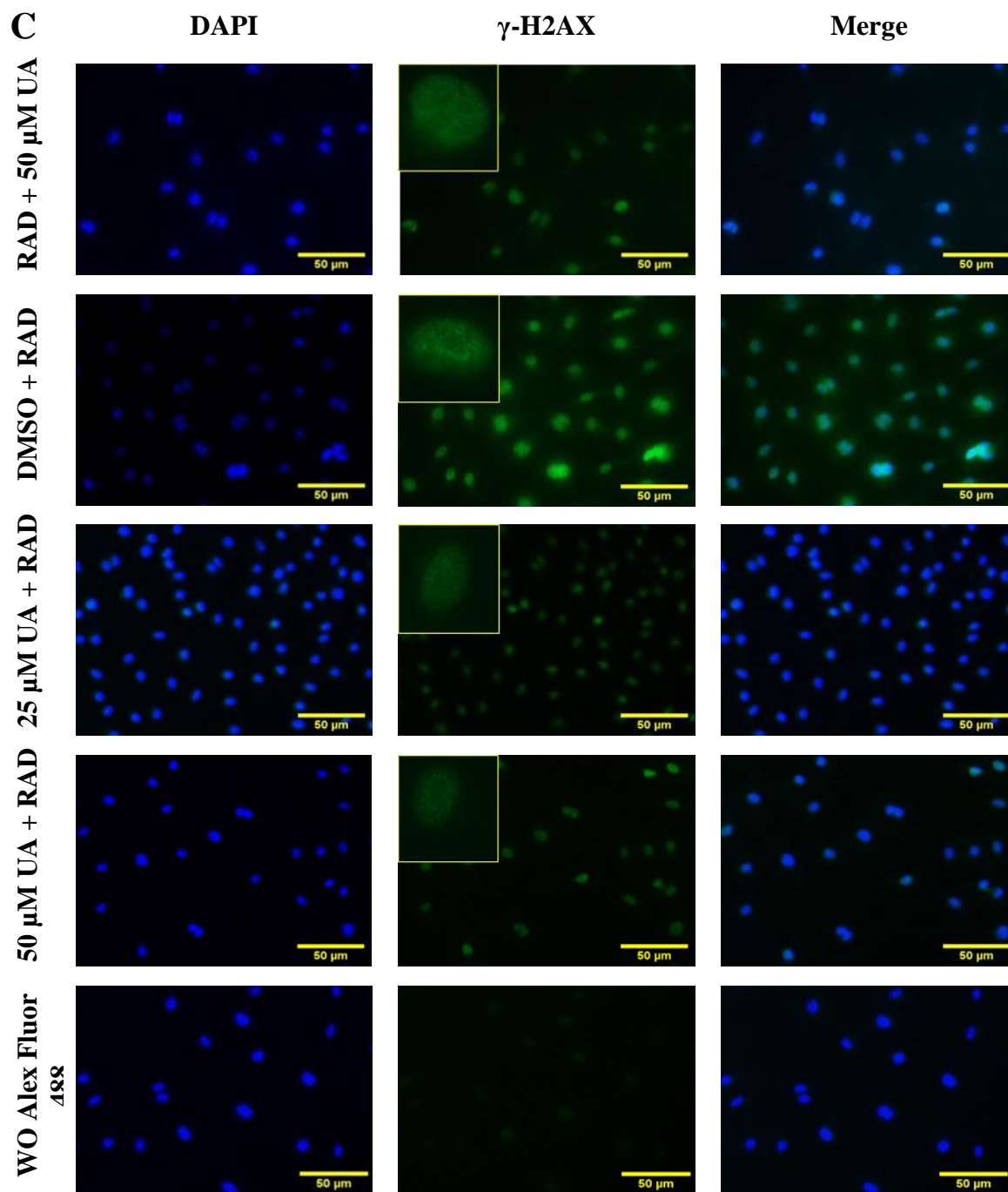
Figure 22 Continued: Influence of urolithin A on DSBs induced by LPS-stimulation or X-irradiation in murine BMDMs after 48h

(C) BMDMs were stimulated with 6 Gy of X-irradiation in the presence or absence of UA (25 µM or 50 µM) for 48h. The irradiated group was subdivided into two, where one received UA 24h before irradiation and the other one received it directly post-irradiation. The pre- and post-administration of UA decreased DSBs induced by X-irradiation which is demonstrated by obvious decrease in green immunofluorescence of Ser139-phosphorylated H2AX. Nuclei were counterstained with DAPI (blue). BMDMs without Alexa Fluor 488 are also indicated. Scale bar represents 50 µm. Abbreviations: DMSO, dimethyl sulfoxide; UA, urolithin A; RAD, radiation; WO, without.
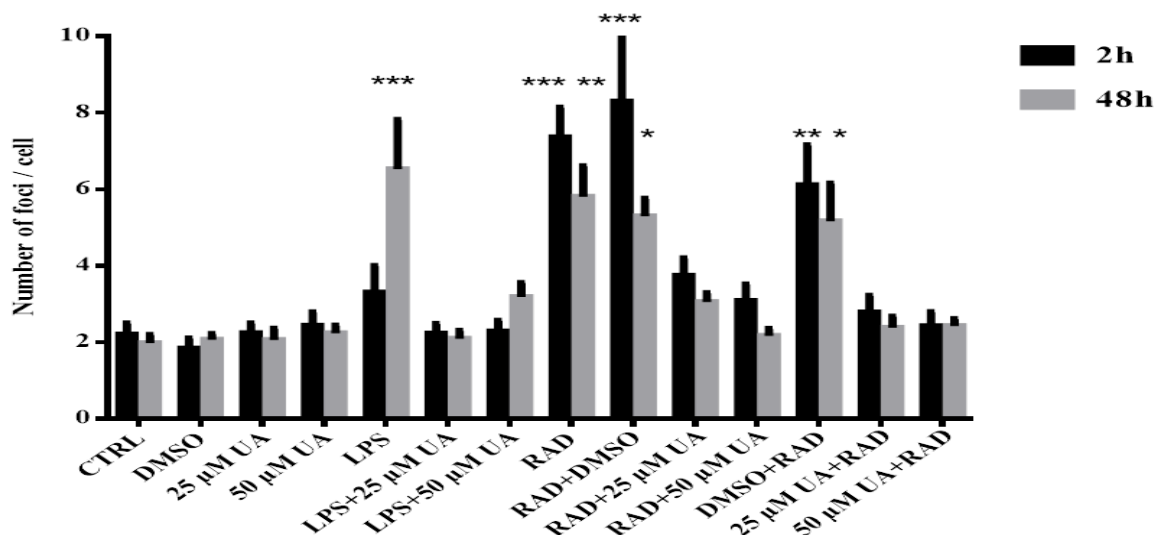
Figure 23 Influence of urolithin A on DNA double strand breaks induced by LPS-stimulation or X-irradiation in murine BMDMs after 2h and 48h

BMDMs were stimulated either by 1µg/ml of LPS or 6 Gy of X-irradiation in the presence or absence of UA (25 µM or 50 µM) for 48h. Graph indicates the number of γ H2AX foci per cell after indicated time points. The unstimulated and untreated BMDMs were used as control. BMDMs treated with DMSO were used as negative control. The irradiated group was subdivided into two, where one received UA (25 or 50 µM) before 24h of irradiation and the other one received it directly post-irradiation. Arithmetic means ± SEM from four independent experiments (600 cells were counted). Two way ANOVA was used and * (p < 0.05), ** (P 0.01), and *** (p < 0.001) indicate statistically significant differences compared to respective control. Abbreviations: DMSO, dimethyl sulfoxide; UA, urolithin A; LPS, lipopolysaccharides; RAD, radiation.

3.7 Effect of urolithin A on TLR signalling pathway in LPS-stimulated or X-irradiated murine BMDMs

As mentioned before, TLRs are well-studied PRRs that are essential for detecting PAMPs and mediate the induction of pro-inflammatory cytokines and costimulatory cell-surface molecules through the activation of transcription factors such as NF-κB (Travassos, Girardin et al. 2004). TLRs are receptive to various components of bacterial cell walls and the best-characterized TLRs are TLR2 and TLR4. Whereas TLR2 recognizes several molecules including lipoteichoic acid (LTA), lipoarabinomannan, lipoproteins and peptidoglycan (PG) and TLR4 recognizes LPS, they subsequently initiate host defense responses against bacteria (Yoshino, Chiba et al. 2014). In the present study, the effects of LPS or X-irradiation on TLR2 and TLR4 expression in the presence or absence of UA (25 µM or 50 µM) were investigated in BMDMs.

3.7.1 Effect of urolithin A on TLR4 expression in LPS-stimulated or X-irradiated murine BMDMs

The influence of UA (25 µM or 50 µM) on TLR4 expression in stimulated BMDMs (LPS or X-irradiation) was investigated. As shown in Figure 24, murine BMDMs expressed TLR4 on the cell surface. The exposure of BMDMs to 1 µg/ml LPS induced remarkable elevations in TLR4 expression after 72h compared to untreated control.

BMDMs receiving both concentrations of UA (25 µM or 50 µM) alone did not record observable changes in TLR4 expression unless a slight decrease was noticed after 72h compared to control. Treatment of LPS-stimulated BMDMs with UA (25 µM or 50 µM) exhibits slightly remarkable changes. Surprisingly, the post-administration of 25 µM UA to LPS-stimulated BMDMs preserved the higher TLR4 expression induced by LPS alone after 48h.

Similarly, the expression of TLR4 in X-irradiated BMDMs was significantly higher than in non-irradiated cells. The pre- and post-administration of 25 µM UA or 50 µM UA was able to induce remarkable downregulations in TLR4 expression achieving values near to control.

In conclusions, both LPS and X-irradiation induced higher expression of cell surface TLR4 in BMDMs. The expression of TLR4 was higher in LPS stimulation than X-irradiated BMDMs. UA (25 µM or 50 µM) was able to induce a remarkable decrease in TLR4 expression in X-irradiated BMDMs but not significant in LPS-stimulated ones.

A
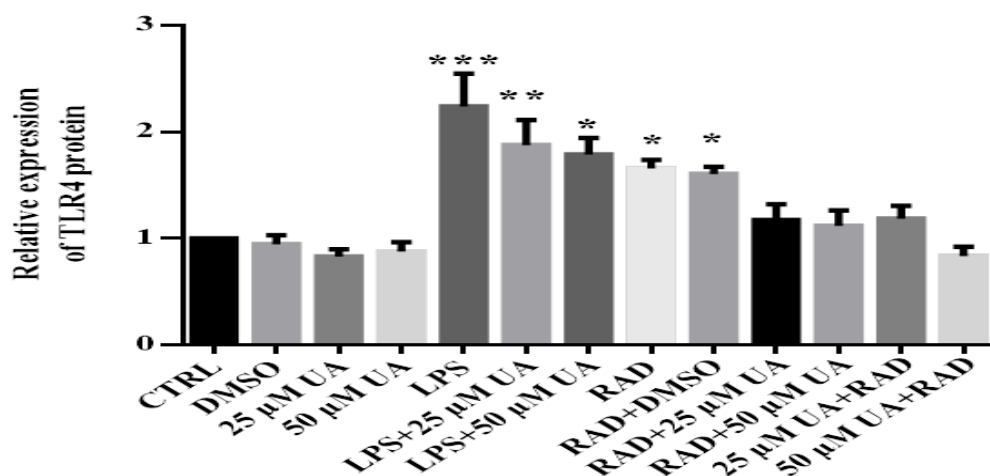
B

Figure 24 Sensitivity of TLR4 expressions to urolithin A in LPS-stimulated or X-irradiated BMDMs

BMDMs were stimulated either by 1μg/ml of LPS or 6 Gy of X-irradiation in the presence or absence of UA (25 μM or 50 μM), harvested after indicated time points and subjected to western blot. The irradiated group was subdivided into two, where one received UA (25 or 50 μM) before 24h of irradiation and the other one received it directly post-irradiation. (A) Bar graph represents relative density normalized to GAPDH after 72h. The unstimulated and untreated BMDMs were used as control. BMDMs treated with DMSO were used as negative control. Data are shown as means ± SEM from four independent experiments. One way ANOVA was used and * ($p < 0.05$) and ** ($p < 0.001$) indicate statistically significant differences compared to control. (B) Representative images of n = 4 for 72h and n = 1 for other time points. Abbreviations: DMSO, dimethyl sulfoxide; LPS, lipopolysaccharides; UA, urolithin A; RAD, radiation; TLR, Toll like receptor.

3.7.2 Effect of urolithin A on TLR2 expression in LPS-stimulated or X-irradiated murine BMDMs

The impact of UA (25 µM or 50 µM) on TLR2 expression in LPS-stimulated or X-irradiated BMDMs was investigated. As shown in Figure 25, BMDMs expressed TLR2. Surprisingly, treatment of BMDMs with UA (25 µM or 50 µM) alone exhibited a significant elevation in TLR2 expression compared to untreated control. In addition, the TLR2 expression was more obviously and higher expressed with the low concentration of 25 µM UA than 50 µM UA.

The stimulation of BMDMs with 1µg of LPS induced significant elevation in TLR2 expression after 2h and increased further until later time points. Unexpectedly, the treatment of LPS-stimulated BMDMs with UA (25 µM or 50 µM) increased TLR2 expression than LPS alone suggesting a role of UA in stimulation of TLR2 expression during the time intervals.

On the other hand, the stimulation of BMDMs with 6 Gy X-irradiation did not induce significant changes in the TLR2 expression during the early 2h and 24h followed by a slight decrease started at 48h and continued to 72h after irradiation.

Administration of UA post-irradiation induced significant dose dependent upregulation in TLR2 expression compared to untreated control during the time intervals. On the contrary, the pre-administration of UA especially with 50 µM preserved the values near to control during the time intervals.

In conclusion, LPS not X-irradiation induced higher expression of TLR2 in BMDMs. UA alone was able to upregulate TLR2 expression. The administration of UA to LPS-stimulated BMDMs raised TLR2 expression induced by LPS alone whereas the values were kept near to control in X-irradiated BMDMs. The sources of variation between groups are summarized in supplementary Table 3.

A
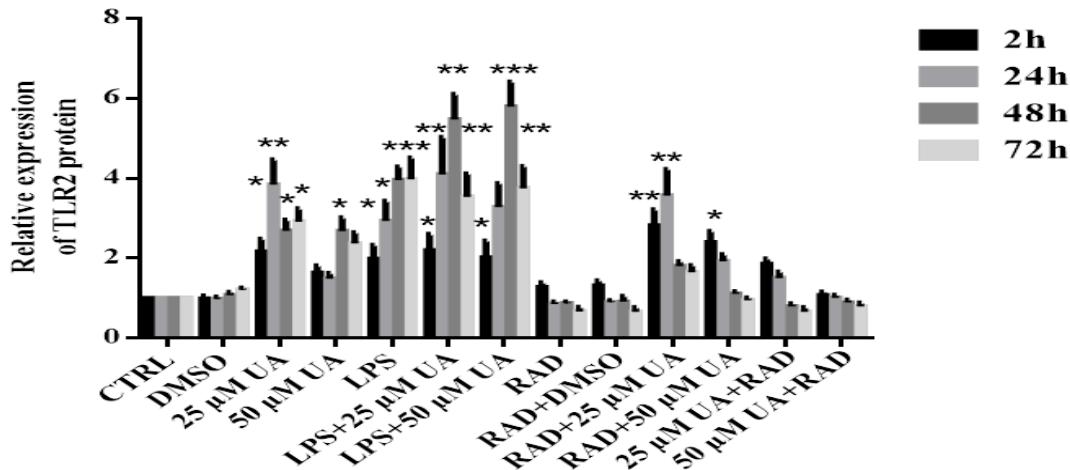
B
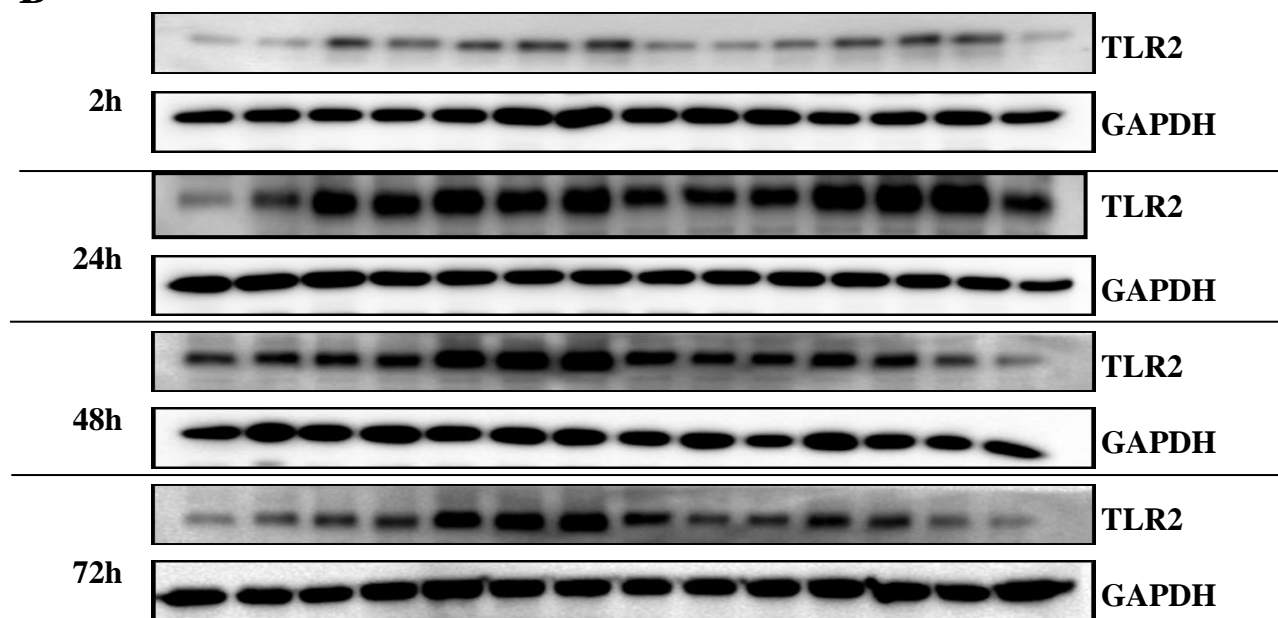
Figure 25 Sensitivity of TLR2 expressions to urolithin A in LPS-stimulated or X-irradiated murine BMDMs

BMDMs were stimulated either by 1μg/ml of LPS or 6 Gy of X-irradiation in the presence or absence of UA (25 or 50 μM) and harvested at different time intervals followed by western blot analysis. The irradiated group was subdivided into two, where one received UA (25 or 50 μM) before 24h of irradiation and the other one received it directly post-irradiation. (A) Bar diagram showing relative band intensities of TLR2 at different time points (n = 4). The unstimulated and untreated BMDMs were used as control. BMDMs treated with DMSO were used as negative control. Arithmetic means ± SEM. Two way ANOVA was used and * ($p < 0.05$), ** (P 0.01), and *** ($p < 0.001$) indicate statistically significant differences compared to respective control. (B) Representative images of TLR2 protein expression was assessed by western blot analysis. GAPDH served as a loading control. Abbreviations: DMSO, dimethyl sulfoxide; LPS, lipopolysaccharides; UA, urolithin A; RAD, radiation.

3.7.3 Effect of urolithin A on MAPK/NF-kB pathway

As mentioned before, in macrophages, evolutionarily conserved signal transduction pathways have been shown to mediate inflammatory processes including MAPK induced effector mechanisms (Kogut, Iqbal et al. 2005, De Nardo, De Nardo et al. 2009). In order to clarify the mechanisms of TLR2 and TLR4 regulation either by LPS or X-irradiation and how gut microbiota metabolite, urolithin A, can drive these signalling pathways, expression of MAPK was evaluated.

The effect of UA on MAPK involved in the regulation of TLR2 and TLR4 expression was investigated after LPS-stimulation or X-irradiation in murine BMDMs. Total and phosphorylated ERK1/2, p38, JNK and IκBα were analysed (immunoblot) and normalized to GAPDH and total protein at indicated time intervals.

3.7.3.1 Effect of urolithin A on MAP kinases ERK1/2 expression and phosphorylation in LPS-stimulated or X-irradiated murine BMDMs

Murine BMDMs were stimulated with 1μg of LPS or 6 Gy X-irradiation in the presence or absence of UA. The activation of MAP kinase ERK1/2 requiring phosphorylation at threonine 202 and tyrosine 204 was monitored by immunoblot analysis using anti-phospho-ERK1/2 antibodies.

As shown in Figure 26, the treatment of murine BMDMs with UA (25 μM or 50 μM) alone did not recorded any significant difference in total ERK1/2 expression (Figure 26A&B) during the time intervals unless a remarkable increase after 24h and 48h of UA administration compared to untreated control was recorded. On the other hand, a highly significant increase in ERK1/2 phosphorylation (Figure 26A&C) started at 24h and continued till 72h while no difference was observed after 2h of UA administration compared to untreated control. UA (25 μM) recorded higher phosphorylation of ERK1/2 at 72h than UA (50 μM).

The stimulation of murine BMDMs with 1μg of LPS exhibited a highly significant upregulation in total ERK1/2 expression (Figure 26A&B) during the time intervals. BMDMs receiving UA25 μM or UA50 μM simultaneously during LPS stimulation induced a dose dependent decrease in total ERK1/2 expression. Similarly, LPS-stimulation induced a highly significant elevation in ERK1/2 phosphorylation (Figure 26A&C) during the time intervals except a slight decrease was recorded after 2h. BMDMs received UA 25 μM or UA 50 μM simultaneously during LPS stimulation exhibited highly significant elevation in pERK1/2 than recorded by LPS alone during the time intervals (Figure 26).

On the other hand, BMDMs receiving 6 Gy X-irradiations showed a non-significant increase in the total ERK1/2 expression (Figure 26B) during the time intervals. Administration of UA pre- and post-irradiation did not record any significant changes in total ERK1/2 expression compared to irradiated cells during the time intervals except a remarkable increase after 2h. While, X-irradiation induced significant upregulation in ERK1/2 phosphorylation (Figure 26A&C) after 2h

followed by a non-significant elevation after 24h and 48h. Again, a significant elevation was registered after 72h.

Administration of UA post-irradiation induced a significant upregulation in ERK1/2 phosphorylation during the time intervals except a non-significant change was recorded after 48h. The pre-administration of UA (24h before irradiation) induced remarkable elevation in ERK1/2 phosphorylation after 2h and 72h while a non-significant decrease was observed after 24h and 48h compared to untreated control.

Figure 26D illustrate the relative densities of pERK1/2 normalized to total ERK1/2. Administration of UA alone induced highly significant increase after 24h and 72h and a non-significant change after 2h and 48h. LPS induced significant upregulations after 48h and administration of UA simultaneously to LPS-stimulation induced remarkable elevation than induced by LPS alone during the time intervals. Concerning X-irradiation stimulation, a non-significant change was recorded in pERK1/2 compared to total ERK1/2 during the time intervals except a highly significant increase after 2h was observed. Administration of UA pre- or post-irradiation revealed a highly significant increase except non-significant change was recorded after 24h.

In conclusion, both LPS and X-irradiation induced phosphorylation of ERK1/2 in BMDMs. UA alone was able to upregulate phosphorylation of ERK1/2. BMDMs receiving UA simultaneously during LPS-stimulation or X-irradiation showed higher phosphorylation of ERK1/2 than induced by LPS or X-irradiation alone. The sources of variations between groups are summarized in supplementary Table 4.

A

DMSO	–	+	–	–	–	–	–	–	–	+	–	–	–	–
25 μM UA	–	–	+	–	–	+	–	–	–	–	+	–	+	–
50 μM UA	–	–	–	+	–	–	+	–	–	–	–	+	–	+
LPS +	–	–	–	–	+	+	+	–	–	–	–	–	–	–
RAD +	–	–	–	–	–	–	–	–	+	+	+	+	–	–
+ RAD	–	–	–	–	–	–	–	–	–	–	–	–	+	+
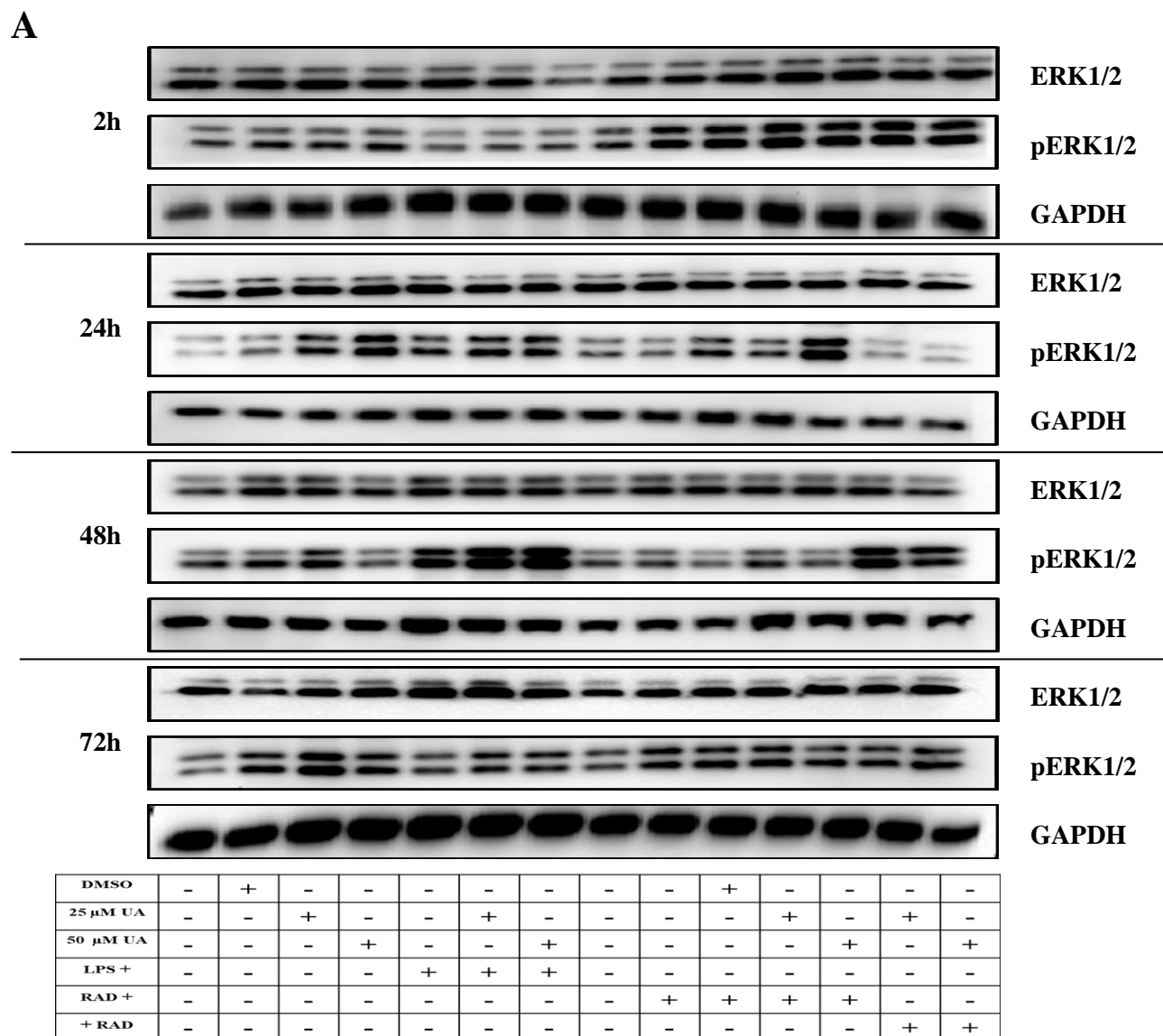
Figure 26 Effect of urolithin A on MAP kinase ERK1/2 expression and phosphorylation in LPS-stimulated or X-irradiated murine BMDMs

BMDMs were stimulated either by 1μg/ml of LPS or 6 Gy of X-irradiation in the presence or absence of UA (25 μM or 50 μM) and harvested at different time intervals followed by western blot analysis. The irradiated group was subdivided into two, where one received UA (25 or 50 μM) before 24h of irradiation and the other one received it directly post-irradiation. (A) Phosphorylation of MAP kinases ERK1/2 was monitored by immunoblot using phospho-p44/42 MAP kinase (Thr202/Tyr204) polyclonal antibodies. Subsequently, blots were stripped and re-incubated with antibody against total ERK1/2. GAPDH served as a loading control. The unstimulated and untreated BMDMs were used as control. BMDMs treated with DMSO were used as negative control. Abbreviations: DMSO, dimethyl sulfoxide; LPS, lipopolysaccharides; UA, urolithin A; RAD, radiation; GAPDH, glyceraldehyde-3-phosphate dehydrogenase.

B
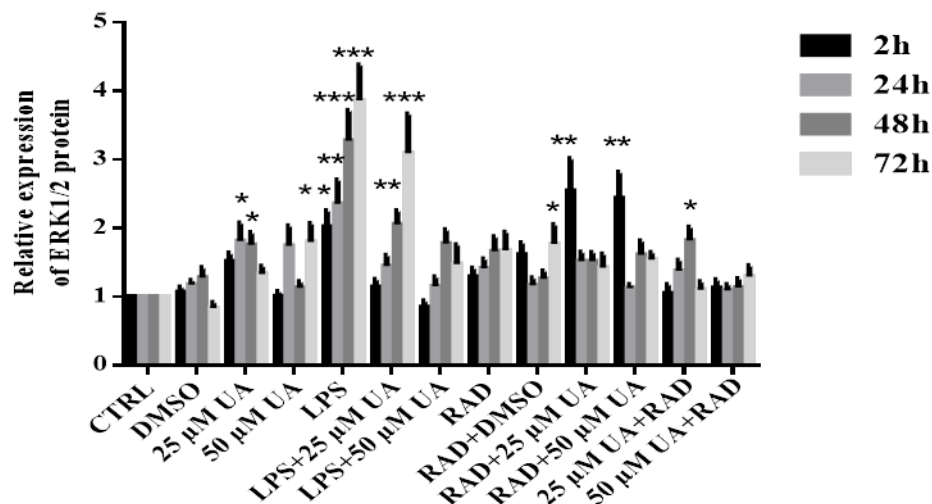
C

Figure 26 Continued: Effect of urolithin A on MAP kinase ERK1/2 expression and phosphorylation in LPS-stimulated or X-irradiated murine BMDMs

Bar diagram showing relative band intensity of total ERK1/2 (B) and pERK1/2 (C) over GAPDH at different time points. Arithmetic means ± SEM from five independent experiments. Two way ANOVA was used and * ($p < 0.05$), ** (P 0.01), and *** ($p < 0.001$) indicates statistically significant difference compared to respective control. Abbreviations: DMSO, dimethyl sulfoxide; LPS, lipopolysaccharides; UA, urolithin A; RAD, radiation.

D

Figure 26 Continued: Effect of urolithin A on MAP kinase ERK1/2 expression and phosphorylation in LPS-stimulated or X-irradiated murine BMDMs

(D) Bar graphs represent relative band densities of pERK1/2 normalized to total ERK1/2. Arithmetic means ± SEM from five independent experiments. Two way ANOVA was used and * ($p < 0.05$) and ** (P 0.01) indicates statistically significant difference compared to respective control. Abbreviations: DMSO, dimethyl sulfoxide; LPS, lipopolysaccharides; UA, urolithin A; RAD, radiation.

3.7.3.2 Effect of urolithin A on MAP kinase p38 expression and phosphorylation in LPS-stimulated or X-irradiated murine BMDMs

Murine BMDMs were stimulated with 1µg/ml of LPS or 6 Gy X-irradiation in the presence or absence of UA. The activation of MAP kinase p38 requiring phosphorylation at threonine 180 and tyrosine 182 was monitored by immunoblot analysis using anti-phospho-p38 antibodies.

Results presented in Figure 27 illustrate a non-significant difference in total p38 expression during the time intervals unless a notable increase after 48h of 25 µM UA administrations. On the other hand, a highly significant increase in phosphorylated p38 (Figure 27A&C) after 48h and 72h was observed in murine BMDMs which received 25 µM UA alone. While, a non-significant difference was observed after 2h and 24h compared to untreated control. UA (25 µM) recorded higher expression of pp38 at 48h and 72h than UA (50 µM) which recorded slight decrease compared to untreated control.

Stimulation of BMDMs with 1µg of LPS exhibited a highly significant elevation in total p38 expression (Figure 27B) during the time intervals. While the treatment of LPS-stimulated BMDMs with 25 µM or 50 µM of UA kept the upregulation of p38 expression induced by LPS alone.

Similarly, BMDMs receiving 1µg of LPS exhibited a significant higher phosphorylation of p38 (Figure 27A&C) during the time intervals. In addition, BMDMs receiving UA (25 µM or 50 µM) simultaneously during LPS-stimulation preserved the highly significant elevation of pp38 induced by LPS alone during the time intervals with respect to the slight decrease observed after 24h (Figure 27A&C).

On the other hand, BMDMs receiving 6 Gy X-irradiations did not show any significant changes in total p38 expression (Figure 27B) during the time intervals except a notable decrease which was observed after 72h (Figure 27B). Administration of UA pre- and post-irradiation did not record any significant changes in total p38 expression compared to irradiated ones during the time intervals. In BMDMs which received 25 µM UA pre- and post-irradiation preserved the p38 expression near to control at 72h.

On the contrary, stimulation of BMDMs with 6 Gy X-irradiation induced early significant upregulation in p38 phosphorylation (Figure 27A&C) after 2h and go on till 48h followed by a decrease after 72h. Administration of UA post-irradiation induced remarkable dose dependent decrease in pp38 expression during the time intervals. While, the pre-administration of UA (24h before irradiation) presented notable decrease in p38 phosphorylation with values near to untreated control.

Figure 27D illustrate the relative protein densities of pp38 normalized to total p38. Administration of UA (25 µM) alone induced highly significant increase after 48h and 72h and a non-significant change after 2h and 24h. LPS induced significant upregulation during the time intervals except a non-significant change was recorded after 48h. Administration of UA simultaneously to LPS-stimulation induced remarkable decrease of pp38 starting from 24h and continued till 72h. Concerning X-irradiation stimulation, a highly significant increase were recorded in pp38 compared to total p38 during the time intervals except a notable change with value near to control was recorded after 72h. Administration of UA pre-irradiation revealed a significant reduction in p38 phosphorylation.

In conclusion, both LPS and X-irradiation induced higher expression of phosphorylation of p38 in BMDMs. UA alone was able to upregulate p38 phosphorylation. BMDMs receiving UA simultaneously during LPS stimulation preserved the higher expression of pp38 induced by LPS alone while BMDMs receiving UA pre- or post-irradiation recorded a reduction of pp38 achieving intermediate value between untreated controls and irradiated ones. The sources of variations between groups are summarized in supplementary Table 5

A

DMSO	–	+	–	–	–	–	–	–	–	+	–	–	–	–
25 μM UA	–	–	+	–	–	+	–	–	–	–	+	–	+	–
50 μM UA	–	–	–	+	–	–	+	–	–	–	–	+	–	+
LPS +	–	–	–	–	+	+	+	–	–	–	–	–	–	–
RAD +	–	–	–	–	–	–	–	–	+	+	+	+	–	–
+ RAD	–	–	–	–	–	–	–	–	–	–	–	–	+	+

Figure 27 Effect of urolithin A on MAP kinase p38 expression and phosphorylation in LPS-stimulated or X-irradiated murine BMDMs

BMDMs were stimulated either by 1μg/ml of LPS or 6 Gy of X-irradiation in the presence or absence of UA (25 μM or 50 μM) and harvested at different time points followed by western blot analysis. The irradiated group was subdivided into two, where one received UA (25 or 50 μM) before 24h of irradiation and the other one received it directly post-irradiation. (A) Phosphorylation of MAP kinase p38 was monitored by immunoblot using phospho-p38 MAP kinase (Thr180/Tyr182) monoclonal antibodies. Subsequently, blots were stripped and re-incubated with antibody against total p38. GAPDH served as a loading control. The unstimulated and untreated BMDMs were used as control. BMDMs treated with DMSO were used as negative control. Abbreviations: DMSO, dimethyl sulfoxide; LPS, lipopolysaccharides; UA, urolithin A; RAD, radiation.
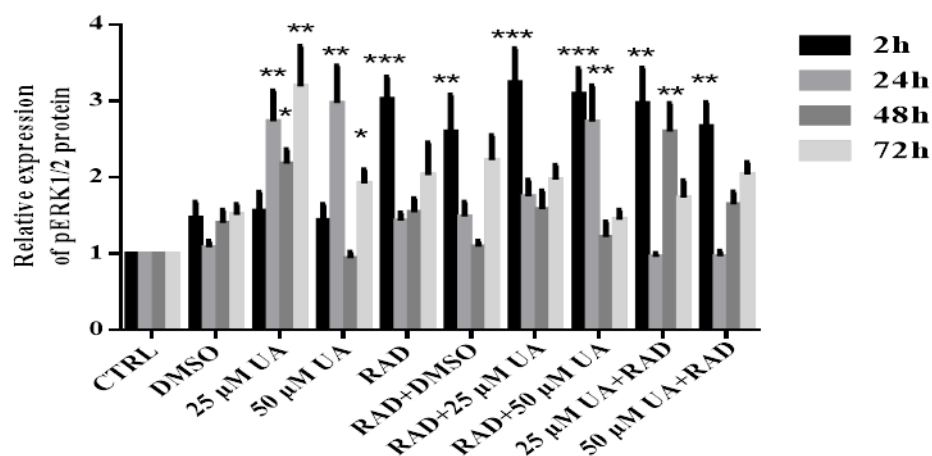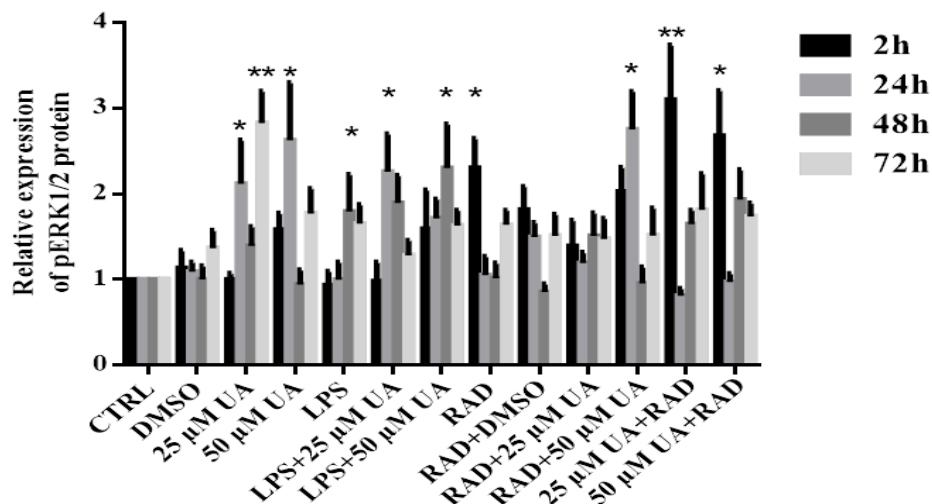
B
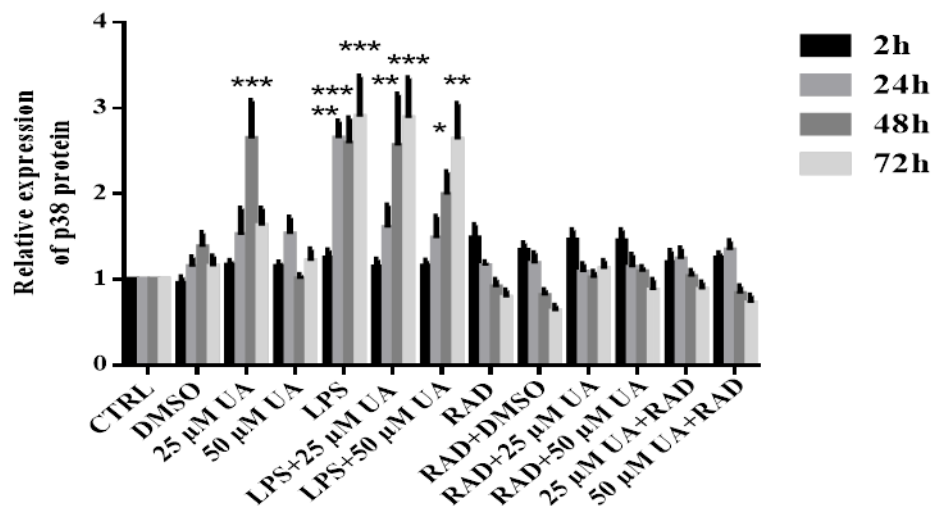
C

Figure 27 Continued: Effect of urolithin A on MAP kinase p38 expression and phosphorylation in LPS-stimulated or X-irradiated murine BMDMs

Bar graphs represent relative band intensities of total p38 (B) and pp38 (C) over GAPDH at different time points. Arithmetic means ± SEM from five independent experiments. Two way ANOVA was used and * ($p < 0.05$), ** (P 0.01), and *** ($p < 0.001$) indicate statistically significant differences compared to respective control. Abbreviations: DMSO, dimethyl sulfoxide; LPS, lipopolysaccharides; UA, urolithin A; RAD, radiation.

D

Figure 27 Continued: Effect of urolithin A on MAP kinase p38 expression and phosphorylation in LPS-stimulated or X-irradiated murine BMDMs

(D) Bar graph represents relative band densities of pp38 normalized to total p38. Arithmetic means ± SEM from five independent experiments. Two way ANOVA was used and * ($p < 0.05$) and ** (P 0.01) indicate statistically significant differences compared to respective control. Abbreviations: DMSO, dimethyl sulfoxide; LPS, lipopolysaccharides; UA, urolithin A; RAD, radiation.

3.7.3.3 Effect of urolithin A on MAP kinases SAPK/JNK expression and phosphorylation in LPS-stimulated or X-irradiated BMDMs

Murine BMDMs were stimulated with 1µg of LPS or 6 Gy X-irradiation in the presence or absence of UA. The activation of MAP kinases SAPK/JNK requiring phosphorylation at threonine 183 and tyrosine 185 was monitored by immunoblot analysis using anti-phospho-SAPK/JNK antibodies.

Results represented in Figure 28 revealed that UA (25 µM or 50 µM) alone induced non-significant changes in the expression of total SAPK/JNK during the time intervals (Figure 28B). On the other hand, UA (25 µM or 50 µM) induced remarkable elevation in phospho-SAPK/JNK expression (Figure 28A&C) in murine BMDMs. But the expression of phospho-SAPK/JNK was more obvious with 25 µM UA during the time intervals.

Stimulations of BMDMs with 1µg/ml of LPS exhibited highly significant elevation in total SAPK/JNK expression (Figure 28B) during the time intervals. While the treatment of LPS-stimulated murine BMDMs with UA (25 µM or 50 µM) induced higher expression of total SAPK/JNK similar to induced by LPS stimulation alone (Figure 28B). Similarly, BMDMs receiving 1µg/ml of LPS showed a significant increase in phospho-SAPK/JNK during the time intervals. In addition, BMDMs receiving UA (25 µM or 50 µM) simultaneously during LPS stimulation preserved the highly significant elevation of phospho-SAPK/JNK expression induced by LPS alone during the time intervals except a remarkable decrease was observed after 48h and 72h compared to LPS-stimulated group (Figure 28C&D). 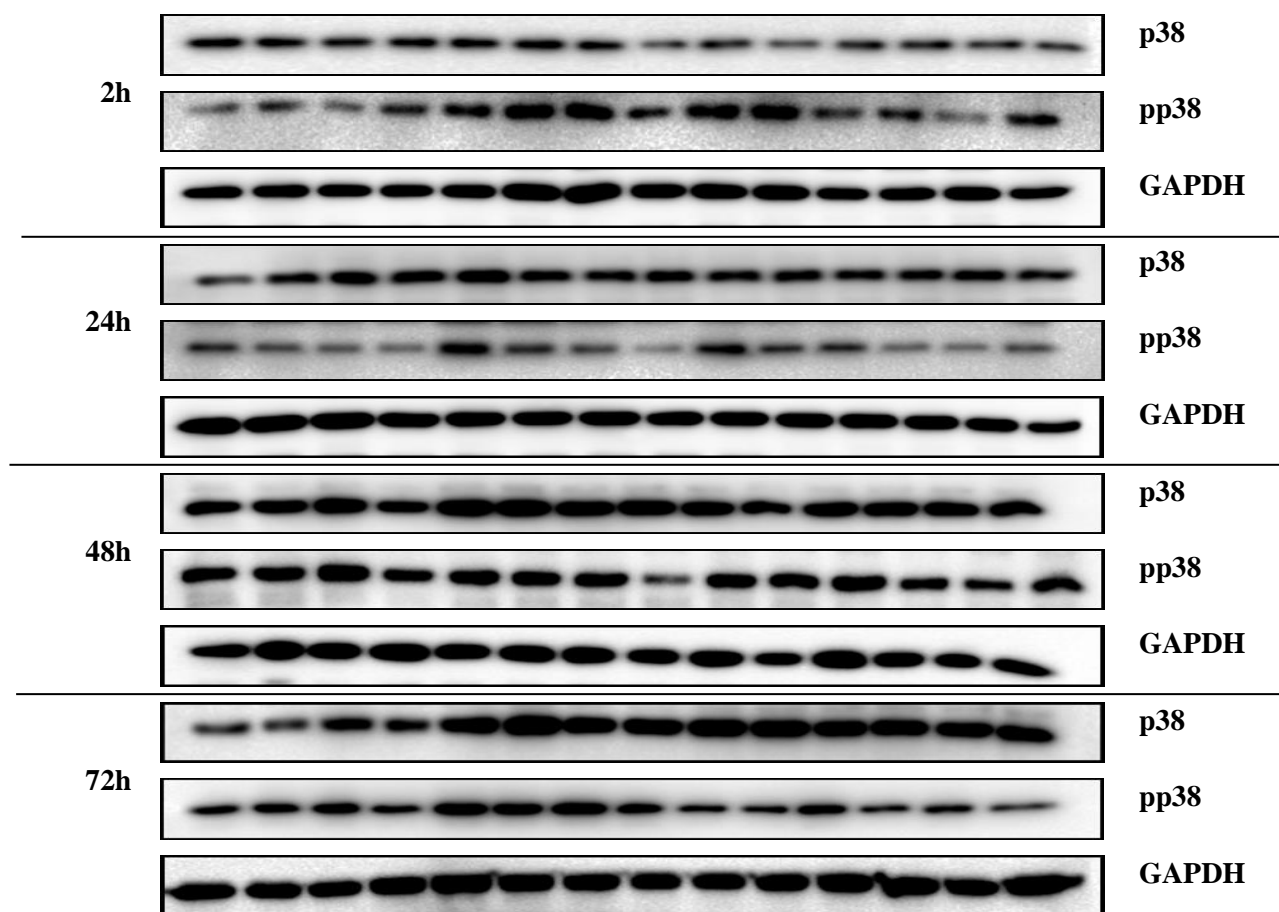On the other hand, BMDMs receiving 6 Gy X-irradiation did not show any significant changes in total SAPK/JNK expression during the time intervals (Figure 28B). Administration of UA pre- and post-irradiation did not record any significant changes in total SAPK/JNK expressions compared to irradiated ones during the time intervals in BMDMs. On the opposite, X-irradiation induced non-significant changes in phospho-SAPK/JNK during the time intervals except a slight increase after 72h. Administration of UA pre- or post-irradiation induced reduction in phospho-SAPK/JNK expression after 2h and non-significant changes were observed during the later time points.

Figure 28D exhibit the relative protein densities of phospho-SAPK/JNK normalized to total SAPK/JNK. Administration of UA (25 µM or 50 µM) alone induced slightly significant increase after 24h and 72h. LPS induced a highly significant upregulation during the time intervals. Administration of UA simultaneously to LPS-stimulation induced a dose dependent decrease of p38 phosphorylation. Concerning X-irradiation, a highly significant increase was recorded in pp38 after 72h compared to total p38. Administration of UA pre- or post-irradiation revealed a significant reduction in p38 phosphorylation.

In conclusion, LPS but not X-irradiation induced higher expression of phosphorylated SAPK/JNK in BMDMs during the time intervals. UA alone was able to upregulate phospho-SAPK/JNK expression especially after 2h and 48h. The pre- or post-administration of UA did not record significant changes in phospho-SAPK/JNK expression compared to the LPS-stimulated BMDMs. The sources of variations between groups are summarized in supplementary Table 6.

A

DMSO	–	+	–	–	–	–	–	–	–	+	–	–	–	–
25 µM UA	–	–	+	–	–	+	–	–	–	–	+	–	+	–
50 µM UA	–	–	–	+	–	–	+	–	–	–	–	+	–	+
LPS +	–	–	–	–	+	+	+	–	–	–	–	–	–	–
RAD +	–	–	–	–	–	–	–	–	+	+	+	+	–	–
+ RAD	–	–	–	–	–	–	–	–	–	–	–	–	+	+
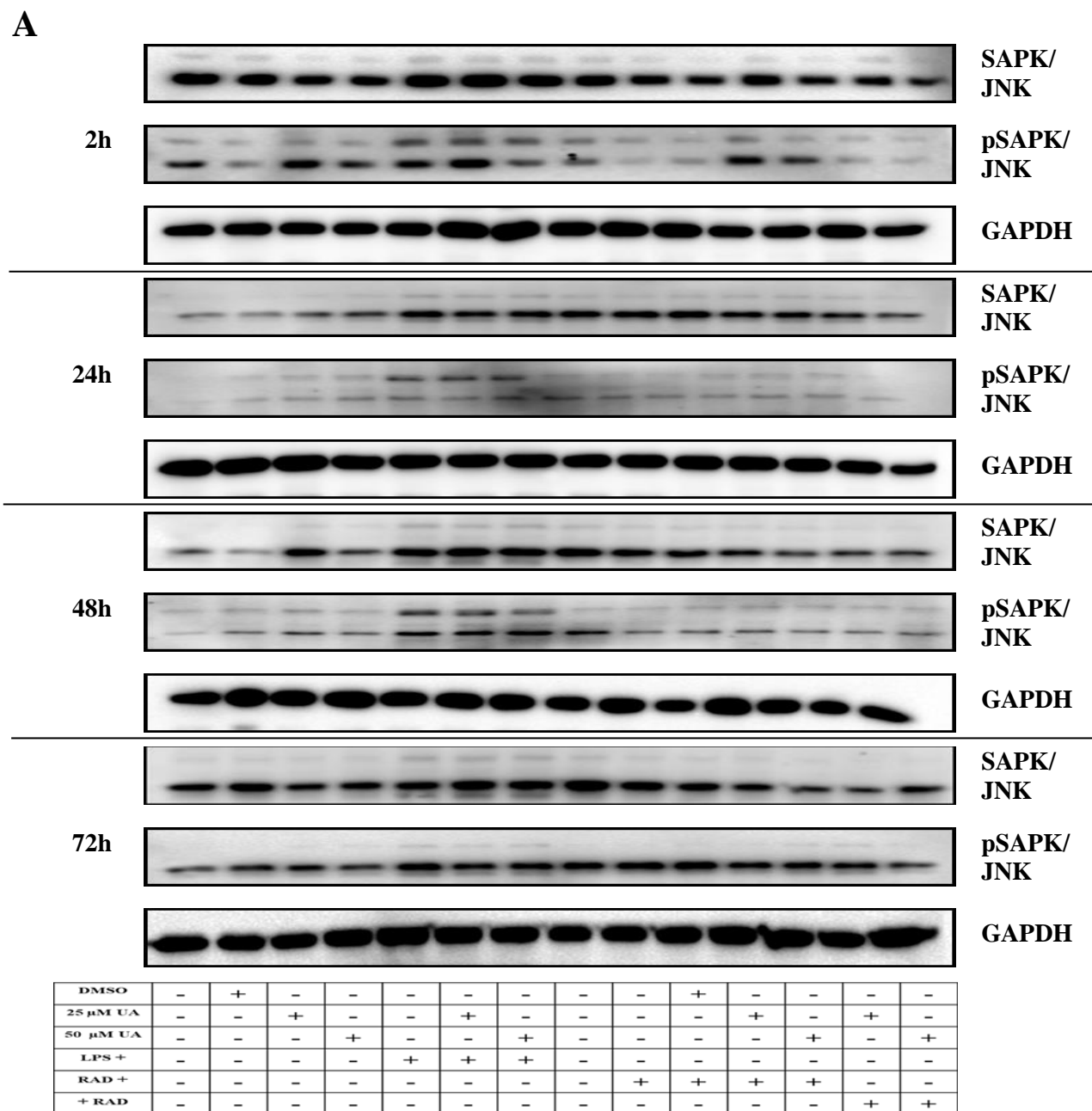
Figure 28 Effect of urolithin A on MAP kinase SAPK/JNK expression and phosphorylation in LPS-stimulated or X-irradiated murine BMDMs

BMDMs were stimulated either by 1µg/ml of LPS or 6 Gy of X-irradiation in the presence or absence of UA (25 µM or 50 µM) and harvested at different time points followed by western blot analysis. The irradiated group was subdivided into two, where one received UA (25 or 50 µM) before 24h of irradiation and the other one received it directly post-irradiation. (A) Phosphorylation of MAP kinase SAPK/JNK was monitored by immunoblot using phospho-SAPK/JNK MAP kinase (Thr183/Tyr185) monoclonal antibodies. Subsequently, blots were stripped and re-incubated with antibody against total SAPK/JNK. GAPDH served as a loading control. The unstimulated and untreated BMDMs were used as control. BMDMs treated with DMSO were used as negative control. Abbreviations: DMSO, dimethyl sulfoxide; LPS, lipopolysaccharides; UA, urolithin A; RAD, radiation
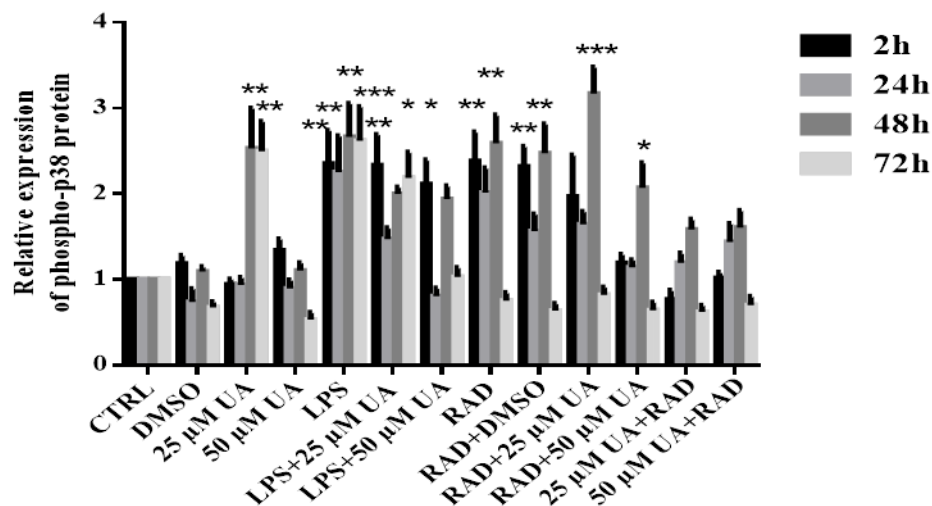
87

B
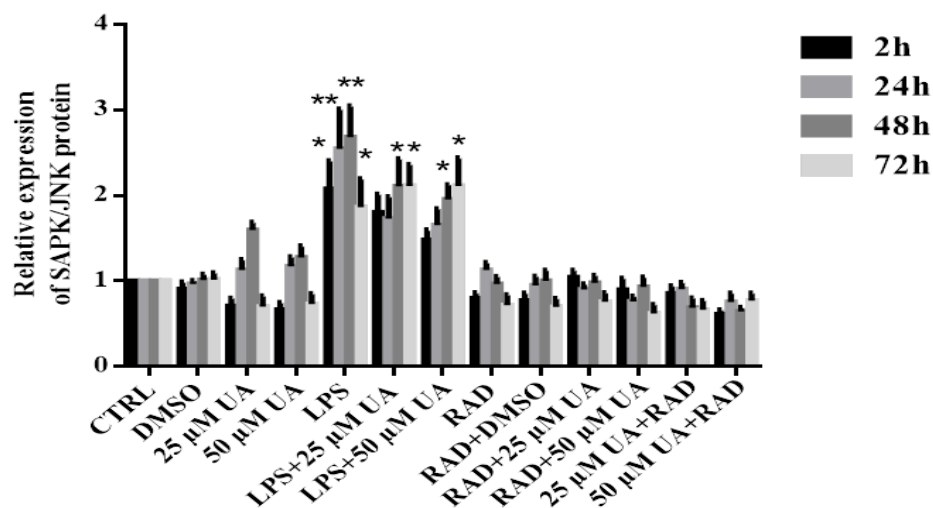
C

Figure 28 Continued: Effect of urolithin A on MAP kinase SAPK/JNK expression and phosphorylation in LPS-stimulated or X-irradiated BMDMs

Bar graphs show relative band intensities of total SAPK/JNK (B) and phospho-SAPK/JNK (C) at different time points. Arithmetic means ± SEM from five independent experiments. Two way ANOVA was used and * ($p < 0.05$), ** (P 0.01), and *** ($p < 0.001$) indicate statistically significant differences compared to respective control. Abbreviations: DMSO, dimethyl sulfoxide; LPS, lipopolysaccharides; UA, urolithin A; RAD, radiation.
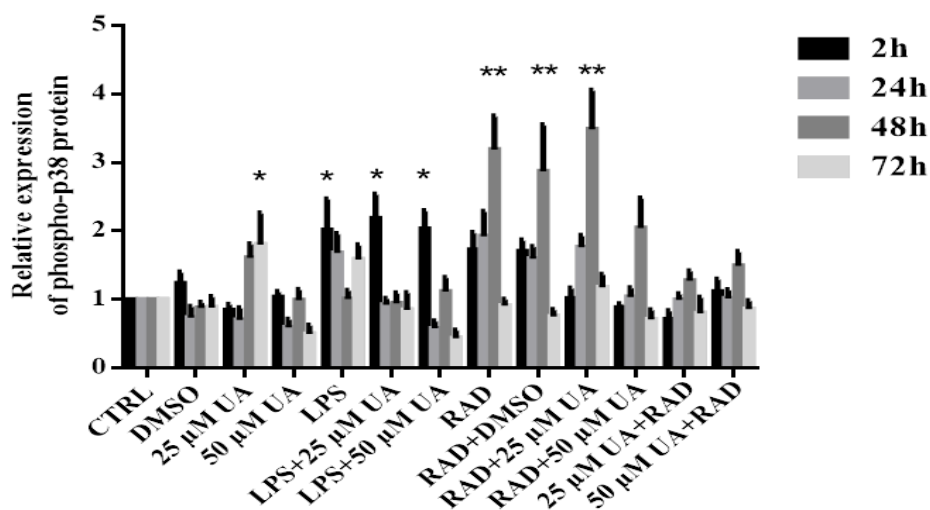
D

Figure 28 Continued: Effect of urolithin A on MAP kinase SAPK/JNK expression and phosphorylation in LPS-stimulated or X-irradiated murine BMDMs

(D) Bar graphs represent relative densities of phospho-SAPK/JNK normalized to total SAPK/JNK. Arithmetic means ± SEM from five independent experiments. Two way ANOVA was used and * ($p < 0.05$) and ** ($P\ 0.01$) indicate statistically significant differences compared to respective control. Abbreviations: DMSO, dimethyl sulfoxide; LPS, lipopolysaccharides; UA, urolithin A; RAD, radiation.

3.7.3.4 Effect of urolithin A on IκBα expression and phosphorylation in LPS-stimulated or X-irradiated BMDMs

As mentioned before, NF-κB is the master transcription factor in inflammatory processes and is normally inhibited by the protein IκBα. When cells are stimulated, IκBα is phosphorylated and polyubiquitinated for proteasome degradation, enabling NF-κB to enter the nucleus and increase the transcription of inflammatory genes. Thus, BMDMs stimulated either with 1μg of LPS or 6 Gy X-irradiation in the presence or absence of UA were evaluated for the level of pIκBα by immunoblot analysis. The activation of IκBα requiring phosphorylation at serine 32/36 was monitored by immunoblot analysis using anti-phospho-IκBα antibodies.

BMDMs receiving UA (25 μM or 50 μM) alone did not express any observed changes neither in total IκBα nor pIκBα expression during the time intervals (Figure 29) except a slight increase after 48h followed by notable decrease after 72h were observed in total IκBα expression. The low dose of UA (25 μM) recorded higher expression of total IκBα after 48h.

Data presented in Figure 29 show that stimulations of BMDMs with 1μg of LPS (Figure 29) exhibited highly significant elevation in total IκBα expression during the time intervals. As well the treatment of LPS-stimulated BMDMs with UA (25 μM or 50 μM) recoded a remarkable decrease in total IκBα expression compared to those receiving LPS alone. Similarly, LPS-stimulated BMDMs induced significant upregulation in pIκBα expression during the time

intervals. In addition, BMDMs received UA (25 μM or 50 μM) simultaneously during LPS stimulation recorded a dose dependent decrease in pIκBα compared to those receiving LPS alone during the time intervals (Figure 29A&C).

On the other hand, BMDMs receiving 6 Gy X-irradiation did not show significant changes in total IκBα expression after 2h while a slight increase was observed after 24h and 48h followed by a slight decrease after 72h (Figure 29). Administration of UA pre- and post-irradiation registered a notable decrease in total IκBα expression compared to untreated control during the time intervals. In addition, the stimulation of BMDMs with 6 Gy X-irradiation was not able to induce a significant effect in IκBα phosphorylation compared to control during the time intervals. Also, the administration of UA pre- or post-irradiation did not record remarkable changes in IκBα phosphorylation compared to untreated control during the time intervals. Figure 29 shows the relative protein expression of phospho-IκBα protein normalized to total IκBα. Administration of UA (25 μM or 50 μM) alone induced non-significant changes during the time intervals. LPS induced a highly significant upregulation during the time intervals.

Administration of UA simultaneously to LPS-stimulation induced a significant dose dependent decrease of IκBα phosphorylation. Concerning X-irradiation, non-significant changes were recorded in phospho-IκBα during the time intervals. Administration of UA pre- or post-irradiation revealed a non-significant change in IκBα phosphorylation.
In conclusion, LPS but not X-irradiation induced a higher upregulation in IκBα phosphorylation expression in BMDMs during the time intervals. UA did not induce observable effects on pIκBα expression during the time intervals except an inconsiderable decrease when co-stimulated with LPS. The sources of variations between groups are summarized in supplementary Table 7.

A

DMSO	–	+	–	–	–	–	–	–	–	+	–	–	–	–
25 µM UA	–	–	+	–	–	+	–	–	–	–	+	–	+	–
50 µM UA	–	–	–	+	–	–	+	–	–	–	–	+	–	+
LPS +	–	–	–	–	+	+	+	–	–	–	–	–	–	–
RAD +	–	–	–	–	–	–	–	–	+	+	+	+	–	–
+ RAD	–	–	–	–	–	–	–	–	–	–	–	–	+	+

Figure 29 Effect of urolithin A on IκBα expression and phosphorylation in LPS-stimulated or X-irradiated BMDMs

BMDMs were stimulated either by 1µg/ml of LPS or 6 Gy of X-irradiation in the presence or absence of UA (25 µM or 50 µM) and harvested at indicated time intervals followed by western blot analysis. The irradiated group was subdivided into two, where one received UA (25 or 50 µM) before 24h of irradiation and the other one received it directly post-irradiation. (A) Phosphorylation of IκBα was monitored by immunoblot using pIκBα (Ser32/36) monoclonal antibodies. Subsequently, blots were stripped and re-incubated with antibody against total IκBα. GAPDH served as a loading control. The unstimulated and untreated BMDMs were used as control. BMDMs treated with DMSO were used as negative control. Abbreviations: DMSO, dimethyl sulfoxide; LPS, lipopolysaccharides; UA, urolithin A; RAD, radiation.
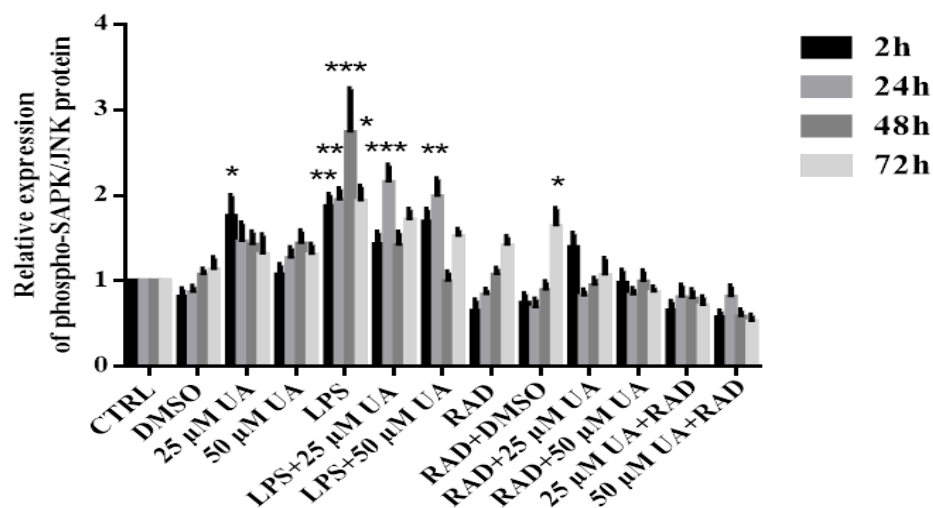
B

C
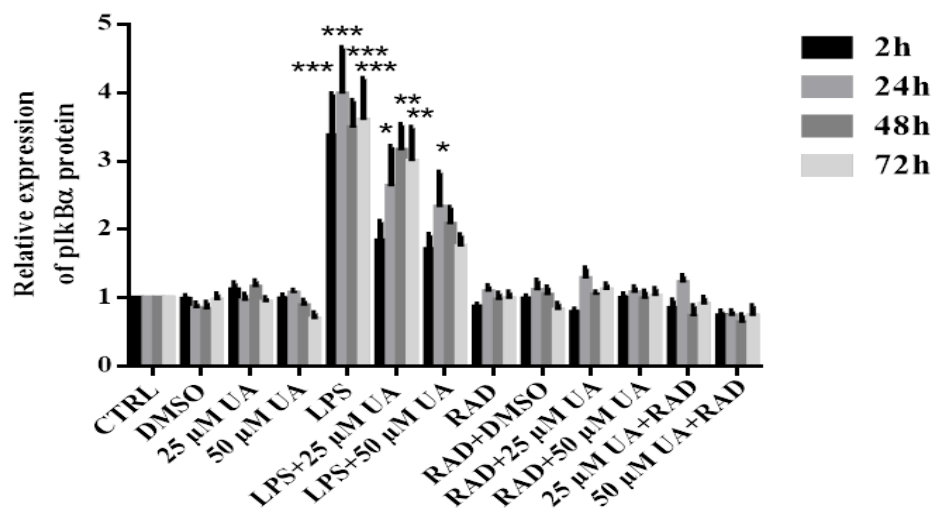
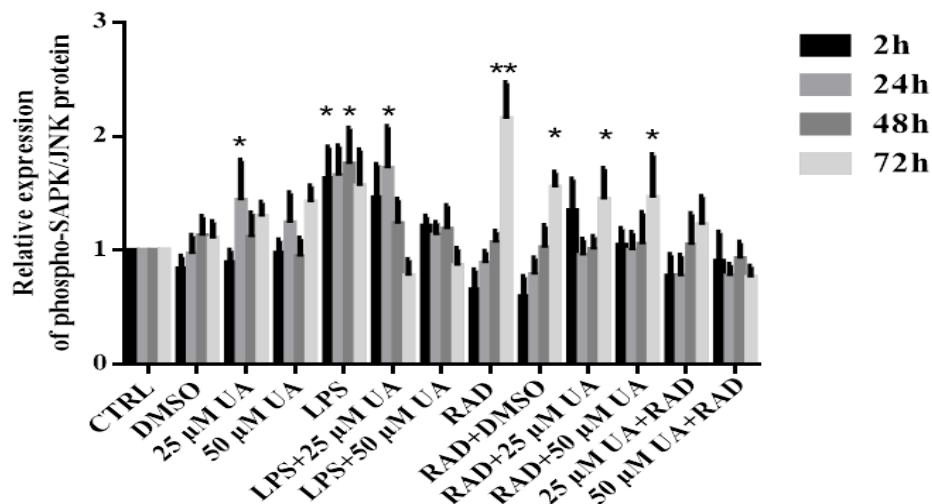**Figure 29 Continued: Effect of urolithin A on IκBα expression and phosphorylation in LPS-stimulated or X-irradiated murine BMDMs**

Bar diagram shows relative band intensities of total IκBα (C) and pIκBα (D) at different time points. Arithmetic means ± SEM from five independent experiments. Two way ANOVA was used and * ($p < 0.05$), ** (P 0.01), and *** ($p < 0.001$) indicate statistically significant differences compared to respective control. Abbreviations: DMSO, dimethyl sulfoxide; LPS, lipopolysaccharides; UA, urolithin A; RAD, radiation.

D

Figure 29 Continued: Effect of urolithin A on IκBα expression and phosphorylation in LPS-stimulated or X-irradiated murine BMDMs

(D) Bar diagram showing relative intensities of pIκBα normalized to total IκBα at indicated time points. Arithmetic means ± SEM from five independent experiments. Two way ANOVA was used and * ($p < 0.05$), *** ($p < 0.001$), and **** ($p < 0.0001$) indicate statistically significant differences compared to respective control. Abbreviations: DMSO, dimethyl sulfoxide; LPS, lipopolysaccharides; UA, urolithin A; RAD, radiation.

3.7.4 Effect of urolithin A on PI3K/AKT/mTOR expression and phosphorylation in LPS-stimulated or X-irradiated BMDMs

Several TLRs induce the PI3K/Akt pathway which can regulate the immune response in a negative or positive manner (Fukao and Koyasu 2003). Both Akt and mTOR are principal signalling pathways that orchestrate the response of macrophages to various metabolic and inflammatory signals (Song, Ouyang et al. 2005). In order to clarify the mechanisms of TLR2 and TLR4 regulation either by LPS or X-irradiation and how the gut microbiota metabolite, urolithin A, can drive these signalling pathway, expression of PI3K/AKT/mTOR were evaluated. The effect of UA on PI3K/Akt/mTOR expression involved in the regulation of TLR expression was investigated in stimulated BMDMs. Total and phosphorylated AKT and mTOR was measured at 2h, 24h, 48h and 72h by western blot.
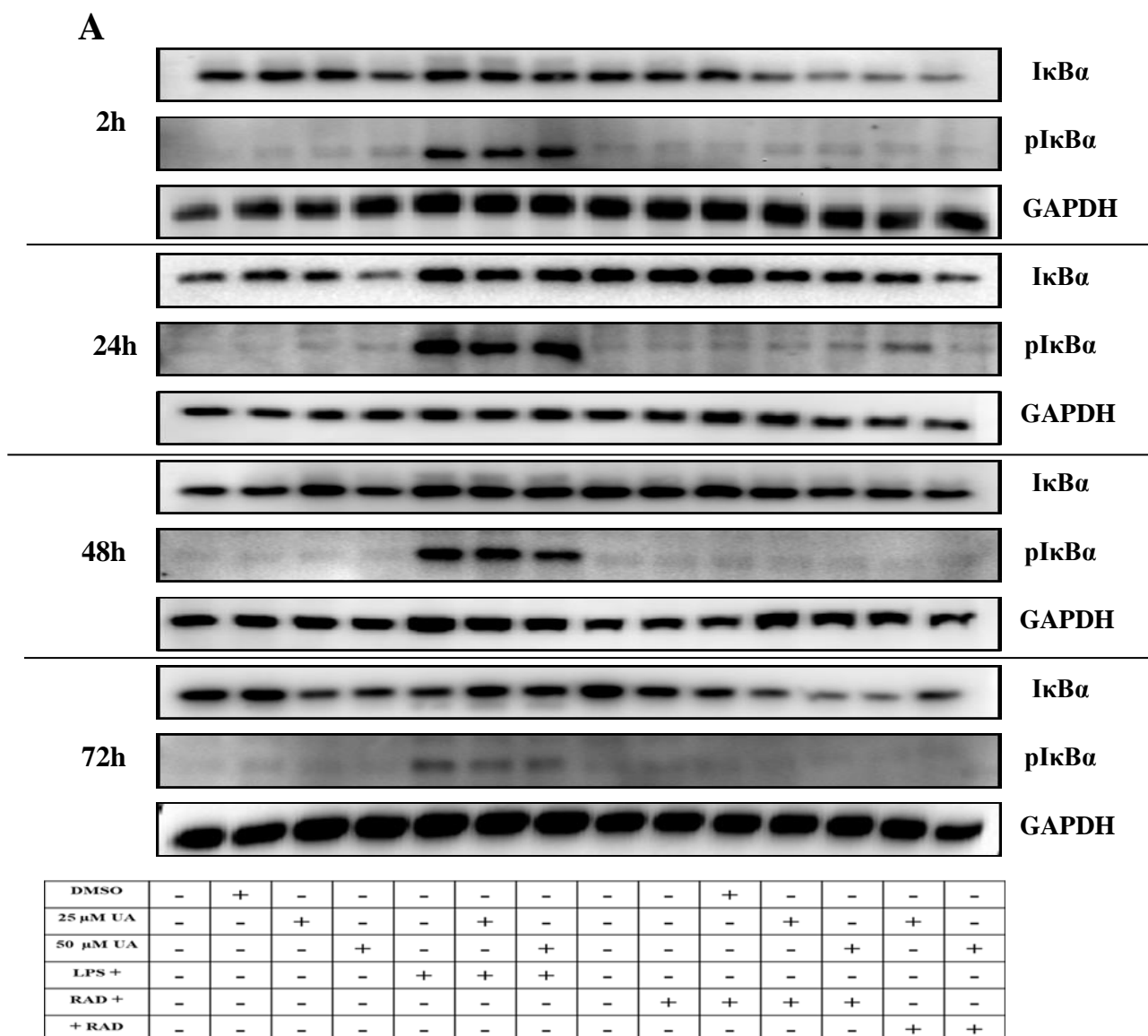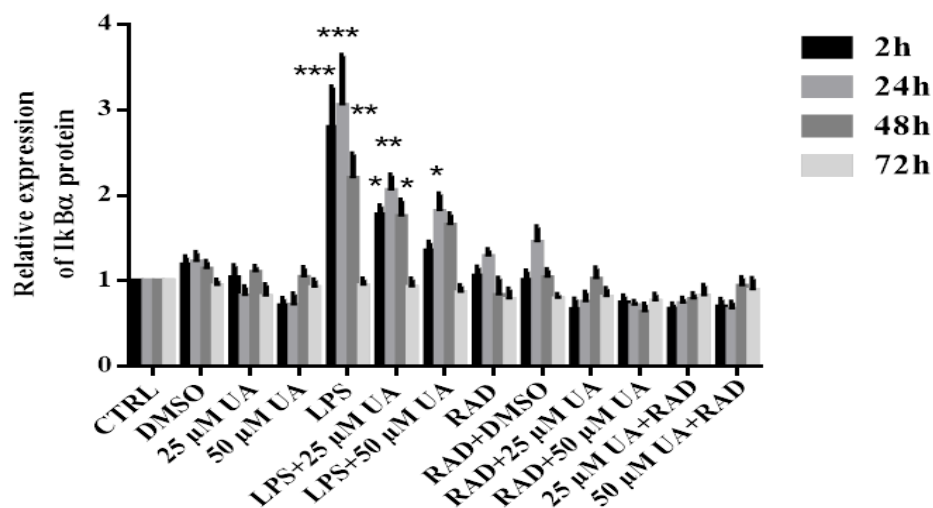
3.7.4.1 Effect of urolithin A on PI3K/AKT expression and phosphorylation in LPS-stimulated or X-irradiated murine BMDMs

Murine BMDMs were stimulated either with 1µg/ml of LPS or 6 Gy X-irradiation in the presence or absence of UA. The activation of PI3 kinases AKT requiring phosphorylation at Serine 473 was monitored by immunoblot analysis using anti-phospho-AKT antibodies.

As shown in Figure 30, the treatment of BMDMs with UA (25 µM or 50 µM) alone show a non-significant disturbance in total AKT expression (Figure 30B) beginning with a slight decrease after 2h followed by an increase at 24h and 48h and a slight depression after 72h. Whereas a remarkable significant increase in pAKT expression (Figure 30A&C) was recorded after UA administration compared to untreated control during the time intervals.

The stimulation of BMDMs with 1µg/ml of LPS was sufficient to induce highly significant upregulation in total AKT expression (Figure 30B) after stimulation of BMDMs with 1 µg/ml LPS during the time intervals. In addition, BMDMs receiving UA (25 µM or 50 µM) simultaneously during LPS stimulation did not show any remarkable changes in total AKT after 2h, 24h and 72h whereas a notable increase was preserved after 48h (Figure 30B). Similarly, a highly significant elevation in pAKT expression (Figure 30A&C) was recorded during the time intervals. In addition, BMDMs receiving UA (25 µM or 50 µM) simultaneously during LPS-stimulation exhibited highly significant elevation in pAKT than recorded by LPS alone after 2h and 24h while a remarkable decrease was observed after 48h followed by a slight increase at 72h (Figure 30A&C).

On the other hand, BMDMs receiving 6 Gy X-irradiations showed a remarkable increase in the total AKT expression (Figure 30B) during the time intervals. As well as, administration of UA pre- and post-irradiation induced non-significant changes in total AKT expression during the time intervals compared to untreated control. Similarly, stimulation of BMDMs with 6 Gy X-irradiation induced significant upregulation in pAKT expression (Figure 30A&C) especially after 72h. Administration of UA pre- or post-irradiation induced remarkable upregulation in pAKT

expression after 24h and 72h while a non-significant change was observed after 2h and 48h compared to untreated control.

Figure 30D explain the relative intensities of pAKT expression normalized to total AKT. Administration of UA (25 µM or 50 µM) alone induced highly significant elevation during the time intervals. LPS induced highly significant upregulation in pAKT starting after 24h and continued after 72h. Administration of UA simultaneously to LPS-stimulation induced non-significant disturbance starting from 2h till 48h while a highly significant increase was recorded after 72h. Concerning X-irradiation, non-significant changes were recorded in pAKT till 48h while a significant increase was observed at 72h. Administration of UA pre- or post-irradiation revealed a non-significant increase in AKT phosphorylation compared to irradiated group.

In conclusion, both LPS and X-irradiation induced higher expression of pAKT as well as total AKT expression in BMDMs during the time intervals. UA alone was able to upregulate pAKT expression. The association of UA with LPS was able to preserve the upregulation induced by LPS alone. The sources of variations between groups are summarized in supplementary Table 8.

A

DMSO	–	+	–	–	–	–	–	–	–	+	–	–	–	–
25 µM UA	–	–	+	–	–	+	–	–	–	–	+	–	+	–
50 µM UA	–	–	–	+	–	–	+	–	–	–	–	+	–	+
LPS +	–	–	–	–	+	+	+	–	–	–	–	–	–	–
RAD +	–	–	–	–	–	–	–	–	+	+	+	+	–	–
+ RAD	–	–	–	–	–	–	–	–	–	–	–	–	+	+

Figure 30 Effect of urolithin A on AKT expression and phosphorylation in LPS-stimulated or X-irradiated murine BMDMs

BMDMs were stimulated either by 1µg/ml of LPS or 6 Gy of X-irradiation in the presence or absence of UA (25 µM or 50 µM) and harvested at indicated time points followed by western blot analysis. The irradiated group was subdivided into two, where one received UA (25 or 50 µM) before 24h of irradiation and the other one received it directly post-irradiation. (A) Phosphorylation of AKT was monitored by immunoblot using pAKT (Ser473) monoclonal antibodies. Subsequently, blots were stripped and re-incubated with antibody against total AKT. GAPDH served as a loading control. The unstimulated and untreated BMDMs were used as control. BMDMs treated with DMSO were used as negative control. Abbreviations: DMSO, dimethyl sulfoxide; LPS, lipopolysaccharides; UA, urolithin A; RAD, radiation.
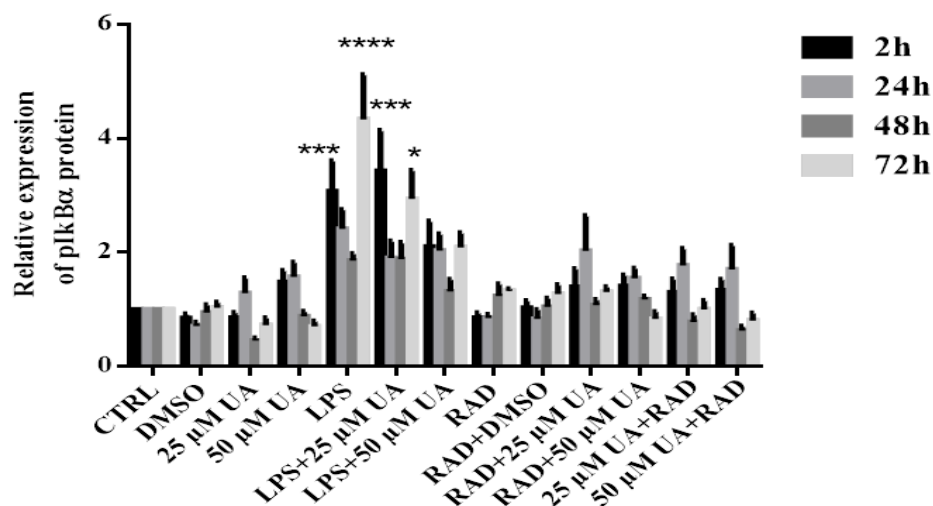
B

C

Figure 30 Continued: Effect of urolithin A on AKT expression and phosphorylation in LPS-stimulated or X-irradiated murine BMDMs

Bar graph shows the relative intensities of total AKT (B) and pAKT (C) at different time points. Arithmetic means ± SEM from five independent experiments. Two way ANOVA was used and * ($p < 0.05$), ** (P 0.01), and *** ($p < 0.001$) indicate statistically significant differences compared to respective control. Abbreviations: DMSO, dimethyl sulfoxide; LPS, lipopolysaccharides; UA, urolithin A; RAD, radiation.

D

Figure 30 Continued: Effect of urolithin A on AKT expression and phosphorylation in LPS-stimulated or X-irradiated murine BMDMs

(D) Bar diagram showing relative band intensities of pAKT normalized to total AKT. Arithmetic means ± SEM from five independent experiments. Two way ANOVA was used and * ($p < 0.05$) and *** ($p < 0.001$) indicate statistically significant differences compared to respective control. Abbreviations: DMSO, dimethyl sulfoxide; LPS, lipopolysaccharides; UA, urolithin A; RAD, radiation.
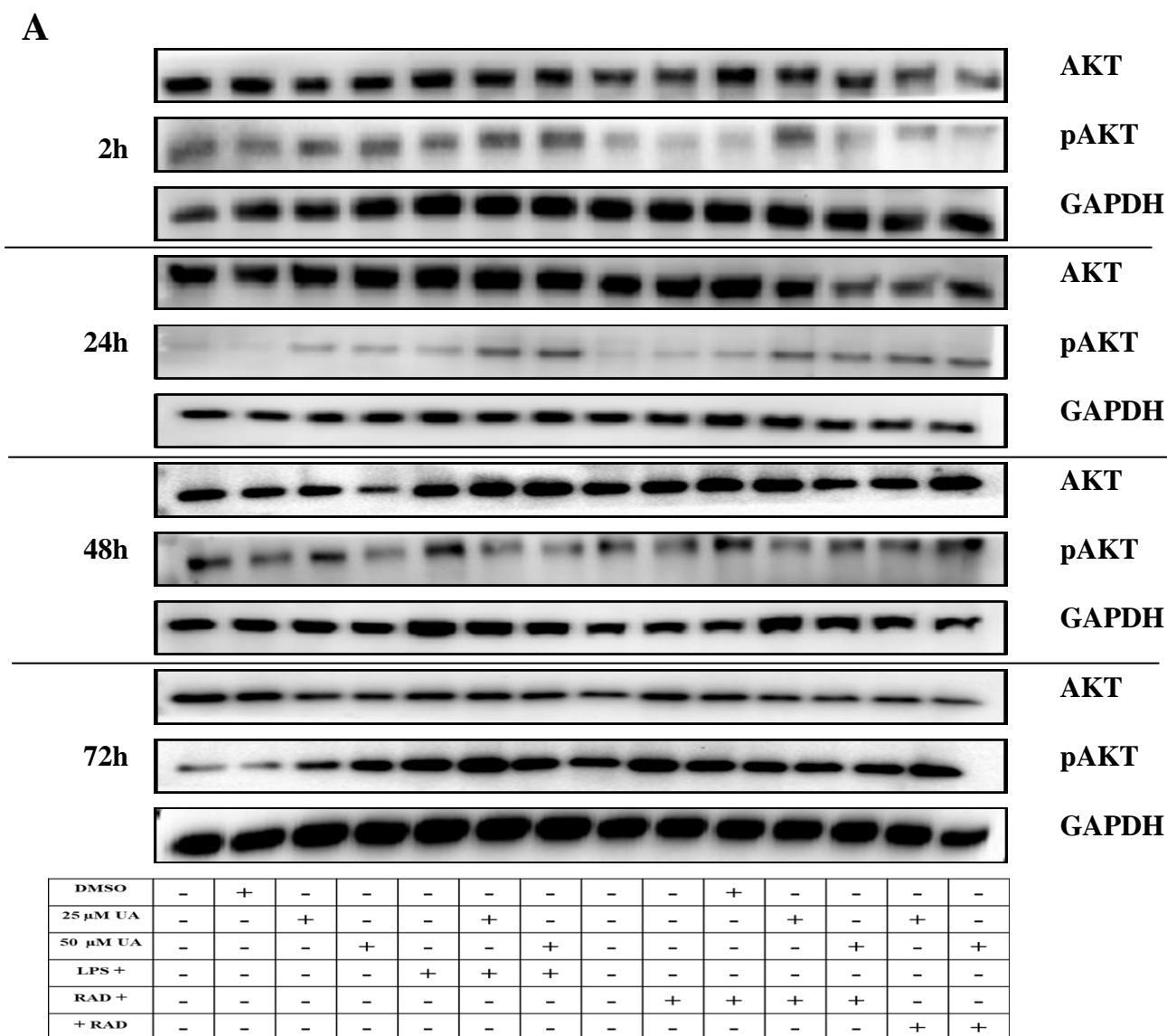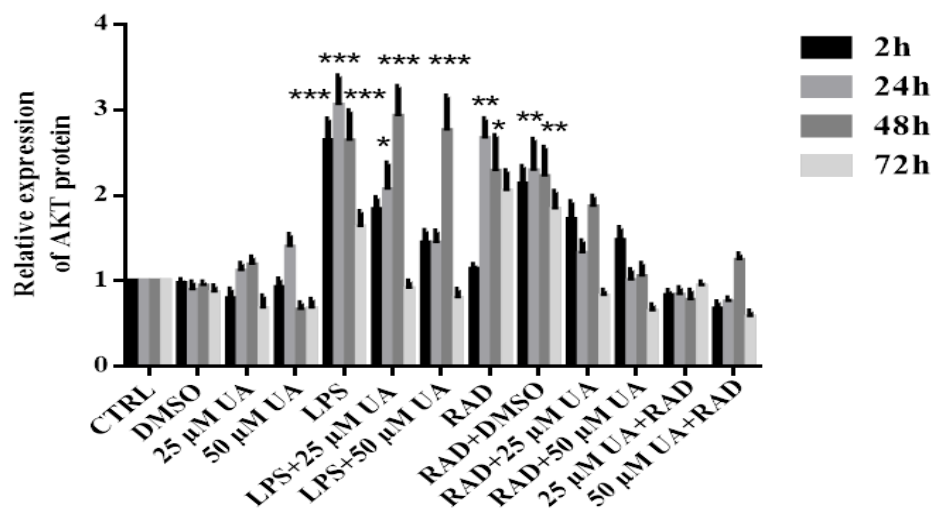
3.7.4.2 Effect of urolithin A on mTOR expression and phosphorylation in LPS-stimulated or X-irradiated murine BMDMs

Murine BMDMs were stimulated with 1µg/ml of LPS or 6 Gy X-irradiation in the presence or absence of UA. The activation of mTOR requiring phosphorylation at Serine 2448 was monitored by immunoblot analysis using anti-phospho-mTOR antibodies.

As presented in Figure 31, the treatment of BMDMs with UA (25 µM or 50 µM) alone showed a remarkable increase in total (Figure 31 A&B) and phospho-mTOR (Figure 31A&C) expression compared to untreated control during the time intervals. Similarly, the stimulation of BMDMs with 1µg/ml LPS was enough to induce highly significant increase in total (Figure 31A&B) and phospho-mTOR (Figure 31A&C) expression during the time intervals.

In addition, BMDMs receiving UA (25 µM or 50 µM) simultaneously during LPS stimulation revealed higher expression of total mTOR than LPS alone during the time intervals (Figure 31A&B). On the contrary, the co-stimulation of UA with LPS exhibited a dose dependent decrease of phospho-mTOR than those receiving LPS alone during the time intervals (Figure 31A&C).

On the other hand, the stimulation of BMDMs with 6 Gy X-irradiation shows non-significant changes in the total mTOR expression (Figure 31B) during the time intervals. In addition, administration of UA pre- and post-irradiations did not record significant changes in total mTOR expression during the time intervals. On the contrary, BMDMs receiving 6 Gy X-irradiation exhibited a significant upregulation in phospho-mTOR expression (Figure 31A&C) during the time intervals except an inconsiderable change was recorded after 2h compared to untreated control. In addition, administration of UA pre- or post-irradiation induced a remarkable decrease in phospho-mTOR expression achieving values near to untreated control during the time intervals.

Figure 31D demonstrate the relative intensities of phospho-mTOR expression normalized to total mTOR. Administration of UA (25 µM or 50 µM) alone induced inconsiderable changes during the time intervals. LPS induced highly significant upregulation in mTOR phosphorylation during the time intervals. Administration of UA simultaneously to LPS-stimulation induced dose dependent decrease in mTOR phosphorylation during the time intervals. Concerning X-irradiation, highly significant increase was recorded in phospho-mTOR expression. Administration of UA pre- or post-irradiation revealed a significant dose dependent decrease in mTOR phosphorylation.

In conclusion, 1 µg/ml LPS was sufficient to induce upregulation of total and phospho-mTOR expression in BMDMs during the time intervals. In addition, 6 Gy X-irradiation was able to induce a significant elevation in phospho-mTOR but not in total mTOR expression. UA alone was able to upregulate total and phospho-mTOR expression. The sources of variations between groups are summarized in supplementary Table 9.

A

DMSO	–	+	–	–	–	–	–	–	–	+	–	–	–	–
25 µM UA	–	–	+	–	–	+	–	–	–	–	+	–	+	–
50 µM UA	–	–	–	+	–	–	+	–	–	–	–	+	–	+
LPS +	–	–	–	–	+	+	+	–	–	–	–	–	–	–
RAD +	–	–	–	–	–	–	–	–	+	+	+	+	–	–
+ RAD	–	–	–	–	–	–	–	–	–	–	–	–	+	+
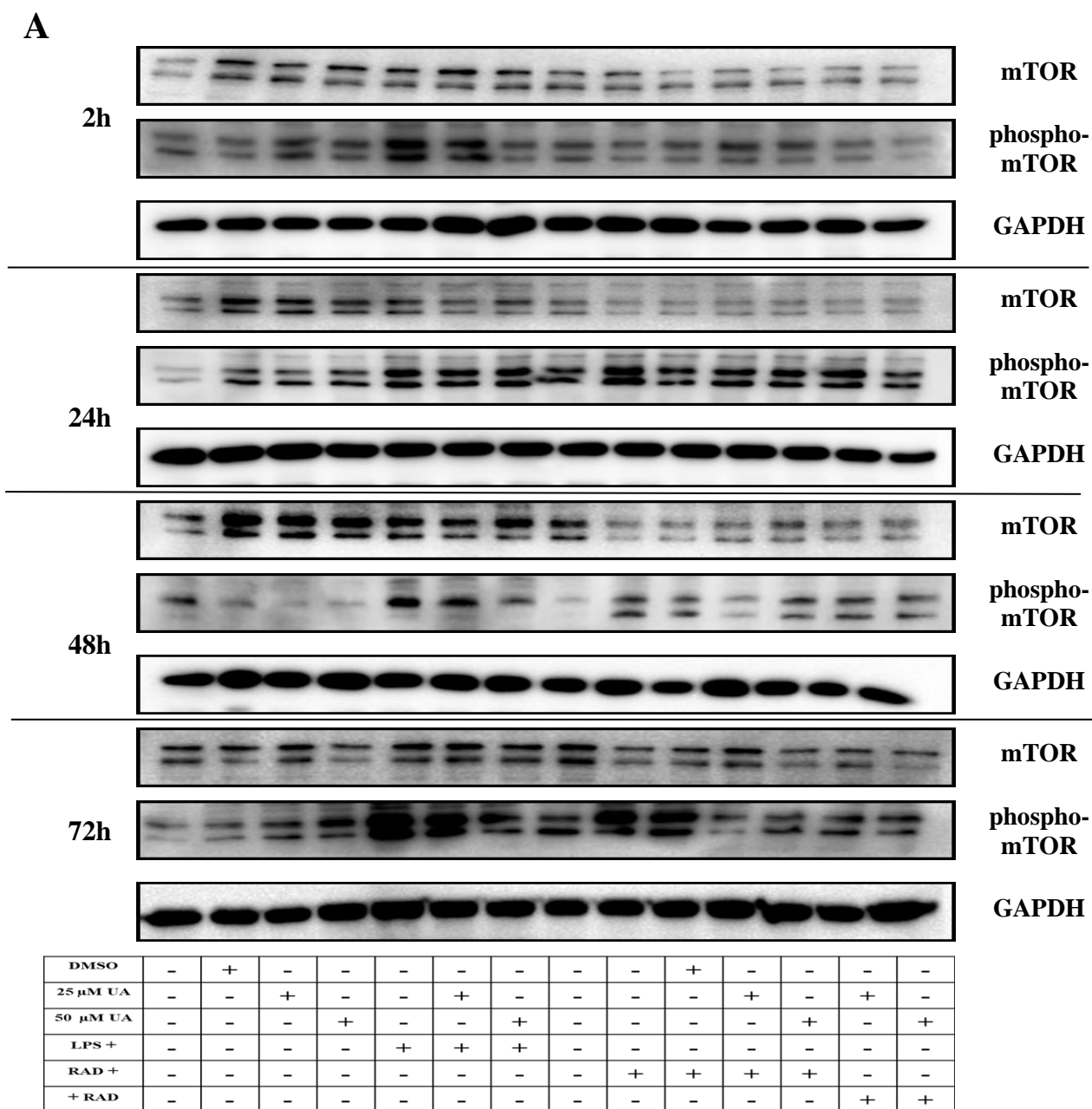
Figure 31 Effect of urolithin A on mTOR expression and phosphorylation in LPS-stimulated or X-irradiated murine BMDMs

BMDMs were stimulated either by 1µg/ml of LPS or 6 Gy of X-irradiation in the presence or absence of UA (25 µM or 50 µM) and harvested at indicated time points followed by western blot analysis. The irradiated group was subdivided into two, where one received UA (25 or 50 µM) before 24h of irradiation and the other one received it directly post-irradiation. (A) Phosphorylation of mTOR was monitored by immunoblot using phospho-mTOR (Ser2448) monoclonal antibodies. Subsequently, blots were stripped and re-incubated with antibody against total mTOR. GAPDH served as a loading control. The unstimulated and untreated BMDMs were used as control. BMDMs treated with DMSO were used as negative control. Abbreviations: DMSO, dimethyl sulfoxide; LPS, lipopolysaccharides; UA, urolithin A; RAD, radiation.
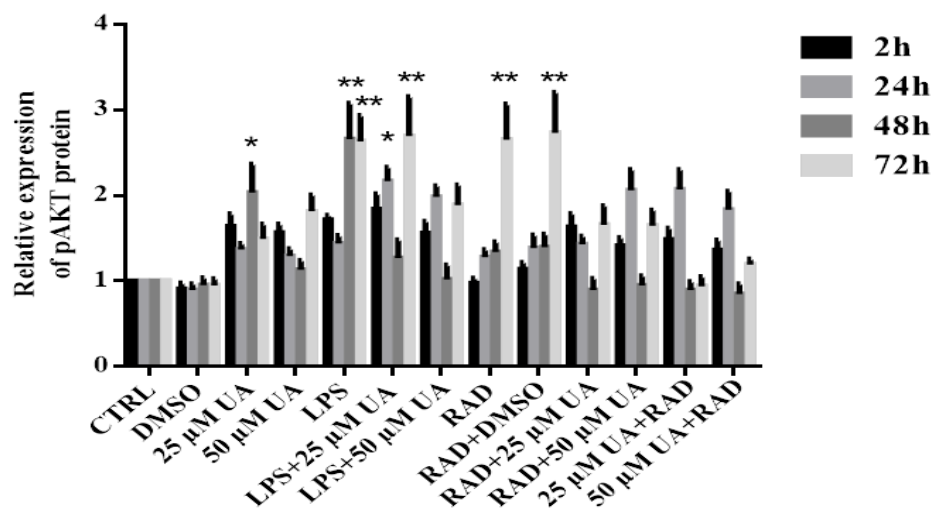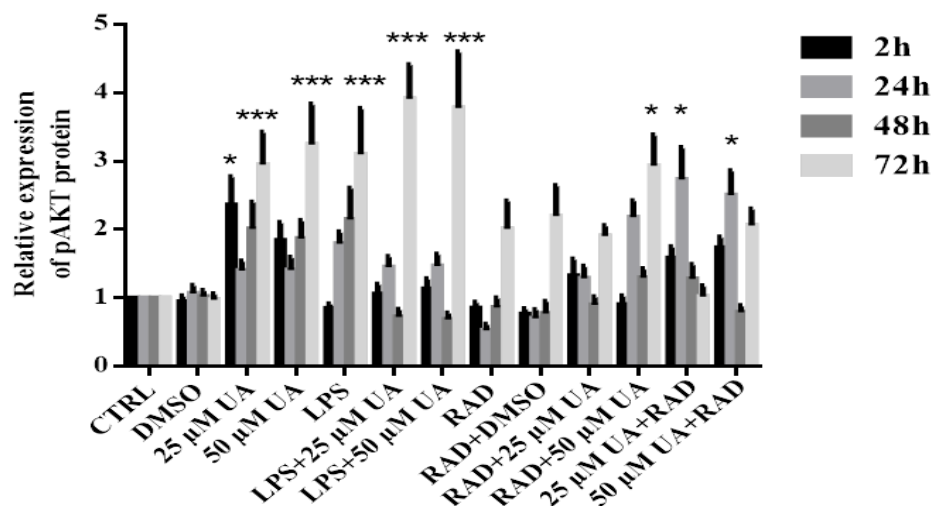
B
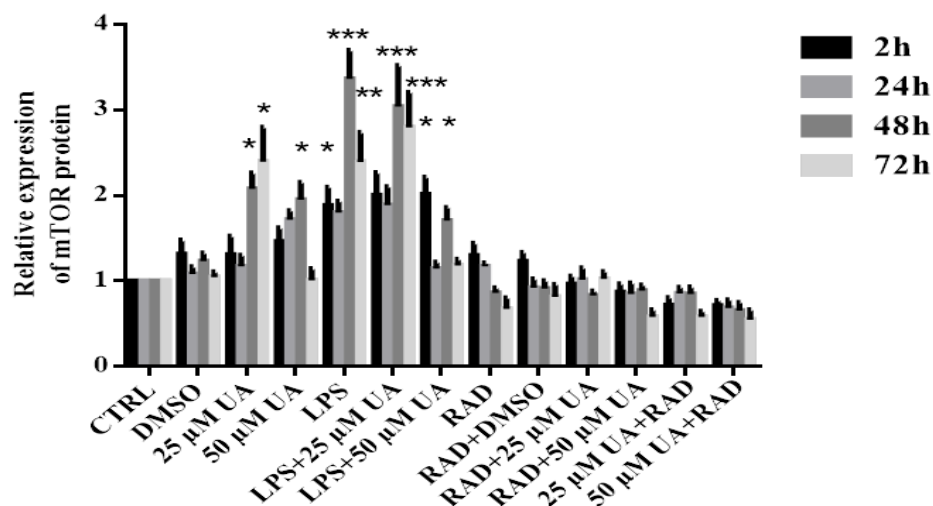
C
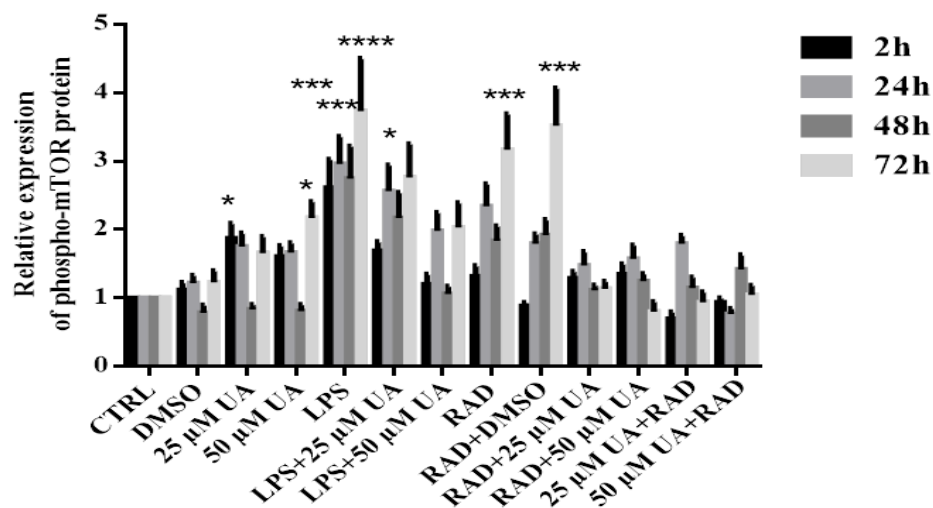
Figure 31 Continued: Effect of urolithin A on mTOR expression and phosphorylation in LPS-stimulated or X-irradiated murine BMDMs

Bar graph shows relative intensities of total mTOR (B) and phospho-mTOR (C) at different time points. Arithmetic means ± SEM from five independent experiments. Two way ANOVA was used and * ($p < 0.05$), ** (P 0.01), *** ($p < 0.001$), and **** ($p < 0.0001$) indicate statistically significant differences compared to respective control. Abbreviations: DMSO, dimethyl sulfoxide; LPS, lipopolysaccharides; UA, urolithin A; RAD, radiation.

D
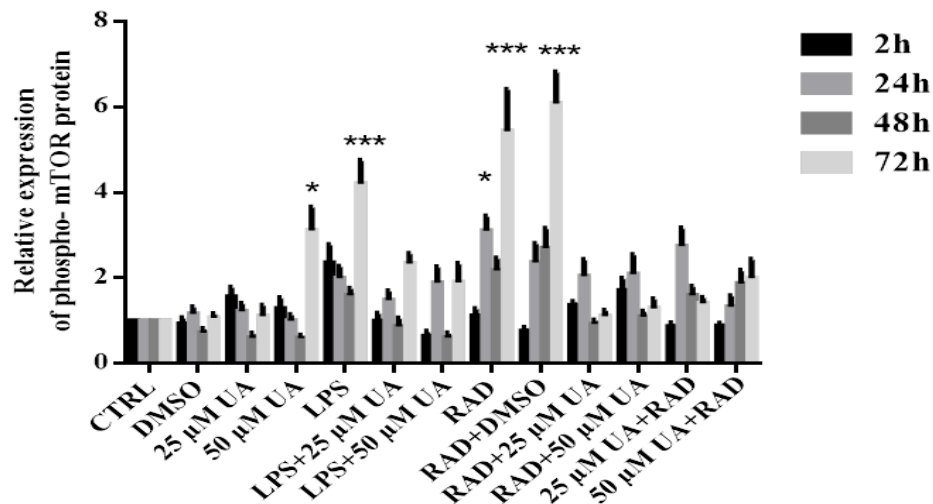
Figure 31 Continued: Effect of urolithin A on mTOR expression and phosphorylation in LPS-stimulated or X-irradiated murine BMDMs

(D) Bar diagram showing relative intensities of phospho-mTOR normalized to total mTOR protein expression. Arithmetic means ± SEM from five independent experiments. Two way ANOVA was used and * ($p < 0.05$) and *** ($p < 0.001$) indicate statistically significant differences compared to respective control. Abbreviations: DMSO, dimethyl sulfoxide; LPS, lipopolysaccharides; UA, urolithin A; RAD, radiation.

3.8 Influence of urolithin A on mRNA expression of inflammatory molecules in LPS-stimulated or X-irradiated murine BMDMs

The effect of UA on pro-inflammatory (IL-1β, IL-2, IL-6, IL-12 and TNF-α) and anti-inflammatory (IL-4, IL-10, IFN-γ, TGF-β and NOS2) cytokine mRNA expression in stimulated BMDMs after 2h, 24h and 48h. Some pro-inflammatory cytokines such as IFN-γ have an anti-inflammatory role and *vice versa*. BMDMs were stimulated either with LPS (1µg/ml) or X-irradiation (6 Gy) in the presence or absence of UA (25 µM or 50 µM). The administration of UA (25 µM or 50 µM) alone did not registered remarkable changes in the tested inflammatory cytokines except a notable, dose dependent, increase was observed for TGF-β and IFN-γ after 2h, 24h and 48h.

3.8.1 Influence of urolithin A on pro-inflammatory cytokine mRNA expression in LPS-stimulated or X-irradiated murine BMDMs

As mentioned before, LPS is known to induce a typical M1 phenotype (Mantovani, Sica et al. 2004). Data presented in Figure 32 illustrate a highly significant elevation in IL-1β (Figure 32A), IL-2 (Figure 32B), IL-6 (Figure 32C), IL-12 (Figure 32D) and TNF-α (Figure 32E) expression of LPS stimulated BMDMs compared to untreated control after 2h, 24h and 48h. Notably, IL-6 and TNF-α expression was significantly higher after 2h and recorded a remarkable decrease at 24h and 48h although they are still significantly higher as compared to untreated control. The post-treatment of LPS-stimulated BMDMs with UA (25 µM or 50 µM) was able to induce a significant decrease of IL-2, IL-6, IL-12 and TNF-α with values near to untreated control. In addition, IL-1β expression recorded a significant decrease as compared to LPS alone and attaining intermediate values between untreated control and LPS-stimulated BMDMs.

On the other hand, exposure of BMDMs to X-irradiation was sufficient to induce a significant increase in IL-2 expression (Figure 32B) during the time intervals. On the opposite side, a slight but non-significant increase in IL-1β (Figure 32A), IL-6 (Figure 32C), IL-12 (Figure 32D) and TNF-α (Figure 32E) expression was observed after X-irradiation during the time intervals. In addition, BMDMs receiving UA (25 µM or 50 µM) pre- or post-irradiation did not record significant changes except a significant decrease in IL-2 after 2h, 24h and 48h and an inconsiderable increase in IL-12 expression after 48h.

In conclusion, LPS alone was enough to induce a significant upregulation in all tested pro-inflammatory cytokine mRNA expression in BMDMs. Exposure of BMDMs to 6 Gy of X-irradiation demonstrated a strongly significant upregulation of IL-2 expression which was canceled by UA (25 µM or 50 µM). In addition, slight non-significant elevations were observed in IL-1β, IL-6 and TNF-α expression during the time intervals. The source of difference between groups and time factor are summarized in supplementary Table 10.

103

A

B

Figure 32 Action of urolithin A on pro-inflammatory cytokine mRNA expression in LPS-stimulated or X-irradiated murine BMDMs after 2h, 24h and 48h

BMDMs were stimulated either by 1μg/ml of LPS or 6 Gy of X-irradiation in the presence or absence of UA (25 μM or 50 μM) for 2h, 24h and 48h. Subsequently, mRNA expression of the pro-inflammatory cytokines IL-1β (A) and IL-2 (B) over GAPDH were measured in BMDMs by qRT-PCR at depicted time points. The irradiated group was subdivided into two, where one received UA (25 or 50 μM) before 24h of irradiation and the other one received it directly post-irradiation. The unstimulated and untreated BMDMs were used as control. BMDMs treated with DMSO were used as negative control. Arithmetic means ± SEM from seven independent experiments are depicted. Two way ANOVA was used and * ($p < 0.05$), ** (P 0.01), *** ($p < 0.001$), and **** ($p < 0.0001$) indicate statistically significant differences compared to respective control. Abbreviations: DMSO, dimethyl sulfoxide; UA, urolithin A; LPS, lipopolysaccharides; RAD, radiation; IL, Interleukin; GAPDH, glyceraldehyde 3-phosphate dehydrogenase.

C

D

Figure 32 Continued: Action of urolithin A on pro-inflammatory cytokine mRNA expression in LPS-stimulated or X-irradiated murine BMDMs after 2h, 24h and 48h

BMDMs were stimulated either by 1μg/ml of LPS or 6 Gy of X-irradiation in the presence or absence of UA (25 μM or 50 μM) for 2h, 24h and 48h. Subsequently, mRNA expression of the pro-inflammatory cytokines IL-6 (C) and IL-12 (D) over GAPDH were measured in BMDMs by qRT-PCR at depicted time points. Arithmetic means ± SEM from seven independent experiments are depicted. Two way ANOVA was used and * ($p < 0.05$), ** ($P\ 0.01$), *** ($p < 0.001$), and **** ($p < 0.0001$) indicate statistically significant differences compared to respective control. Abbreviations: DMSO, dimethyl sulfoxide; UA, urolithin A; LPS, lipopolysaccharides; RAD, radiation; IL, Interleukin; GAPDH, glyceraldehyde 3-phosphate dehydrogenase.

E

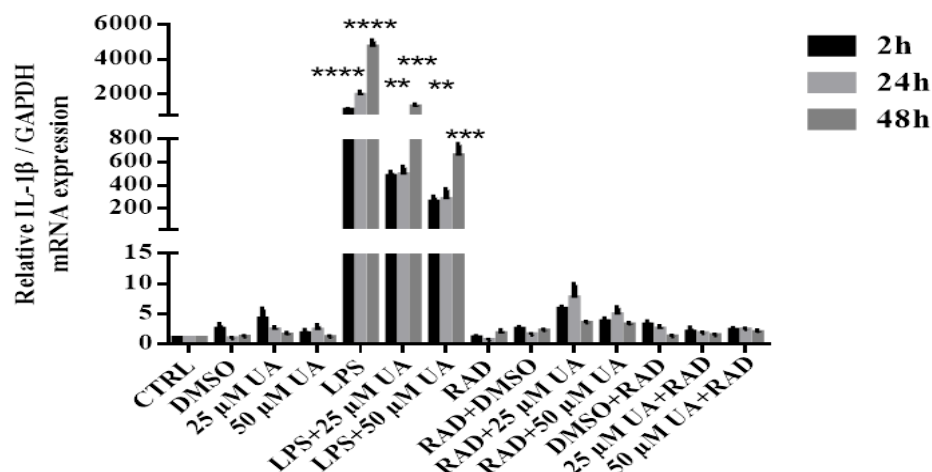**Figure 32 Continued: Action of urolithin A on pro-inflammatory cytokine mRNA expression in LPS-stimulated or X-irradiated murine BMDMs after 2h, 24h and 48h**

(E) BMDMs were stimulated either by 1µg/ml of LPS or 6 Gy of X-irradiation in the presence or absence of UA (25 µM or 50 µM) for 2h, 24h and 48h. Subsequently, mRNA expression of the pro-inflammatory cytokine TNF-α over GAPDH was measured in BMDMs by qRT-PCR at depicted time points. Arithmetic means ± SEM from seven independent experiments are depicted. Two way ANOVA was used and ** (P 0.01) and **** (p < 0.0001) indicate statistically significant differences compared to respective control. Abbreviations: DMSO, dimethyl sulfoxide; UA, urolithin A; LPS, lipopolysaccharides; RAD, radiation; TNF, tumor necrosis factor; GAPDH, glyceraldehyde 3-phosphate dehydrogenase.

3.8.2 Influence of urolithin A on anti-inflammatory cytokine mRNA expression in LPS-stimulated or X-irradiated murine BMDMs

Results presented in Figure 33 show that LPS alone was sufficient to induce significant elevation in IL-10 (Figure 33B), IFN-γ (Figure 33D) and NOS2 (Figure 33E) expression but a slight non-significant increase was observed in IL-4 expression (Figure 33A). In addition, an inconsiderable decrease in TGF-β expression (Figure 33C) was reported in BMDMs as compared to untreated control during the time intervals. Notably, LPS induced a highly significant increase after 2h followed by remarkable decreases but still significant after 24h and 48h. The post-treatment with UA (25 µM or 50 µM) was able to induce significant depressions in IFN-γ and NOS2 expression attaining intermediate values between untreated control and LPS group. Significant elevation was observed in IL-4 (Figure 33) expression after 2h and 24h followed by a decrease at 72h with values near to untreated control. Concerning IL-10 and TGF-β, UA did not record any significant changes at all as compared to LPS ones.

On the other hand, exposure of BMDMs to 6 Gy of X-irradiation induced remarkable upregulation of IL-4 (Figure 33A), IL-10 (Figure 33B), TGF-β (Figure 33C), IFN-γ (Figure 33 D) and NOS2 (Figure 33E) expression during the time intervals. Notably, IL-4 exhibited highly significant elevations after 2h followed by a sudden decrease still significant after 24h and 48h. BMDMs received DMSO 2h before or post-irradiation also registered a highly significant increase in all examined anti-inflammatory cytokine mRNA expression as compared to control cells.

In addition, BMDMs receiving UA (25 µM or 50 µM) pre- or post-irradiation induced remarkable inhibition in TGF-β, IFN-γ and NOS2 expression as compared to irradiated ones and attaining the values near to untreated control. The pre-administration of UA recorded better effects than the post ones.

In conclusion, 1 µg/ml of LPS was enough to induce remarkable increases in IL-10, IFN-γ and NOS2 expression in BMDMs during the time intervals. Similarly, exposure of BMDMs to X-irradiation alone was able to induce significant elevation in all mentioned anti-inflammatory cytokine mRNA expressions during the time intervals. The pre- and post-administration of UA (25 µM or 50 µM) showed a significant decrease of TGFβ, IFN-γ and NOS2 expression as compared to irradiated cells as well as a notable increase was recorded in IL-4 and IL-10 mRNA expressions during the time intervals. The source of variation between groups is summarized in supplementary Table 11.
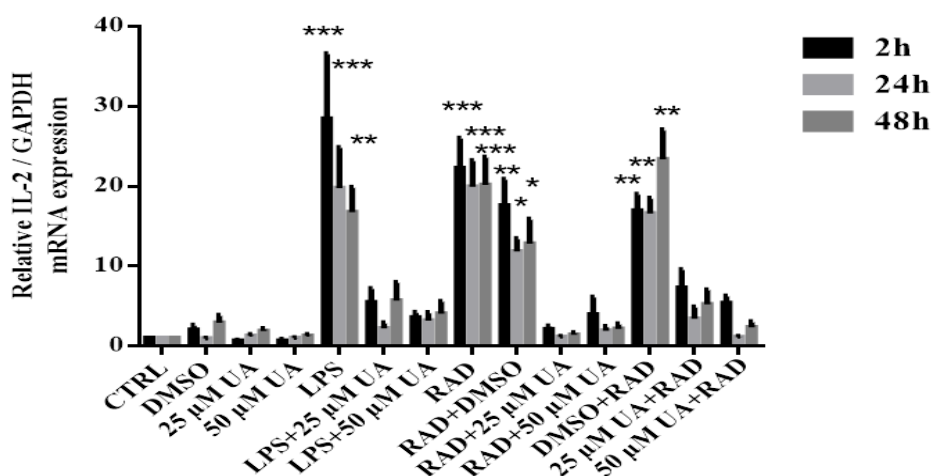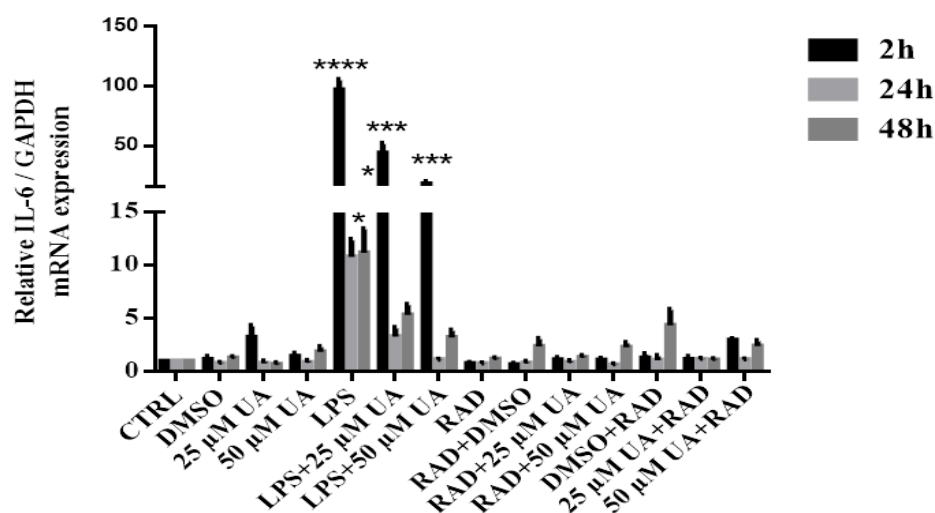
A
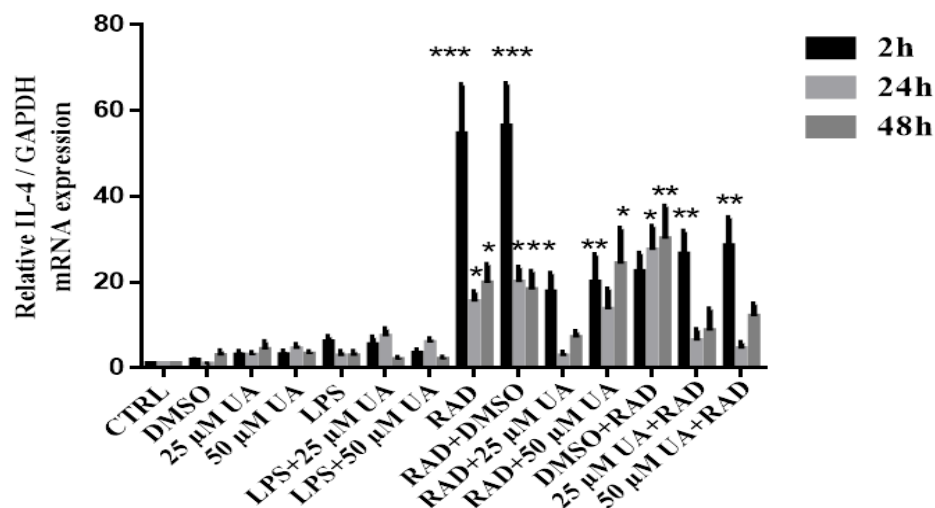
B
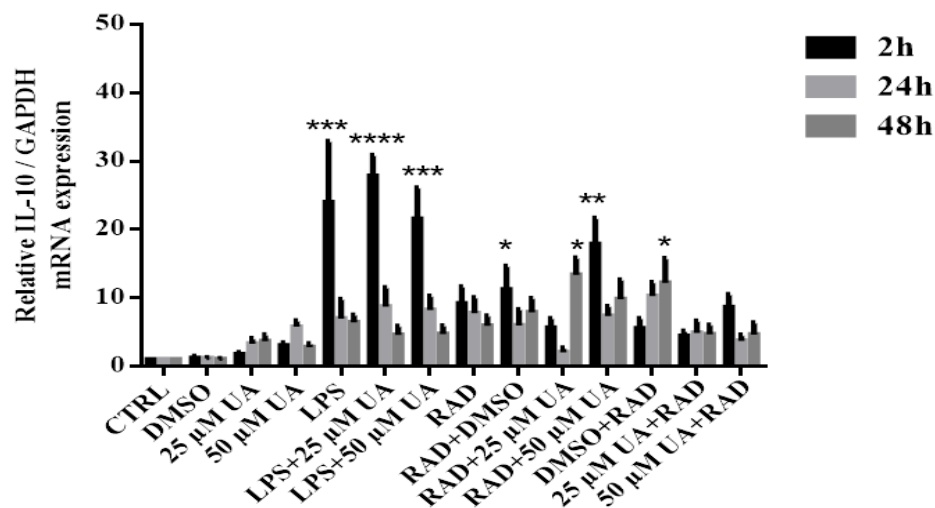
Figure 33 Action of urolithin A on anti-inflammatory cytokine mRNA expression in LPS-stimulated or X-irradiated murine BMDMs after 2h, 24h and 48h

BMDMs were stimulated either by 1μg/ml of LPS or 6 Gy of X-irradiation in the presence or absence of UA (25 μM or 50 μM) for 2h, 24h and 48h. Subsequently, mRNA expression of the anti-inflammatory cytokines IL-4 (A) and IL-10 (B) over GAPDH were measured in BMDMs by qRT-PCR at depicted time points. The irradiated group was subdivided into two, where one received UA (25 or 50 μM) before 24h of irradiation and the other one received it directly post-irradiation. The unstimulated and untreated BMDMs were used as control. BMDMs treated with DMSO were used as negative control. Arithmetic means ± SEM from seven independent experiments are depicted. Two way ANOVA was used and * ($p < 0.05$), ** (P 0.01), and *** ($p < 0.001$) indicate statistically significant differences compared to respective control. Abbreviations: DMSO, dimethyl sulfoxide; UA, urolithin A; LPS, lipopolysaccharides; RAD, radiation; IL, Interleukin; GAPDH, glyceraldehyde 3-phosphate.
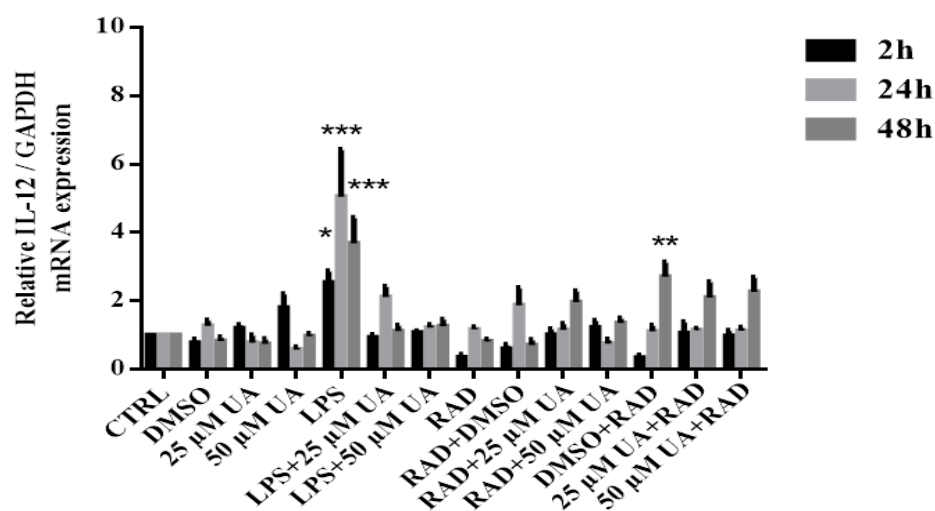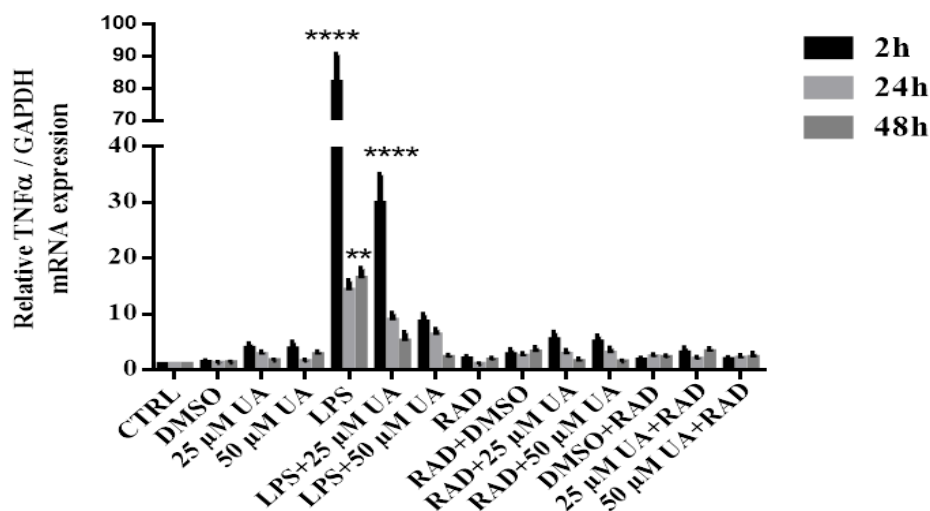
C

D

Figure 33 Continued: Action of urolithin A on anti-inflammatory cytokine mRNA expression in LPS-stimulated or X-irradiated murine BMDMs after 2h, 24h and 48h

BMDMs were stimulated either by 1μg/ml of LPS or 6 Gy of X-irradiation in the presence or absence of UA (25 μM or 50 μM) for 2h, 24h and 48h. Subsequently, mRNA expression of the anti-inflammatory cytokines TGF-β (C) and IFN-γ (D) over GAPDH were measured in BMDMs by qRT-PCR at depicted time points. Arithmetic means ± SEM from seven independent experiments are depicted. Two way ANOVA was used and * (p < 0.05), ** (P 0.01), *** (p < 0.001), and **** (p < 0.0001) indicate statistically significant differences compared to respective control. Abbreviations: DMSO, dimethyl sulfoxide; UA, urolithin A; LPS, lipopolysaccharides; RAD, radiation; TGF, tumor growth factor; IFN, interferon gamma; GAPDH, glyceraldehyde 3-phosphate.

E

Figure 33 Continued: Action of urolithin A on anti-inflammatory cytokine mRNA expression in LPS-stimulated or X-irradiated murine BMDMs after 2h, 24h and 48h

(E) BMDMs were stimulated either by 1µg/ml of LPS or 6 Gy of X-irradiation in the presence or absence of UA (25 µM or 50 µM) for 2h, 24h and 48h. Subsequently, mRNA expression of the anti-inflammatory mediator NOS2 over GAPDH was measured in BMDMs by qRT-PCR at depicted time points. Arithmetic means ± SEM from seven independent experiments are depicted. Two way ANOVA was used and * ($p < 0.05$), ** (P 0.01), and **** ($p < 0.0001$) indicate statistically significant differences compared to respective control. Abbreviations: DMSO, dimethyl sulfoxide; UA, urolithin A; LPS, lipopolysaccharides; RAD, radiation; NOS, nitric oxide synthase; GAPDH, glyceraldehyde 3-phosphate.

3.9   Action of urolithin A on inflammatory cytokine production by BMDMs

Next, the effect of UA on secretion of pro-inflammatory (IL-1β, IL-6, IL-12 and TNF-α) and anti-inflammatory (IL-4, IL-10, IFN-γ and TGF-β) cytokines in stimulated BMDMs after 24h and 48h were evaluated. BMDMs were stimulated either with LPS (1µg/ml) or X-irradiation (6 Gy) in the presence or absence of UA (25 µM or 50 µM).

3.9.1   Action of urolithin A on pro-inflammatory cytokine production

LPS is known to induce a typical M1 phenotype (Mantovani, Sica et al. 2004). BMDMs receiving 25 µM UA or 50 µM UA recorded remarkable dose dependent increase in IL-6 and TNF-α production after 24h and 48h. In addition, UA did not show any significant impact on IL-1β and IL-12 secretion.

Data represented in Figure 34 demonstrate a highly significant elevation in IL-1β (Figure 34A), IL-6 (Figure 34B), IL-12 (Figure 34C), and TNF-α (Figure 34D) in LPS stimulated BMDMs compared to untreated control after 24h and 48h with respect to a notable decrease of TNF-α production after 48h.

The post-administration of UA (25 µM or 50 µM) was able to induce significant depression of IL-1β and IL-12 after 24h and 48h while for TNF-α, the inhibition was only detected after 24h. However, UA was insufficient to suppress IL-6 cytokine production, unless a slight non-significant decrease was registered after 48h.

On the other hand, exposure of BMDMs to 6 Gy of X-irradiation did not record any significant secretion of tested pro-inflammatory cytokines. In addition, the post-administration of UA (25 µM or 50 µM) had no impact on IL-1β and IL-12 production at all and reported an inconsiderable increase in IL-6 and TNF-α level compared to untreated control and irradiated group. The post-administration of UA had no effect on IL-1β and IL-6 at all and induced an inconsiderable increase in IL-12 and TNF-α in particular after 24h and reached nearly the level of the control cells at 48h.

In conclusion, LPS stimulated BMDMs demonstrated a highly significant increase of pro-inflammatory cytokines while X-irradiated BMDMs did not show any significant effect. UA was able to suppress the upregulation of IL-1β and IL-12 production after LPS-stimulation. The source of variations between groups is summarized in supplementary Table 12**.**

A
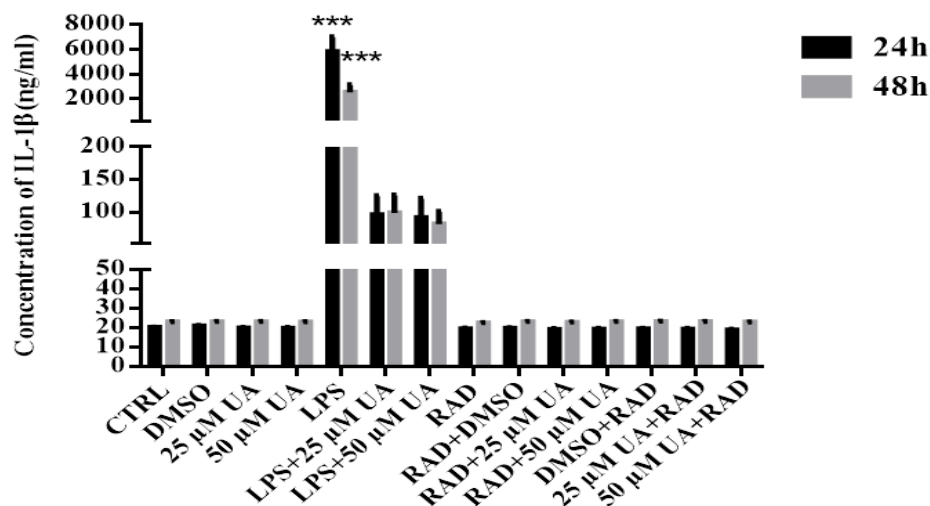
B

Figure 34 Effect of urolithin A on pro-inflammatory cytokine production induced by LPS-stimulation or X-irradiation in murine BMDMs after 24h and 48h

BMDMs were stimulated either by 1μg/ml of LPS or 6 Gy of X-irradiation in the presence or absence of UA (25 μM or 50 μM) for 24h or 48h. IL-1β (A) and IL-6 (B) pro-inflammatory cytokines were measured in the culture supernatants of stimulated BMDMs. The irradiated group was subdivided into two, where one received UA (25 or 50 μM) before 24h of irradiation and the other one received it directly post-irradiation. The unstimulated and untreated BMDMs were used as control. BMDMs treated with DMSO were used as negative control. Arithmetic means ± SEM from seven independent experiments. Two way ANOVA was used and ** (P 0.01) and *** (p < 0.001) indicate statistically significant differences compared to respective control. Abbreviations: DMSO, dimethyl sulfoxide; UA, urolithin A; LPS, lipopolysaccharides; RAD, radiation; IL, Interleukin.
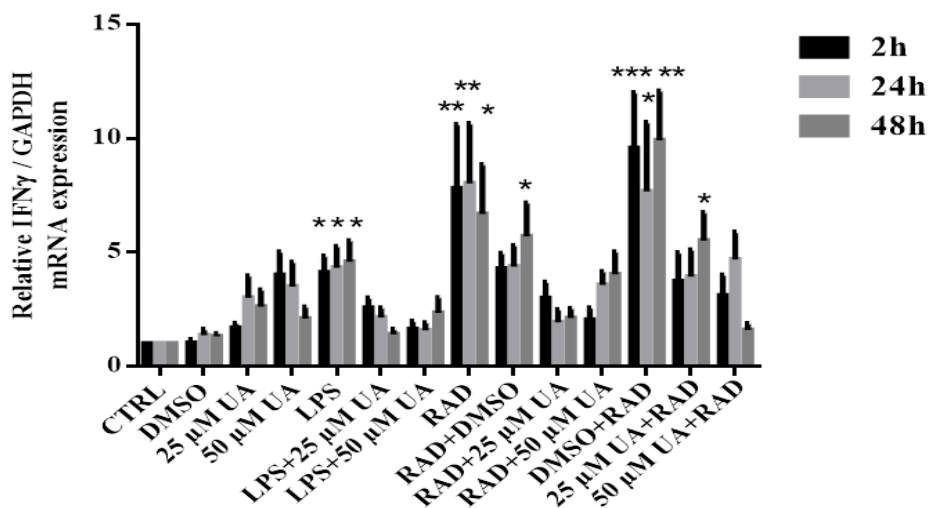
C

D

Figure 34 Continued: Effect of urolithin A on pro-inflammatory cytokine production induced by LPS-stimulation or X-irradiation in murine BMDMs after 24h and 48h

BMDMs were stimulated either by 1μg/ml of LPS or 6 Gy of X-irradiation in the presence or absence of UA (25 μM or 50 μM) for 24h or 48h. IL-12 (C) and TNFα (D) pro-inflammatory cytokines were measured in the culture supernatants of stimulated BMDMs. Arithmetic means ± SEM from seven independent experiments. Two way ANOVA was used and ** (P 0.01) and *** (p < 0.001) indicate statistically significant differences compared to respective control. Abbreviations: DMSO, dimethyl sulfoxide; UA, urolithin A; LPS, lipopolysaccharides; RAD, radiation; IL, Interleukin; TNF, tumor necrosis factor.

3.9.2 Action of urolithin A on anti-inflammatory cytokine production

First, both concentrations of UA 25 µM or UA 50 µM had no observable effect on IL-4, IL-10, IFN-γ and TGF-β production during the time intervals.

Data presented in Figure 35 show significant depression in IL-4 (Figure 35A) and TGF-β (Figure 35C) production in LPS stimulated BMDMs as well as a slight decrease of IFN-γ (Figure 35D) secretion was observed compared to untreated control after 24h and 48h. Surprisingly, a highly significant elevation of IL-10 (Figure 35B) production was registered in LPS stimulated BMDMs after 24h and still significant at 48h.

The post-administration of UA (25 µM or 50 µM) to LPS stimulated BMDMs was able to preserve the production of IL-4, TGF-β and IFN-γ with values near to untreated control after 24h and 48h. In addition, UA was able to induce a considerable decrease of IL-10 production and attaining intermediate values between normal control and LPS stimulated BMDMs.

On the other hand, exposure of BMDMs to 6 Gy of X-irradiation induced significant upregulation of IL-4 and IFN-γ while IL-10 and TGF-β did not registered any significant secretion after 24h and 48h. The pre- or post-administration of UA (25 µM or 50 µM) maintained the secretion of IL-4 and IFN-γ with values near to control ones. While UA did not recorded any significant change, even pre- or post-administration, in IL-10 and TGF-β production after 24h and 48h compared to untreated control and irradiated group.

In conclusion, exposure of BMDMs to 6 Gy of X-irradiation demonstrated strong significant upregulation of IL-4 and IFN-γ production and inconsiderable impact on IL-10 and TGF-β after 24h and 48h. The pre- or post-administration of UA (25 µM or 50 µM) was able to preserve the production of tested cytokines with values near to untreated control. The source of difference between groups and time factor are summarized in supplementary Table 13.

A
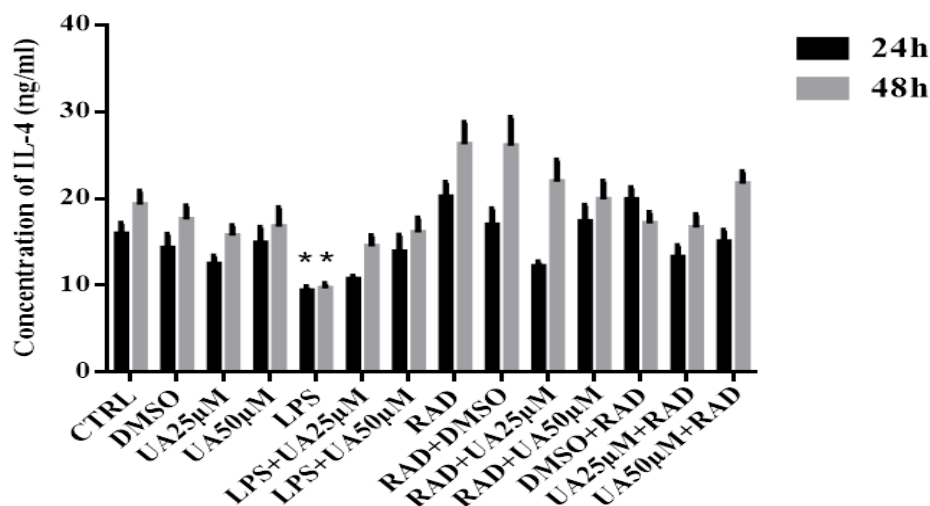
B
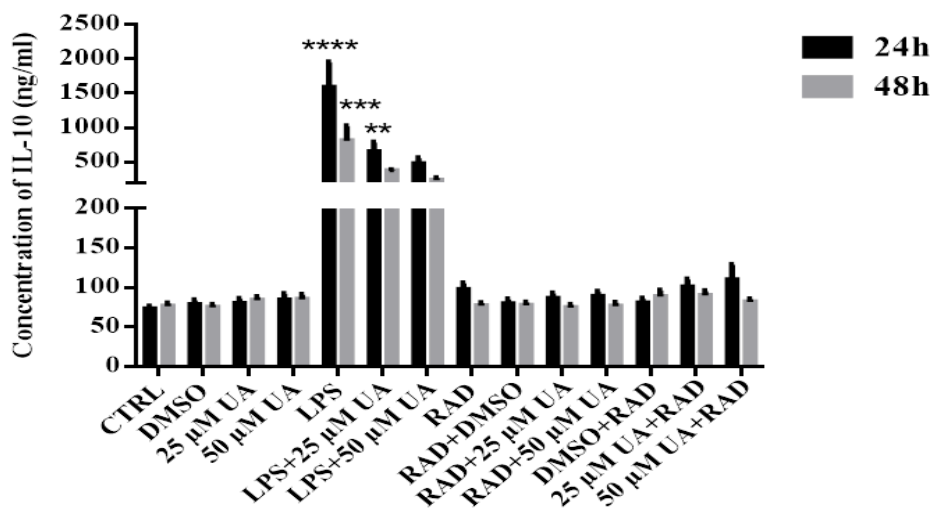
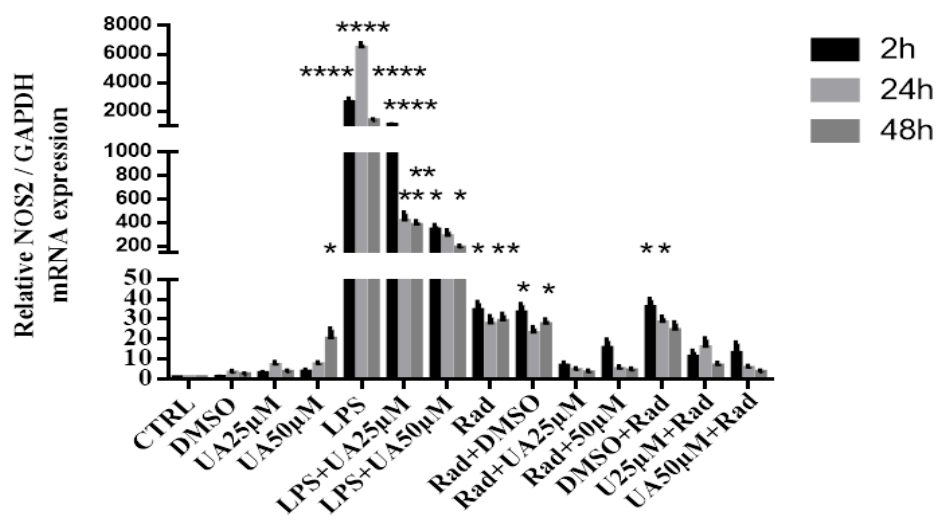**Figure 35 Effect of urolithin A on anti-inflammatory cytokine production in LPS-stimulated or X-irradiated murine BMDMs after 24h and 48h.**

BMDMs were stimulated either by 1µg/ml of LPS or 6 Gy of X-irradiation in the presence or absence of UA (25 µM or 50 µM) for 24h or 48h. IL-4 (A) and IL-10 (B) anti-inflammatory cytokines were measured in the culture supernatants of stimulated BMDMs. The irradiated group was subdivided into two, where one received UA (25 or 50 µM) before 24h of irradiation and the other one received it directly post-irradiation. The unstimulated and untreated BMDMs were used as control. BMDMs treated with DMSO were used as negative control. Arithmetic means ± SEM from seven independent experiments are depicted. Two way ANOVA was used and * ($p < 0.05$), ** (P 0.01), *** ($p < 0.001$), and **** ($p < 0.0001$) indicate statistically significant differences compared to respective conreol. Abbreviations: DMSO, dimethyl sulfoxide; UA, urolithin A; LPS, lipopolysaccharides; RAD, radiation; IL, Interleukin.
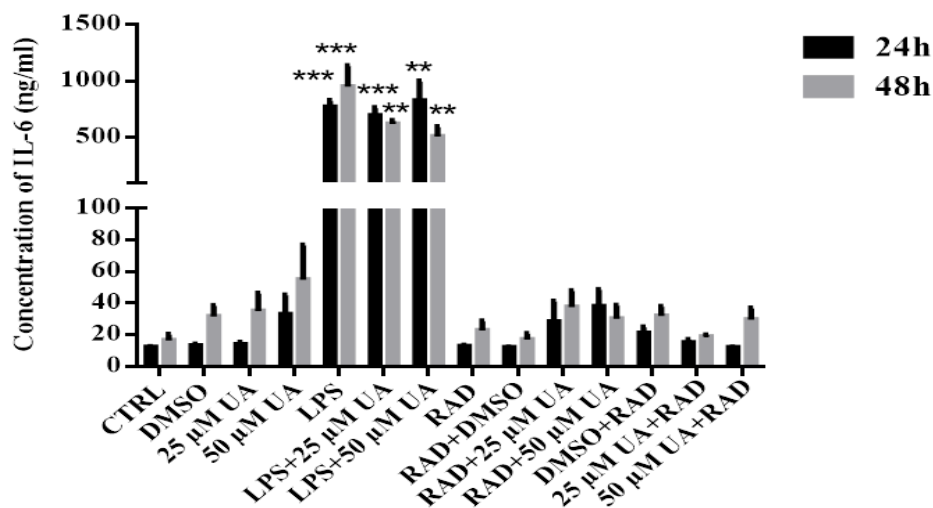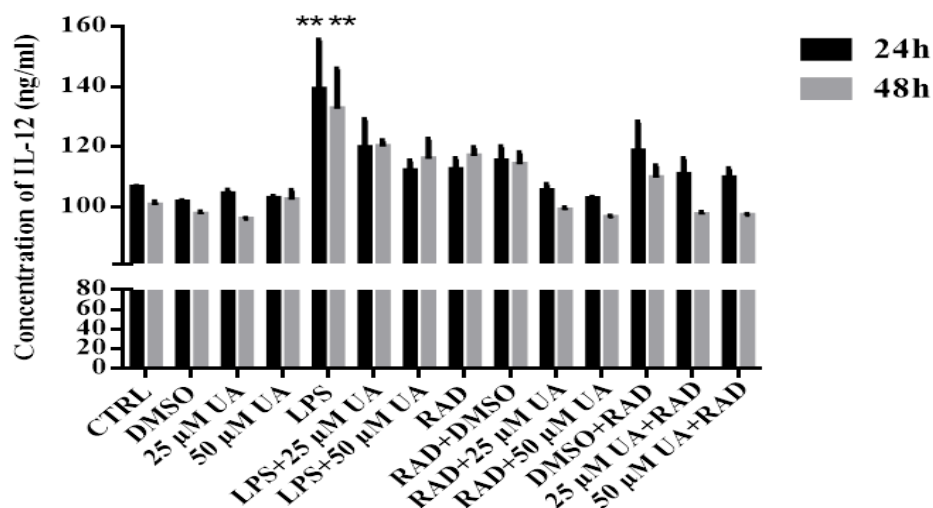
C
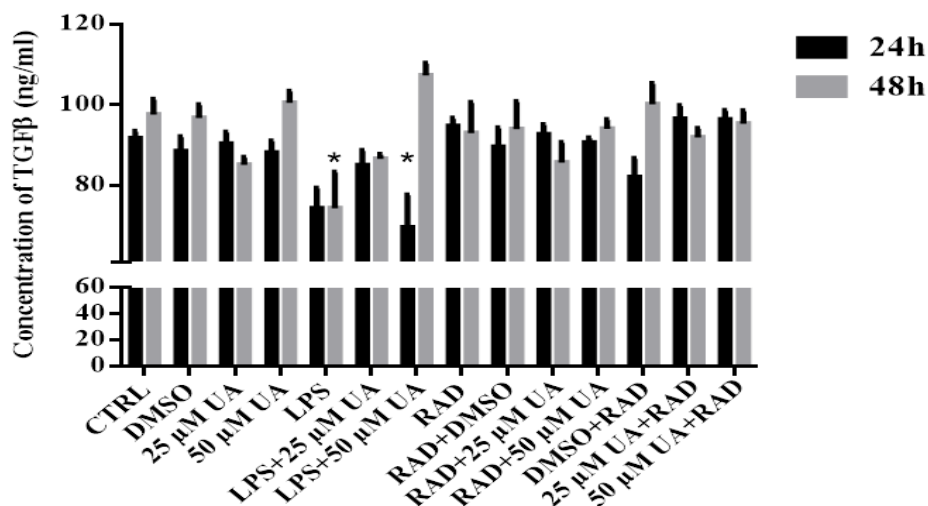
D

Figure 35 Continued: Effect of urolithin A on anti-inflammatory cytokine production in LPS-stimulated or X-irradiated murine BMDMs after 24h and 48h.

BMDMs were stimulated either by 1µg/ml of LPS or 6 Gy of X-irradiation in the presence or absence of UA (25 µM or 50 µM) for 24h or 48h. TGF-β (C) and IFN-γ (D) anti-inflammatory cytokines were measured in the culture supernatants of stimulated BMDMs. Arithmetic means ± SEM from seven independent experiments are depicted. Two way ANOVA was used and * ($p < 0.05$) and *** ($p < 0.001$) indicate statistically significant differences compared to respective control. Abbreviations: DMSO, dimethyl sulfoxide; UA, urolithin A; LPS, lipopolysaccharides; RAD, radiation; TGF, tumor growth factor; IFNγ, interferon gamma.
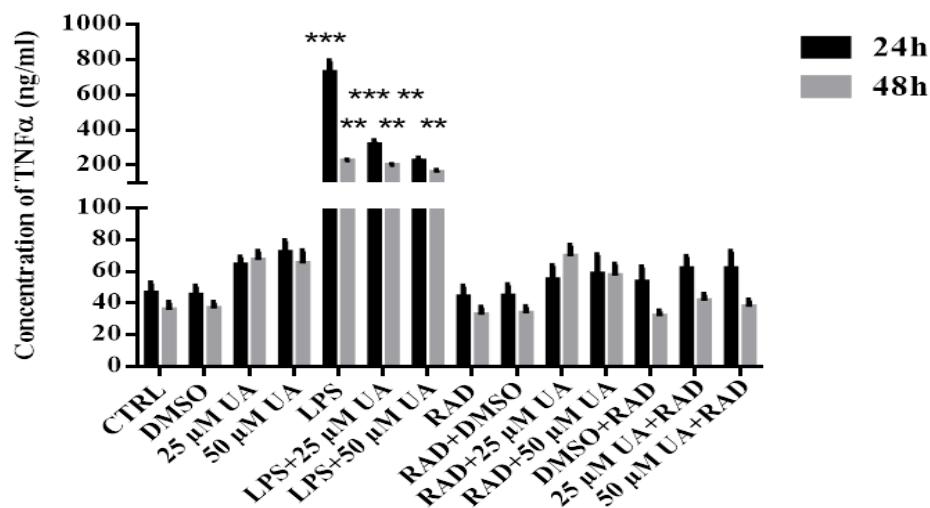
3.10 Effect of urolithin A on miRNA expression in LPS-stimulated or X-irradiated murine BMDMs

MicroRNAs (miRNA) are emerging as central regulators of inflammation. In addition, post-transcriptional regulation is an important control mechanism for the expression of genes involved in inflammation like cytokines and chemokines (Ishmael, Fang et al. 2008, Fan, Ishmael et al. 2011). Thus, the influence of UA (25 µM or 50 µM) on miR-9 (Figure 36A), miR-10 (Figure 36B), miR-99b (Figure 36C), miR-146a (Figure 36D) and miR-155 (Figure 36E) expression in LPS-stimulated or X-irradiated BMDMs was investigated. BMDMs receiving UA (25 µM or 50 µM) alone did not record any significant change in examined miRNA expression except a slight non-significant elevation was observed in miR-99b expression.

Data presented in Figure 36 demonstrate a significant decrease in miR-9 expression while a strong significant upregulation in miR-10, miR-99b, miR-146a and miR-155 was found in LPS-stimulated BMDMs compared to untreated control. Treatment of stimulated murine BMDMs (1 µg/ml LPS) with UA (25 µM or 50 µM) was enough to induce a remarkable decrease in miR-10, miR-99b, miR-146a and miR-155 expression with values near to untreated control. In addition, a slight progress to miR-9 expression was recorded.

On the other side, exposure of BMDMs to 6 Gy of X-irradiation induced non-significant changes in all tested miRNA. Notably, BMDMs treated with DMSO 2h before irradiation exhibited a remarkable significant increase in miR-99b expression and a non-significant increase in miR-9, miR-10, miR-146a and miR-155 expression compared to the irradiated group.

Furthermore, the post-administration of UA (25 µM or 50 µM) induced slightly progress in miR-9 expression at 25 µM UA compared to the irradiated group and a remarkable increase in miR-155 expression at 50 µM UA compared to untreated control and irradiated ones. The pre-administration of UA (25 µM or 50 µM) was able to induce significant elevation in miR-99b and a slight increase in miR-9, miR-10, miR-146a and miR-155 expression compared to untreated control and irradiated group was observed.

In conclusion, 1 µg/ml LPS induced significant rising in miR-10, miR-99b, miR-146a and miR-155 and a significant depression in miR-9 expression in BMDMs after 72h. On the other hand, X-irradiated BMDMs recorded an inconsiderable decrease in all examined miRNA. UA (25 µM or 50 µM) induced a remarkable decrease in LPS-stimulated BMDMs.

A
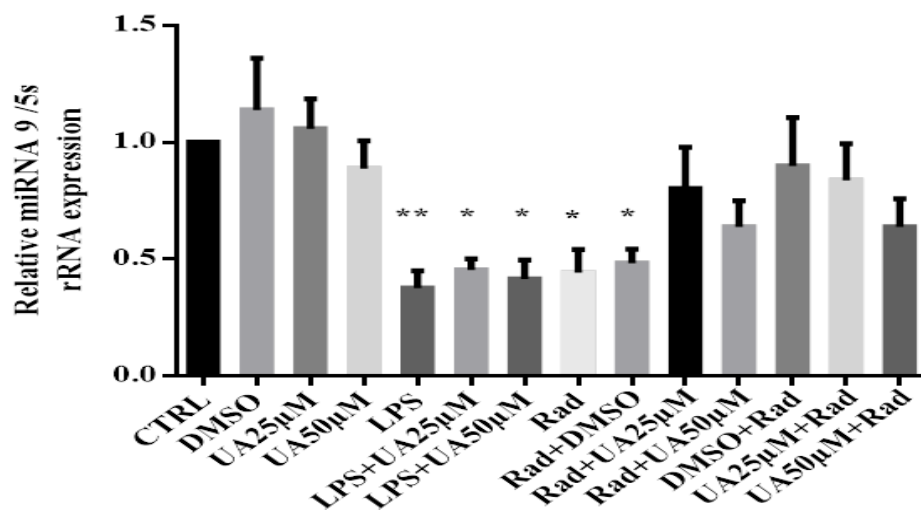
B
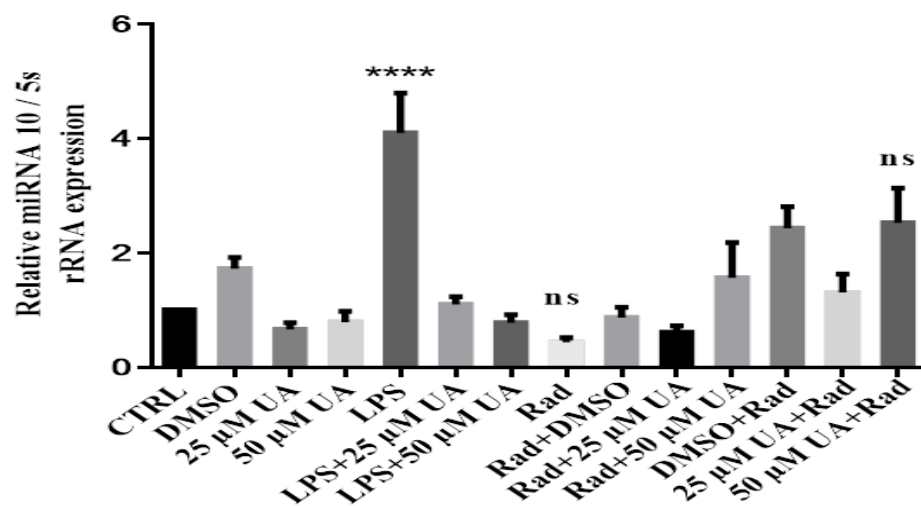
Figure 36 Influence of urolithin A on miRNA expression in LPS-stimulated or X-irradiated murine BMDMs

BMDMs were stimulated either by 1µg/ml of LPS or 6 Gy of X-irradiation in the presence or absence of UA (25 µM or 50 µM). The expression of miR-9 (A) and miR-10 (B) over 5S rRNA was evaluated in stimulated BMDMs after 72h. The irradiated group was subdivided into two, where one received UA (25 or 50 µM) before 24h of irradiation and the other one received it directly post-irradiation. The unstimulated and untreated BMDMs were used as control. BMDMs treated with DMSO were used as negative control. Arithmetic means ± SEM from seven independent experiments are depicted. One way ANOVA was used and * (p < 0.05), ** (P 0.01), and **** (p < 0.0001) indicate statistically significant differences compared to control. Abbreviations: DMSO, dimethyl sulfoxide; UA, urolithin A; LPS, lipopolysaccharides; RAD, radiation; miR, micro RNA; ns, non-significant.

C
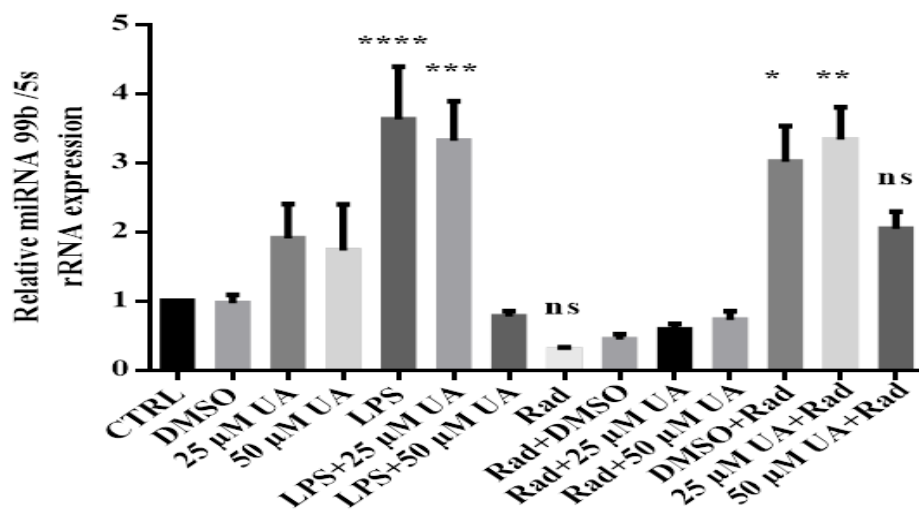
D
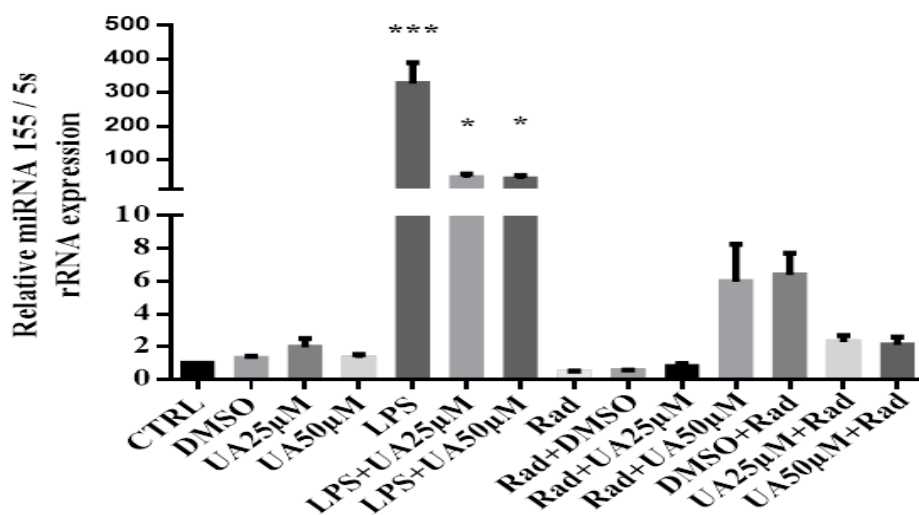
Figure 36 Continued: Influence of urolithin A on miRNA expression in LPS-stimulated or X-irradiated murine BMDMs

BMDMs were stimulated either by 1µg/ml of LPS or 6 Gy of X-irradiation in the presence or absence of UA (25 µM or 50 µM). The expression of miR-99b (C) and miR-155 (D) over 5S rRNA were evaluated in stimulated BMDMs after 72h. Arithmetic means ± SEM from seven independent experiments are depicted. One way ANOVA was used and * ($p < 0.05$), ** (P 0.01), and *** ($p < 0.001$) indicate statistically significant differences compared to control. Abbreviations: DMSO, dimethyl sulfoxide; UA, urolithin A; LPS, lipopolysaccharides; RAD, radiation; miR, micro RNA; ns, non-significant.
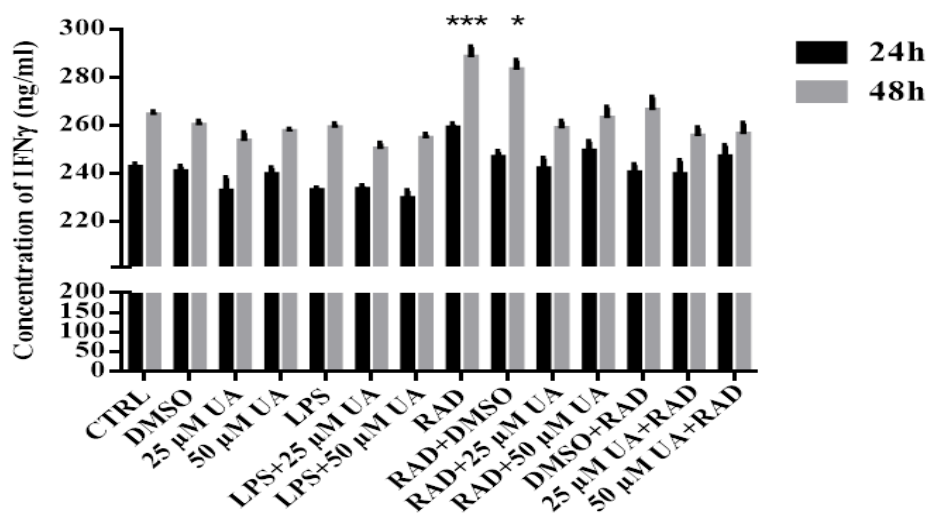
E
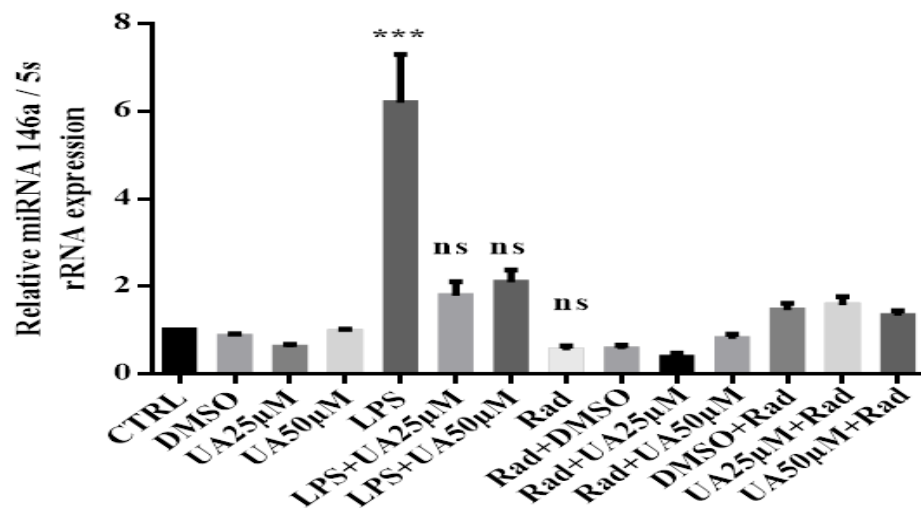
Figure 36 Continued: Influence of urolithin A on miRNA expression in LPS-stimulated or X-irradiated murine BMDMs

BMDMs were stimulated either by 1μg/ml of LPS or 6 Gy of X-irradiation in the presence or absence of UA (25 μM or 50 μM). The expression of miR-146a (E) over 5S rRNA was evaluated in stimulated BMDMs after 72h. Arithmetic means ± SEM from seven independent experiments are depicted. One way ANOVA was used and *** ($p < 0.001$) indicate statistically significant differences compared to control. Abbreviations: LPS, lipopolysaccharides; UA, urolithin A; DMSO, dimethyl sulfoxide; RAD, radiation; miR, micro RNA; ns, non-significant.

4 Discussion

4.1 Targeting macrophage TLRs in inflammatory immune response using gut microbiota metabolite of ellagitannins urolithin A

Inflammation is a complex physiological response towards noxious stimuli, such as physical or chemical injuries, or microbial infections. Inflammatory bowel disease (IBD), arthritis, cardiovascular disease (CVD), diabetes, and cancer are the main chronic inflammation associated disease and they are the main cause of mortality and morbidity. Accordingly, 3 of 5 people die due to these diseases worldwide. IBD is generally considered to be associated with dietary patterns, genetic susceptibility, and abnormal immune and environmental factors, chemotherapy, intestinal microbiota dysfunction as well as radiation therapy (RT). Antibiotic exposure in early life can lead to a significant change of the gut microbiota and may contribute to later onset of IBD (Amal, Mohamed et al. 2018).

Radiation is everywhere and every year millions of people are exposed to ionizing radiation resulting from diagnostic, interventional radiology and radiotherapy. Furthermore, nuclear and radiologic accidents pose a threat to all individuals all over the world. In addition to the lethal effects of ionizing radiation at high doses, exposure to sub-lethal doses may result in many diseases, such as carcinogenesis and cardiovascular disease (Wong, Yamada et al. 1993).

Several reports revealed that exposure to IR can strongly affect immune system responses, leading to various diseases among exposed people (Georgakilas, Pavlopoulou et al. 2015). Wu, Antony et al. proposed that chronic inflammation and continuous free radical production are responsible for several diseases after radiotherapy or radiation accident as well proposed that 25% to 50% of all cancers may be related to chronic inflammation. In addition, the continuous production of free radical, resulting from inflammatory responses, can disrupt organ function (Wu, Antony et al. 2014). For example, in diabetic patients the chronic oxidative damage in kidneys is mediated by insulin-like growth actor 1 (IGF-1) and NADPH oxidase enzymes. This situation has been confirmed for other organs, such as Crohn's disease and ulcerative colitis in the gastrointestinal system, pancreatitis, and rheumatoid arthritis (New, Block et al. 2012).

The innate immune response to bacterial infection or damage induced by radiation is initiated and guided by macrophages, which are the key components of the immune system (Sharif, Bolshakov et al. 2007). MicroRNA control multiple regulatory checkpoints to fine-tune macrophage inflammatory responses (Roy and Sen 2011).

TLRs play essential roles in triggering innate immune responses against bacteria and viruses (McCoy and O'neill 2008). Therefore, targeting TLR signaling to dampen the deleterious immune response is considered as a therapeutic approach for various diseases involving IBD. In addition, it has been demonstrated that activation of TLRs alleviated radiation damage *in vitro* and *in vivo* (Liu, Lei et al. 2018). Considering reports suggested that triggering TLRs exhibit lower side

effects and higher protective efficiency than traditional radioprotective drugs, which make TLRs as a potential candidate in ionizing radiation protection (Liu, Lei et al. 2018).

TLR2 and TLR4 have gained enormous importance due to their extreme ability of identifying distinct molecular patterns from invading pathogens. These PRRs not only act as innate sensor but also shape and bridge innate and adaptive immune response. Furthermore, they play a crucial role in regulating the balance between Th1 and Th2 type of response essential for the survivability of the host (Mukherjee, Karmakar et al. 2016). Interestingly, activation of TLRs has been a target for cancer treatment. It is shown that TLRs can induce preferable anti-tumor effect by eliciting inflammatory cytokines expression and cytotoxic T lymphocytes response. As adjuvant, TLRs agonists can launch a strong immune response to support cancer radiotherapy and bio-chemotherapy (Cen, Liu et al. 2018).

In the present study two scenarios were used to stimulate inflammation. The first one is the commercially available LPS isolated from Escherichia coli O111:B4 (Limtrakul, Yodkeeree et al. 2015). It is used to mimic the bacterial invasion as in the real scenario of bacterial infection. The second one is exposure of macrophages to ionizing radiation to mimic inflammation induced to radiation sickness.

Wherein most of the studies involving natural products used plant extracts or compounds found in food matrix and only a few used the metabolite obtained after the biotransformation in the body. So, the gut microbiota metabolite of ellagitannins (poorly absorbed in the gastrointestinal tract) urolithin A was selected in this study.

Ellagitannins-rich food has beneficial effects on IBD and other inflammatory diseases such as CVD and arthritis (Selma, Beltrán et al. 2014). The bioavailability of ellagitannins and ellagic acid is limited and they need further digestion by the gut microbiota to produce their bioactive molecules as UA that can be easily absorbed (Espín, Larrosa et al. 2013). The most common gut bacterial metabolites such as short chain fatty acids (propionic acid, acetic acid, and butyric acid) can positively contribute to generation of the adaptive immune regulatory T cells (Smith, Howitt et al. 2013)(. Furthermore, the bacterial metabolite acetate is involved in the reduction of inflammation in Type 1 diabetes model by reducing the autoimmune CD8+ T cells (Mariño, Richards et al. 2017). In addition, only 1 in each 3 people has the right microbiota and can perform this metabolism with maximum efficiency (Garcia-Villalba, Vissenaekens et al. 2017). The role of UA in macrophage activation remained elusive. Thus, our study investigates how this gut microbiota metabolite drives the TLR2 and TLR4 signalling at the transcriptional and translational levels.

4.2 Urolithin A abolished the increase of intracellular calcium induced by LPS-stimulation or X-irradiation in mouse BMDMs

Calcium is an important second messenger involved in intra- and extracellular signaling cascades and plays a crucial role in cell life and death decisions. The Ca^{2+} signaling network acts in

various ways to regulate many cellular processes. In addition, changes in intracellular calcium will influence the functional properties of the immune cells, including activation, chemokine and cytokine expression, cytotoxicity and granule exocytosis, and accompany pharmacological responses to ligands of specific cell receptors (Clapham 2007, Rahman and Dickenson 2013).

The current data revealed that LPS-stimulation or X-irradiation induced significant upregulation in intracellular calcium in BMDMs. Such results have been reported by several authors (Drysdale, Yapundich et al. 1987, Hoffmann, Kann et al. 2003, Racioppi, Noeldner et al. 2012, Zhang, Wang et al. 2014, Liu, Wang et al. 2016). In agreement with Carafoli, Santella, et al., such increase in intracellular Ca^{2+} can arise from different sources including the entry of extracellular Ca^{2+} via Ca^{2+} channels (voltage-gated channels, receptor-mediated channels) and the transient receptor potential channel of store-operated Ca^{2+} influx (SOCI), or the release of stored Ca^{2+} from intracellular stores via IP3 receptors and ryanodine receptors in intracellular Ca^{2+} stores (Carafoli, Santella et al. 2001, Berridge, Bootman et al. 2003).

Noteworthy, Hoffmann, Kann et al. revealed that LPS-stimulation of mouse microglia *in vitro* leads to elevated basal intracellular calcium along with attenuated calcium signalling in response to extracellular stimulation of selected purinoreceptors and complement receptors. Moreover, they present evidence that the rise in intracellular calcium is essential for microglial activation, such as release of NO and certain cytokines and chemokines. They hypothesized that an activation-related lasting increase in the basal intracellular calcium level critically determines receptor signalling efficacy and executive behavior of macrophage-like cells (Hoffmann, Kann et al. 2003).

On the other hand, both the extracellular space and intracellular Ca^{2+} stores can participate in the radiation-induced Ca^{2+} response (Claro, Oshiro et al. 2008). Several studies revealed a prominent role for IP3-induced intracellular calcium increases during radiation and activate the downstream signalling of Raf-1 and MAPK pathway. Feske, Wulff et al. revealed that radiation induces tyrosine phosphorylation of EGFR and activation of phospholipase C (PLC) followed by IP3 production which leads to opening of IP3 receptor channels in the membrane of ER and release of calcium from ER stores (Feske, Wulff et al. 2015). Calcium which releases from the ER results in a transient increase in intracellular Ca^{2+} concentrations and a decrease in ER Ca^{2+} concentrations. The latter causes the opening of store-operated CRAC channels in the plasma membrane via the activation of stromal interaction molecule STIM1 and STIM2, which are single-pass transmembrane protein, located in the ER membrane. Dissociation of Ca^{2+} from the ER luminal part of STIM proteins results in their translocation to ER–plasma membrane junctions and binding to ORAI1, the pore-forming subunit of the CRAC channel (Feske, Gwack et al. 2006). Opening of ORAI1 results in store operated Ca^{2+} entry (SOCE), thus called because this form of Ca^{2+} influx is regulated by the ER Ca^{2+} concentrations (Shaw, Qu et al. 2013).

In addition, several reports have demonstrated that TLRs induced rapid changes in the intracellular Ca^{2+} concentration (Zhou, Yang et al. 2006). Ca^{2+} signaling regulates downstream signaling molecules, such as nuclear factor of activated T cells (NF-ATc) transcriptional

complexes and calcineurin, followed by many cellular responses through the change of gene expression (Gallo, Canté-Barrett et al. 2006). Zhou, Yang et al., demonstrated that Ca^{2+}-dependent signaling pathway results in stimulation of iNOS expression as well as TNF-α production upon LPS stimulation of rat peritoneal macrophages (Zhou, Yang et al. 2006).

Furthermore, it has been suggested that TLR-dependent PLCγ2 activation participated in this event (Chun and Prince 2006, Zhou, Yang et al. 2006). In 2008, Aki, Minoda et al., using PLCγ2 knockdown cells and BMDMs from PLCγ2-disrupted mice clearly demonstrated the role of PLCγ2 in TLR2 and TLR4 mediated calcium mobilization and signal transduction (Aki, Minoda et al. 2008).

Our results revealed that UA administration inhibit intracellular calcium in LPS-stimulation or X-irradiated BMDMs and this inhibition may be through modulation of IP3R activity where UA was able to decrease the AKT phosphorylation. In addition, the inhibition of pro-inflammatory cytokines such as IL-6, TNF-α, NOS2 mediator and ROS production also mediate this inhibitory effect of UA on intracellular calcium.

4.3 Urolithin A diminished ROS production induced by LPS-stimulation or X-irradiation in mouse BMDMs

The interactions between ROS and calcium signaling can be considered as bidirectional, wherein ROS can regulate cellular calcium signaling and calcium signaling is essential for ROS production (Gordeeva, Zvyagilskaya et al. 2003). Thus, any increase in Ca^{2+} levels will activate ROS-generating enzymes and formation of free radicals. However, the mutual interplay and communication of ROS and calcium is highly dependent on the cell and tissue types (Zhang, Kang et al. 2013). Increasing evidence suggests that this cross-talk plays a crucial role in various pathophysiological conditions also in other systems, including neurodegenerative diseases such as Parkinson disease and Alzheimer disease, inflammatory diseases, but also cancer (Sharma and Nehru 2015).

The present study showed that LPS or X-irradiation induce higher production of ROS that may change DNA structure, result in modification of proteins and lipids, activation of several stress-induced transcription factors, and production of pro-inflammatory and anti-inflammatory cytokines. In addition, LPS was able to trigger the production of inflammatory cytokines and ROS in mouse peritoneal macrophages and RAW 264.7 cells (Lim, Choi et al. 2020, More and Makola 2020).

LPS induces ROS production via multiple mechanisms including the activation and induction of NADPH oxidase, as well as a significant decrease in antioxidant defense enzymes with an increase in lipid peroxidation and NO levels as detected by Amal et al. (Amal, Mohamed et al. 2018). On the other hand, X-irradiation can directly breakup the respiratory chain of mitochondria leading to respiratory chain dysfunction and thus reducing ATP production, increasing ROS production, reducing anti-oxidant capacity and inducing apoptosis (Vona,

Gambardella et al. 2019). In addition, ionizing radiation activates NADPH oxidase (NOXs), the main enzymatic source of ROS, which catalyze the transfer of electrons from NADPH to oxygen molecules to produce oxygen free radicals (Seddon, Looi et al. 2007). Noteworthy, radiation can not only change the upstream source of ROS but also change the balance of endogenous antioxidant defense mechanisms, including glutathione, ascorbic acid, catalase, and superoxide dismutase (SOD) (Gajowik and Dobrzyńska 2014). So, the inhibition of anti-oxidant enzymes is one of the important effects of ionizing radiation on irradiated organs and off-site organs, which leads to the production and accumulation of ROS (Najafi, Shirazi et al. 2017).

However, Li, Maitra et al., demonstrated that IRAK-1 is critically involved in generation of ROS induced by LPS and mechanistically, they observed that IRAK-1 is required for LPS-induced expression of NOX-1, via multiple transcription factors including p65/RelA, C/EBPβ and C/EBPδ. On the other hand, they demonstrated that IRAK-1 associated with and activated small GTPase Rac1, a known activator of NOX-1 oxidase enzymatic activity. IRAK-1 forms a close complex with Rac1 via a poly-proline motif within the variable region of IRAK-1 (Li, Maitra et al. 2010).

In agreement with Liu, Sun et al. our results show that excessive ROS production induced by LPS stimulates MAPK and NF-κB pathways and initiates inflammatory responses (Liu, Sun et al. 2012, Liu, Wu et al. 2016). In our study, we recorded that UA treatment apparently blocked ROS generation and restored the balance of the intracellular redox state by attenuating the oxidative stress. The inhibition of pro-inflammatory cytokines such as IL-1β, IL-2, IL-6, IL-12 and TNF-α and NOS2 mediator as well as inhibition of inflammatory transcription factor NF-kB and MAPK (p38 and JNK) activity mediate this inhibitory effect of UA on ROS. Based on our results, it would be interesting to investigate whether UA is able to ameliorate oxidative stress induced mitochondrial ROS (mROS) production as well as DNA damage in mouse BMDMs.

4.4 Urolithin A decreased mROS production induced by LPS-stimulation or X-irradiation in mouse BMDMs

The mitochondria are the major sites of intracellular oxygen consumption, and the respiratory chain of mitochondria is the main source of cellular ROS, and ATP synthesis produces ROS during the normal oxygen metabolism (Bedard and Krause 2007). Moreover, TLR2 and TLR4 can enhance ROS production by recruiting mitochondria to macrophage phagosomes and translocating TRAF6 to mitochondria to engage in evolutionarily conserved signalling intermediate in Toll pathways (ECSIT) (West, Brodsky et al. 2011). Next, we designed the experiment to investigate the effect of UA on mitochondria superoxide production using immunofluorescence MitoSOX red fluorescence dye.

The results of the current study demonstrated that UA decreases mROS production induced by LPS-stimulation or X-irradiation by displaying a remarkable decrease in red fluorescence. The major factors responsible for ROS production are respiratory chain complexes (Yang and Lian 2020) and LPS attenuates macrophage respiration by inhibiting complexes II and III (Kato 1972)

and slowing state of complexes III respiration (McGivney and Bradley 1979). In addition, LPS induces alterations in mitochondrial metabolism and can alter Krebs cycle by breaking it after citrate and after succinate (Jha, Huang et al. 2015, Mills, Kelly et al. 2016). Accordingly, Mills, Kelly et al. and Sena and Chandel et al., suggested that LPS-stimulation induced mitochondrial ROS generation following the oxidation of succinate is central to determine the inflammatory phenotype of macrophages (Sena and Chandel 2012, Mills, Kelly et al. 2016).

On the other hand, we observed that radiation triggered the generation of mitochondria ROS was essential for robust induction of pro-inflammatory cytokines such as IL-1β, IL-2, IL-6, IL-12 and TNF-α mRNA. Also, radiation exposure induced NF-kB signalling, and MAPK and PI3K activation were regulated by mROS in macrophages (Kim, Choe et al. 2016). UA was able to block ROS production through suppression of pro-inflammatory cytokines and inhibition of p38, JNK, AKT/mTOR and NF-kB signalling.

4.5 Urolithin A reduced DSBs availability induced by LPS-stimulation or X-irradiation in mouse BMDMs

The results obtained in the present study revealed that a significant higher number of γ-H2AX foci were observed in LPS-stimulated (after 48h) or X-irradiated (after 2h and 48h) BMDMs . Noteworthy, a prominent self-repair was recorded after 48h of irradiation compared to those observed after 2h. UA was able to decrease the DNA double strand breaks. This result was in agreement with the findings of Chumduri, Gurumurthy et al., who indicated that LPS can induce DSBs either directly or indirectly through ROS (Chumduri, Gurumurthy et al. 2013). Moreover, the unrepaired DSBs activate the cytosolic DNA sensor stimulator of interferon genes, thus inducing the production of IFNα and IFNβ, which promote innate immune responses (Härtlova, Erttmann et al. 2015). According to Qiao, Huang et al. LPS-induced DSBs activated the NF-κB signalling pathway in human dental pulp tissues (Qiao, Huang et al. 2019).

On the other hand, radiation induced DNA damage including base damage, cross-linking, SSBs and DSBs (Musa and Shabeeb 2019). Whereas, DSBs recruit the damage sensor 53BP1 to the chromatin domain surrounding the DSBs and 53BP1 co-localizes with γ-H2AX (Eberlein, Peper et al. 2015). So, phosphorylation of H2Ax is responsible for the accumulation of 53BP1 at the DSB site (Ward, Minn et al. 2004). Moreover, 53BP1 facilitates the DSB repair by increasing the mobility of DSB chromatin (Krawczyk, Borovski et al. 2012). However, the lack of chromatin structure, histone protection, and an inefficient repair system, mtDNA is vulnerable to oxidative stress-related damage. If not repaired, it will lead to the destruction of the electronic transport chain and produce more ROS, which exceeds the protective ability of the ant-ioxidant system (Alam and Jabeen 2007). Reactive oxygen-induced mitochondrial DNA oxidative damage and mitochondrial damage lead to the pathological production of ROS, and the formation of the vicious cycle leads to cell energy consumption and apoptosis.

Our data revealed a prominent self-repair after 48h of irradiation compared to those observed after 2h. UA induce remarkable disappearance of DSB foci by γ-H2AX dephosphorylation after a

DSB is repaired. In addition, UA exhibited significant improvement by reducing the availability of DSBs. The prominent inhibition of intracellular calcium, ROS and mtROS production induced by UA provide another support for reduction of DSBs availability. In addition, inhibition of NF-κB signalling and suppression of MAPK and PI3K activity as well as the inhibition of pro-inflammatory cytokines may also mediate the remarkable decrease of DSBs in BMDMs.

The obtained data showed that UA was capable of suppressing intracellular calcium increase, cellular and mitochondrial ROS production, and DSBs as well as the pro-inflammatory cytokines and mediators, thereby providing us a concrete justification that UA has a potential value to be carried forward for a more advanced anti-inflammatory study. However, the suppression activity of UA is incomplete without its inhibitory mechanism studied.

4.6 Effect of UA on TLRs signalling

TLRs are important PRRs in innate immunity and activated by specific ligands. TLRs initiate some downstream signaling pathways, and thus participate in various cellular processes such as proliferation, apoptosis, and immune response regulation (Liu, Lei et al. 2018). Next, we investigated the effect of UA on TLR2 and TLR4 signalling pathway including MAPK, PI3K activity and NF-kB pathway.

TLRs play essential roles in triggering innate immune responses against bacteria and viruses. TLR4, which recognizes LPS, is highly expressed by macrophages, dendritic cells, and monocytes (McCoy and O'neill 2008). When gram-negative bacteria are encountered, LPS binds to TLR4 on the surface of macrophages. Then, activated macrophages trigger inflammatory responses to exert innate immune responses, followed by acquired immune responses driven by T and B cells. However, excessive or uncontrolled activation of macrophages is associated with chronic inflammatory diseases (McNelis and Olefsky 2014). Therefore, targeting TLR4 signaling to dampen this deleterious immune response is considered as a therapeutic approach for various diseases involving dysregulated macrophage activation. On the other hand, TLR2 forms heterodimers with TLR1 and TLR6, which is the initial step in a cascade of events leading to significant innate immune responses followed by development of adaptive immunity to pathogens and protection from immune sequelae related to infection (Oliveira-Nascimento, Massari et al. 2012). Thus, stimulation of host immune response with TLR2 and TLR4 agonist can be the option of choice to treat such diseases in future (Mukherjee, Karmakar et al. 2016).

4.6.1 Urolithin A stimulated TLR2 activation in LPS-stimulated or X-irradiated mouse BMDMs

Surprisingly, the current data revealed that UA alone induced significant elevation in TLR2 expression. In addition, LPS-stimulation, but not X-irradiation induced upregulation of cell surface TLR2 expression in BMDMs. The administration of UA to LPS-stimulated or post-irradiated BMDMs raised TLR2 expression than induced by LPS or X-irradiation alone (Matsuguchi, Musikacharoen et al. 2000). Several studies demonstrated that LPS-stimulation or X-irradiation induce TLR2 stimulation and a series of intracellular signalling pathway is activated, which ultimately induce the transcription/translation of inflammatory cytokines (Ioannou and Voulgarelis 2010, Ratikan, Micewicz et al. 2015).
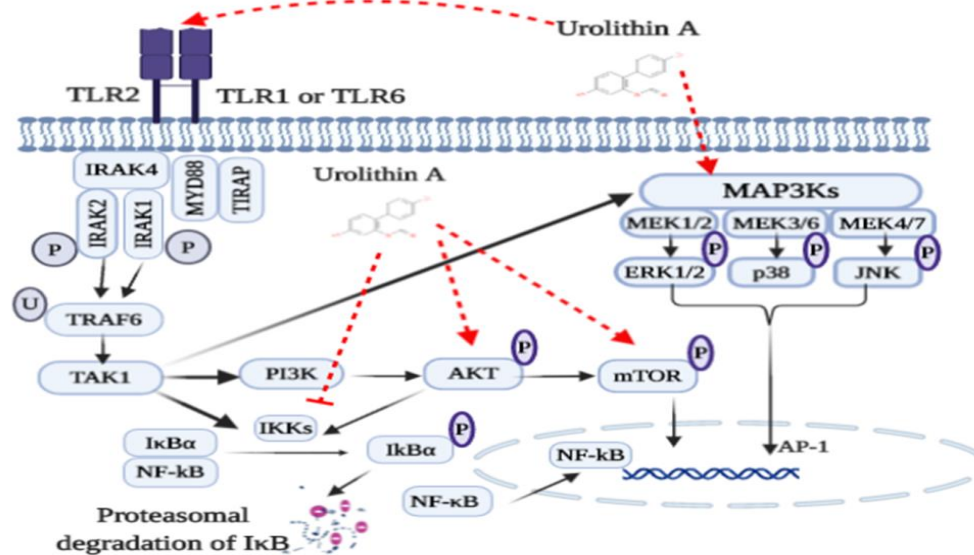
Figure 37 Urolithin A stimulated TLR2 signalling pathway

Urolithin A activates TLR2 signalling cascade through activation of MAPK and PI3K signalling pathway. UA inhibits IKK activation and suppresses NF-kB translocation and activation. TLR2 signalling, after ligand recognition and consequent TLR2 dimer rearrangement, the TIR domain of TIRAP binds the TIR domain of TLR2 and recruits the adaptor protein MyD88. IRAKs are then recruited and IRAK 4 phosphorylates IRAK1 which activates TRAF6. Since IRAK1 is rapidly dissociated, IRAK2 also activates TRAF6 in latter responses. Ubiquitinated (U) TRAF6 triggers the activation sequence of TAK1 complex. IκB phosphorylation and ubiquitination by the IKK complex leads to its degradation and release of NF-κB translocation to the nucleus for gene up-regulation. TAK1 also activates MAPKs (ERK, JNK and p38) and PI3K activation, leading to AP-1 and NF-kB activation that trigger gene transcription of cytokines and accessory molecules. Abbreviation: TIRAP, TIR adaptor protein; MyD88, myeloid differentiation primary-response gene 88; IRAK, interleukin-1 receptor associated kinase; TRAF, TNF receptor associated factor; RIP, receptor-interacting protein kinases; TAK, transforming growth factor beta-activated kinase 1; IKK, IκB kinase; PI3K, phosphatidylinositol 3-kinases; mTOR, mechanistic target of rapamycin; ERK, extracellular regulated kinase; JNK, c-Jun N-terminal kinase; NF-κB, nuclear factor-κB; IκB, kinase complex; AP, activator protein. The figure adapted from (El-Zayat, Sibaii et al. 2019).

Surprisingly, treatment of murine BMDMs with UA alone induces remarkable elevation in TLR2 expression during the time intervals. The association of UA with LPS or X-irradiation induced upregulation of TLR2 expression than LPS or X-irradiation alone. Notably, X-irradiation alone did not induce remarkable effects on TLR2 expression compared to control BMDMs (Figure 37).

4.6.2 Urolithin A suppressed TLR4 activation in LPS-stimulated or X-irradiated mouse BMDMs

On the one hand, the present data showed that stimulation of BMDMs with LPS or X-irradiated induced significant elevation of TLR4 expression . Where, activation of TLR4-dependent signalling processes in macrophages was estimated with different methods, especially IκBα degradation and NF-κB phosphorylation and nuclear translocation followed by a series of intracellular signaling pathways, which finally leads to the transcription/translation of inflammatory cytokines (Bagaev, Garaeva et al. 2019). Our data revealed that treatment with UA did not induce significant changes on LPS-stimulated BMDMs. While in X-irradiated BMDMs, the pre- and post-administration of UA induced significant decrease with values near to control in TLR4 expression.

In order to elucidate the effect of UA alone on TLR2 as well as TLR4 expression and the underlying molecular mechanism by which UA exerts anti-inflammatory activity, its influence on the activation of the NF-κB, MAPK and PI3K pathways were evaluated in BMDMs challenged with LPS or X-irradiation (Figure 37).

4.6.3 Urolithin A inhibited NF-κB activation in LPS-stimulated or X-irradiated mouse BMDMs

Concerning NF-κB activation, the results obtained in the present study demonstrated that LPS-stimulation, but not X-irradiation induced a significant increase in IκBα phosphorylation as described previously by (Ahmed and Li 2008, Hobbs, Reynoso et al. 2018, Bagaev, Garaeva et al. 2019). Administration of UA alone did not have any effects on the phosphorylation of IκBα and a dose dependent decrease in the IκBα phosphorylation was recorded after LPS-stimulation. This finding indicates that the suppressive effects of UA against IL-1β, IL-2, IL-6, IL-12, NOS2 and TNF-α are due to inhibition/impairment of activation of NF-κB signaling (Figure 38).
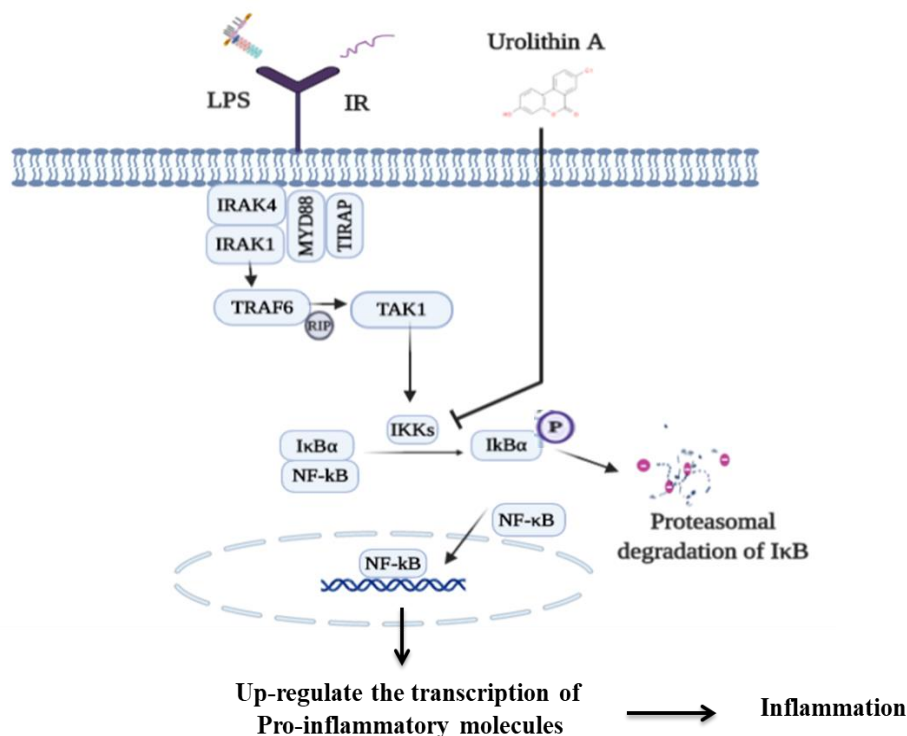
Figure 38 Urolithin A inhibited IKKs kinase activity

Urolithin A has inhibited the phosphorylation, ubiquitination, and degradation of the inhibitory protein, IκBα complex. Whereas, UA makes the NF-κB subunit (p65 and p50) stayed intact with IκBα and stopping their translocation to the nucleus to activate the pro-inflammatory gene expression. Abbreviation: LPS, lipopolysaccharides; IR, ionizing radiation; TIRAP, TIR adaptor protein; MyD88, myeloid differentiation primary-response gene 88; IRAK, interleukin-1 receptor associated kinase; TRAF, TNF receptor associated factor; RIP, receptor-interacting protein kinases; TAK, transforming growth factor beta-activated kinase 1; IKK, IκB kinase; NF-κB, nuclear factor-κB; IκB, kinase complex; AP, activator protein. The figure is adapted from (El-Zayat, Sibaii et al. 2019).

4.6.4 Urolithin A diminished MAPK activation in LPS-stimulated or X-irradiated mouse BMDMs

The MAPK pathway (ERK, p38, and JNK) is also triggered by LPS-stimulation or X-irradiation and mediates the transcription of various cytokines and chemokines (Dent, Yacoub et al. 2003, Narang and Krishna 2008, Marampon, Ciccarelli et al. 2019). Here we found, that in LPS-stimulated BMDMs, UA suppressed the phosphorylation of both p38 and JNK while it did not induce significant effect on ERK1/2. On the other hand, in X-irradiated BMDMs, the pre- and post-administration of UA was able to suppress the phosphorylation of JNK while the pre-administration only was able to suppress the p38 phosphorylation. Moreover, UA did not affect ERK1/2 phosphorylation. Noteworthy, administration of UA (25 µM) alone was able to induce significantly increase in phosphorylation of ERK and p38 expression and this is may be correlated to TLR2 overexpression with this dose of UA. Taken together, these results suggest that these two signaling pathways (p38 and JNK) are possible targets of UA and could be involved in mediating the reduction in levels of pro-inflammatory cytokines (Figure 39).
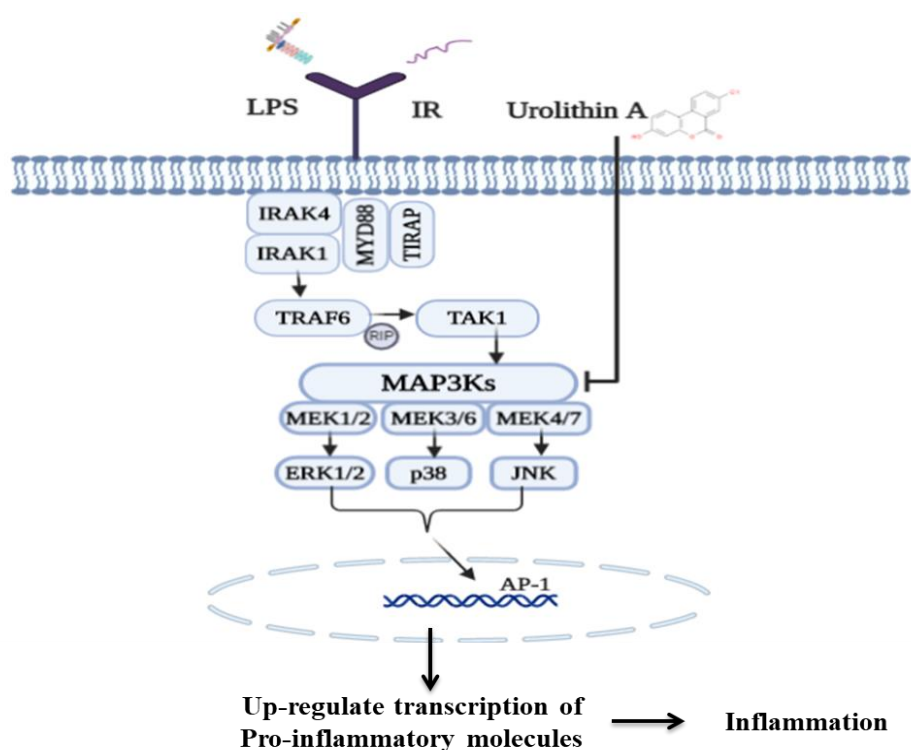
Figure 39 Urolithin A inhibited MAPKs signalling pathway

Urolithin A has inhibited the phosphorylation of ERK, p38 and JNK protein. Hence, UA suppresses MAPK downstream signalling cascade including NF-κB activation, pro-inflammatory gene expression and reduces inflammation. Abbreviation: TIRAP, TIR adaptor protein; MyD88, myeloid differentiation primary-response gene 88; IRAK, interleukin-1 receptor associated kinase; TRAF, TNF receptor associated factor; TAK, transforming growth factor beta-activated kinase 1; ERK, extracellular regulated kinase; JNK, c-Jun N-terminal kinase; NF-κB, nuclear factor-κB; IκB, kinase complex; AP, activator protein. The figure is adapted from (El-Zayat, Sibaii et al. 2019).

4.6.5 Urolithin A suppressed PI3K/AKT/mTOR activation in LPS-stimulated or X-irradiated mouse BMDMs

The activation of PI3K/AKT/mTOR pathway is also triggered by LPS-stimulation or X-irradiation and mediates the transcription of various cytokines in BMDMs (McGuire, Gray et al. 2013, Vergadi, Ieronymaki et al. 2017). UA 25 µM suppressed the phosphorylation of AKT up to 48h while UA 50 µM suppressed the phosphorylation of AKT up to 72h in LPS-stimulated macrophages. While UA was able to suppress AKT phosphorylation pre- and post-irradiation in BMDMs. Concerning mTOR, UA achieved a significant decrease in mTOR phosphorylation in LPS-stimulated or X-irradiated BMDMs. Noteworthy, administration of UA alone was able to induce slightly increase in phosphorylation of AKT and mTOR expression (Figure 40).
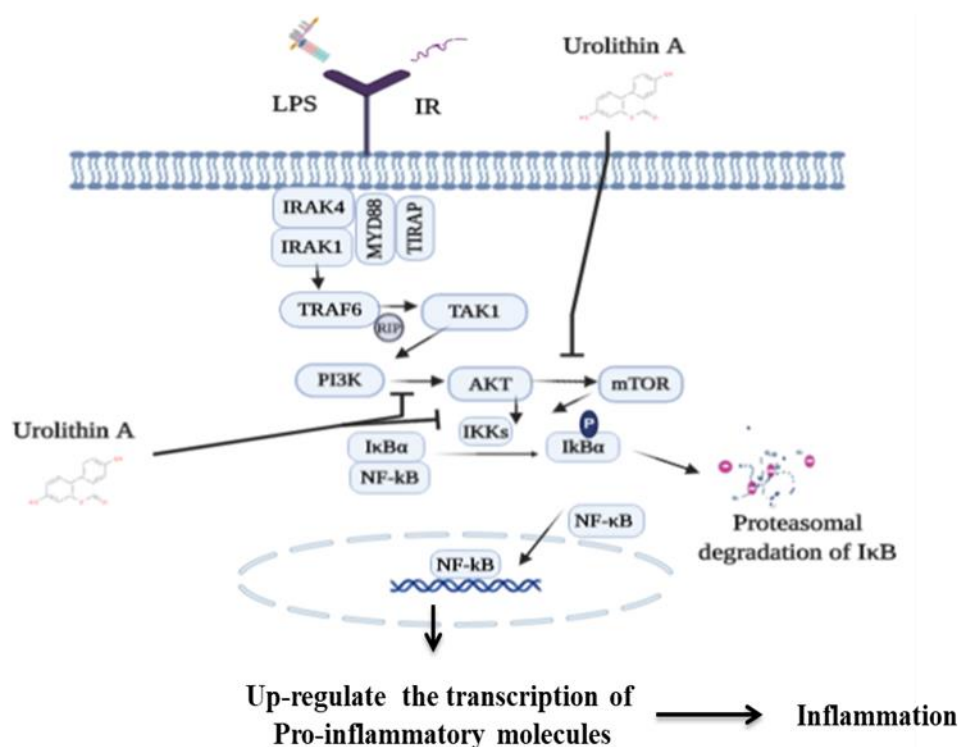
Figure 40 Urolithin A suppressed PI3K/AKT/mTOR signalling pathway

Urolithin A has inhibited the phosphorylation of AKT and mTOR protein. On the other hand, Urolithin A suppressed NF-κB activation and pro-inflammatory gene expression. Abbreviation: TIRAP, TIR adaptor protein; MyD88, myeloid differentiation primary-response gene 88; IRAK, interleukin-1 receptor associated kinase; TRAF, TNF receptor associated factor; RIP, receptor-interacting protein kinases; TAK, transforming growth factor beta-activated kinase 1; IKK, IκB kinase; PI3K, phosphatidylinositol 3-kinases; mTOR, mechanistic target of rapamycin; NF-κB, nuclear factor-κB; IκB, kinase complex; AP, activator protein. The figure is adapted from (El-Zayat, Sibaii et al. 2019).

4.7 Urolithin A suppressed production of pro-inflammatory cytokines induced by LPS-stimulation or X-irradiation in mouse BMDMs

Cytokines which function as a messenger between cells (small sized proteins) play an important role during inflammation. The influence of UA on pro- and anti-inflammatory cytokines expression (mRNA) and production (ELISA) were investigated in LPS-stimulated or X-irradiated murine BMDMs. The results obtained in the present study showed that UA significantly inhibited IL-1β, IL-2, IL-6, IL-10, IL-12 and TNF-α cytokines as well as NOS2 mediators in BMDMs. The pleiotropic nature of the protein indicates that the accumulation of a high level of pro-inflammatory cytokines amplifies inflammation due to the complexity of the interdependency of one on the other as the production of pro-inflammatory cytokines that work in a cascade mechanism by downstream effects of earlier released cytokines (Schulte, Bernhagen et al. 2013). Therefore, suppressing the production of a cytokine may influence the reduction of another dependent cytokine. Accordingly, in this analysis, UA was able to suppress the level of IL-1β, IL-2, IL-6, IL-12, IFN-γ, and TNF-α cytokines as well as NOS2 mediators in a dose dependent manner.

Taken together, the results presented in this study demonstrated for the first time that the gut microbiota metabolites of ellagitannins, UA stimulate TLR2 activation as well as differentially modulate the production of inflammatory cytokines and exerted suppressive effects on IL-1β, IL-2, IL-6, IL-12 and TNF-α and NOS2 mediator. These effects may be mediated by the suppression of MAPK (p38 and JNK) and PI3K/AKT/mTOR signaling pathways. Our findings highlight the potential role of UA as a novel therapeutic agent for treating inflammatory diseases as CVD and IBD and a promising drug for radiation sickness. Further *in vivo* studies are essential to confirm the therapeutic or preventive effect of UA in animal disease models (Figure 41).

4.8 Urolithin A suppressed the production of pro-inflammatory miRNA expression induced by LPS-stimulation or X-irradiation in mouse BMDMs

Emerging evidence has demonstrated that non-coding RNAs such as miRNAs are involved in almost all known cellular processes, including innate and adaptive immune responses, via modulation of gene expression (Calin, Liu et al. 2004). Chaudhuri, So et al., demonstrated that miR-146a/b, miR-132, and miR-155 were identified as LPS-responsive miRNAs (Chaudhuri, So et al. 2011). Promoter analysis studies recognized miR-146a as a NF-κB-inducible miRNA. Also, the study identified a crucial role of miR-146 in controlling TLR and cytokine signalling via a negative feedback regulation loop (Chaudhuri, So et al. 2011). In addition, O'Connell, Taganov et al. showed that miR-155 tightly controlled the expression of SHIPI and SOCS1, both critical regulators of the inflammatory response in macrophages (O'Connell, Taganov et al. 2007). Bala, Marcos et al. reported that increased miR-155 levels contribute to alcohol-induced elevation in TNF-α production (Bala, Marcos et al. 2011).

The results obtained in the present study, showed that UA was able to supress the expression level of miR-10, miR-99b, miR146a and miR-155 after LPS-stimulation. Concerning X-irradiation, there were no significant changes recorded in the tested miRNA except a significant decrease in miR-9 of X-irradiated as well as LPS-stimulation BMDMs. On the contrary, Bazzoni, Rossato et al.(Bazzoni, Rossato et al. 2009) revealed that miR-9 is activated by TLR4 in human PMNs and monocytes targeting NF-κB subunit p50. Therefore, suppressing the production of a pro-inflammatory cytokine as inhibition of NF-κB and MAPK activation may influence or mediate the reduction of miRNA expression (Figure 41).
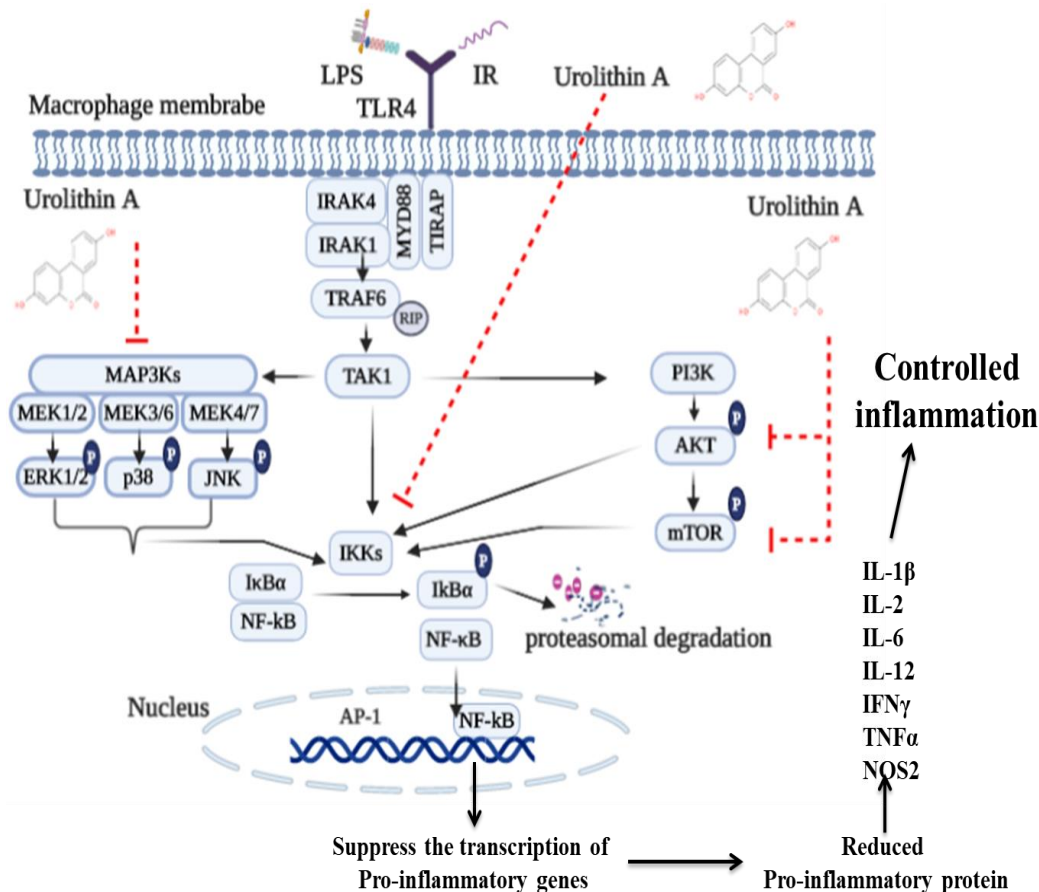
Figure 41 Urolithin A controlled NF-kB inflammatory response

LPS or ionizing radiation stimulate TLR4 signalling cascades. Urolithin A impaired the NF-kB activation through the inactivation of IKKs. Urolithin A suppresses MAPKs activation through blocking ERK, p38 and JNK phosphorylation. Additionally, urolithin A inhibits the phosphorylation of AKT and mTOR protein. Abbreviation: LPS; lipopolysaccharide; IR, ionizing radiation; TIRAP, TIR adaptor protein; MyD88, myeloid differentiation primary-response gene 88; IRAK, interleukin-1 receptor associated kinase; TRAF, TNF receptor associated factor; RIP, receptor-interacting protein kinases; TAK, transforming growth factor beta-activated kinase 1; IKK, IκB kinase; MAPK, mitogen activated protein kinase; PI3K, phosphatidylinositol 3-kinases; mTOR, mechanistic target of rapamycin; ERK, extracellular regulated kinase; JNK, c-Jun N-terminal kinase; NF-κB, nuclear factor-κB; IκB, kinase complex; AP, activator protein; IL, interleukin; IFN, interferon; TNF, tumor necrosis factor; and NOS, nitric oxide. The figure adapted from (El-Zayat, Sibaii et al. 2019),.

4.9 Conclusions and Outlook

In summary, this study elucidates that UA has effectively and efficiently quenched ROS production, prevented oxidative stress-associated disorders and suppressed the production of pro-inflammatory cytokines and mediators in LPS-stimulated or X-irradiated mouse BMDMs by inhibiting their corresponding genes at the transcriptional level and by preventing the activation of PI3K, MAPK and the NF-κB pathway that was achieved by obstructing the phosphorylation of IκBα (Figure 41). Therefore, based on the finding, UA may be considered as an impending anti-inflammatory therapeutic agent against inflammatory-associated diseases such as IBD, CVD, arthritis and cancer and an effective treatment for radiation exposure (radioprotector). UA may ameliorate the symptoms of inflammatory bowel disease as ulcerative colitis via anti-inflammatory activities. Although, Kaisho and Akira revealed that most TLR ligands are derived from pathogens and not found in the host making them critical in sensing invading microorganisms (Kaisho and Akira 2002). Here and for the first time our data revealed the ability of gut microbiota metabolites of ellagitannins, urolithin A to stimulate TLR2 expression and activate the downstream signalling pathways of MAPK (through ERK and p38) and PI3K/AKT/mTOR, while inhibiting the NF-kB activation. Thus these results provide a fertile field for continued research. Finally, in order to directly extrapolate the biological activity of UA, animal studies should be included to study its bioactivity, molecular mechanism (s), and drug distribution in an inflammation-induced animal model.

5 SUMMARY

Macrophages are the first line of defense in innate immunity and play a crucial role in initiation of excessive inflammatory responses involved in the pathogenesis of various inflammatory autoimmune diseases, including inflammatory bowel disease (IBD), rheumatoid arthritis (RA), and sepsis. These cells express the pathogen recognition receptor (PRR) system that detects various microbial and dangerous components. Urolithin A (UA) is a natural polyphenolic metabolite generated from ellagic acid and ellagitannins by the intestinal microbiota after consumption of fruits such as pomegranates or strawberries.

The present study has been designed to evaluate a possible effect of UA as an anti-inflammatory, anti-oxidant and radio-protector agent against chronic inflammation induced by chemotherapy, radiotherapy and intestinal microbiota dysfunction. As well as studying the influences of UA on TLR2 and TLR4 signalling pathway in murine BMDMs. For this, two stimulation models were used, first bacterial LPS (1µg/ml) as it mimics many inflammatory effects, and second 6 Gy of X-ray radiation exposures where pelvic and abdominal radiotherapy can damage the gut commensal bacteria increasing the susceptibility to gastrointestinal toxicity beside loss of gut homeostasis.

The results revealed for the first time that the non-pathogenic molecule but gut microbiota metabolite UA stimulated TLR2 expression and activated the downstream signalling cascade in murine BMDMs. In particular, UA exhibits its anti-oxidant and anti-inflammatory ability through inhibition of intracellular calcium, cellular and mitochondrial ROS production and lessen DNA damage induced by LPS-stimulation or X-irradiation in BMDMs. Interestingly, the prophylactic use as well as the low dose of UA (25 µM) were more efficient and recorded better effects than the post-administration and high dose of UA (50 µM). Furthermore, the analysis of TLR downstream pathways as NF-κB (IκBα), MAPK (ERK, p38, JNK), and PI3K/AKT/mTOR revealed that UA suppressed the activation of MAPK and PI3K and impaired the phosphorylation of NF-κB induced by LPS-stimulation or X-irradiation. UA activated TLR2 downstream signalling through MAPK (ERK and p38) and PI3K (AKT and mTOR) and did not activate IκBα (NF-κB inhibitor). Accordingly, UA quenched the high expression of pro-inflammatory mRNA, cytokines and mediators (NOS2) as well as pro-inflammatory miRNA expression induced by LPS-stimulation or X-irradiation. Noteworthy, UA alone induced a remarkable increase in IFNγ and slight increases in TNFα, IL-10, TGFβ and NOS2 production.

In conclusion, the present study provides molecular and biochemical evidence for the anti-inflammatory and anti-oxidant activity of UA making it a promising therapeutic agent for chronic inflammatory diseases such as IBD as well as a radioprotector for radiation sickness.

ZUSAMMENFASSUNG

Makrophagen sind die erste Verteidigungslinie bei der angeborenen Immunität und spielen eine entscheidende Rolle bei der Initiierung von übermäßigen Entzündungsreaktionen, die an der Pathogenese verschiedener (Auto-)Immunerkrankungen, wie entzündliche Darmerkrankungen, Rheumatoide Arthritis, aber auch Sepsis beteiligt sind. Diese Zellen exprimieren ein PRR-System, das verschiedene mikrobielle und gefährliche Substanzen erkennt. Urolithin A (UA) ist ein natürlicher polyphenolischer Metabolit, der aus Ellagsäure und Ellagitannine durch die Darmmikrobiota nach dem Verzehr von Früchten wie Granatäpfeln oder Erdbeeren erzeugt wird.

Die vorliegende Studie wurde durchgeführt, um eine mögliche entzündungshemmende Wirkung von UA als Antioxidans und Strahlenschutzmittel gegen chronische Entzündungen durch Chemotherapie, Strahlentherapie und intestinale Mikrobiota-Dysfunktion zu bewerten. Darüber hinaus sollten die Einflüsse von UA auf TLR (TLR2 und TLR4) Signalwege in murinen BMDMs untersucht werden. Hierfür wurden zwei Modelle verwendet, um die Entzündungen zu untersuchen. Erstens bakterielles LPS (1µg/ml), da es viele entzündliche Wirkungen nachahmt und zweitens 6 Gy Röntgenstrahlungsexpositionen, bei denen die Becken- und abdominale Strahlentherapie die Darmbakterien schädigen und neben dem Verlust der Darmhomöostase die Anfälligkeit für gastrointestinale Toxizität erhöhen kann.

Die Ergebnisse zeigen zum ersten Mal, dass ein nicht pathogenes Molekül, aber ein Darm-Mikrobiota-Metabolit die TLR2-Expression stimulieren und die Downstream-Signalkaskade in murinen BMDMs aktivieren kann. Insbesondere zeigte UA seine anti-oxidative und entzündungshemmende Fähigkeit durch die Hemmung des intrazellulären Kalziums und der zellulären und mitochondrialen ROS-Produktion sowie die Verringerung von DNA Schäden, welche durch LPS-Stimulation oder Röntgenbestrahlung in BMDMs induziert wurden. Interessanterweise waren die prophylaktische Anwendung sowie die niedrige UA-Dosis (25 µM) effizienter und zeigten bessere Wirkungen als die Behandlung nach Stimulation und eine hohe UA-Dosis (50 µM). Darüber hinaus zeigten die Analysen der TLR Downstream-Signalwege wie NF-κB (IκBα), MAPK (ERK, p38, JNK) und PI3K/AKT/mTOR, dass UA die Aktivierung von MAPK und PI3K, die durch LPS-Stimulation oder Röntgenbestrahlung aktiviert wurden, unterdrückte und die Phosphorylierung von NF-κB beeinträchtigte. UA alleine aktivierte die TLR2-Signalisierung über MAPK (ERK und p38) und PI3K (AKT und mTOR), jedoch nicht IκBα. Dementsprechend reduzierte UA, die durch LPS-Stimulation oder Röntgenbestrahlung induzierte, hohe mRNA Expression von pro-inflammatorischen Molekülen, wie Zytokine und andere Mediatoren (NOS2) sowie pro-inflammatorische miRNAs. Interessanterweise induzierte UA allein einen bemerkenswerten Anstieg von IFNγ, und eine leichte Erhöhung der TNFα, IL-10, TGFβ, und NOS2-Produktion.

Zusammenfassend liefert die vorliegende Studie molekulare und biochemische Belege für die anti-entzündliche und anti-oxidative Aktivität von UA und macht es zu einem vielversprechenden Therapeutikum für chronisch entzündliche Erkrankungen sowie ein Strahlenschutzmittel gegen Strahlenkrankheit.

6 REFERENCES

Aderem, A. (2003). "Phagocytosis and the Inflammatory Response." The Journal of Infectious Diseases **187**(Supplement_2): S340-345.

Ahmed, K. M. and J. J. Li (2008). "NF-kappa B-mediated adaptive resistance to ionizing radiation." Free radical biology & medicine **44**(1): 1-13.

Aki, D., Y. Minoda, H. Yoshida, S. Watanabe, R. Yoshida, G. Takaesu, T. Chinen, T. Inaba, M. Hikida, T. Kurosaki, K. Saeki and A. Yoshimura (2008). "Peptidoglycan and lipopolysaccharide activate PLCγ2, leading to enhanced cytokine production in macrophages and dendritic cells." Genes to Cells **13**(2): 199-208.

Akira, S., T. Taga and T. Kishimoto (1993). "Interleukin-6 in biology and medicine." Advances in immunology **54**: 1-78.

Akira, S., K. Takeda and T. Kaisho (2001). "Toll-like receptors: critical proteins linking innate and acquired immunity." Nature immunology **2**(8): 675-680.

Akira, S., S. Uematsu and O. Takeuchi (2006). "Pathogen Recognition and Innate Immunity." Cell **124**(4): 783-801.

Alam, K. and S. Jabeen (2007). "Immunogenicity of mitochondrial DNA modified by hydroxyl radical." Cellular immunology **247**(1): 12-17.

Alasalvar, C. and B. W. Bolling (2015). "Review of nut phytochemicals, fat-soluble bioactives, antioxidant components and health effects." The British journal of nutrition **113 Suppl 2**: S68-S78.

Amal, A. H., A. E.-A. Mohamed, F. H. Mohamed, Z. B. Ahmed and A. E. Mohammed (2018). "Lipopolysaccharide Prompts Oxidative Stress and Apoptosis in Rats' Testicular Tissue." Journal of Veterinary Healthcare **1**(3): 20-31.

Angelini, C. (2017). "Metabolites-mitochondria-macrophages (MMM): new therapeutic avenues for inflammation and muscle atrophy." Translational Cancer Research; Vol 6, Supplement 1 (February 2017): Translational Cancer Research.

Anthoney, N., I. Foldi and A. Hidalgo (2018). "Toll and Toll-like receptor signalling in development." Development **145**(9): dev156018.

Arthur, J. S. C. and S. C. Ley (2013). "Mitogen-activated protein kinases in innate immunity." Nature Reviews Immunology **13**(9): 679-692.

Austin, P. E., E. A. McCulloch and J. E. Till (1971). "Characterization of the factor in L-cell conditioned medium capable of stimulating colony formation by mouse marrow cells in culture." Journal of cellular physiology **77**(2): 121-134.

Azzam, E. I., J.-P. Jay-Gerin and D. Pain (2012). "Ionizing radiation-induced metabolic oxidative stress and prolonged cell injury." Cancer letters **327**(1-2): 48-60.

Bäckhed, F., R. E. Ley, J. L. Sonnenburg, D. A. Peterson and J. I. Gordon (2005). "Host-bacterial mutualism in the human intestine." Science **307**(5717): 1915-1920.

Bagaev, A. V., A. Y. Garaeva, E. S. Lebedeva, A. V. Pichugin, R. I. Ataullakhanov and F. I. Ataullakhanov (2019). "Elevated pre-activation basal level of nuclear NF-κB in native macrophages accelerates LPS-induced translocation of cytosolic NF-κB into the cell nucleus." Scientific Reports **9**(1): 4563.

Bala, S., M. Marcos, K. Kodys, T. Csak, D. Catalano, P. Mandrekar and G. Szabo (2011). "Up-regulation of microRNA-155 in macrophages contributes to increased tumor necrosis factor {alpha} (TNF{alpha}) production via increased mRNA half-life in alcoholic liver disease." J Biol Chem **286**(2): 1436-1444.

Banerjee, S., H. Cui, N. Xie, Z. Tan, S. Yang, M. Icyuz, V. J. Thannickal, E. Abraham and G. Liu (2013). "miR-125a-5p regulates differential activation of macrophages and inflammation." The Journal of biological chemistry **288**(49): 35428-35436.

Bates, J. M., J. Akerlund, E. Mittge and K. Guillemin (2007). "Intestinal alkaline phosphatase detoxifies lipopolysaccharide and prevents inflammation in zebrafish in response to the gut microbiota." Cell host & microbe **2**(6): 371-382.

Bäumler, A. J. and V. Sperandio (2016). "Interactions between the microbiota and pathogenic bacteria in the gut." Nature **535**(7610): 85-93.

Bazzoni, F., M. Rossato, M. Fabbri, D. Gaudiosi, M. Mirolo, L. Mori, N. Tamassia, A. Mantovani, M. A. Cassatella and M. Locati (2009). "Induction and regulatory function of miR-9 in human monocytes and neutrophils exposed to proinflammatory signals." Proceedings of the National Academy of Sciences **106**(13): 5282-5287.

Bedard, K. and K. H. Krause (2007). "The NOX family of ROS-generating NADPH oxidases: physiology and pathophysiology." Physiol Rev **87**(1): 245-313.

Belgiovine, C., M. D'Incalci, P. Allavena and R. Frapolli (2016). "Tumor-associated macrophages and anti-tumor therapies: complex links." Cellular and molecular life sciences : CMLS **73**(13): 2411-2424.

Belkaid, Y. and S. Naik (2013). "Compartmentalized and systemic control of tissue immunity by commensals." Nature immunology **14**(7): 646-653.

Bellacosa, A., S. Staal and P. Tsichlis (1991). "A retroviral oncogene, akt, encoding a serine-threonine kinase containing an SH2-like region." Science **254**(5029): 274-277.

Bengmark, S. (1998). "Ecological control of the gastrointestinal tract. The role of probiotic flora." Gut **42**(1): 2-7.

Berridge, M. J., M. D. Bootman and H. L. Roderick (2003). "Calcium signalling: dynamics, homeostasis and remodelling." Nat Rev Mol Cell Biol **4**(7): 517-529.

Bertani, B. and N. Ruiz (2018). "Function and Biogenesis of Lipopolysaccharides." EcoSal Plus **8**(1): 10.1128/ecosalplus.ESP-0001-2018.

Bertani, B. and N. Ruiz (2018). "Function and Biogenesis of Lipopolysaccharides." EcoSal Plus **8**(1).

Beutler, B. and E. T. Rietschel (2003). "Innate immune sensing and its roots: the story of endotoxin." Nature reviews. Immunology **3**(2): 169-176.

Blyth, B. J. and P. J. Sykes (2011). "Radiation-induced bystander effects: what are they, and how relevant are they to human radiation exposures?" Radiation research **176**(2): 139-157.

Boakye, Y. D., L. Groyer and E. H. Heiss (2018). "An increased autophagic flux contributes to the anti-inflammatory potential of urolithin A in macrophages." Biochim Biophys Acta Gen Subj **1862**(1): 61-70.

Borzęcka, K., A. Płóciennikowska, H. Björkelund, A. Sobota and K. Kwiatkowska (2013). "CD14 mediates binding of high doses of LPS but is dispensable for TNF-α production." Mediators of inflammation **2013**: 824919-824919.

Botos, I., David M. Segal and David R. Davies (2011). "The Structural Biology of Toll-like Receptors." Structure **19**(4): 447-459.

Bouquet, F., C. Muller and B. Salles (2006). "The loss of gammaH2AX signal is a marker of DNA double strand breaks repair only at low levels of DNA damage." Cell Cycle **5**(10): 1116-1122.

Braga, T. T., J. S. H. Agudelo and N. O. S. Camara (2015). "Macrophages During the Fibrotic Process: M2 as Friend and Foe." Frontiers in immunology **6**: 602-602.

Bryant, C. E., D. R. Spring, M. Gangloff and N. J. Gay (2010). "The molecular basis of the host response to lipopolysaccharide." Nat Rev Microbiol **8**(1): 8-14.

Cai, X., Y.-H. Chiu and Zhijian J. Chen (2014). "The cGAS-cGAMP-STING Pathway of Cytosolic DNA Sensing and Signaling." Molecular Cell **54**(2): 289-296.

Cai, X., Y. Yin, N. Li, D. Zhu, J. Zhang, C.-Y. Zhang and K. Zen (2012). "Re-polarization of tumor-associated macrophages to pro-inflammatory M1 macrophages by microRNA-155." Journal of molecular cell biology **4**(5): 341-343.

Calin, G. A., C.-G. Liu, C. Sevignani, M. Ferracin, N. Felli, C. D. Dumitru, M. Shimizu, A. Cimmino, S. Zupo and M. Dono (2004). "MicroRNA profiling reveals distinct signatures in B cell chronic lymphocytic leukemias." Proceedings of the National Academy of Sciences **101**(32): 11755-11760.

Carafoli, E., L. Santella, D. Branca and M. Brini (2001). "Generation, control, and processing of cellular calcium signals." Crit Rev Biochem Mol Biol **36**(2): 107-260.

Cassetta, L., E. Cassol and G. Poli (2011). "Macrophage polarization in health and disease." TheScientificWorldJournal **11**: 2391-2402.

Celeste, A., S. Petersen, P. J. Romanienko, O. Fernandez-Capetillo, H. T. Chen, O. A. Sedelnikova, B. Reina-San-Martin, V. Coppola, E. Meffre, M. J. Difilippantonio, C. Redon, D. R. Pilch, A. Olaru, M. Eckhaus, R. D. Camerini-Otero, L. Tessarollo, F. Livak, K. Manova, W. M. Bonner, M. C. Nussenzweig and A. Nussenzweig (2002). "Genomic instability in mice lacking histone H2AX." Science **296**(5569): 922-927.

Celhar, T., R. Magalhães and A. M. Fairhurst (2012). "TLR7 and TLR9 in SLE: when sensing self goes wrong." Immunologic Research **53**(1): 58-77.

Cen, X., S. Liu and K. Cheng (2018). "The Role of Toll-Like Receptor in Inflammation and Tumor Immunity." Frontiers in pharmacology **9**: 878-878.

Cerdá, B., J. C. Espín, S. Parra, P. Martínez and F. A. Tomás-Barberán (2004). "The potent in vitro antioxidant ellagitannins from pomegranate juice are metabolised into bioavailable but poor antioxidant hydroxy-6H-dibenzopyran-6-one derivatives by the colonic microflora of healthy humans." European journal of nutrition **43**(4): 205-220.

Cerdá, B., R. Llorach, J. J. Cerón, J. C. Espín and F. A. Tomás-Barberán (2003). "Evaluation of the bioavailability and metabolism in the rat of punicalagin, an antioxidant polyphenol from pomegranate juice." European journal of nutrition **42**(1): 18-28.

Cerdá, B., P. Periago, J. C. Espín and F. A. Tomás-Barberán (2005). "Identification of urolithin a as a metabolite produced by human colon microflora from ellagic acid and related compounds." Journal of agricultural and food chemistry **53**(14): 5571-5576.

Cerdá, B., F. A. Tomás-Barberán and J. C. Espín (2005). "Metabolism of antioxidant and chemopreventive ellagitannins from strawberries, raspberries, walnuts, and oak-aged wine in humans: identification of biomarkers and individual variability." Journal of agricultural and food chemistry **53**(2): 227-235.

Chaplin, D. D. (2010). "Overview of the immune response." The Journal of allergy and clinical immunology **125**(2 Suppl 2): S3-S23.

Charles A. Janeway, J. and R. Medzhitov (2002). "Innate Immune Recognition." Annual Review of Immunology **20**(1): 197-216.

Chaudhuri, A. A., A. Y.-L. So, N. Sinha, W. S. J. Gibson, K. D. Taganov, R. M. O'Connell and D. Baltimore (2011). "MicroRNA-125b potentiates macrophage activation." Journal of immunology (Baltimore, Md. : 1950) **187**(10): 5062-5068.

Chen, L., H. Deng, H. Cui, J. Fang, Z. Zuo, J. Deng, Y. Li, X. Wang and L. Zhao (2017). "Inflammatory responses and inflammation-associated diseases in organs." Oncotarget **9**(6): 7204-7218.

Chen, Q., H. Wang, Y. Liu, Y. Song, L. Lai, Q. Han, X. Cao and Q. Wang (2012). "Inducible microRNA-223 down-regulation promotes TLR-triggered IL-6 and IL-1β production in macrophages by targeting STAT3." PloS one **7**(8): e42971-e42971.

Chen, T. Y., M. G. Lei, T. Suzuki and D. C. Morrison (1992). "Lipopolysaccharide receptors and signal transduction pathways in mononuclear phagocytes." Current topics in microbiology and immunology **181**: 169-188.

Chertov, O., D. Yang, O. M. Howard and J. J. Oppenheim (2000). "Leukocyte granule proteins mobilize innate host defenses and adaptive immune responses." Immunol Rev **177**: 68-78.

Chistiakov, D. A., Y. V. Bobryshev, N. G. Nikiforov, N. V. Elizova, I. A. Sobenin and A. N. Orekhov (2015). "Macrophage phenotypic plasticity in atherosclerosis: The associated features and the peculiarities of the expression of inflammatory genes." International journal of cardiology **184**: 436-445.

Chomczynski, P. (1993). "A reagent for the single-step simultaneous isolation of RNA, DNA and proteins from cell and tissue samples." BioTechniques **15**(3): 532-537.

Chomczynski, P. and N. Sacchi (1987). "Single-step method of RNA isolation by acid guanidinium thiocyanate-phenol-chloroform extraction." Analytical biochemistry **162**(1): 156-159.

Chua, C. L. L., G. Brown, J. A. Hamilton, S. Rogerson and P. Boeuf (2013). "Monocytes and macrophages in malaria: protection or pathology?" Trends in parasitology **29**(1): 26-34.

Chumduri, C., R. K. Gurumurthy, P. K. Zadora, Y. Mi and T. F. Meyer (2013). "Chlamydia infection promotes host DNA damage and proliferation but impairs the DNA damage response." Cell Host Microbe **13**(6): 746-758.

Chun, J. and A. Prince (2006). "Activation of Ca2+-dependent signaling by TLR2." J Immunol **177**(2): 1330-1337.

Ciccia, A. and S. J. Elledge (2010). "The DNA damage response: making it safe to play with knives." Molecular cell **40**(2): 179-204.

Clapham, D. E. (2007). "Calcium signaling." Cell **131**(6): 1047-1058.

Claro, S., M. E. M. Oshiro, E. Freymuller, E. Katchburian, E. G. Kallas, P. S. Cerri and A. T. Ferreira (2008). "γ-Radiation induces apoptosis via sarcoplasmatic reticulum in guinea pig ileum smooth muscle cells." European journal of pharmacology **590**(1-3): 20-28.

Covarrubias, A. J., H. I. Aksoylar and T. Horng (2015). "Control of macrophage metabolism and activation by mTOR and Akt signaling." Semin Immunol **27**(4): 286-296.

Crifo, B. and C. T. Taylor (2016). "Crosstalk between toll-like receptors and hypoxia-dependent pathways in health and disease." Journal of Investigative Medicine **64**(2): 369.

Curtale, G., T. A. Renzi, M. Mirolo, L. Drufuca, M. Albanese, M. De Luca, M. Rossato, F. Bazzoni and M. Locati (2018). "Multi-Step Regulation of the TLR4 Pathway by the miR-125a~99b~let-7e Cluster." Frontiers in Immunology **9**(2037).

Curtale, G., M. Rubino and M. Locati (2019). "MicroRNAs as Molecular Switches in Macrophage Activation." Frontiers in Immunology **10**(799).

Czaja, A. J. (2014). "Hepatic inflammation and progressive liver fibrosis in chronic liver disease." World J Gastroenterol **20**(10): 2515-2532.

Daniel-Issakani, S., A. M. Spiegel and B. Strulovici (1989). "Lipopolysaccharide response is linked to the GTP binding protein, Gi2, in the promonocytic cell line U937." The Journal of biological chemistry **264**(34): 20240-20247.

Davies, L. C., S. J. Jenkins, J. E. Allen and P. R. Taylor (2013). "Tissue-resident macrophages." Nature immunology **14**(10): 986-995.

De Nardo, D., C. M. De Nardo, T. Nguyen, J. A. Hamilton and G. M. Scholz (2009). "Signaling crosstalk during sequential TLR4 and TLR9 activation amplifies the inflammatory response of mouse macrophages." J Immunol **183**(12): 8110-8118.

den Besten, G., K. van Eunen, A. K. Groen, K. Venema, D. J. Reijngoud and B. M. Bakker (2013). "The role of short-chain fatty acids in the interplay between diet, gut microbiota, and host energy metabolism." J Lipid Res **54**(9): 2325-2340.

Dent, P., A. Yacoub, P. B. Fisher, M. P. Hagan and S. Grant (2003). "MAPK pathways in radiation responses." Oncogene **22**(37): 5885-5896.

Deretic, V. (2016). "Autophagy in leukocytes and other cells: mechanisms, subsystem organization, selectivity, and links to innate immunity." Journal of leukocyte biology **100**(5): 969-978.

Desouky, O., N. Ding and G. Zhou (2015). "Targeted and non-targeted effects of ionizing radiation." Journal of Radiation Research and Applied Sciences **8**(2): 247-254.

Divangahi, M., I. L. King and E. Pernet (2015). "Alveolar macrophages and type I IFN in airway homeostasis and immunity." Trends in immunology **36**(5): 307-314.

Dorrington, M. G. and I. D. C. Fraser (2019). "NF-κB Signaling in Macrophages: Dynamics, Crosstalk, and Signal Integration." Frontiers in Immunology **10**(705).

Drysdale, B. E., R. A. Yapundich, M. L. Shin and H. S. Shin (1987). "Lipopolysaccharide-mediated macrophage activation: the role of calcium in the generation of tumoricidal activity." J Immunol **138**(3): 951-956.

Eberlein, U., M. Peper, M. Fernández, M. Lassmann and H. Scherthan (2015). "Calibration of the γ-H2AX DNA Double Strand Break Focus Assay for Internal Radiation Exposure of Blood Lymphocytes." PLOS ONE **10**(4): e0123174.

Ehses, J. A., M. Böni-Schnetzler, M. Faulenbach and M. Y. Donath (2008). "Macrophages, cytokines and beta-cell death in Type 2 diabetes." Biochemical Society transactions **36**(Pt 3): 340-342.

Einstein, A. (1905). "Über einen die Erzeugung und Verwandlung des Lichtes betreffenden heuristischen Gesichtspunkt." Annalen der physik **322**(6): 132-148.

El-Zayat, S. R., H. Sibaii and F. A. Mannaa (2019). "Toll-like receptors activation, signaling, and targeting: an overview." Bulletin of the National Research Centre **43**(1): 187.

Epelman, S., K. J. Lavine and G. J. Randolph (2014). "Origin and functions of tissue macrophages." Immunity **41**(1): 21-35.

Espín, J. C., R. González-Barrio, B. Cerdá, C. López-Bote, A. I. Rey and F. A. Tomás-Barberán (2007). "Iberian Pig as a Model To Clarify Obscure Points in the Bioavailability and Metabolism of Ellagitannins in Humans." Journal of Agricultural and Food Chemistry **55**(25): 10476-10485.

Espín, J. C., M. Larrosa, M. T. García-Conesa and F. Tomás-Barberán (2013). "Biological significance of urolithins, the gut microbial ellagic Acid-derived metabolites: the evidence so far." Evidence-based complementary and alternative medicine : eCAM **2013**: 270418-270418.

Espín, J. C., M. Larrosa, M. T. García-Conesa and F. Tomás-Barberán (2013). "Biological Significance of Urolithins, the Gut Microbial Ellagic Acid-Derived Metabolites: The Evidence So Far." Evidence-Based Complementary and Alternative Medicine **2013**: 1-15.

Fajardo, L. (1982). "Pathology of radiation injury." Masson Pub. USA: 285 pages.

Fan, J., F. T. Ishmael, X. Fang, A. Myers, C. Cheadle, S.-K. Huang, U. Atasoy, M. Gorospe and C. Stellato (2011). "Chemokine Transcripts as Targets of the RNA-Binding Protein HuR in Human Airway Epithelium." The Journal of Immunology **186**(4): 2482.

Ferrante, C. J., G. Pinhal-Enfield, G. Elson, B. N. Cronstein, G. Hasko, S. Outram and S. J. Leibovich (2013). "The adenosine-dependent angiogenic switch of macrophages to an M2-like phenotype is independent of interleukin-4 receptor alpha (IL-4Rα) signaling." Inflammation **36**(4): 921-931.

Ferrero-Miliani, L., O. H. Nielsen, P. S. Andersen and S. E. Girardin (2007). "Chronic inflammation: importance of NOD2 and NALP3 in interleukin-1beta generation." Clin Exp Immunol **147**(2): 227-235.

Feske, S., Y. Gwack, M. Prakriya, S. Srikanth, S. H. Puppel, B. Tanasa, P. G. Hogan, R. S. Lewis, M. Daly and A. Rao (2006). "A mutation in Orai1 causes immune deficiency by abrogating CRAC channel function." Nature **441**(7090): 179-185.

Feske, S., H. Wulff and E. Y. Skolnik (2015). "Ion channels in innate and adaptive immunity." Annu Rev Immunol **33**: 291-353.

Fujiwara, N. and K. Kobayashi (2005). "Macrophages in inflammation." Current drug targets. Inflammation and allergy **4**(3): 281-286.

Fukao, T. and S. Koyasu (2003). "PI3K and negative regulation of TLR signaling." Trends Immunol **24**(7): 358-363.

Gajowik, A. and M. M. Dobrzyńska (2014). "Lycopene - antioxidant with radioprotective and anticancer properties. A review." Rocz Panstw Zakl Hig **65**(4): 263-271.

Gallo, E. M., K. Canté-Barrett and G. R. Crabtree (2006). "Lymphocyte calcium signaling from membrane to nucleus." Nat Immunol **7**(1): 25-32.

García-Villalba, R., M. V. Selma, J. C. Espín and F. A. Tomás-Barberán (2019). "Identification of Novel Urolithin Metabolites in Human Feces and Urine after the Intake of a Pomegranate Extract." Journal of Agricultural and Food Chemistry **67**(40): 11099-11107.

Garcia-Villalba, R., H. Vissenaekens, J. Pitart, M. Romo-Vaquero, J. C. Espin, C. Grootaert, M. V. Selma, K. Raes, G. Smagghe, S. Possemiers, J. Van Camp and F. A. Tomas-Barberan (2017). "Gastrointestinal Simulation Model TWIN-SHIME Shows Differences between Human Urolithin-Metabotypes in Gut Microbiota Composition, Pomegranate Polyphenol Metabolism, and Transport along the Intestinal Tract." J Agric Food Chem **65**(27): 5480-5493.

Gee, K. R., K. A. Brown, W. N. U. Chen, J. Bishop-Stewart, D. Gray and I. Johnson (2000). "Chemical and physiological characterization of fluo-4 Ca2+-indicator dyes." Cell Calcium **27**(2): 97-106.

Gensollen, T., S. S. Iyer, D. L. Kasper and R. S. Blumberg (2016). "How colonization by microbiota in early life shapes the immune system." Science **352**(6285): 539-544.

Georgakilas, A. G., A. Pavlopoulou, M. Louka, Z. Nikitaki, C. E. Vorgias, P. G. Bagos and I. Michalopoulos (2015). "Emerging molecular networks common in ionizing radiation, immune and inflammatory responses by employing bioinformatics approaches." Cancer Lett **368**(2): 164-172.

Gill, S. R., M. Pop, R. T. Deboy, P. B. Eckburg, P. J. Turnbaugh, B. S. Samuel, J. I. Gordon, D. A. Relman, C. M. Fraser-Liggett and K. E. Nelson (2006). "Metagenomic analysis of the human distal gut microbiome." Science **312**(5778): 1355-1359.

Ginhoux, F. and M. Guilliams (2016). "Tissue-Resident Macrophage Ontogeny and Homeostasis." Immunity **44**(3): 439-449.

Gong, Z., J. Huang, B. Xu, Z. Ou, L. Zhang, X. Lin, X. Ye, X. Kong, D. Long, X. Sun, X. He, L. Xu, Q. Li and A. Xuan (2019). "Urolithin A attenuates memory impairment and neuroinflammation in APP/PS1 mice." Journal of Neuroinflammation **16**(1): 62.

Gordeeva, A. V., R. A. Zvyagilskaya and Y. A. Labas (2003). "Cross-talk between reactive oxygen species and calcium in living cells." Biochemistry (Mosc) **68**(10): 1077-1080.

Gordon, S. (2016). "Phagocytosis: The Legacy of Metchnikoff." Cell **166**(5): 1065-1068.

Gordon, S. and L. Martinez-Pomares (2017). "Physiological roles of macrophages." Pflügers Archiv - European Journal of Physiology **469**(3-4): 365-374.

Guo, H., J. B. Callaway and J. P. Y. Ting (2015). "Inflammasomes: mechanism of action, role in disease, and therapeutics." Nature medicine **21**(7): 677-687.

Hall, E. J. and A. J. Giaccia (2006). Radiobiology for the Radiologist, Lippincott Williams & Wilkins.

Haneklaus, M., M. Gerlic, L. A. J. O'Neill and S. L. Masters (2013). "miR-223: infection, inflammation and cancer." Journal of internal medicine **274**(3): 215-226.

Härtlova, A., S. F. Erttmann, F. A. Raffi, A. M. Schmalz, U. Resch, S. Anugula, S. Lienenklaus, L. M. Nilsson, A. Kröger, J. A. Nilsson, T. Ek, S. Weiss and N. O. Gekara (2015). "DNA damage primes the type I interferon system via the cytosolic DNA sensor STING to promote anti-microbial innate immunity." Immunity **42**(2): 332-343.

Hayden, M. S. and S. Ghosh (2012). "NF-kappaB, the first quarter-century: remarkable progress and outstanding questions." Genes Dev **26**(3): 203-234.

Heber, D. (2008). "Multitargeted therapy of cancer by ellagitannins." Cancer letters **269**(2): 262-268.

Heinrichs, D. E., J. A. Yethon and C. Whitfield (1998). "Molecular basis for structural diversity in the core regions of the lipopolysaccharides of Escherichia coli and Salmonella enterica." Molecular microbiology **30**(2): 221-232.

Hinz, B., S. H. Phan, V. J. Thannickal, M. Prunotto, A. Desmoulière, J. Varga, O. De Wever, M. Mareel and G. Gabbiani (2012). "Recent developments in myofibroblast biology: paradigms for connective tissue remodeling." The American journal of pathology **180**(4): 1340-1355.

Hirayama, D., T. Iida and H. Nakase (2017). "The Phagocytic Function of Macrophage-Enforcing Innate Immunity and Tissue Homeostasis." International journal of molecular sciences **19**(1): 92.

Hirayama, D., T. Iida and H. Nakase (2017). "The Phagocytic Function of Macrophage-Enforcing Innate Immunity and Tissue Homeostasis." Int J Mol Sci **19**(1).

Hirschfeld, M., J. J. Weis, V. Toshchakov, C. A. Salkowski, M. J. Cody, D. C. Ward, N. Qureshi, S. M. Michalek and S. N. Vogel (2001). "Signaling by Toll-Like Receptor 2 and 4 Agonists Results in Differential Gene Expression in Murine Macrophages." Infection and Immunity **69**(3): 1477.

Ho, M. and T. Springer (1982). "Mac-1 antigen: quantitative expression in macrophage populations and tissues, and immunofluorescent localization in spleen." The Journal of Immunology **128**(5): 2281-2286.

Hobbs, S., M. Reynoso, A. V. Geddis, A. Y. Mitrophanov and R. W. Matheny, Jr. (2018). "LPS-stimulated NF-κB p65 dynamic response marks the initiation of TNF expression and transition to IL-10 expression in RAW 264.7 macrophages." Physiological reports **6**(21): e13914-e13914.

Hoffmann, A., O. Kann, C. Ohlemeyer, U.-K. Hanisch and H. Kettenmann (2003). "Elevation of basal intracellular calcium as a central element in the activation of brain macrophages (microglia): suppression of receptor-evoked calcium signaling and control of release function." The Journal of neuroscience : the official journal of the Society for Neuroscience **23**(11): 4410-4419.

Iguchi, A. (2016). "A complete view of the Escherichia coli O-antigen biosynthesis gene cluster and the development of molecular-based O-serogrouping methods." Nihon saikingaku zasshi. Japanese journal of bacteriology **71**(4): 209-215.

Imlay, J. A., S. M. Chin and S. Linn (1988). "Toxic DNA damage by hydrogen peroxide through the Fenton reaction in vivo and in vitro." Science **240**(4852): 640-642.

Ioannou, S. and M. Voulgarelis (2010). "Toll-Like Receptors, Tissue Injury, and Tumourigenesis." Mediators of Inflammation **2010**: 581837.

Ishmael, F. T., X. Fang, M. R. Galdiero, U. Atasoy, W. F. Rigby, M. Gorospe, C. Cheadle and C. Stellato (2008). "Role of the RNA-binding protein tristetraprolin in glucocorticoid-mediated gene regulation." J Immunol **180**(12): 8342-8353.

Iwasaki, A. and R. Medzhitov (2004). "Toll-like receptor control of the adaptive immune responses." Nat Immunol **5**(10): 987-995.

Jackson, S. P. and J. Bartek (2009). "The DNA-damage response in human biology and disease." Nature **461**(7267): 1071-1078.

Janeway, C. A., Jr. (1989). "Approaching the asymptote? Evolution and revolution in immunology." Cold Spring Harbor symposia on quantitative biology **54 Pt 1**: 1-13.

Janeway, C. A., Jr. and R. Medzhitov (2002). "Innate immune recognition." Annual review of immunology **20**: 197-216.

Jaumouillé, V. and S. Grinstein (2016). "Molecular Mechanisms of Phagosome Formation." Microbiology spectrum **4**(3): 10.1128/microbiolspec.MCHD-0013-2015.

Jha, A. K., S. C. Huang, A. Sergushichev, V. Lampropoulou, Y. Ivanova, E. Loginicheva, K. Chmielewski, K. M. Stewart, J. Ashall, B. Everts, E. J. Pearce, E. M. Driggers and M. N. Artyomov (2015). "Network integration of parallel metabolic and transcriptional data reveals metabolic modules that regulate macrophage polarization." Immunity **42**(3): 419-430.

Jiang, P., R. Liu, Y. Zheng, X. Liu, L. Chang, S. Xiong and Y. Chu (2012). "MiR-34a inhibits lipopolysaccharide-induced inflammatory response through targeting Notch1 in murine macrophages." Experimental cell research **318**(10): 1175-1184.

Johnson, G. L. and R. Lapadat (2002). "Mitogen-Activated Protein Kinase Pathways Mediated by ERK, JNK, and p38 Protein Kinases." Science **298**(5600): 1911-1912.

Kadhim, H., B. Tabarki, G. Verellen, C. De Prez, A. M. Rona and G. Sébire (2001). "Inflammatory cytokines in the pathogenesis of periventricular leukomalacia." Neurology **56**(10): 1278-1284.

Kaisho, T. and S. Akira (2002). "Toll-like receptors as adjuvant receptors." Biochim Biophys Acta **1589**(1): 1-13.

Kalynych, S., R. Morona and M. Cygler (2014). "Progress in understanding the assembly process of bacterial O-antigen." FEMS microbiology reviews **38**(5): 1048-1065.

Karin, M. (1999). "How NF-kappaB is activated: the role of the IkappaB kinase (IKK) complex." Oncogene **18**(49): 6867-6874.

Kato, M. (1972). "Site of action of lipid A on mitochondria." Journal of bacteriology **112**(1): 268-275.

Kawabata, K., R. Mukai and A. Ishisaka (2015). "Quercetin and related polyphenols: new insights and implications for their bioactivity and bioavailability." Food & function **6**(5): 1399-1417.

Kawai, T. and S. Akira (2010). "The role of pattern-recognition receptors in innate immunity: update on Toll-like receptors." Nature Immunology **11**(5): 373-384.

Kawai, T. and S. Akira (2011). "Toll-like receptors and their crosstalk with other innate receptors in infection and immunity." Immunity **34**(5): 637-650.

Kawasaki, T. and T. Kawai (2014). "Toll-Like Receptor Signaling Pathways." Frontiers in Immunology **5**(461).

Khanna, K. K. and S. P. Jackson (2001). "DNA double-strand breaks: signaling, repair and the cancer connection." Nat Genet **27**(3): 247-254.

Khosravi, A., A. Yáñez, J. G. Price, A. Chow, M. Merad, H. S. Goodridge and S. K. Mazmanian (2014). "Gut microbiota promote hematopoiesis to control bacterial infection." Cell host & microbe **15**(3): 374-381.

Kielian, T. L. and F. Blecha (1995). "CD14 and other recognition molecules for lipopolysaccharide: a review." Immunopharmacology **29**(3): 187-205.

Kim, S., J. H. Choe, G. J. Lee, Y. S. Kim, S. Y. Kim, H.-M. Lee, H. S. Jin, T. S. Kim, J.-M. Kim, M.-J. Cho, E.-C. Shin, E.-K. Jo and J.-S. Kim (2016). "Ionizing Radiation Induces Innate Immune Responses in Macrophages by Generation of Mitochondrial Reactive Oxygen Species." Radiation Research **187**(1): 32-41, 10.

Klein, G. and S. Raina (2015). "Regulated Control of the Assembly and Diversity of LPS by Noncoding sRNAs." BioMed research international **2015**: 153561-153561.

Klug, F., H. Prakash, P. E. Huber, T. Seibel, N. Bender, N. Halama, C. Pfirschke, R. H. Voss, C. Timke, L. Umansky, K. Klapproth, K. Schäkel, N. Garbi, D. Jäger, J. Weitz, H. Schmitz-Winnenthal, G. J. Hämmerling and P. Beckhove (2013). "Low-dose irradiation programs macrophage differentiation to an iNOS[+]/M1 phenotype that orchestrates effective T cell immunotherapy." Cancer cell **24**(5): 589-602.

Koch, W. (2019). "Dietary Polyphenols-Important Non-Nutrients in the Prevention of Chronic Noncommunicable Diseases. A Systematic Review." Nutrients **11**(5).

Kogut, M. H., M. Iqbal, H. He, V. Philbin, P. Kaiser and A. Smith (2005). "Expression and function of Toll-like receptors in chicken heterophils." Dev Comp Immunol **29**(9): 791-807.

Kolch, W. (2000). "Meaningful relationships: the regulation of the Ras/Raf/MEK/ERK pathway by protein interactions." Biochem J **351 Pt 2**(Pt 2): 289-305.

Kollmann, T. R., O. Levy, R. R. Montgomery and S. Goriely (2012). "Innate immune function by Toll-like receptors: distinct responses in newborns and the elderly." Immunity **37**(5): 771-783.

Krawczyk, P. M., T. Borovski, J. Stap, T. Cijsouw, R. ten Cate, J. P. Medema, R. Kanaar, N. A. Franken and J. A. Aten (2012). "Chromatin mobility is increased at sites of DNA double-strand breaks." J Cell Sci **125**(Pt 9): 2127-2133.

Kryston, T. B., A. B. Georgiev, P. Pissis and A. G. Georgakilas (2011). "Role of oxidative stress and DNA damage in human carcinogenesis." Mutat Res **711**(1-2): 193-201.

Kurowska-Stolarska, M., B. Stolarski, P. Kewin, G. Murphy, C. J. Corrigan, S. Ying, N. Pitman, A. Mirchandani, B. Rana, N. van Rooijen, M. Shepherd, C. McSharry, I. B. McInnes, D. Xu and F. Y. Liew (2009). "IL-33 amplifies the polarization of alternatively activated macrophages that contribute to airway inflammation." Journal of immunology (Baltimore, Md. : 1950) **183**(10): 6469-6477.

Kyriakis, J. M. and J. Avruch (2001). "Mammalian mitogen-activated protein kinase signal transduction pathways activated by stress and inflammation." Physiol Rev **81**(2): 807-869.

Laplante, M. and David M. Sabatini (2012). "mTOR Signaling in Growth Control and Disease." Cell **149**(2): 274-293.

Larrosa, M., A. González-Sarrías, M. J. Yáñez-Gascón, M. V. Selma, M. Azorín-Ortuño, S. Toti, F. Tomás-Barberán, P. Dolara and J. C. Espín (2010). "Anti-inflammatory properties of a pomegranate extract and its metabolite urolithin-A in a colitis rat model and the effect of colon inflammation on phenolic metabolism☆." The Journal of Nutritional Biochemistry **21**(8): 717-725.

Lawrence, T. (2009). "The nuclear factor NF-kappaB pathway in inflammation." Cold Spring Harb Perspect Biol **1**(6): a001651.

Leatherbarrow, E. L., J. V. Harper, F. A. Cucinotta and P. O'Neill (2006). "Induction and quantification of gamma-H2AX foci following low and high LET-irradiation." Int J Radiat Biol **82**(2): 111-118.

Lee, B. L., J. E. Moon, J. H. Shu, L. Yuan, Z. R. Newman, R. Schekman and G. M. Barton (2013). "UNC93B1 mediates differential trafficking of endosomal TLRs." eLife **2**: e00291-e00291.

Lemaitre, B., E. Nicolas, L. Michaut, J. M. Reichhart and J. A. Hoffmann (1996). "The dorsoventral regulatory gene cassette spätzle/Toll/cactus controls the potent antifungal response in Drosophila adults." Cell **86**(6): 973-983.

Les, F., J. M. Arbonés-Mainar, M. S. Valero and V. López (2018). "Pomegranate polyphenols and urolithin A inhibit α-glucosidase, dipeptidyl peptidase-4, lipase, triglyceride accumulation and adipogenesis related genes in 3T3-L1 adipocyte-like cells." J Ethnopharmacol **220**: 67-74.

Letari, O., S. Nicosia, C. Chiavaroli, P. Vacher and W. Schlegel (1991). "Activation by bacterial lipopolysaccharide causes changes in the cytosolic free calcium concentration in single peritoneal macrophages." The Journal of Immunology **147**(3): 980-983.

Ley, R. E., M. Hamady, C. Lozupone, P. J. Turnbaugh, R. R. Ramey, J. S. Bircher, M. L. Schlegel, T. A. Tucker, M. D. Schrenzel, R. Knight and J. I. Gordon (2008). "Evolution of mammals and their gut microbes." Science (New York, N.Y.) **320**(5883): 1647-1651.

Li, L., U. Maitra, N. Singh and L. Gan (2010). "Molecular mechanism underlying LPS-induced generation of reactive oxygen species in macrophages." The FASEB Journal **24**(S1): 422.423-422.423.

Libby, P. (2007). "Inflammatory mechanisms: the molecular basis of inflammation and disease." Nutr Rev **65**(12 Pt 2): S140-146.

Lieber, M. R., Y. Ma, U. Pannicke and K. Schwarz (2003). "Mechanism and regulation of human non-homologous DNA end-joining." Nat Rev Mol Cell Biol **4**(9): 712-720.

Lim, D.-W., H.-J. Choi, S.-D. Park, H. Kim, G.-R. Yu, J.-E. Kim and W.-H. Park (2020). "Activation of the Nrf2/HO-1 Pathway by <i>Amomum villosum</i> Extract Suppresses LPS-Induced Oxidative Stress <i>In Vitro</i> and <i>Ex Vivo</i>." Evidence-Based Complementary and Alternative Medicine **2020**: 2837853.

Lim, J. E., E. Chung and Y. Son (2017). "A neuropeptide, Substance-P, directly induces tissue-repairing M2 like macrophages by activating the PI3K/Akt/mTOR pathway even in the presence of IFNγ." Sci Rep **7**(1): 9417.

Limtrakul, P., S. Yodkeeree, P. Pitchakarn and W. Punfa (2015). "Suppression of Inflammatory Responses by Black Rice Extract in RAW 264.7 Macrophage Cells via Downregulation of NF-kB and AP-1 Signaling Pathways." Asian Pac J Cancer Prev **16**(10): 4277-4283.

Little, J. B. (2006). "Cellular radiation effects and the bystander response." Mutat Res **597**(1-2): 113-118.

Liu, C. M., Y. Z. Sun, J. M. Sun, J. Q. Ma and C. Cheng (2012). "Protective role of quercetin against lead-induced inflammatory response in rat kidney through the ROS-mediated MAPKs and NF-κB pathway." Biochim Biophys Acta **1820**(10): 1693-1703.

Liu, F., Y. Cui, F. Yang, Z. Xu, L. T. Da and Y. Zhang (2019). "Inhibition of polypeptide N-acetyl-α-galactosaminyltransferases is an underlying mechanism of dietary polyphenols preventing colorectal tumorigenesis." Bioorg Med Chem **27**(15): 3372-3382.

Liu, F., Y. Li, R. Jiang, C. Nie, Z. Zeng, N. Zhao, C. Huang, Q. Shao, C. Ding, C. Qing, L. Xia, E. Zeng and K. Qian (2015). "miR-132 inhibits lipopolysaccharide-induced inflammation in alveolar macrophages by the cholinergic anti-inflammatory pathway." Experimental lung research **41**(5): 261-269.

Liu, G. and E. Abraham (2013). "MicroRNAs in immune response and macrophage polarization." Arteriosclerosis, thrombosis, and vascular biology **33**(2): 170-177.

Liu, P., W. Gan, Y. R. Chin, K. Ogura, J. Guo, J. Zhang, B. Wang, J. Blenis, L. C. Cantley, A. Toker, B. Su and W. Wei (2015). "PtdIns(3,4,5)P₃-Dependent Activation of the mTORC2 Kinase Complex." Cancer Discovery **5**(11): 1194.

Liu, T., L. Wu, D. Wang, H. Wang, J. Chen, C. Yang, J. Bao and C. Wu (2016). "Role of reactive oxygen species-mediated MAPK and NF-κB activation in polygonatum cyrtonema lectin-induced apoptosis and autophagy in human lung adenocarcinoma A549 cells." J Biochem **160**(6): 315-324.

Liu, T., L. Zhang, D. Joo and S.-C. Sun (2017). "NF-κB signaling in inflammation." Signal transduction and targeted therapy **2**: 17023.

Liu, T., L. Zhang, D. Joo and S. C. Sun (2017). "NF-kappaB signaling in inflammation." Signal Transduct Target Ther **2**.

Liu, X., N. Wang, Y. Zhu, Y. Yang, X. Chen, S. Fan, Q. Chen, H. Zhou and J. Zheng (2016). "Inhibition of Extracellular Calcium Influx Results in Enhanced IL-12 Production in LPS-Treated Murine Macrophages by Downregulation of the CaMKKβ-AMPK-SIRT1 Signaling Pathway." Mediators of inflammation **2016**: 6152713-6152713.

Liu, Z., X. Lei, X. Li, J. M. Cai, F. Gao and Y. Y. Yang (2018). "Toll-like receptors and radiation protection." Eur Rev Med Pharmacol Sci **22**(1): 31-39.

Liu, Z., Y. Wang, Y. Wang, Q. Ning, Y. Zhang, C. Gong, W. Zhao, G. Jing and Q. Wang (2016). "Dexmedetomidine attenuates inflammatory reaction in the lung tissues of septic mice by activating cholinergic anti-inflammatory pathway." Int Immunopharmacol **35**: 210-216.

López-Peláez, M., I. Soria-Castro, L. Boscá, M. Fernández and S. Alemany (2011). "Cot/tpl2 activity is required for TLR-induced activation of the Akt p70 S6k pathway in macrophages: Implications for NO synthase 2 expression." Eur J Immunol **41**(6): 1733-1741.

Luckey, T. D. (1972). "Introduction to intestinal microecology." Am J Clin Nutr **25**(12): 1292-1294.

Mah, L. J., A. El-Osta and T. C. Karagiannis (2010). "GammaH2AX as a molecular marker of aging and disease." Epigenetics **5**(2): 129-136.

Mahaney, B. L., K. Meek and S. P. Lees-Miller (2009). "Repair of ionizing radiation-induced DNA double-strand breaks by non-homologous end-joining." Biochem J **417**(3): 639-650.

Mantovani, A., S. K. Biswas, M. R. Galdiero, A. Sica and M. Locati (2013). "Macrophage plasticity and polarization in tissue repair and remodelling." The Journal of pathology **229**(2): 176-185.

Mantovani, A., S. K. Biswas, M. R. Galdiero, A. Sica and M. Locati (2013). "Macrophage plasticity and polarization in tissue repair and remodelling." J Pathol **229**(2): 176-185.

Mantovani, A., A. Sica, S. Sozzani, P. Allavena, A. Vecchi and M. Locati (2004). "The chemokine system in diverse forms of macrophage activation and polarization." Trends Immunol **25**(12): 677-686.

Mantovani, A., A. Sica, S. Sozzani, P. Allavena, A. Vecchi and M. Locati (2004). "The chemokine system in diverse forms of macrophage activation and polarization." Trends in immunology **25**(12): 677-686.

Mantovani, A., S. Sozzani, M. Locati, P. Allavena and A. Sica (2002). "Macrophage polarization: tumor-associated macrophages as a paradigm for polarized M2 mononuclear phagocytes." Trends in immunology **23**(11): 549-555.

Marampon, F., C. Ciccarelli and B. M. Zani (2019). "Biological Rationale for Targeting MEK/ERK Pathways in Anti-Cancer Therapy and to Potentiate Tumour Responses to Radiation." International journal of molecular sciences **20**(10): 2530.

Marchesi, J. R., D. H. Adams, F. Fava, G. D. A. Hermes, G. M. Hirschfield, G. Hold, M. N. Quraishi, J. Kinross, H. Smidt, K. M. Tuohy, L. V. Thomas, E. G. Zoetendal and A. Hart (2016). "The gut microbiota and host health: a new clinical frontier." Gut **65**(2): 330-339.

Mariño, E., J. L. Richards, K. H. McLeod, D. Stanley, Y. A. Yap, J. Knight, C. McKenzie, J. Kranich, A. C. Oliveira, F. J. Rossello, B. Krishnamurthy, C. M. Nefzger, L. Macia, A. Thorburn, A. G. Baxter, G. Morahan, L. H. Wong, J. M. Polo, R. J. Moore, T. J. Lockett, J. M. Clarke, D. L. Topping, L. C. Harrison and C. R. Mackay (2017). "Gut microbial metabolites limit the frequency of autoimmune T cells and protect against type 1 diabetes." Nature immunology **18**(5): 552-562.

Martinez, F. O. and S. Gordon (2014). "The M1 and M2 paradigm of macrophage activation: time for reassessment." F1000Prime Rep **6**: 13.

Martinez, F. O., A. Sica, A. Mantovani and M. Locati (2008). "Macrophage activation and polarization." Frontiers in bioscience : a journal and virtual library **13**: 453-461.

Matozaki, T., Y. Murata, Y. Saito, H. Okazawa and H. Ohnishi (2009). "Protein tyrosine phosphatase SHP-2: A proto-oncogene product that promotes Ras activation." Cancer Science **100**(10): 1786-1793.

Matsuguchi, T., T. Musikacharoen, T. Ogawa and Y. Yoshikai (2000). "Gene expressions of Toll-like receptor 2, but not Toll-like receptor 4, is induced by LPS and inflammatory cytokines in mouse macrophages." J Immunol **165**(10): 5767-5772.

McCain, J. (2013). "The MAPK (ERK) Pathway: Investigational Combinations for the Treatment Of BRAF-Mutated Metastatic Melanoma." P t **38**(2): 96-108.

McCoy, C. E. and L. O'neill (2008). "The role of toll-like receptors in macrophages." Front Biosci **13**(13): 62-70.

McGarry, M. P. and C. C. Stewart (1991). "Murine eosinophil granulocytes bind the murine macrophage-monocyte specific monoclonal antibody F4/80." J Leukoc Biol **50**(5): 471-478.

McGivney, A. and S. G. Bradley (1979). "Action of bacterial endotoxin and lipid A on mitochondrial enzyme activities of cells in culture and subcellular fractions." Infect Immun **25**(2): 664-671.

McGuire, V. A., A. Gray, C. E. Monk, S. G. Santos, K. Lee, A. Aubareda, J. Crowe, N. Ronkina, J. Schwermann, I. H. Batty, N. R. Leslie, J. L. E. Dean, S. J. O'Keefe, M. Boothby, M. Gaestel and J. S. C. Arthur (2013). "Cross talk between the Akt and p38α pathways in macrophages downstream of Toll-like receptor signaling." Molecular and cellular biology **33**(21): 4152-4165.

McNelis, J. C. and J. M. Olefsky (2014). "Macrophages, immunity, and metabolic disease." Immunity **41**(1): 36-48.

Medzhitov, R., P. Preston-Hurlburt and C. A. Janeway, Jr. (1997). "A human homologue of the Drosophila Toll protein signals activation of adaptive immunity." Nature **388**(6640): 394-397.

Meng, Y., M. A. Beckett, H. Liang, H. J. Mauceri, N. van Rooijen, K. S. Cohen and R. R. Weichselbaum (2010). "Blockade of tumor necrosis factor alpha signaling in tumor-associated macrophages as a radiosensitizing strategy." Cancer research **70**(4): 1534-1543.

Meshkani, R. and S. Vakili (2016). "Tissue resident macrophages: Key players in the pathogenesis of type 2 diabetes and its complications." Clinica chimica acta; international journal of clinical chemistry **462**: 77-89.

Metchnikoff, E. (1893). "Lectures on the Comparative Pathology of Inflammation." London: Kegan Paul, Trench, Trubner & Co. Ltd.

Metchnikoff, E. (1905). "Immunity in Infective Diseases." London: Cambridge University Press.

Meziani, L., E. Deutsch and M. Mondini (2018). "Macrophages in radiation injury: a new therapeutic target." OncoImmunology **7**(10): e1494488.

Meziani, L., M. Mondini, B. Petit, A. Boissonnas, V. Thomas de Montpreville, O. Mercier, M.-C. Vozenin and E. Deutsch (2018). "CSF1R inhibition prevents radiation pulmonary fibrosis by depletion of interstitial macrophages." The European respiratory journal **51**(3): 1702120.

Mills, E. L., B. Kelly, A. Logan, A. S. H. Costa, M. Varma, C. E. Bryant, P. Tourlomousis, J. H. M. Däbritz, E. Gottlieb, I. Latorre, S. C. Corr, G. McManus, D. Ryan, H. T. Jacobs, M. Szibor, R. J. Xavier, T. Braun, C. Frezza, M. P. Murphy and L. A. O'Neill (2016). "Succinate Dehydrogenase Supports Metabolic Repurposing of Mitochondria to Drive Inflammatory Macrophages." Cell **167**(2): 457-470.e413.

Mogensen, T. H. (2009). "Pathogen Recognition and Inflammatory Signaling in Innate Immune Defenses." Clinical Microbiology Reviews **22**(2): 240.

Mohammadi, A., C. N. Blesso, G. E. Barreto, M. Banach, M. Majeed and A. Sahebkar (2019). "Macrophage plasticity, polarization and function in response to curcumin, a diet-derived polyphenol, as an immunomodulatory agent." The Journal of Nutritional Biochemistry **66**: 1-16.

Mohammed Saleem, Y. I., H. Albassam and M. Selim (2019). "Urolithin A induces prostate cancer cell death in p53-dependent and in p53-independent manner." Eur J Nutr.

More, G. K. and R. T. Makola (2020). "In-vitro analysis of free radical scavenging activities and suppression of LPS-induced ROS production in macrophage cells by Solanum sisymbriifolium extracts." Scientific Reports **10**(1): 6493.

Morrison, D. C. and J. L. Ryan (1987). "Endotoxins and disease mechanisms." Annual review of medicine **38**: 417-432.

Moynagh, P. N. (2005). "The NF-kappaB pathway." J Cell Sci **118**(Pt 20): 4589-4592.

Mukherjee, D., P. J. Coates, S. A. Lorimore and E. G. Wright (2014). "Responses to ionizing radiation mediated by inflammatory mechanisms." The Journal of pathology **232**(3): 289-299.

Mukherjee, S., S. Karmakar and S. P. S. Babu (2016). "TLR2 and TLR4 mediated host immune responses in major infectious diseases: a review." The Brazilian Journal of Infectious Diseases **20**(2): 193-204.

Murray, P. J. (2017). "Macrophage Polarization." Annual review of physiology **79**: 541-566.

Murray, P. J. and T. A. Wynn (2011) "Protective and pathogenic functions of macrophage subsets." Nature reviews. Immunology **11**, 723-737 DOI: 10.1038/nri3073.

Musa, A. E. and D. Shabeeb (2019). "Radiation-induced heart diseases: protective effects of natural products." Medicina **55**(5): 126.

Na, Y. R., D. Jung, G. J. Gu and S. H. Seok (2016). "GM-CSF Grown Bone Marrow Derived Cells Are Composed of Phenotypically Different Dendritic Cells and Macrophages." Molecules and cells **39**(10): 734-741.

Najafi, M., A. Shirazi, E. Motevaseli, G. Geraily, F. Norouzi, M. Heidari and S. Rezapoor (2017). "The melatonin immunomodulatory actions in radiotherapy." Biophys Rev **9**(2): 139-148.

Narang, H. and M. Krishna (2008). "P4. Effect of nitric oxide donor on radiation induced MAPK signaling in mouse peritoneal macrophages." Nitric Oxide **19**: 43-44.

Nathan, C. and A. Ding (2010). "Nonresolving inflammation." Cell **140**(6): 871-882.

Natividad, J. M. and E. F. Verdu (2013). "Modulation of intestinal barrier by intestinal microbiota: pathological and therapeutic implications." Pharmacol Res **69**(1): 42-51.

Needham, B. D. and M. S. Trent (2013). "Fortifying the barrier: the impact of lipid A remodelling on bacterial pathogenesis." Nature reviews. Microbiology **11**(7): 467-481.

Neish, A. S. (2009). "Microbes in gastrointestinal health and disease." Gastroenterology **136**(1): 65-80.

New, D. D., K. Block, B. Bhandhari, Y. Gorin and H. E. Abboud (2012). "IGF-I increases the expression of fibronectin by Nox4-dependent Akt phosphorylation in renal tubular epithelial cells." Am J Physiol Cell Physiol **302**(1): C122-130.

Newton, K. and V. M. Dixit (2012). "Signaling in innate immunity and inflammation." Cold Spring Harb Perspect Biol **4**(3).

Ngkelo, A., K. Meja, M. Yeadon, I. Adcock and P. A. Kirkham (2012). "LPS induced inflammatory responses in human peripheral blood mononuclear cells is mediated through NOX4 and Giα dependent PI-3kinase signalling." Journal of inflammation (London, England) **9**(1): 1-1.

Nichols, G. J., J. Schaack and D. A. Ornelles (2009). "Widespread phosphorylation of histone H2AX by species C adenovirus infection requires viral DNA replication." J Virol **83**(12): 5987-5998.

Noda, A. (2018). "Radiation-induced unrepairable DSBs: their role in the late effects of radiation and possible applications to biodosimetry." Journal of radiation research **59**(suppl_2): ii114-ii120.

Nonnenmacher, Y. and K. Hiller (2018). "Biochemistry of proinflammatory macrophage activation." Cellular and Molecular Life Sciences **75**(12): 2093-2109.

Norden, E. and E. H. Heiss (2018). "Urolithin A gains in antiproliferative capacity by reducing the glycolytic potential via the p53/TIGAR axis in colon cancer cells." Carcinogenesis **40**(1): 93-101.

Nuñez-Sánchez, M. A., R. García-Villalba, T. Monedero-Saiz, N. V. García-Talavera, M. B. Gómez-Sánchez, C. Sánchez-Álvarez, A. M. García-Albert, F. J. Rodríguez-Gil, M. Ruiz-Marín, F. A. Pastor-Quirante, F. Martínez-Díaz, M. J. Yáñez-Gascón, A. González-Sarrías, F. A. Tomás-Barberán and J. C. Espín (2014). "Targeted metabolic profiling of pomegranate polyphenols and urolithins in plasma, urine and colon tissues from colorectal cancer patients." Molecular nutrition & food research **58**(6): 1199-1211.

Nüsslein-Volhard, C., M. Lohs-Schardin, K. Sander and C. Cremer (1980). "A dorso-ventral shift of embryonic primordia in a new maternal-effect mutant of Drosophila." Nature **283**(5746): 474-476.

O'Connell, R. M., K. D. Taganov, M. P. Boldin, G. Cheng and D. Baltimore (2007). "MicroRNA-155 is induced during the macrophage inflammatory response." Proceedings of the National Academy of Sciences of the United States of America **104**(5): 1604-1609.

O'Hara, A. M. and F. Shanahan (2006). "The gut flora as a forgotten organ." EMBO reports **7**(7): 688-693.

O'Neill, L. A. J., D. Golenbock and A. G. Bowie (2013). "The history of Toll-like receptors — redefining innate immunity." Nature Reviews Immunology **13**(6): 453-460.

O'Shea, J. J. and W. E. Paul (2010). "Mechanisms underlying lineage commitment and plasticity of helper CD4+ T cells." Science (New York, N.Y.) **327**(5969): 1098-1102.

Oliveira-Nascimento, L., P. Massari and L. M. Wetzler (2012). "The Role of TLR2 in Infection and Immunity." Front Immunol **3**: 79.

Orecchioni, M., Y. Ghosheh, A. B. Pramod and K. Ley (2019). "Macrophage Polarization: Different Gene Signatures in M1(LPS+) vs. Classically and M2(LPS-) vs. Alternatively Activated Macrophages." Front Immunol **10**: 1084.

Owens, D. M. and S. M. Keyse (2007). "Differential regulation of MAP kinase signalling by dual-specificity protein phosphatases." Oncogene **26**(22): 3203-3213.

Patel, B., R. Banerjee, M. Basu, S. S. Lenka, M. Paichha, M. Samanta and S. Das (2019). "Toll like receptor induces Ig synthesis in Catla catla by activating MAPK and NF-kappaB signalling." Mol Immunol **105**: 62-75.

Pearson, G., F. Robinson, T. Beers Gibson, B. E. Xu, M. Karandikar, K. Berman and M. H. Cobb (2001). "Mitogen-activated protein (MAP) kinase pathways: regulation and physiological functions." Endocr Rev **22**(2): 153-183.

Peti, W. and R. Page (2013). "Molecular basis of MAP kinase regulation." Protein Science **22**(12): 1698-1710.

Petkau, A. (1987). "Role of superoxide dismutase in modification of radiation injury." Br J Cancer Suppl **8**: 87-95.

Piwowarski, J. P., I. Stanisławska, S. Granica, J. Stefańska and A. K. Kiss (2017). "Phase II Conjugates of Urolithins Isolated from Human Urine and Potential Role of β-Glucuronidases in Their Disposition." Drug Metabolism and Disposition **45**(6): 657-665.

Porta, C., C. Paglino and A. Mosca (2014). "Targeting PI3K/Akt/mTOR Signaling in Cancer." Front Oncol **4**: 64.

Qian, B.-Z. and J. W. Pollard (2010). "Macrophage Diversity Enhances Tumor Progression and Metastasis." Cell **141**(1): 39-51.

Qiao, W., Y. Huang, Z. Bian, X. Sun, X. Wang, Q. Gao, Y. Peng and L. Meng (2019). "Lipopolysaccharide-induced DNA damage response activates nuclear factor κB signalling pathway via GATA4 in dental pulp cells." International Endodontic Journal **52**(12): 1704-1715.

Racioppi, L., P. K. Noeldner, F. Lin, S. Arvai and A. R. Means (2012). "Calcium/calmodulin-dependent protein kinase kinase 2 regulates macrophage-mediated inflammatory responses." J Biol Chem **287**(14): 11579-11591.

Racioppi, L., P. K. Noeldner, F. Lin, S. Arvai and A. R. Means (2012). "Calcium/calmodulin-dependent protein kinase kinase 2 regulates macrophage-mediated inflammatory responses." Journal of Biological Chemistry **287**(14): 11579-11591.

Raetz, C. R. H., C. M. Reynolds, M. S. Trent and R. E. Bishop (2007). "Lipid A modification systems in gram-negative bacteria." Annual review of biochemistry **76**: 295-329.

Raetz, C. R. H. and C. Whitfield (2002). "Lipopolysaccharide endotoxins." Annual review of biochemistry **71**: 635-700.

Rahman, W. and A. H. Dickenson (2013). "Voltage gated sodium and calcium channel blockers for the treatment of chronic inflammatory pain." Neuroscience Letters **557**: 19-26.

Raingeaud, J., A. J. Whitmarsh, T. Barrett, B. Dérijard and R. J. Davis (1996). "MKK3- and MKK6-regulated gene expression is mediated by the p38 mitogen-activated protein kinase signal transduction pathway." Mol Cell Biol **16**(3): 1247-1255.

Ramond, E., A. Jamet, M. Coureuil and A. Charbit (2019). "Pivotal Role of Mitochondria in Macrophage Response to Bacterial Pathogens." Frontiers in Immunology **10**(2461).

Ratikan, J. A., E. D. Micewicz, M. W. Xie and D. Schaue (2015). "Radiation takes its Toll." Cancer letters **368**(2): 238-245.

Redon, C., D. Pilch, E. Rogakou, O. Sedelnikova, K. Newrock and W. Bonner (2002). "Histone H2A variants H2AX and H2AZ." Curr Opin Genet Dev **12**(2): 162-169.

Redon, C. E., J. S. Dickey, A. J. Nakamura, I. G. Kareva, D. Naf, S. Nowsheen, T. B. Kryston, W. M. Bonner, A. G. Georgakilas and O. A. Sedelnikova (2010). "Tumors induce complex DNA damage in distant proliferative tissues in vivo." Proceedings of the National Academy of Sciences **107**(42): 17992-17997.

Rietschel, E. T., T. Kirikae, F. U. Schade, U. Mamat, G. Schmidt, H. Loppnow, A. J. Ulmer, U. Zähringer, U. Seydel, F. Di Padova and et al. (1994). "Bacterial endotoxin: molecular relationships of structure to activity and function." Faseb j **8**(2): 217-225.

Rossato, M., G. Curtale, N. Tamassia, M. Castellucci, L. Mori, S. Gasperini, B. Mariotti, M. De Luca, M. Mirolo, M. A. Cassatella, M. Locati and F. Bazzoni (2012). "IL-10–induced microRNA-187 negatively

regulates TNF-α, IL-6, and IL-12p40 production in TLR4-stimulated monocytes." Proceedings of the National Academy of Sciences **109**(45): E3101-E3110.

Rossol, M., H. Heine, U. Meusch, D. Quandt, C. Klein, M. J. Sweet and S. Hauschildt (2011). "LPS-induced cytokine production in human monocytes and macrophages." Critical reviews in immunology **31**(5): 379-446.

Rothkamm, K., I. Krüger, L. H. Thompson and M. Löbrich (2003). "Pathways of DNA double-strand break repair during the mammalian cell cycle." Mol Cell Biol **23**(16): 5706-5715.

Roy, S. and C. K. Sen (2011). "MiRNA in innate immune responses: novel players in wound inflammation." Physiol Genomics **43**(10): 557-565.

Rubin, P. and G. W. Casarett (1968). "Clinical radiation pathology as applied to curative radiotherapy." Cancer **22**(4): 767-778.

Ruffell, B. and L. M. Coussens (2015). "Macrophages and therapeutic resistance in cancer." Cancer cell **27**(4): 462-472.

Ryu, D., L. Mouchiroud, P. A. Andreux, E. Katsyuba, N. Moullan, A. A. Nicolet-Dit-Félix, E. G. Williams, P. Jha, G. Lo Sasso, D. Huzard, P. Aebischer, C. Sandi, C. Rinsch and J. Auwerx (2016). "Urolithin A induces mitophagy and prolongs lifespan in C. elegans and increases muscle function in rodents." Nature medicine **22**(8): 879-888.

Sabers, C. J., M. M. Martin, G. J. Brunn, J. M. Williams, F. J. Dumont, G. Wiederrecht and R. T. Abraham (1995). "Isolation of a protein target of the FKBP12-rapamycin complex in mammalian cells." J Biol Chem **270**(2): 815-822.

Sahin, E., S. Colla, M. Liesa, J. Moslehi, F. L. Müller, M. Guo, M. Cooper, D. Kotton, A. J. Fabian, C. Walkey, R. S. Maser, G. Tonon, F. Foerster, R. Xiong, Y. A. Wang, S. A. Shukla, M. Jaskelioff, E. S. Martin, T. P. Heffernan, A. Protopopov, E. Ivanova, J. E. Mahoney, M. Kost-Alimova, S. R. Perry, R. Bronson, R. Liao, R. Mulligan, O. S. Shirihai, L. Chin and R. A. DePinho (2011). "Telomere dysfunction induces metabolic and mitochondrial compromise." Nature **470**(7334): 359-365.

Sánchez-González, C., M. Izquierdo-Pulido and V. Noé (2016). "Urolithin A causes p21 up-regulation in prostate cancer cells." European journal of nutrition **55**(3): 1099-1112.

Sassi, N., C. Paul, A. Martin, A. Bettaieb and J.-F. Jeannin (2010). "Lipid A-induced responses in vivo." Advances in experimental medicine and biology **667**: 69-80.

Schroeder, B. O. and F. Bäckhed (2016). "Signals from the gut microbiota to distant organs in physiology and disease." Nat Med **22**(10): 1079-1089.

Schulte, W., J. Bernhagen and R. Bucala (2013). "Cytokines in sepsis: potent immunoregulators and potential therapeutic targets--an updated view." Mediators Inflamm **2013**: 165974.

Scott, A. J., B. L. Oyler, D. R. Goodlett and R. K. Ernst (2017). "Lipid A structural modifications in extreme conditions and identification of unique modifying enzymes to define the Toll-like receptor 4 structure-activity relationship." Biochimica et biophysica acta. Molecular and cell biology of lipids **1862**(11): 1439-1450.

Seddon, M., Y. H. Looi and A. M. Shah (2007). "Oxidative stress and redox signalling in cardiac hypertrophy and heart failure." Heart **93**(8): 903-907.

Seeram, N. P., W. J. Aronson, Y. Zhang, S. M. Henning, A. Moro, R.-P. Lee, M. Sartippour, D. M. Harris, M. Rettig, M. A. Suchard, A. J. Pantuck, A. Belldegrun and D. Heber (2007). "Pomegranate ellagitannin-

derived metabolites inhibit prostate cancer growth and localize to the mouse prostate gland." Journal of agricultural and food chemistry **55**(19): 7732-7737.

Seeram, N. P., S. M. Henning, Y. Zhang, M. Suchard, Z. Li and D. Heber (2006). "Pomegranate juice ellagitannin metabolites are present in human plasma and some persist in urine for up to 48 h." J. Nutr. **136**: 2481.

Selma, M. V., D. Beltrán, R. García-Villalba, J. C. Espín and F. A. Tomás-Barberán (2014). "Description of urolithin production capacity from ellagic acid of two human intestinal Gordonibacter species." Food & function **5**(8): 1779-1784.

Sena, L. A. and N. S. Chandel (2012). "Physiological roles of mitochondrial reactive oxygen species." Molecular cell **48**(2): 158-167.

Shapira, L., S. Takashiba, C. Champagne, S. Amar and T. E. Van Dyke (1994). "Involvement of protein kinase C and protein tyrosine kinase in lipopolysaccharide-induced TNF-alpha and IL-1 beta production by human monocytes." Journal of immunology (Baltimore, Md. : 1950) **153**(4): 1818-1824.

Shapouri-Moghaddam, A., S. Mohammadian, H. Vazini, M. Taghadosi, S.-A. Esmaeili, F. Mardani, B. Seifi, A. Mohammadi, J. T. Afshari and A. Sahebkar (2018). "Macrophage plasticity, polarization, and function in health and disease." Journal of Cellular Physiology **233**(9): 6425-6440.

Sharif, O., V. N. Bolshakov, S. Raines, P. Newham and N. D. Perkins (2007). "Transcriptional profiling of the LPS induced NF-κB response in macrophages." BMC immunology **8**(1): 1.

Sharma, N. and B. Nehru (2015). "Characterization of the lipopolysaccharide induced model of Parkinson's disease: Role of oxidative stress and neuroinflammation." Neurochem Int **87**: 92-105.

Shaw, P. J., B. Qu, M. Hoth and S. Feske (2013). "Molecular regulation of CRAC channels and their role in lymphocyte function." Cell Mol Life Sci **70**(15): 2637-2656.

Shroff, R., A. Arbel-Eden, D. Pilch, G. Ira, W. M. Bonner, J. H. Petrini, J. E. Haber and M. Lichten (2004). "Distribution and dynamics of chromatin modification induced by a defined DNA double-strand break." Current Biology **14**(19): 1703-1711.

Sica, A., P. Allavena and A. Mantovani (2008). "Cancer related inflammation: the macrophage connection." Cancer letters **267**(2): 204-215.

Sica, A., M. Erreni, P. Allavena and C. Porta (2015). "Macrophage polarization in pathology." Cellular and molecular life sciences : CMLS **72**(21): 4111-4126.

Sica, A. and A. Mantovani (2012). "Macrophage plasticity and polarization: in vivo veritas." The Journal of clinical investigation **122**(3): 787-795.

Singh, A., P. Andreux, W. Blanco-Bose, D. Ryu, P. Aebischer, J. Auwerx and C. Rinsch (2017). "ORALLY ADMINISTERED UROLITHIN A IS SAFE AND MODULATES MUSCLE AND MITOCHONDRIAL BIOMARKERS IN ELDERLY." Innovation in Aging **1**(suppl_1): 1223-1224.

Singh, R., S. Chandrashekharappa, S. R. Bodduluri, B. V. Baby, B. Hegde, N. G. Kotla, A. A. Hiwale, T. Saiyed, P. Patel, M. Vijay-Kumar, M. G. I. Langille, G. M. Douglas, X. Cheng, E. C. Rouchka, S. J. Waigel, G. W. Dryden, H. Alatassi, H. G. Zhang, B. Haribabu, P. K. Vemula and V. R. Jala (2019). "Enhancement of the gut barrier integrity by a microbial metabolite through the Nrf2 pathway." Nat Commun **10**(1): 89.

Smith, P. M., M. R. Howitt, N. Panikov, M. Michaud, C. A. Gallini, M. Bohlooly-Y, J. N. Glickman and W. S. Garrett (2013). "The microbial metabolites, short-chain fatty acids, regulate colonic Treg cell homeostasis." Science (New York, N.Y.) **341**(6145): 569-573.

Soares-Silva, M., F. F. Diniz, G. N. Gomes and D. Bahia (2016). "The Mitogen-Activated Protein Kinase (MAPK) Pathway: Role in Immune Evasion by Trypanosomatids." Front Microbiol **7**: 183.

Sobhani, I., J. Tap, F. Roudot-Thoraval, J. P. Roperch, S. Letulle, P. Langella, G. Corthier, J. Tran Van Nhieu and J. P. Furet (2011). "Microbial dysbiosis in colorectal cancer (CRC) patients." PloS one **6**(1): e16393-e16393.

Song, G., G. Ouyang and S. Bao (2005). "The activation of Akt/PKB signaling pathway and cell survival." J Cell Mol Med **9**(1): 59-71.

Spitz, D. R., E. I. Azzam, J. J. Li and D. Gius (2004). "Metabolic oxidation/reduction reactions and cellular responses to ionizing radiation: a unifying concept in stress response biology." Cancer Metastasis Rev **23**(3-4): 311-322.

Stanley, E. R. (1985). "The macrophage colony-stimulating factor, CSF-1." Methods Enzymol **116**: 564-587.

Stevenson, G., B. Neal, D. Liu, M. Hobbs, N. H. Packer, M. Batley, J. W. Redmond, L. Lindquist and P. Reeves (1994). "Structure of the O antigen of Escherichia coli K-12 and the sequence of its rfb gene cluster." Journal of bacteriology **176**(13): 4144-4156.

Stiff, T., S. A. Walker, K. Cerosaletti, A. A. Goodarzi, E. Petermann, P. Concannon, M. O'Driscoll and P. A. Jeggo (2006). "ATR-dependent phosphorylation and activation of ATM in response to UV treatment or replication fork stalling." Embo j **25**(24): 5775-5782.

Stucki, M., J. A. Clapperton, D. Mohammad, M. B. Yaffe, S. J. Smerdon and S. P. Jackson (2005). "MDC1 directly binds phosphorylated histone H2AX to regulate cellular responses to DNA double-strand breaks." Cell **123**(7): 1213-1226.

Sun, S. C. (2011). "Non-canonical NF-κB signaling pathway." Cell Res **21**(1): 71-85.

Sun, S. C., J. H. Chang and J. Jin (2013). "Regulation of nuclear factor-κB in autoimmunity." Trends Immunol **34**(6): 282-289.

Surapaneni, K. M., V. V. Priya and J. Mallika (2014). "Pioglitazone, quercetin and hydroxy citric acid effect on cytochrome P450 2E1 (CYP2E1) enzyme levels in experimentally induced non alcoholic steatohepatitis (NASH)." European review for medical and pharmacological sciences **18**(18): 2736-2741.

Tabas, I. and K. E. Bornfeldt (2016). "Macrophage Phenotype and Function in Different Stages of Atherosclerosis." Circulation research **118**(4): 653-667.

Tabeta, K., K. Hoebe, E. M. Janssen, X. Du, P. Georgel, K. Crozat, S. Mudd, N. Mann, S. Sovath, J. Goode, L. Shamel, A. A. Herskovits, D. A. Portnoy, M. Cooke, L. M. Tarantino, T. Wiltshire, B. E. Steinberg, S. Grinstein and B. Beutler (2006). "The Unc93b1 mutation 3d disrupts exogenous antigen presentation and signaling via Toll-like receptors 3, 7 and 9." Nature Immunology **7**(2): 156-164.

Taganov, K. D., M. P. Boldin, K.-J. Chang and D. Baltimore (2006). "NF-kappaB-dependent induction of microRNA miR-146, an inhibitor targeted to signaling proteins of innate immune responses." Proceedings of the National Academy of Sciences of the United States of America **103**(33): 12481-12486.

Tak, P. P. and G. S. Firestein (2001). "NF-kappaB: a key role in inflammatory diseases." J Clin Invest **107**(1): 7-11.

Takahashi, K., F. Yamamura and M. Naito (1989). "Differentiation, maturation, and proliferation of macrophages in the mouse yolk sac: a light-microscopic, enzyme-cytochemical, immunohistochemical, and ultrastructural study." Journal of leukocyte biology **45**(2): 87-96.

Takashiba, S., T. E. Van Dyke, S. Amar, Y. Murayama, A. W. Soskolne and L. Shapira (1999). "Differentiation of monocytes to macrophages primes cells for lipopolysaccharide stimulation via accumulation of cytoplasmic nuclear factor kappaB." Infection and immunity **67**(11): 5573-5578.

Takeda, K. and S. Akira (2005). "Toll-like receptors in innate immunity." International immunology **17**(1): 1-14.

Takeuchi, O. and S. Akira (2010). "Pattern recognition receptors and inflammation." Cell **140**(6): 805-820.

Tanaka, H., H. Arakawa, T. Yamaguchi, K. Shiraishi, S. Fukuda, K. Matsui, Y. Takei and Y. Nakamura (2000). "A ribonucleotide reductase gene involved in a p53-dependent cell-cycle checkpoint for DNA damage." Nature **404**(6773): 42-49.

Teresa Pinto, A., M. Laranjeiro Pinto, A. Patrícia Cardoso, C. Monteiro, M. Teixeira Pinto, A. Filipe Maia, P. Castro, R. Figueira, A. Monteiro, M. Marques, M. Mareel, S. G. dos Santos, R. Seruca, M. Adolfo Barbosa, S. Rocha and M. José Oliveira (2016). "Ionizing radiation modulates human macrophages towards a pro-inflammatory phenotype preserving their pro-invasive and pro-angiogenic capacities." Scientific Reports **6**(1): 18765.

Thorpe, L. M., H. Yuzugullu and J. J. Zhao (2015). "PI3K in cancer: divergent roles of isoforms, modes of activation and therapeutic targeting." Nat Rev Cancer **15**(1): 7-24.

Thulin, P., T. Wei, O. Werngren, L. Cheung, R. M. Fisher, D. Grandér, M. Corcoran and E. Ehrenborg (2013). "MicroRNA-9 regulates the expression of peroxisome proliferator-activated receptor δ in human monocytes during the inflammatory response." International journal of molecular medicine **31**(5): 1003-1010.

Tomás-Barberán, F. A., R. García-Villalba, A. González-Sarrías, M. V. Selma and J. C. Espín (2014). "Ellagic Acid Metabolism by Human Gut Microbiota: Consistent Observation of Three Urolithin Phenotypes in Intervention Trials, Independent of Food Source, Age, and Health Status." Journal of Agricultural and Food Chemistry **62**(28): 6535-6538.

Tomás-Barberán, F. A., A. González-Sarrías, R. García-Villalba, M. A. Núñez-Sánchez, M. V. Selma, M. T. García-Conesa and J. C. Espín (2017). "Urolithins, the rescue of "old" metabolites to understand a "new" concept: Metabotypes as a nexus among phenolic metabolism, microbiota dysbiosis, and host health status." Mol Nutr Food Res **61**(1).

Tomkovich, S. and C. Jobin (2016). "Microbiota and host immune responses: a love-hate relationship." Immunology **147**(1): 1-10.

Toney, A. and S. Chung (2019). "Urolithin A, a Gut Metabolite, Induces Metabolic Reprogramming of Adipose Tissue by Promoting M2 Macrophage Polarization and Mitochondrial Function (OR12-02-19)." Current Developments in Nutrition **3**(Supplement_1).

Travassos, L. H., S. E. Girardin, D. J. Philpott, D. Blanot, M.-A. Nahori, C. Werts and I. G. Boneca (2004). "Toll-like receptor 2-dependent bacterial sensing does not occur via peptidoglycan recognition." EMBO reports **5**(10): 1000-1006.

Travis, E. L. (1980). "The sequence of histological changes in mouse lungs after single doses of x-rays." International journal of radiation oncology, biology, physics **6**(3): 345-347.

Travis, E. L. (1980). "The sequence of histological changes in mouse lungs after single doses of x-rays." Int J Radiat Oncol Biol Phys **6**(3): 345-347.

Troutman, T. D., J. F. Bazan and C. Pasare (2012). "Toll-like receptors, signaling adapters and regulation of the pro-inflammatory response by PI3K." Cell Cycle **11**(19): 3559-3567.

Tucureanu, M. M., D. Rebleanu, C. A. Constantinescu, M. Deleanu, G. Voicu, E. Butoi, M. Calin and I. Manduteanu (2017). "Lipopolysaccharide-induced inflammation in monocytes/macrophages is blocked by liposomal delivery of G(i)-protein inhibitor." International journal of nanomedicine **13**: 63-76.

Tulipani, S., M. Urpi-Sarda, R. García-Villalba, M. Rabassa, P. López-Uriarte, M. Bulló, O. Jáuregui, F. Tomás-Barberán, J. Salas-Salvadó, J. C. Espín and C. Andrés-Lacueva (2012). "Urolithins are the main urinary microbial-derived phenolic metabolites discriminating a moderate consumption of nuts in free-living subjects with diagnosed metabolic syndrome." Journal of agricultural and food chemistry **60**(36): 8930-8940.

Turner, M. D., B. Nedjai, T. Hurst and D. J. Pennington (2014). "Cytokines and chemokines: At the crossroads of cell signalling and inflammatory disease." Biochim Biophys Acta **1843**(11): 2563-2582.

Vacchelli, E., I. Vitale, E. Tartour, A. Eggermont, C. Sautès-Fridman, J. Galon, L. Zitvogel, G. Kroemer and L. Galluzzi (2013). "Trial Watch: Anticancer radioimmunotherapy." Oncoimmunology **2**(9): e25595-e25595.

Vacchelli, E., I. Vitale, E. Tartour, A. Eggermont, C. Sautès-Fridman, J. Galon, L. Zitvogel, G. Kroemer and L. Galluzzi (2013). "Trial Watch: Anticancer radioimmunotherapy." Oncoimmunology **2**(9): e25595.

Valerie, K., A. Yacoub, M. P. Hagan, D. T. Curiel, P. B. Fisher, S. Grant and P. Dent (2007). "Radiation-induced cell signaling: inside-out and outside-in." Mol Cancer Ther **6**(3): 789-801.

Vallabhapurapu, S. and M. Karin (2009). "Regulation and function of NF-kappaB transcription factors in the immune system." Annu Rev Immunol **27**: 693-733.

van Furth, R. and Z. A. Cohn (1968). "The origin and kinetics of mononuclear phagocytes." The Journal of experimental medicine **128**(3): 415-435.

Vanhaesebroeck, B., J. Guillermet-Guibert, M. Graupera and B. Bilanges (2010). "The emerging mechanisms of isoform-specific PI3K signalling." Nat Rev Mol Cell Biol **11**(5): 329-341.

Varol, C., A. Mildner and S. Jung (2015). "Macrophages: development and tissue specialization." Annual review of immunology **33**: 643-675.

Veremeyko, T., S. Siddiqui, I. Sotnikov, A. Yung and E. D. Ponomarev (2013). "IL-4/IL-13-dependent and independent expression of miR-124 and its contribution to M2 phenotype of monocytic cells in normal conditions and during allergic inflammation." PloS one **8**(12): e81774-e81774.

Vergadi, E., E. Ieronymaki, K. Lyroni, K. Vaporidi and C. Tsatsanis (2017). "Akt Signaling Pathway in Macrophage Activation and M1/M2 Polarization." J Immunol **198**(3): 1006-1014.

Vergadi, E., K. Vaporidi, E. E. Theodorakis, C. Doxaki, E. Lagoudaki, E. Ieronymaki, V. I. Alexaki, M. Helms, E. Kondili, B. Soennichsen, E. N. Stathopoulos, A. N. Margioris, D. Georgopoulos and C. Tsatsanis (2014). "Akt2 deficiency protects from acute lung injury via alternative macrophage activation and miR-146a induction in mice." Journal of immunology (Baltimore, Md. : 1950) **192**(1): 394-406.

Vieira, O. V., R. J. Botelho and S. Grinstein (2002). "Phagosome maturation: aging gracefully." The Biochemical journal **366**(Pt 3): 689-704.

Vogel, S. Z., S. Schlickeiser, K. Jürchott, L. Akyuez, J. Schumann, C. Appelt, K. Vogt, M. Schröder, M. Vaeth and F. Berberich-Siebelt (2015). "TCAIM decreases T cell priming capacity of dendritic cells by inhibiting TLR-induced Ca2+ influx and IL-2 production." The Journal of Immunology **194**(7): 3136-3146.

Vona, R., L. Gambardella, C. Cittadini, E. Straface and D. Pietraforte (2019). "Biomarkers of oxidative stress in metabolic syndrome and associated diseases." Oxidative medicine and cellular longevity **2019**.

Wang, D. D., W. J. Pan, S. Mehmood, X. D. Cheng and Y. Chen (2018). "Polysaccharide isolated from Sarcodon aspratus induces RAW264.7 activity via TLR4-mediated NF-κB and MAPK signaling pathways." Int J Biol Macromol **120**(Pt A): 1039-1047.

Wang, L.-X., S.-X. Zhang, H.-J. Wu, X.-L. Rong and J. Guo (2019). "M2b macrophage polarization and its roles in diseases." Journal of leukocyte biology **106**(2): 345-358.

Wang, N., H. Liang and K. Zen (2014). "Molecular mechanisms that influence the macrophage m1-m2 polarization balance." Front Immunol **5**: 614.

Wang, W., P. Liu, C. Hao, L. Wu, W. Wan and X. Mao (2017). "Neoagaro-oligosaccharide monomers inhibit inflammation in LPS-stimulated macrophages through suppression of MAPK and NF-κB pathways." Sci Rep **7**: 44252.

Wang, Z., A. L. Koenig, K. J. Lavine and R. S. Apte (2019). "Macrophage Plasticity and Function in the Eye and Heart." Trends in Immunology **40**(9): 825-841.

Ward, I. M., K. Minn and J. Chen (2004). "UV-induced ataxia-telangiectasia-mutated and Rad3-related (ATR) activation requires replication stress." J Biol Chem **279**(11): 9677-9680.

Wassenaar, T. M. and K. Zimmermann (2018). "Lipopolysaccharides in Food, Food Supplements, and Probiotics: Should We be Worried?" European journal of microbiology & immunology **8**(3): 63-69.

Watts, C. (1997). "Capture and processing of exogenous antigens for presentation on MHC molecules." Annu Rev Immunol **15**: 821-850.

Weagel, E., C. Smith, P. Liu, R. Robison and K. O'Neill (2015). "Macrophage polarization and its role in cancer." J Clin Cell Immunol **6**(4): 338.

Wei, Y. and A. Schober (2016). "MicroRNA regulation of macrophages in human pathologies." Cellular and molecular life sciences : CMLS **73**(18): 3473-3495.

Weinstein, S. L., J. S. Sanghera, K. Lemke, A. L. DeFranco and S. L. Pelech (1992). "Bacterial lipopolysaccharide induces tyrosine phosphorylation and activation of mitogen-activated protein kinases in macrophages." The Journal of biological chemistry **267**(21): 14955-14962.

Weiss, G. and U. E. Schaible (2015). "Macrophage defense mechanisms against intracellular bacteria." Immunological Reviews **264**(1): 182-203.

Werts, C., R. I. Tapping, J. C. Mathison, T. H. Chuang, V. Kravchenko, I. Saint Girons, D. A. Haake, P. J. Godowski, F. Hayashi, A. Ozinsky, D. M. Underhill, C. J. Kirschning, H. Wagner, A. Aderem, P. S. Tobias and R. J. Ulevitch (2001). "Leptospiral lipopolysaccharide activates cells through a TLR2-dependent mechanism." Nature immunology **2**(4): 346-352.

West, A. P., I. E. Brodsky, C. Rahner, D. K. Woo, H. Erdjument-Bromage, P. Tempst, M. C. Walsh, Y. Choi, G. S. Shadel and S. Ghosh (2011). "TLR signalling augments macrophage bactericidal activity through mitochondrial ROS." Nature **472**(7344): 476-480.

Wong, F. L., M. Yamada, H. Sasaki, K. Kodama, S. Akiba, K. Shimaoka and Y. Hosoda (1993). "Noncancer disease incidence in the atomic bomb survivors: 1958-1986." Radiat Res **135**(3): 418-430.

Woollard, K. J. and F. Geissmann (2010). "Monocytes in atherosclerosis: subsets and functions." Nature reviews. Cardiology **7**(2): 77-86.

Wright, E. G. (2010). "Manifestations and mechanisms of non-targeted effects of ionizing radiation." Mutation research **687**(1-2): 28-33.

Wu, Y., S. Antony, J. L. Meitzler and J. H. Doroshow (2014). "Molecular mechanisms underlying chronic inflammation-associated cancers." Cancer Lett **345**(2): 164-173.

Wyllie, D. H., E. Kiss-Toth, A. Visintin, S. C. Smith, S. Boussouf, D. M. Segal, G. W. Duff and S. K. Dower (2000). "Evidence for an Accessory Protein Function for Toll-Like Receptor 1 in Anti-Bacterial Responses." The Journal of Immunology **165**(12): 7125.

Wynn, T. A., A. Chawla and J. W. Pollard (2013). "Macrophage biology in development, homeostasis and disease." Nature **496**(7446): 445-455.

Xu, F., Y. Kang, H. Zhang, Z. Piao, H. Yin, R. Diao, J. Xia and L. Shi (2013). "Akt1-mediated regulation of macrophage polarization in a murine model of Staphylococcus aureus pulmonary infection." The Journal of infectious diseases **208**(3): 528-538.

Yamamoto, M. and K. Takeda (2010). "Current views of toll-like receptor signaling pathways." Gastroenterol Res Pract **2010**: 240365.

Yang, H., D. G. Rudge, J. D. Koos, B. Vaidialingam, H. J. Yang and N. P. Pavletich (2013). "mTOR kinase structure, mechanism and regulation." Nature **497**(7448): 217-223.

Yang, S. and G. Lian (2020). "ROS and diseases: role in metabolism and energy supply." Molecular and cellular biochemistry **467**(1-2): 1-12.

Ying, H., Y. Kang, H. Zhang, D. Zhao, J. Xia, Z. Lu, H. Wang, F. Xu and L. Shi (2015). "MiR-127 modulates macrophage polarization and promotes lung inflammation and injury by activating the JNK pathway." Journal of immunology (Baltimore, Md. : 1950) **194**(3): 1239-1251.

Yoshino, H., K. Chiba, T. Saitoh and I. Kashiwakura (2014). "Ionizing radiation affects the expression of Toll-like receptors 2 and 4 in human monocytic cells through c-Jun N-terminal kinase activation." J Radiat Res **55**(5): 876-884.

Yu, T., M. Gao, P. Yang, D. Liu, D. Wang, F. Song, X. Zhang and Y. Liu (2019). "Insulin promotes macrophage phenotype transition through PI3K/Akt and PPAR-γ signaling during diabetic wound healing." J Cell Physiol **234**(4): 4217-4231.

Yu, X.-Q. and M. R. Kanost (2004). "Immulectin-2, a pattern recognition receptor that stimulates hemocyte encapsulation and melanization in the tobacco hornworm, Manduca sexta." Developmental and comparative immunology **28**(9): 891-900.

Zhang, G., T. C. Meredith and D. Kahne (2013). "On the essentiality of lipopolysaccharide to Gram-negative bacteria." Current opinion in microbiology **16**(6): 779-785.

Zhang, K., P. Wang, S. Huang, X. Wang, T. Li, Y. Jin, M. Hehir and C. Xu (2014). "Different mechanism of LPS-induced calcium increase in human lung epithelial cell and microvascular endothelial cell: a cell culture study in a model for ARDS." Mol Biol Rep **41**(7): 4253-4259.

Zhang, L., P. T. Kang, C. L. Chen, K. B. Green and Y. R. Chen (2013). "Oxidative modifications of mitochondria complex II." Methods Mol Biol **1005**: 143-156.

Zhang, S., T. Al-Maghout, H. Cao, L. Pelzl, M. S. Salker, M. Veldhoen, A. Cheng, F. Lang and Y. Singh (2019). "Gut Bacterial Metabolite Urolithin A (UA) Mitigates Ca(2+) Entry in T Cells by Regulating miR-10a-5p." Front Immunol **10**: 1737.

Zhang, S. Q., W. Yang, M. I. Kontaridis, T. G. Bivona, G. Wen, T. Araki, J. Luo, J. A. Thompson, B. L. Schraven, M. R. Philips and B. G. Neel (2004). "Shp2 regulates SRC family kinase activity and Ras/Erk activation by controlling Csk recruitment." Mol Cell **13**(3): 341-355.

Zhang, W., H. Liu, W. Liu, Y. Liu and J. Xu (2015). "Polycomb-mediated loss of microRNA let-7c determines inflammatory macrophage polarization via PAK1-dependent NF-κB pathway." <u>Cell death and differentiation</u> **22**(2): 287-297.

Zhang, W. and H. T. Liu (2002). "MAPK signal pathways in the regulation of cell proliferation in mammalian cells." <u>Cell Res</u> **12**(1): 9-18.

Zhang, Y., M. Zhang, M. Zhong, Q. Suo and K. Lv (2013). "Expression profiles of miRNAs in polarized macrophages." <u>International journal of molecular medicine</u> **31**(4): 797-802.

Zhao, W. and M. E. C. Robbins (2009). "Inflammation and chronic oxidative stress in radiation-induced late normal tissue injury: therapeutic implications." <u>Current medicinal chemistry</u> **16**(2): 130-143.

Zhao, W., F. Shi, Z. Guo, J. Zhao, X. Song and H. Yang (2018). "Metabolite of ellagitannins, urolithin A induces autophagy and inhibits metastasis in human sw620 colorectal cancer cells." <u>Mol Carcinog</u> **57**(2): 193-200.

Zhou, X., W. Yang and J. Li (2006). "Ca2+- and protein kinase C-dependent signaling pathway for nuclear factor-kappaB activation, inducible nitric-oxide synthase expression, and tumor necrosis factor-alpha production in lipopolysaccharide-stimulated rat peritoneal macrophages." <u>J Biol Chem</u> **281**(42): 31337-31347.

Zhou, Y., Y. Hong and H. Huang (2016). "Triptolide Attenuates Inflammatory Response in Membranous Glomerulo-Nephritis Rat via Downregulation of NF-κB Signaling Pathway." <u>Kidney Blood Press Res</u> **41**(6): 901-910.

Zizzo, G., B. A. Hilliard, M. Monestier and P. L. Cohen (2012). "Efficient clearance of early apoptotic cells by human macrophages requires M2c polarization and MerTK induction." <u>Journal of immunology (Baltimore, Md. : 1950)</u> **189**(7): 3508-3520.

Zorova, L. D., V. A. Popkov, E. Y. Plotnikov, D. N. Silachev, I. B. Pevzner, S. S. Jankauskas, V. A. Babenko, S. D. Zorov, A. V. Balakireva, M. Juhaszova, S. J. Sollott and D. B. Zorov (2018). "Mitochondrial membrane potential." <u>Anal Biochem</u> **552**: 50-59.

7 SUPPLEMENTARY

Table 1 The source of variation in intracellular calcium in LPS-stimulated or X-irradiated murine BMDMs

Source of variation	% of total variation	F(DFn, DFd)	P value
Interaction	7.747	$F_{(13, 145)} = 1.645$	P = 0.0792
Group factor	33.64	$F_{(13, 145)} = 7.144$	P < 0.0001
Time factor	4.312	$F_{(1, 145)} = 11.91$	P = 0.0007

Table 2 The source of variation in γH2AX phosphorylation in LPS-stimulated or X-irradiated murine BMDMs

Source of variation	% of total variation	F (DFn, DFd)	P value
Interaction	6.728	$F_{(13, 318)} = 2.730$	P = 0.0011
Group factor	32.27	$F_{(13, 318)} = 13.09$	P < 0.0001
Time factor	0.4730	$F_{(1, 318)} = 2.495$	P = 0.1152

Table 3 The source of variation in protein expression of TLR2 in LPS-stimulated or X-irradiated murine BMDMs

Source of variation / TLR2	% of total variation	F (DFn, DFd)	P value	P value summary
Interaction	15.61	$F_{(36, 507)} = 5.298$	P < 0.0001	****
Group factor	39.95	$F_{(12, 507)} = 40.67$	P < 0.0001	****
Time factor	1.481	$F_{(3, 507)} = 6.032$	P = 0.0005	***

Table 4 The source of variation in protein expression and phosphorylation of ERK1/2 in LPS-stimulated or X-irradiated murine BMDMs

Source of variation / pERK1/2 over GAPDH	% of total variation	F (DFn, DFd)	P value	P value summary
Interaction	42.83	F (36, 286) = 7.898	P < 0.0001	****
Group factor	13.38	F (12, 286) = 7.402	P < 0.0001	****
Time factor	0.5391	F (3, 286) = 1.193	P = 0.3126	ns
Source of variation / ERK1/2 over GAPDH	**% of total variation**	**F (DFn, DFd)**	**P value**	**P value summary**
Interaction	20.60	F (36, 386) = 4.361	P < 0.0001	****
Group factor	29.42	F (12, 386) = 18.68	P < 0.0001	****
Time factor	2.287	F (3, 386) = 5.808	P = 0.0007	***
Source of variation / pERK1/2 over ERK	**% of total variation**	**F (DFn, DFd)**	**P value**	**P value summary**
Interaction	31.32	F (36, 260) = 3.921	P < 0.0001	****
Group factor	9.705	F (12, 260) = 3.645	P < 0.0001	****
Time factor	1.286	F (3, 260) = 1.931	P = 0.1249	ns

Table 5 The source of variation in protein expression and phosphorylation of MAPK p38 in LPS-stimulated or X-irradiated murine BMDMs

Source of variation / pp38 over GAPDH	% of total variation	F (DFn, DFd)	P value	P value summary
Interaction	19.15	F (36, 351) = 4.448	P < 0.0001	****
Group factor	26.46	F (12, 351) = 18.44	P < 0.0001	****
Time factor	12.37	F (3, 351) = 34.48	P < 0.0001	****
Source of variation / p38 over GAPDH	**% of total variation**	**F (DFn, DFd)**	**P value**	**P value summary**
Interaction	27.15	F (36, 247) = 5.127	P < 0.0001	****
Group factor	37.25	F (12, 247) = 21.10	P < 0.0001	****
Time factor	1.456	F (3, 247) = 3.299	P = 0.0211	*
Source of variation / phospho/p38 over p38	**% of total variation**	**F (DFn, DFd)**	**P value**	**P value summary**
Interaction	29.43	F (36, 247) = 5.008	P < 0.0001	****
Group factor	18.45	F (12, 247) = 9.419	P < 0.0001	****
Time factor	10.60	F (3, 247) = 21.65	P < 0.0001	****

Table 6 The source of variation in protein expression and phosphorylation of MAPK SAPK/JNK in LPS-stimulated or X-irradiated murine BMDMs

Source of variation / phospho-SAPK/JNK over GAPDH	% of total variation	F (DFn, DFd)	P value	P value summary
Interaction	15.06	F (36, 273) = 3.122	P < 0.0001	****
Group factor	45.48	F (12, 273) = 28.28	P < 0.0001	****
Time factor	0.4262	F (3, 273) = 1.060	P = 0.3665	ns
Source of variation / SAPK/JNK over GAPDH	**% of total variation**	**F (DFn, DFd)**	**P value**	**P value summary**
Interaction	6.266	F (36, 286) = 1.394	P = 0.0740	ns
Group factor	53.30	F (12, 286) = 35.57	P < 0.0001	****
Time factor	2.454	F (3, 286) = 6.551	P = 0.0003	***
Source of variation / pSAPK/JNK over SAPK/JNK	**% of total variation**	**F (DFn, DFd)**	**P value**	**P value summary**
Interaction	20.37	F (36, 208) = 1.877	P = 0.0034	**
Group factor	13.73	F (12, 208) = 3.795	P < 0.0001	****
Time factor	3.194	F (3, 208) = 3.531	P = 0.0158	*

Table 7 The source of variation in protein expression of IκBα expression and phosphorylation in LPS-stimulated or X-irradiated murine BMDMs

Source of variation / pIκBα over GAPDH	% of total variation	F (DFn, DFd)	P value	P value summary
Interaction	3.277	F (36, 208) = 0.7886	P = 0.8001	ns
Group factor	71.94	F (12, 208) = 51.93	P < 0.0001	****
Time factor	0.7713	F (3, 208) = 2.227	P = 0.0861	ns
Source of variation / IκBα over GAPDH	**% of total variation**	**F (DFn, DFd)**	**P value**	**P value summary**
Interaction	19.38	F (36, 208) = 4.482	P < 0.0001	****
Group factor	46.84	F (12, 208) = 32.49	P < 0.0001	****
Time factor	8.799	F (3, 208) = 24.42	P < 0.0001	****
Source of variation / pIκBα over IκBα	**% of total variation**	**F (DFn, DFd)**	**P value**	**P value summary**
Interaction	16.26	F (36, 208) = 2.714	P < 0.0001	****
Group factor	45.24	F (12, 208) = 22.65	P < 0.0001	****
Time factor	3.884	F (3, 208) = 7.780	P < 0.0001	****

Table 8 The source of variation in protein expression and phosphorylation of AKT in LPS-stimulated or X-irradiated murine BMDMs

Source of variation / pAKT over GAPDH	% of total variation	F (DFn, DFd)	P value	P value summary
Interaction	29.06	F (36, 299) = 5.809	P < 0.0001	****
Group factor	22.32	F (12, 299) = 13.39	P < 0.0001	****
Time factor	8.092	F (3, 299) = 19.41	P < 0.0001	****
Source of variation / AKT over GAPDH	**% of total variation**	**F (DFn, DFd)**	**P value**	**P value summary**
Interaction	15.74	F (36, 312) = 4.524	P < 0.0001	****
Group factor	46.02	F (12, 312) = 39.68	P < 0.0001	****
Time factor	8.075	F (3, 312) = 27.84	P < 0.0001	****
Source of variation / pAKT over AKT	**% of total variation**	**F (DFn, DFd)**	**P value**	**P value summary**
Interaction	25.51	F (36, 299) = 5.331	P < 0.0001	****
Group factor	15.43	F (12, 299) = 9.674	P < 0.0001	****
Time factor	19.95	F (3, 299) = 50.05	P < 0.0001	****

Table 9 The source of variation in protein expression and phosphorylation of mTOR in LPS-stimulated or X-irradiated murine BMDMs

Source of variation / phospho-mTOR over GAPDH	% of total variation	F (DFn, DFd)	P value	P value summary
Interaction	15.42	F (36, 387) = 3.499	P < 0.0001	****
Group factor	30.73	F (12, 387) = 20.92	P < 0.0001	****
Time factor	6.764	F (3, 387) = 18.41	P < 0.0001	****
Source of variation / mTOR over GAPDH	**% of total variation**	**F (DFn, DFd)**	**P value**	**P value summary**
Interaction	13.69	F (36, 351) = 3.984	P < 0.0001	****
Group factor	50.05	F (12, 351) = 43.70	P < 0.0001	****
Time factor	3.277	F (3, 351) = 11.44	P < 0.0001	****
Source of variation / phospho-mTOR over mTOR	**% of total variation**	**F (DFn, DFd)**	**P value**	**P value summary**
Interaction	27.85	F (36, 351) = 7.738	P < 0.0001	****
Group factor	24.93	F (12, 351) = 20.78	P < 0.0001	****
Time factor	14.17	F (3, 351) = 47.24	P < 0.0001	****

Table 10 The source of variation of pro-inflammatory cytokine mRNA expression in LPS-stimulated or X-irradiated murine BMDMs

Source of variation / IL-1β	% of total variation	F (DFn, DFd)	P value	P value summary
Interaction	24.47	F (26, 166) = 49.58	P < 0.0001	****
Group factor	68.95	F (13, 166) = 279.4	P < 0.0001	****
Time factor	3.339	F (2, 166) = 87.96	P < 0.0001	****
Source of variation / IL-2	**% of total variation**	**F (DFn, DFd)**	**P value**	**P value summary**
Interaction	3.335	F (26, 192) = 0.8858	P = 0.6283	ns
Group factor	66.63	F (13, 192) = 35.40	P < 0.0001	****
Time factor	1.049	F (2, 192) = 3.624	P = 0.0285	*
Source of variation / IL-6	**% of total variation**	**F (DFn, DFd)**	**P value**	**P value summary**
Interaction	44.60	F (26, 252) = 51.81	P < 0.0001	****
Group factor	38.68	F (13, 252) = 89.86	P < 0.0001	****
Time factor	8.371	F (2, 252) = 126.4	P < 0.0001	****
Source of variation / IL-12	**% of total variation**	**F (DFn, DFd)**	**P value**	**P value summary**
Interaction	21.03	F (26, 230) = 4.485	P < 0.0001	****
Group factor	37.76	F (13, 230) = 16.11	P < 0.0001	****
Time factor	4.157	F (2, 230) = 11.53	P < 0.0001	****
Source of variation / TNF-α	**% of total variation**	**F (DFn, DFd)**	**P value**	**P value summary**
Interaction	36.46	F (26, 246) = 34.51	P < 0.0001	****
Group factor	46.95	F (13, 246) = 88.90	P < 0.0001	****
Time factor	6.413	F (2, 246) = 78.93	P < 0.0001	****

Table 11 The source of variation in anti-inflammatory cytokine mRNA expression in LPS-stimulated or X-irradiated murine BMDMs

Source of variation / IL-4	% of total variation	F (DFn, DFd)	P value	P value summary
Interaction	23.18	F (26, 259) = 6.454	P < 0.0001	****
Group factor	30.00	F (13, 259) = 16.71	P < 0.0001	****
Time factor	11.90	F (2, 259) = 43.07	P < 0.0001	****
Source of variation / IL-10	% of total variation	F (DFn, DFd)	P value	P value summary
Interaction	23.35	F (26, 235) = 4.678	P < 0.0001	****
Group factor	24.39	F (13, 235) = 9.770	P < 0.0001	****
Time factor	6.672	F (2, 235) = 17.37	P < 0.0001	****
Source of variation / TGF-β	% of total variation	F (DFn, DFd)	P value	P value summary
Interaction	2.195	F (26, 248) = 0.4064	P = 0.9960	ns
Group factor	46.23	F (13, 248) = 17.12	P < 0.0001	****
Time factor	0.05814	F (2, 248) = 0.1399	P = 0.8695	ns
Source of variation / IFN-γ	% of total variation	F (DFn, DFd)	P value	P value summary
Interaction	3.315	F (26, 239) = 0.5017	P = 0.9808	ns
Group factor	33.54	F (13, 239) = 10.15	P < 0.0001	****
Time factor	0.05949	F (2, 239) = 0.1170	P = 0.8896	ns
Source of variation / NOS2	% of total variation	F (DFn, DFd)	P value	P value summary
Interaction	27.23	F (26, 243) = 103.5	P < 0.0001	****
Group factor	68.19	F (13, 243) = 518.4	P < 0.0001	****
Time factor	1.943	F (2, 243) = 95.99	P < 0.0001	****

Table 12 The source of variation of pro-inflammatory cytokines production in LPS-stimulated or X-irradiated murine BMDMs

Source of variation / IL-1β	% of total variation	F (DFn, DFd)	P value	P value summary
Interaction	10.39	F (12, 156) = 5.966	P < 0.0001	****
Group factor	66.12	F (12, 156) = 37.96	P < 0.0001	****
Time factor	0.8422	F (1, 156) = 5.802	P = 0.0172	*

Source of variation / IL-6	% of total variation	F (DFn, DFd)	P value	P value summary
Interaction	2.344	F (13, 168) = 1.764	P = 0.0525	ns
Group factor	80.47	F (13, 168) = 60.56	P < 0.0001	****
Time factor	0.01169	F (1, 168) = 0.1144	P = 0.7356	ns

Source of variation / IL-12	% of total variation	F (DFn, DFd)	P value	P value summary
Interaction	2.439	F (13, 166) = 0.5166	P = 0.9122	ns
Group factor	35.28	F (13, 166) = 7.472	P < 0.0001	****
Time factor	1.956	F (1, 166) = 5.386	P = 0.0215	*

Source of variation / TNF-α	% of total variation	F (DFn, DFd)	P value	P value summary
Interaction	16.29	F (13, 168) = 29.95	P < 0.0001	****
Group factor	73.38	F (13, 168) = 134.9	P < 0.0001	****
Time factor	3.299	F (1, 168) = 78.83	P < 0.0001	****

Table 13 The source of variation of anti-inflammatory cytokines production in LPS-stimulated or X-irradiated BMDMs

Source of variation/ IL-4	% of total variation	F (DFn, DFd)	P value	P value summary
Interaction	7.409	F (13, 168) = 1.965	P = 0.0265	*
Group factor	33.41	F (13, 168) = 8.861	P < 0.0001	****
Time factor	10.46	F (1, 168) = 36.07	P < 0.0001	****
Source of variation/ IL-10	**% of total variation**	**F (DFn, DFd)**	**P value**	**P value summary**
Interaction	7.302	F (13, 168) = 3.094	P = 0.0004	***
Group factor	60.59	F (13, 168) = 25.68	P < 0.0001	****
Time factor	1.609	F (1, 168) = 8.866	P = 0.0033	**
Source of variation/ TGF-β	**% of total variation**	**F (DFn, DFd)**	**P value**	**P value summary**
Interaction	17.89	F (13, 168) = 3.691	P < 0.0001	****
Group factor	15.77	F (13, 168) = 3.253	P = 0.0002	***
Time factor	3.698	F (1, 168) = 9.917	P = 0.0019	**
Source of variation/ IFN-γ	**% of total variation**	**F (DFn, DFd)**	**P value**	**P value summary**
Interaction	4.273	F (13, 168) = 2.040	P = 0.0203	*
Group factor	27.07	F (13, 168) = 12.92	P < 0.0001	****
Time factor	41.59	F (1, 168) = 258.1	P < 0.0001	****

8 ACKNOWLEDGEMENT

I can't forget to extend my deep thanks and gratitude to my family for being an unstinting source of support and encouragement, patience and support throughout the entire period of my work. Thanks to my beloved **mother**, **brothers**, **and sisters**. Thanks to my beloved wife **Fatma Refat** and my daughters **Sarah** and **Elham**.

Khalid Nady Mohammed Abdelazeem

9   DECLARATION OF CONTRIBUTIONS

I assure that the submitted work has not been submitted previously or used by another examination authority for the purpose of a doctoral or other examination procedure and is all written by me, and all the used sources are cited properly.

Professor Stephen Huber provided the facility for radiation exposure.

Flow cytometry, miRNA, qPCR, western blot and ELISA experiments were carried out by me.

Immunofluorescences Imaging was carried out by me and M. Zaher Kalo.

Professor Sandra Beer-Hammer and me designed the study.

Professor Florian Lang and Professor Sandra Beer-Hammer provided me with the reagents and lab facility.

The work in this thesis will be submitted under the title.

1- Inhibiting NF-kB activation by gut microbiota metabolite urolithin A in LPS-stimulated BMDMs

2- The non-pathogenic gut microbiota metabolite UA augments TLR2 expression and dwindling DNA double strand breaks in X-irradiated BMDMs

The author

Khalid Nady Mohammed Abdelazeem

LIST OF PUBLICATIONS

1- Abdelazeem, K. N. M., Y. Singh, F. Lang and M. S. Salker (2017). "**Negative Effect of Ellagic Acid on Cytosolic pH Regulation and Glycolytic Flux in Human Endometrial Cancer Cells.**" Cell Physiol Biochem 41(6): 2374-2382.

2- Singh, Y., Y. Zhou, S. Zhang, Abdelazeem, K. N. M., B. Elvira, M. S. Salker and F. Lang (2017). "**Enhanced Reactive Oxygen Species Production, Acidic Cytosolic pH and Upregulated Na+/H+ Exchanger (NHE) in Dicer Deficient CD4+ T Cells.**" Cell Physiol Biochem 42(4): 1377-1389.

3- Abdelazeem, K. N. M., B. Droppova, B. Sukkar, T. Al-Maghout, L. Pelzl, N. Zacharopoulou, N. H. Ali Hassan, K. I. Abdel-Fattah, C. Stournaras and F. Lang (2019). "**Upregulation of Orai1 and STIM1 expression as well as store-operated Ca(2+) entry in ovary carcinoma cells by placental growth factor**." Biochem Biophys Res Commun 512(3): 467-472.

4- Abd El Salam, S.; Elnady, K.; Zahran, W.M.; Ayobe, M.H. **Protective Effects Of ALPHA Lipoic Acid On GAMMA Irradiation Hazards In Male Rats**. Isotope and Radiation Research; ISSN 0021-1907; ; v. 43(1); p. 223-232.

5- Abdelazeem, K. N. M., Kalo Z. M., Singh Y., F. Lang and S. Beer-Hammer (2020). "**Inhibiting NF-kB activation by gut microbiota metabolite urolithin A in LPS-stimulated BMDMs.**" in Submission.

6- Abdelazeem, K. N. M., Kalo Z. M., S. Huber, F. Lang and S. Beer-Hammer (2020). "**The non-pathogenic gut microbiota metabolite UA augments TLR2 expression and dwindling DNA double strand breaks in X-irradiated BMDMs**. " in Submission

Eidesstattliche Erklärung

Ich erkläre hiermit, dass ich die zur Promotion eingereichte Arbeit mit dem Titel „Effect of the gut microbiota metabolite urolithin A on the inflammatory responses induced by LPS or X-irradiation in BMDMs" selbständig verfasst, nur die angegebenen Quellen und Hilfsmittel benutzt und wörtlich oder inhaltlich übernommene Stellen als solche gekennzeichnet habe. Ich erkläre, dass die Richtlinien zur Sicherung guter wissenschaftlicher Praxis der Universität Tübingen (Beschluss des Senats vom 25.05.2000) beachtet wurden. Ich versichere an Eides statt, dass diese Angaben wahr sind und dass ich nichts verschwiegen habe. Mir ist bekannt, dass die falsche Abgabe einer Versicherung an Eides statt mit Freiheitstrafe bis zu drei Jahren oder mit Geldstrafe bestraft wird.

The author

Khalid Nady Mohammed Abdelazeem